Damage Sensitive Feature Extraction and Classification in the Structural Systems using Time Series Representation in Phase-Space Portrait

Thesis Submitted in Partial Fulfilment of the Requirements for the Degree of

DOCTOR OF PHILOSOPHY

By

Lavish Gobind Pamwani

(156104003)

to

DEPARTMENT OF CIVIL ENGINEERING

INDIAN INSTITUTE OF TECHNOLOGY GUWAHATI

December-2019

Dedicated to my

Mother ***Mrs. Komal Pamwani***

and

Father ***Mr. Gobind Pamwani***

DECLARATION

I hereby certify that the work compiled in this thesis is the outcome of the research work, performed by myself, else stated, under the guidance of Dr. Amit Shelke.

Any part of this work has not been submitted for the award of any degree, diploma, associate-fellowship, fellowship or its equivalent to any university or institution.

Lavish Gobind Pamwani
Registration No. 156104003
Department of Civil Engineering
Indian Institute of Technology Guwahati

CERTIFICATE

It is certified that the work contained in the thesis entitled "**Damage Sensitive Feature Extraction and Classification in the Structural Systems using Time Series Representation in Phase-Space Portrait"** by **Mr. Lavish Gobind Pamwani (156104003)**, a student, in the Department of Civil Engineering, Indian Institute of Technology Guwahati, India, for the award of the degree of the Doctor of Philosophy, has been carried out under my supervision and, that this work has not been submitted elsewhere for the degree.

Date:

Dr. Amit Shelke

Assistant Professor

Department of Civil Engineering

Indian Institute of Technology Guwahati

Guwahati-781039

India

ACKNOWLEDGMENTS

I want to grab this opportunity to acknowledge the greatness of all those people who help and support me to complete this thesis. First of all, I want to thank my supervisor, Dr. Amit Shelke for giving endless important suggestions and critical reviews of my work through their guidance. His endless reassurance, recommendations and co-operation have been a great motivation for me while carrying out my research work. I will always be grateful to him for the knowledge he conveyed from his enormous experience.

Besides my supervisor, I would like to acknowledge the doctoral committee members, Prof. Arbind Kumar Singh, Dr. Karuna Kalita, Dr. Hrishikesh Sharma, and Dr. Nelson Muthu for their valuable recommendations and insightful remarks throughout the course of research activities, which has constantly engaged me towards undertaking a meaningful thesis work. I would specially like to thank Dr. Budhaditya Hazra for his advice and help in my research work.

Further, special appreciation for the senior technician and support staff of the Department of Civil Engineering for their valuable help namely, Mr. Biswajit Debnath, Mr. Pranab Hazarika, Mr. Saurabh Mudoi, and Mr. Suresh Boro.

I would also gratefully acknowledge the financial support provided by the Department of Science and Technology (SERB/F/2242/2015-2016) and Defence Research and Development Organization (Grant No. ARMREB/CDSW/2017/192), Government of India.

I am truly grateful to my colleague-turned-friends: Anupoju Rajeev, Dharmendra Dhaka, Shekhar Singh, Ayush Maheshwari, Basuraj Bhowmik, Prashank Yadav and Sai Sharath for their contributions towards my dissertation: be it preparing drafts or assisting me in experiments/coding is greatly acknowledged. I have very fond memories of my time here. I would deeply thank all my fellow lab-mates in NDT Laboratory: Pallab, Pranjal, Kasturi, Subhadip, Sulaem Da, Bonisha, Monjusha, Saroj, Prinza and Tori for all the enriching and valuable discussions. Without this group, my journey perhaps would have been of less fun.

There were days that went by with frustrations and disappointments; and all I had to do was make a simple phone call. Thank you Bhavna for always being available, sharing my feelings, and believing in me.

Last but not the least; I owe my gratitude towards my parents Mr. Gobind Pamwani Mrs. Komal Pamwani and my brother Mr. Bhavesh Pamwani for being the constant guiding, and supporting force throughout my journey.

Lavish Gobind Pamwani

Indian Institute of Technology Guwahati

December 2019

ABSTRACT

Due to increase in urbanization of the world population, the utilization of urban infrastructure has been accelerated. Therefore, the development of resilient, intelligent, smart and sustainable infrastructure is essential to deal with the ever-increasing needs. Unceasing utilization of the structural services has always necessitated timely and effective maintenance systems. Past two decades are evident of numerous accidents and sudden failure of structures due to extreme loading, that could have been easily averted by detailed inspection and routine maintenance. The requirement for a capable maintenance system and asset management is the availability of robust health monitoring background. The decision-making for reinstating the utility and safe operation of the critical infrastructure is often doubtful in absence of availability of robust structural health monitoring (SHM) and damage assessment framework. Therefore, the development and implementation of health monitoring algorithms to monitor the health of different structural systems subjected to the extreme scenario is a key aspect of current work.

In order to monitor health of structural systems subjected to the extreme loadings, the current work initially develops an algorithm based on a combination of Empirical mode decomposition (EMD) and principal component analysis (PCA) to monitor the health of three storey shear building subjected to repetitive seismic excitation of high return period. Under the influence of repetitive base excitation, an extreme loading scenario, the shear building is expected to incur a reduction in its service life (i.e. damage is induced). The process of "EMD" gives the dominant intrinsic mode function that has no noise and redundant information. This step helps to avoid false alarm, as any redundant information if present, will alter the Eigen-structure of signal even in case of no damage. Later, with the help of "PCA", the change in the Eigen-structure is evaluated and a sensitive condition indicator (CI) was proposed. The proposed CI quantifies damage by evaluating the normalized Euclidean norm of the change in principal angles, corresponding to pristine and damage state.

The interesting case of extreme loading is shockwave loading, high pressure, and short duration pulse. The shock loading can induce significant damage in any structure and leads to its catastrophic failure. Therefore, in current work a health monitoring approach to quantify the damage of structure subjected to such an extreme loading was developed. To demonstrate the efficacy of the proposed approach, shockwave experiments were conducted on a three storey shear building, where repetitive localized shock loads were imparted to manifest progressive damage states. A two-phase novel damage detection algorithm was proposed, that quantify and segregate perturbative damage from microscale damage. The first phase performs dimension reduction and damage state segregation using principal component analysis. In the second phase, initially, the embedding dimension was reduced through Empirical Mode Decomposition. Thereafter, the embedding parameters were derived using singular system analysis and average mutual information function. Now, based on Takens' theorem and embedding parameters, the response was represented in a multi-dimensional phase space trajectory (PST). The dissimilarity in the multi-dimensional "PST" was used to derive the damage sensitive features (DSFs). The "DSFs" namely: (i) Change in phase space topology (CPST) and (ii) Mahalanobis distance between phase space topology (MDPST) are evaluated to quantify progressive damage states. These "DSFs" are based on Euclidean norm and Mahalanobis distance.

Seismic excitation of high magnitude, a case of an extreme loading is also considered in the current study. The monitoring approach to quantify the damage due to extreme vibration was developed. The proposed approach was tested on a test model: a steel moment resisting frame that experiences the excessive magnitude of vibration due to base excitation. Under the influence of prolonging ambient vibration, the beam-to-column connection of "MRF" will undergo fatigue resulting in loosing of bolts causing the reduction in stiffness These extreme vibrations can lead to catastrophic failure if the health of structure is left unmonitored. Also, the structural damage to the steel frame might get unnoticed during structural damage assessment. Therefore, current work develops two different approaches to

monitor the health of steel moment resisting frame. The first approach is based on the time-varying autoregressive (TVAR) model is integrated with K-means -- clustering technique to detect damage in the steel moment resisting frame. The damage is detected in the frame using non-stationary acceleration response of the structure excited using ambient white noise. The proposed technique identifies and quantifies the damage in the beam-to-column connection and column-to-column splice plate connection caused due to loosening of the connecting bolts. The algorithm models the non-stationary acceleration time history and evaluates the "TVAR" coefficients (TVARC) for pristine and damage states. These coefficients are represented as a cluster in the "TVARC" subspace and segregated and classified using K means -- segmentation technique. The K-means -- approach is adapted to simultaneously perform partition clustering and remove outliers. Eigenstructure evaluation of the segregated "TVARC" cluster is performed to detect temporal damage. The topological and statistical parameters of the "TVARC" clusters are used to quantify the magnitude of the damage. The damage is quantified using Mahalanobis distance (MD) and Itakura distance (ID) serving as the statistical distance between the healthy and damage "TVARC" clusters.

The second damage detection algorithm proposed is based on the amalgamation of Independent component analysis (ICA) and Phase space reconstruction (PSR). An experimental investigation is conducted by inducing damage in steel moment resisting frame (SMRF) and exciting it with ambient white noise base excitation. The experimental study was conducted for a healthy state and multiple progressive damage state. The damage in "SMRF" was manifested progressively by loosening the bolts of the beam-to-column and column-to-column bolted connection. The proposed algorithm analyzes the acquired acceleration response of "SMRF" subjected to white noise base excitation (WNBE). The algorithm consists of two segments; in the first segment, the modal responses are obtained from the acquired response with the help of Independent component analysis (ICA). The optimal embedding parameters for modal responses are evaluated with the help of average mutual information function (AMIF) and Singular System Analysis (SSA). The second

segment deals with the reconstruction of "PST" with the help of modal responses and embedding parameters. Lastly, the damage sensitive features (DSFs) are evaluated to identify and quantify the induced damage. The "DSFs" evaluated in the presented study are namely; (i) Change in phase space topology (CPST), (ii) Mahalanobis distance between phase space topology (MDPST), and (iii) Itakura distance (ID). The "DSFs", "CPST", and "MDPST" measure the dissimilarity between the "PST" of healthy and damage states. Whereas, ID measures the dissimilarity between the set of Auto-Regressive (AR) coefficients of healthy and damage states of "SMRF".

TABLE OF CONTENTS

LIST OF FIGURES

LIST OF TABLES

LIST OF ABBREVIATIONS AND SYMBOLS

Abbreviations

AMIF	Average Mutual Information Function
AR	Auto-Regressive
ARMA	Auto-Regressive Moving Average
ALAVR	Average Local Attractor Variance Ratio
AMUSE	Algorithm For Multiple Unknown Signals Extraction
BSS	Blind Source Separation
CI	Condition Indicator
CPST	Change In Phase Space Topology
DSF	Damage Sensitive Feature
EMD	Empirical Mode Decomposition
FFT	Fast Fourier Transform
IMF	Intrinsic Mode Function
ID	Itakura Distance
ISMB	India Standard Medium Weight Beam
ICA	Independent Component Analysis
KF	Kalman Filter
MRF	Moment Resisting Frame
MD	Mahalanobis Distance
MDPST	Mahalanobis Distance between Phase Space Topology
MAC	Modal Assurance Criterion
MDOF	Multiple Degree Of Freedom
MSE	Mean Square Error
PCA	Principal Component Analysis
PST	Phase Space Trajectory
PSR	Phase Space Reconstruction
POC	Principal Orthogonal Component
SMRF	Steel Moment Resisting Frame
SSA	Singular System Analysis

SHM	Structural Health Monitoring
SI	System Identification
SVD	Singular Value Decomposition
TVAR	Time-Varying Autoregressive
TVARC	Time-Varying Autoregressive Cluster
VBM	Vibration-Based Methods

Symbols

σ	Standard Deviation
μ	Mean
α	Damage Feature
τ	Time Delay/Lag
λ	Eigen Value
a_k	Time-Varying Autoregressive Coefficients
$c_{xx}(t)$	Autocorrelation Function
m	Embedding Dimension
$p(x)$	Probability Density Function
$p(x,y)$	Joint Probability Density Function
$v(n)$	Zero Mean Gaussian White Noise
$I(t)$	Average Mutual Information Function
$J_{K-means}$	Objective Function
$K(n)$	Kalman Gain Matrix
X_c	Coefficient Matrix
$X(n)$	Attractor at time step 'n'
C	Covariance Matrix
I	Identity Matrix
K	Stiffness Matrix
M	Mass Matrix
R	Autocorrelation Matrix

The following notations are considered for equations, if not stated explicitly.

Bold in first bracket	[**X**]	Matrix
Italics in second bracket	{X}	Vector
Bold with no brackets	**X**	Scalar constant
Italics with no brackets	X	Scalar variable

Chapter 1

Introduction

1.1 Background

According to world health observatory (WHO) data, in the year 2015, more than 54 % of the world population have migrated from rural areas to reside in urban communities (United-Nations, 2017) . The dramatic demographic transformation of the major cities has altered the urban landscape and accelerated the exploitation of urban infrastructure. Therefore, the development of resilient and sustainable infrastructure is essential for catering the increasing needs of modern society. One important component to address the strenuous growth in urban communities is to build intelligent and smart infrastructure. The technological advancement has increased our reliance by multiple folds on the utilization of civil, mechanical, aerospace and nuclear structures. Continuous utilization of the structural services has always demanded timely and efficient maintenance systems. Past two decades are evident of innumerable accidents and mishaps due to sudden failure of structural operations and performance of the civil systems for example I-35W Mississippi River Bridge collapse USA 2007 and many more. These accidents could have been easily averted by detailed inspection and routine maintenance. The prerequisite for an efficient maintenance system and asset management is the availability of robust health monitoring framework. Under ambient environments, structures undergo aging and degradation of strength and stiffness that requires long term periodic collection and evaluation of structural responses. Also, under the catastrophic events such as earthquake loading, blast, shock, and impact loading, the structures are often subjected to the large magnitude of loads (Yim and Krauthammer, 2009, Kurata et al., 2013, Li et al., 2015). These extreme loads cause severe damage to the structures and their components that affect its overall performance. The decision-making for reinstating the

utility and safe operation of the critical infrastructure is often questionable in absence of availability of robust structural health monitoring (SHM) and damage assessment framework (Balageas et al., 2010).

Damage detection is a central focusing theme in various diagnosis and prognosis frameworks such as structural health monitoring (SHM), condition based monitoring (CBM), non-destructive testing and evaluation (NDT-E), health and usage monitoring system (HUMS), statistical process control (SPC) and diagnosis and prognosis evaluation (DPE) (Farrar et al., 2001). Structural health monitoring (SHM) is referred to a framework that deals with detection and quantification of damages using a various non-destructive technique based on structural dynamics, ultrasonic, electromagnetic, optical and radiographic methods (Farrar and Worden, 2007). The definition of damage from the perspective of vibration based "SHM" framework is the change in the structural system parameters such as mass, stiffness, and damping. These system changes could arise from initiation and evolution of crack and changes in boundary condition such as loosening of bolts or fracture of welded joints etc. (Giurgiutiu et al., 1999, Yang and Chang, 2006, Doyle et al., 2010). However, the definition of damage is not universal and is ill-defined because it depends on the spatial and temporal scale of the defect in the structural system.

The "SHM" framework includes the acquisition of sensitive responses, extraction of dominant features and quantification of damage using a statistical metric based on sensitive features. Statistical process control in conjunction with "SHM" provides an opportunity in extracting the essential damage sensitive feature that is useful not only in diagnosis but also in the prognosis of the damage (Sohn et al., 2000, Fugate et al., 2001, Catbas et al., 2008). The fundamental principles that serve as a guideline for the development of damage detection framework in "SHM" are as follows (Worden et al., 2007)

- All structural systems have inherent flaws, defects, and micro-scale cracks.
- The presence of damage is diagnosed by comparison of response from pristine state and damage state

- Sensors are only capable of response acquisition. Damage sensitive feature extraction and classification algorithms are needed to segregate and quantify the damage.
- The efficiency and robustness of the damage detecting algorithm are dictated by the spatial and temporal length scale of the damage under investigation.

Referring to the above axioms, the signal processing techniques need to be implemented for the detection and quantification of damage by extracting the damage sensitive features.

1.2 Motivation for structural health monitoring (SHM)

Health monitoring of structures under the post-earthquake scenario is one of the crucial aspects of ensuring the future safety of people and infrastructure. The decision capabilities of municipal authorities are often paralyzed due to inadequate and unreliable certified assurances of the health assessment of the structures (Bruneau and MacRae, 2017). For instance, the Tohoku earthquake in Japan, 2011 has resulted in 20,896 casualties and induced severe distress to 95,000 residential and commercial buildings (Japan Building Disaster Prevention Association, 2001). The 1994 Northridge (Los Angeles) earthquake in the USA and the 1995 Kobe earthquake in Japan has a substantial influence on the health of moment resisting steel structure (Bruneau et al., 1998). The magnitude of damage can be witnessed from the collapse of steel building during the 1995 Kobe earthquake, Japan (Figure 1.1). The structural damage to the steel moment resisting frame (MRF) buildings was significant and widespread but remain unnoticed during structural damage assessment. The beam-to-column moment connections of "MRF", prior to 1994 Northridge experience brittle fracture due to excessive stress concentration near full penetration welds of the beam. These dramatic events have triggered a paradigm shift in the design philosophy, which has led to capacity based ductile designing of the steel structure that avoids brittle failure of beam-to-column connections (Bruneau et al., 1998). The efforts towards ductile designing of steel structure have resulted in design provisions and standards in North America namely; Specifications for Structural Steel Buildings (AISC, 1999), Seismic Provisions for Structural Steel

Buildings (AISC, 2010b), and Prequalified Connections for Special and Intermediate Steel Moment Frames for Seismic Applications (AISC, 2010a). As per ASCE-7's, Design Basis Earthquake (DBE), the plastic hinge will form hierarchical at the predefined location in the steel moment resisting frame (MRF) (ASCE-7). However, under the influence of prolonging ambient vibration, the beam-to-column connection of "MRF" will undergo fatigue resulting in loosing of bolts causing the reduction in stiffness (Amezquita-Sanchez and Adeli, 2016). Additionally, under extreme loadings such as earthquake, blast and impact loading, the "MRF" connections undergo excessive magnitude of vibration (Krauthammer, 1999). These extreme vibrations can lead to catastrophic failure if the health of structure is not monitored periodically. Therefore, it is utmost important to undertake structural health monitoring techniques seriously for assessing the global health and localize the damage in the structure.

Figure 1.1 Collapse of steel building during January 17, 1995, Kobe earthquake, Japan (Elkholy S & Meguro K (2004))

1.3 Local and global damage detection

The quantitative global health assessment is needed before probing for element level damages for the structures possessing a large degree of freedom and redundant supports. Any significant change in the mass, stiffness, and energy dissipative properties will affect the vibration characteristic of the dynamic system (Doebling et al., 1996). The vibration-based

damage detection scheme may suffer serious limitations for highly damped structures possessing large degrees of freedom (Yan et al., 2007). Also, a global system identification (SI) is challenging for structures possessing closely spaced structural modes (Paultre et al., 1995). The major limitation of global SI is that the localized damages in the structures do not significantly affect the fundamental modal frequency responses (Martinez-Flores, 2005). Global SI indeed offers the knowledge of the presence of damage but fails to localize and quantify the magnitude and location of the defect.

Therefore, local damage detection is widely accepted and preferred framework for defect localization in the spatial and temporal domain. There is a paradigm shift in the "SHM" to detect the inception and incubation of the damages at the microscale (Van Den Abeele et al., 2001, Zagrai et al., 2008). The detection of the inception of microscale damage before its evolution at macroscale offers a unique opportunity to adopt remedial measures for the arresting the propagation of defect and cracks. However, in civil and mechanical infrastructure, detection and quantification of incubation of damage are often challenging due to over-exploitation of financial resources and time.

The local damage detection involves the diagnosis of damage in the spatial scale ranging from sub-micron to sub-millimeter range. Ultrasonic guided waves offer a promising technique to detect the damage of the size of a quarter of a wavelength (Kundu, 2016). The local damage detection techniques require the knowledge of the probable location of the hot spot regions. The salient characteristics of the local and global SI are summarized in Table 1.1. A "SHM" framework which coherently combines the advantages of global SI and interweaves with the philosophies of local damage detection is ideal for health monitoring of critical infrastructure (Kim et al., 2006, Park et al., 2010).

Table 1.1 Salient features of local and global system identification

Global damage detection (vibration based)	Local damage detection (ultrasonic)
➢ Changes in mass, stiffness, and energy dissipation mechanics cause changes in vibration characteristic. ➢ Lower frequency modes are insensitive to damage at the element level. ➢ Provide an overall assessment of the presence of damage. ➢ Rapid screening of damage and feasible under ambient vibration. Suited well for structure subjected to earthquake loading as the natural period is close to the excitation period.	➢ Capable of quantifying inception and incubation of damage. ➢ Localize the damage in space and time ➢ Micro-scale damage significantly affects the wave velocity, dispersion characteristics, and mode conversion. ➢ Interaction of guided wave with crack causes mode conversion and metamorphosis of waves.

1.4 Statistical damage detection in SHM

In this thesis, the efforts are focused towards extraction of geometrical and statistical damage sensitive feature in the time domain using time series analysis and change in phase space portrait. Time domain SI techniques are sensitive to local level perturbation and can localize the damage in the temporal and spatial domain. The time domain methods are mainly categorized as parametric and non-parametric approaches. The parametric approaches extract the modal parameters in the time domain using advanced signal processing techniques (Hayes, 2009). Hilbert Huang Transform (Yang et al., 2004a), Empirical Mode Decomposition (Huang et al., 1998), Wavelet Transform (Taha et al., 2006), and Singular Spectrum Analysis (Lakshmi et al., 2017), Auto-Regressive (AR) Model (Lu and Gao, 2005), Auto-Regressive Moving Average Model (ARMA) (Bodeux and Golinval, 2001) are the popular approaches to evaluate the system modal parameters from the response. Two time-series techniques which have not been well studied in literature are explored in the thesis *i.e.*

i) Change in phase space topology

ii) Clustering of time-varying autoregressive (TVAR) coefficients.

Auto-regression modeling is a widely accepted tool to model non-stationary signal using time-invariant coefficients. In "AR" modeling, the physical response is assumed to be an auto-regressive process in the sense that the current state depends on the linear combination of past observations. The model error for an "AR" process is stationary, zero-mean Gaussian white noise. Sohn et al. (2000), Bodeux and Golinval (2001), Sohn et al. (2001), Omenzetter and Brownjohn (2006), and Yao and Pakzad (2012) have proposed feature extraction algorithm based on the "AR", "AR" with exogenous input and "ARMA" for damage identification. These approaches assume linearity of the structural response and categorize the damage by alterations in the system modal parameters and novel damage index (Worden et al., 2008). This time-varying autoregressive coefficient forms the damage sensitive features defined as feature vectors. The dominant feature vectors are extracted based on the model order of the "TVAR" model. Based, on the damage sensitive features, a statistical metric needs to be explored for quantification of damage. The damage sensitive indicators ideally suited for statistical quantification of dissimilarity of the time series coefficients are explored and presented in the thesis.

As the damage is induced in any structural system, it manifests nonlinearity in the structure. This nonlinearity is generally idealized as linear for conventional "SHM" methods to work. However, for a large magnitude of damage the idealization of nonlinear system as linear lead to wrong interpretation of systems condition as conventional "SHM" methods do not work satisfactorily. The nonlinear system is the one in which any change in the input (i.e. Input loading) is not proportional to change observed in output (i.e. Dynamic response). The nonlinearity can be caused in a structural system by various factors such as loosening of structural joints, shock absorbers, base isolators, friction characteristic of joint, bearings, plastification of structural member etc. The nonlinear behavior of structure is simulated numerically with help of nonlinear models such as Bouc-Wen model, Duffing oscillator etc. (Ismail et al., 2009, Kovacic and Brennan, 2011). These models approximate the realistic

nonlinear behavior of a structural system. The majority of "SHM" procedures currently available are for linear system or linearizing the nonlinear system. Very few conclusive methods exist for damage identification of nonlinear systems. Therefore, it would be particularly helpful if "SHM" techniques developed are employed on experimental model where nonlinearity is induced due to damage. In current thesis, for nonlinear dynamical systems, the damage sensitive features (DSFs) extracted from phase space topology are superior to conventional modal features (Todd et al., 2001). The dynamic responses are correlated that are transformed into linear uncorrelated time series using orthogonal decomposition and representation in phase space portrait. Some of the popular "DSFs" that accommodate non-linearity in the structure are Phase Space Warping (PSW), Local Attractor Variance Ratio (LAVR) and Change of Phase Space Topology (CPST). PSW refers to changes in the vector field of the phase space of the damaged system and healthy system (Chelidze and Liu, 2006). Todd et al. (2001) proposed LAVR feature calculated as the variance ratio of the clusters corresponding to baseline data and damage data. Change of Phase Space Topology (CPST) is a prominent "DSFs" that identifies nonlinearity in the structure using the Euclidean distance between phase portrait of progressive damage states (Nie et al., 2012, Nie et al., 2013). The applicability of phase space methodology is demonstrated for system excited using nonstationary excitations (Nichols et al., 2003, Paul et al., 2017).

The other class of damage sensitive feature for nonlinear system are, statistical "DSFs". Statistical "DSF" is a numeric statistical parameter extracted from the acquired response that identifies the presence of damage in the system. One of the prime focus of this thesis is regarding the selection of an appropriate statistical "DSF" that can accurately segregate the damaged system from healthy one. The statistical feature selection process is based on the higher sensitivity of a statistical parameter to damage. Out of numerous statistical features few are explored in thesis such as Mahalanobis distance, Itakura distance etc. Mahalanobis distance (MD) is a multidimensional statistical measure that exploits the

statistical information of all the sensitive feature in a unified manner to quantify the distance between two clusters using covariance between the states vectors. Nair and Kiremidjian (2007) have utilized the MD to measure the extent of damage using damage sensitive clusters in the framed structure. In the multi-dimensional statistical analysis, Mahalanobis distance (MD) is referred to a measure of a distance in the scale of standard deviation between an observation and reference sample (Mahalanobis, 1936, McLachlan, 1999, De Maesschalck et al., 2000). Mahalanobis metric considers direction dependent variance and accounts for covariance between the samples. Another powerful statistical measure to quantify the similarity of the "AR" coefficients for segmented data is using Itakura distance (ID) and Cepstral distance (CD) (Zheng and Mita, 2009). The ID is a parameter that measures the distance between two datasets of the auto-regressive model and is commonly used in speech and signal processing applications. ID tests how optimally the "AR" parameter of known state signal fits the signal of the unknown state. The distance between the cluster of damage sensitive features and dissimilarity of time series coefficients are evaluated to quantify the damage and will be discussed in the thesis.

1.5 Aim and objective of the thesis

The main objectives of the thesis are to explore various statistical signal processing techniques to detect and quantify the severity of the damage in the structure. The aim is to explore relevant data reduction and feature extraction techniques to diagnose the damage. Furthermore, the focus of the thesis is the representation of the temporal response in a multidimensional space that facilities the feature extraction. The dominant features are integrated and damage state classification is performed using supervised learning and clustering techniques. Based on the cluster, the damage is evaluated using statistical distance indicators that determines the proximity of two temporal signals.

In order to overcome some of the gap areas in literature, the specific objectives of the current study are listed below:

- Development of "SHM" techniques to detect damage in a dynamical system induced due to extreme loadings such as blast, shock, and earthquake.
- Application of statistical process control technique based on the principal component analysis (PCA) and independent component analysis (ICA) to detect minor structural damage by extracting principal features using Eigen analysis.
- Exploring the dissimilarity of phase space topology of dynamic response towards nonlinear structural damage detection.
- Damage identification, classification, and quantification in the structural system by exploring time-varying features obtained via time series analysis (a pseudo real-time approach) that can be extended to be a complete online "SHM" approach.
- Development of damage sensitive features based on Euclidian distance (geometrical), Mahalanobis distance (statistical) and Itakura distance (autoregressive model) to quantify the initiation and evolution of damage.

The structural health monitoring approach proposed in current work is explained by general steps presented in Figure 1.2 and also mentioned below:

Step-1: Experimental model

In this step the experimental investigation of structure is carried out for an extreme loading. The damage is manifested in the structure either manually or structure is allowed to damage due to application of extreme loading.

Step-2: Data acquisition

The dynamic acceleration response or displacement response for healthy as well as damage state is acquired in this step. The raw data acquired is used further for analysis.

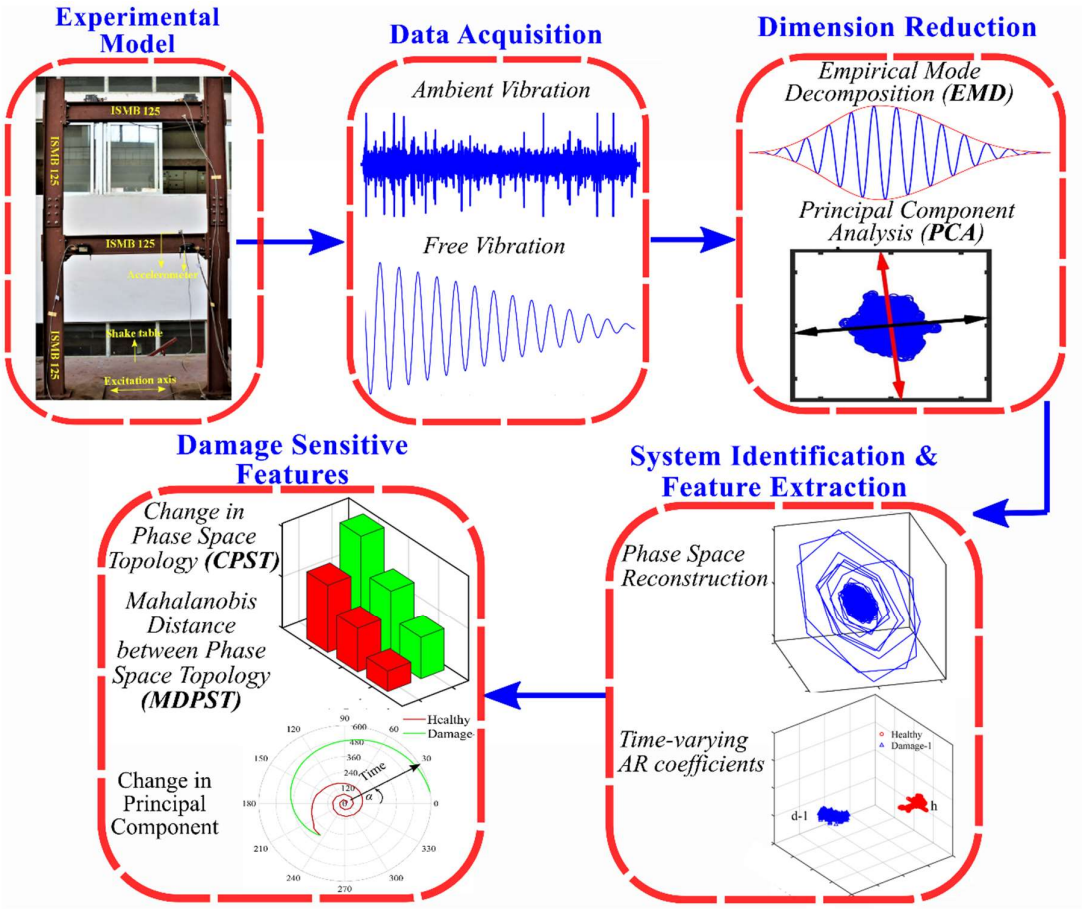

Figure 1.2 General steps of a structural health monitoring approach

Step-3: Dimension reduction

For a particular case where number of degrees are more, the data set acquire will be of high dimension. Hence in order to reduce the computation time the dimension reduction of acquired data set is carried out with help of techniques such as "PCA".

Step-4: System identification and feature extraction

In this step the reduced dimension data is processed by signal processing techniques to get the damage sensitive features.

Step-5: Damage sensitive features (DSF)

The variation of "DSF" for healthy and damage state can be tracked to identify the occurrence of damage. The relative change in the "DSF" corresponding to healthy and damage state quantifies the magnitude of damage.

1.6 Organization of the thesis

The studies reported in this thesis for fulfilling the objectives mentioned above are presented in seven chapters. An introduction and objectives of the presented work are concisely presented in Chapter-1.

Chapter 2 presents the literature review of the vibration based health monitoring domains involved in the current study. The entire literature review is carried out in five sub-categories as (i) Natural frequency-based methods, (ii) Mode-shape based methods, (iii) Changes in Mode-shape curvature or strain energy, (iv) Methods based on other modal parameters (Damping, Flexibility etc.), and (v) Time-domain based methods.

The chapter-3 discusses a novel technique based on the single input and multiple outputs to detect and quantify the progressive damage of shear building subjected to repetitive base excitation. Three output accelerations are acquired at three floors of the shear building. Damage detection algorithms based on Empirical Mode Decomposition (EMD) and Principal Component Analysis (PCA) are implemented to quantify the evolution of damage in the shear building. The evolution of the progressive damage was quantified using proposed condition indicator (CI) based on normalized Euclidean norm of the change in principal angles, corresponding to pristine and damage state. CI indicator provides a robust and accurate metric for detection and quantification of progressive damage.

The chapter-4 discusses a phase space based damage detection technique that is able to detect damages in a shear building subjected to shock loading. The two-phase novel damage detection algorithm proposed is explained in chapter-2, the proposed algorithm quantifies and segregates perturbative damage from microscale damage. The first phase performs dimension reduction and damage state segregation using principal component analysis. In the second phase, the embedding dimension is reduced through Empirical Mode Decomposition and the embedding parameters are evaluated. With the help of embedding parameters, the response is represented in a multi-dimensional phase space trajectory (PST). The dissimilarity in the multi-dimensional "PST" is used to derive the damage sensitive features (DSFs). The "DSFs"

namely: (i) Change in phase space topology (CPST) and (ii) Mahalanobis distance between phase space topology (MDPST) are evaluated to quantify progressive damage states.

The chapter-5 discusses the time-varying autoregressive (TVAR) model integrated with a K-means -- clustering technique to detect damage in the steel moment resisting frame. The proposed technique identifies and quantifies the damage in the beam-to-column connection and column-to-column splice plate connection caused due to loosening of the connecting bolts. The algorithm models the non-stationary acceleration response of the frame subjected to white noise and evaluates the "TVAR" coefficients (TVARC). These coefficients are represented as a cluster in the "TVARC" subspace and segregated and classified using K means -- segmentation technique. Eigenstructure evaluation of the segregated "TVARC" cluster is performed to detect temporal damage. The damage in the steel frame is quantified using Mahalanobis distance (MD) and Itakura distance (ID) serving as the statistical distance between the healthy and damage "TVARC" clusters.

Chapter 6 presents a novel damage detection algorithm based on the amalgamation of Independent component analysis (ICA) and Phase space reconstruction (PST). An experimental investigation is conducted by inducing damage in steel moment resisting frame (SMRF) and exciting it with ambient white noise base excitation. The algorithm consists of two segments; in the first segment, the modal responses are obtained from the acquired response with the help of Independent component analysis (ICA). The optimal embedding parameters for modal responses are evaluated with the help of average mutual information function (AMIF) and Singular System Analysis (SSA). The second segment deals with the reconstruction of "PST" with the help of modal responses and embedding parameters. Lastly, the damage sensitive features (DSFs) are evaluated to identify and quantify the induced damage. In the end, Chapter 7 summarizes and concludes the major findings of this thesis and also provides the recommendations for future research work.

Chapter 2

Literature review

The conventional health monitoring techniques are mainly characterized as vibration-based damage detection techniques. The vibration-based methods (VBM) work on the principle that change in vibration characteristics of the structure can be directly correlated to damage. This is because the damage/fault in any structure due to change in stiffness or mass will eventually cause changes in frequency response in spectral domain. The change in mass or stiffness matrix will alter the dynamic characteristics such as natural frequency, damping, and mode-shape. Therefore, the quantification of damage can be predicted by quantifying the change in dynamic characteristics of a damaged system with respect to the reference system.

An extensive review of various vibration based methods for damage identification is presented in Sohn et al. (2003) and Doebling et al. (1996). The presented literature review is organized by classification based on "SHM" methods categorized as mentioned below and also presented in Figure 2.1, 2.2 and 2.3.

Vibration based methods

- Natural frequency-based methods
- Mode-shape based methods
- Changes in Mode-shape curvature or strain energy
- Methods based on other modal parameters (Damping, Flexibility, etc.)

Time-domain based methods

- Wavelet decomposition
- Empirical mode decomposition
- Principal component analysis
- Independent component analysis
- Time-varying autoregressive
- Phase space based methods

❖ Recursive/online methods

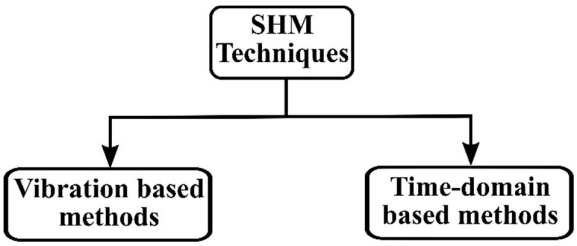

Figure 2.1 Classification of structural health monitoring techniques

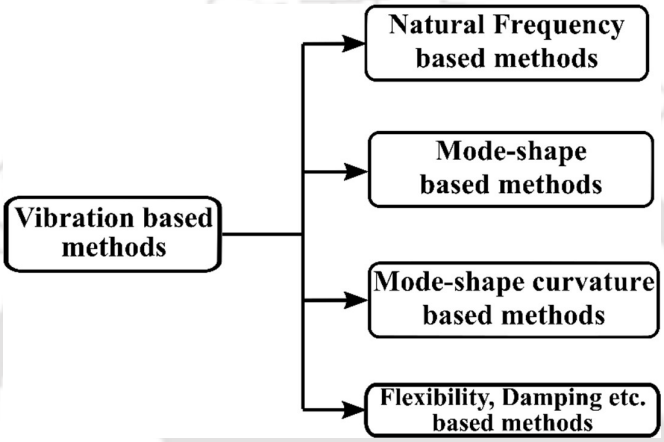

Figure 2.2 Classification of vibration based methods

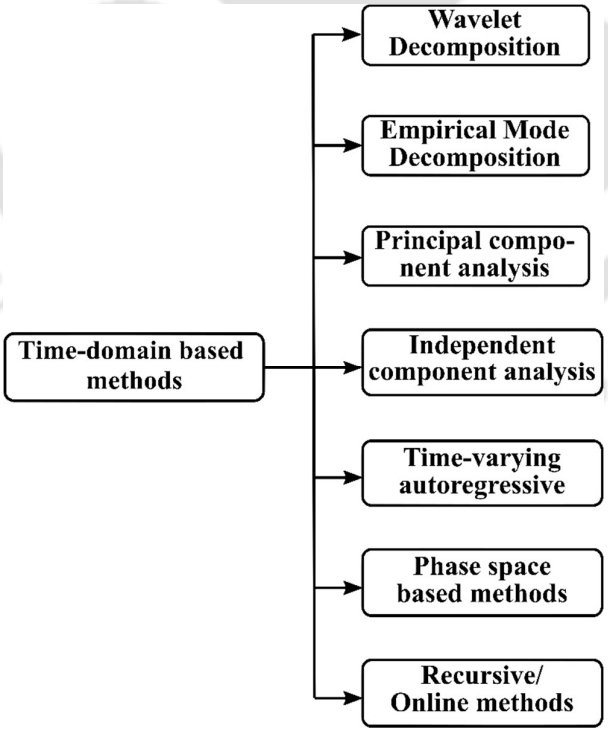

Figure 2.3 Classification time-domain based methods

2.1 Natural frequency-based methods

Natural frequency-based methods quantify the damage with the help of a damage sensitive feature based on changes in the natural frequency of the structure. The advantage of the natural frequency-based method is its moderate accuracy and ease of measurement. Natural frequency-based methods are generally categorized as forward and inverse problem. The former one deals with evaluation of variations in frequency based on severity of damage and location. Whereas, the latter one deals with evaluation of damage location, size, and severity based on frequency measurements. However, to precisely detect and quantify the damage induced in any structure, the measurement of natural frequency is insufficient. Moreover, this method is not so reliable to be used as a damage detection approach, because the natural frequency is less sensitive to initial damages in a structure. If the methods based on frequency are used for practical application, then these can only assure existence of large damage. A brief review of research works carried out based on these methods is discussed.

Penny et al. (1993) presented a procedure to identify the location and size of crack in a one-dimensional beam structure with the help of measurements of natural frequency. The entire procedure proposed in this work is based on non-destructive testing (NDT). The proposed method considers the changes in natural frequency numerically that would occur mostly for all the cases of damage under consideration. Thereafter using the least-square technique, the measured frequencies are fitted to the frequencies obtained numerically for different damage scenarios. In the last stage, the true case of damage is the one for which the goodness of fit is maximal or for which the error of fit is minimal.

Lee and Chung (2000) discussed a nondestructive identification procedure for detecting size of crack and its precise location for a one-dimensional beam in a two-step procedure. The first step is to evaluate first four natural frequencies of a damaged/cracked structure with help of a developed finite element model (FEM). Now, the frequencies evaluated in first step is utilized by Armon's Rank-ordering method to get the approximate location of crack. The second step deals with development of a FEM model with help of the results of approximate

crack location obtained in first step. Lastly, the exact location of crack can be identified by Gudmundson's equation that utilizes the evaluated crack size. Lee and Chung applied above procedure to the cracked beam and the maximum error regarding exact size of crack were estimated to be 25%.

Patil and Maiti (2003) proposed a frequency shift-based method to detect multiple open cracks in a Euler-Bernoulli beam with different boundary conditions. The method was based on transfer matrix method where the cracks were represented by a rotational spring. To estimate the damage locally, the beam was divided into a number of parts and for each part, a damage parameter was evaluated. The damage parameters proposed here were determined with the help of information regarding changes in the natural frequencies. After obtaining the results for each part, these parts were studied individually to exactly pinpoint the location of crack in a particular part.

Zhong et al. (2008) presented a new approach that is based on auxiliary mass spatial probing, the mass probing was done with the help of the spectral center correction method (SCCM). In this approach, just by using the output time history of structure a simple damage detection solution was proposed. To identify the crack with help of SCCM, a highly accurate auxiliary mass location versus natural frequency curve was plotted along with curves of its derivative up to third order. However, the SCCM method was illustrated only with the help of FE model, no experimental investigation was carried out. In the experimental investigation, it is very difficult to get a high-resolution auxiliary mass location versus natural frequency curve. The same difficulty also arises for FE simulation, therefore the practicality and applicability of the method in situ testing or laboratory testing are questionable.

2.2 Mode shape based methods

"VBMs" based on mode-shape are more advantageous than natural frequency-based methods. This is because; 1) local information of any structure is contained in mode-shape, therefore these methods are also sensitive to localize the damage, 2) The sensitivity of mode-shape for the effects of environment is very less compared to natural frequencies (Farrar and

James III, 1997). In spite of many advantages of mode shape over natural frequency, they have several limitations in its application (Hua, 2006), i.e. (i) mode-shape based methods require a very high sampling measurement for precise estimation of the information regarding mode shapes and its curvature, (ii) these methods have larger statistical variation, (iii) For the structures with complex geometry or material property, the mode shape based methods, especially the methods based on the curvature of mode shape are very inaccurate and incapable of accurate estimation, and (iv) the information regarding a particular mode-shape that will undergo significant changes due to a particular type of damage is unknown.

In the past three decades, based on indirect or direct use of mode shapes several damage detection methodologies have been developed. These methods are generally classified into two categories. One of them being the traditional mode shape change methods. With help of experimental tests and FEM analysis, these methods establish a relationship between change in mode shape and damage. The second category being a relatively new damage detection method that utilizes a signal processing technique for damage detection. These modern methods use signal processing technique to identify the location of damage by detecting the local discontinuity of curvature of mode shape due to damage.

Ko et al. (1994) provided a method to identify and locate the damage in steel frame structures. The method proposed here utilizes a combination of Coordinate Modal Assurance Criterion (COMAC), Modal Assurance Criterion(MAC), and the sensitivity analysis. The sensitivities of the numerically or analytically obtained mode shapes to a particular type of damage are calculated to determine which degree of freedom are most related and is damaged. The "MAC" number used in this study gives information about the correlation between the n^{th} mode of damaged model vector $\{\phi\}_D$ and m^{th} mode of undamaged modal vector $\{\phi\}_U$ and is defined as:

$$\mathrm{MAC} = \frac{\left|\{\phi_U\}_m^T \{\phi_D\}_n\right|^2}{\{\phi_U\}_m^T \{\phi_U\}_m \{\phi_D\}_n^T \{\phi_D\}_n} \tag{2.1}$$

When all the "MAC" number values are arranged in matrix form the diagonal entries of the matrix should be greater than the rest of entries for the structure to be intact. "COMAC" is a modified form of "MAC" number such that the correlation is related to the coordinate of the modal vector instead of the mode number. As a result, when "COMAC" is applied to particular sets of modal vectors of a structure, it can indicate at which point the two sets of modal vectors are much different from one another and thus localizing the damage. "COMAC" is formulated as:

$$COMAC = \frac{\left(\sum_{L=1}^{L_{\max}} \left|(\phi_{i,L}^{U}).(\phi_{i,L}^{D})\right|\right)^2}{\sum_{L=1}^{L_{\max}} (\phi_{i,L}^{U})^2 \sum_{L=1}^{L_{\max}} (\phi_{i,L}^{D})^2} \tag{2.2}$$

where i is the number of degree of freedoms in the modal vector, $L_{\max}$ is the highest correlated mode pair number and L is the incremental counter.

Hadjileontiadis et al. (2005) proposed a response-based damage detection algorithm for beams and plates. For beam-type structures, the Fractal Dimension (FD) of a mode-shape curve is evaluated by:

$$FD = \frac{\log_{10}(n)}{\log_{10}(d/L) + \log_{10}(n)} \tag{2.3}$$

Where,

'n' is the number of steps in the curve.

'd' is the distance between the first point (P_1) the ith point of the sequence P_i.

'L' is the total length of the curve or the sum of distances between successive points.

$$d = \max dist(P_1, P_i) \tag{2.4}$$

$$L = \sum_{i}^{n-1} dist(P_i, P_{i+1}) \tag{2.5}$$

The damage features are evaluated by implementing a sliding window of length M across the mode shape and FD is estimated at each position inside the window for the regional mode

shape. Damage size and location are determined by a peak on the FD curve that indicates local irregularity introduced by the damage to fundamental mode shape.

Pawar et al. (2007) studied the effect of damage on beams using Fourier analysis of mode shapes. The FEM was developed to obtain the mode shapes of a damaged beam, the evaluate mode shapes were expanded using a spatial Fourier analysis. It was observed that the Fourier coefficients of mode shapes are sensitive to damage, therefore the vector form of Fourier coefficients was considered as damage index. Artificial neural network (ANN) was trained to detect the size and location of damage using input as Fourier coefficients. Damage identification using neural networks and Fourier coefficients has the capability to detect the size and location of damage precisely and this is proved by numerical studies. However, the drawback of this method is that its use is limited to beams with clamped-clamped boundary conditions.

2.3 Mode Shape curvature/strain energy change

Many researchers have mentioned that the mode shape based methods are not much sensitive to minor initial damages, even if the data is acquired at a high sampling rate (Huth et al., 2005). Instead of using the information regarding mode shape, the information regarding mode shape curvature (MSC) will increase the sensitivity of damage detection methods. The changes in MSC are more with the reduction in stiffness value or with the progressive damage. Therefore, the magnitude of change in MSC is used as a damage feature in MSC based methods. Several peaks were observed in MSC change for higher modes, this the main drawback of this method as pointed out by Wahab and De Roeck (1999). These peaks are not only at location of damaged but also at other locations, which concludes false damage detection. These methods are only suitable for continuous structure and not discrete structure; this is the other drawback. Hence to get rid of false damage detection only lower mode shape curvature can be used.

Pandey et al. (1991) assumed that the effect on damage on any structure is only reflected in its stiffness matrix and not the mass matrix. They expressed the undamaged condition as the eigenvalue problem formulated as:

$$\left([\mathbf{K}]-\lambda_i[\mathbf{M}]\right)\{\phi_i\}=\{0\} \tag{2.6}$$

Where [**M**] and [**K**] are mass and stiffness matrix respectively, $\boldsymbol{\lambda}_i$ and ϕ_i are i^{th} Eigenvalue and Eigenvector. Similarly, the eigenvalue problem for the damaged structure is formulated as:

$$\left([\mathbf{K}^*]-\boldsymbol{\lambda}_i^*[\mathbf{M}]\right)\{\phi_i^*\}=\{0\} \tag{2.7}$$

where an asterisk (*) sign indicated the structural property for damaged structure. Here, the pre and post damage structural properties are the basis for damage detection. In this study, mode shape curvature for the beam corresponding to the intact and damaged condition was evaluated numerically. For a particular case of damaged and intact mode shapes, consider a beam cross-section is subjected to a bending moment $M(a)$ at location '$_a$' and its curvature is given by:

$$v^{"}=\frac{M(a)}{EI} \tag{2.8}$$

Where, E is the modulus of elasticity, $I$the moment of area of the section.

Hence, for a given applied moment $M(a)$ to the pristine and damaged structure, an increase in curvature is associated with a reduction of stiffness. Also, the magnitude of change in curvature of mode shape was correlated with the severity of damage in a continuous beam.

Shi et al. (2000), presented an approach based on the change in modal strain energy (MSE) between pristine and damaged structure. The elemental "MSE" is defined as the product of the second power of the mode shape component and the elemental stiffness matrix. The "MSE" after and before the occurrence of damage is mathematically represented as:

$$\begin{aligned} MSE_{ij} &= \{\phi_i^T\}[\mathbf{K}_j]\{\phi_i\} \\ MSE_{ij}^d &= \{\phi_i^d\}^T[\mathbf{K}]_j\{\phi_i^d\} \end{aligned} \tag{2.9}$$

Where MSE_{ij} and MSE_{ij}^{d} are healthy and damaged "MSE" of j^{th} element for i^{th} mode shape. As the exact estimation of stiffness matrix for damaged structure is difficult or was nearly impossible, therefore they considered modal strain energy change ratio (MSECR) to identify the location of damage.

$$MSECR = \frac{\left| MSE_{ij}^{d} - MSE_{ij} \right|}{MSE_{ij}} \tag{2.10}$$

The approach proposed by them was illustrated by using an experimental and numerical study of a two-storey portal steel frame. The results of the study indicated that the proposed method is highly accurate in identifying the location of damage. One of the limitations of proposed method is its sensitivity to noise.

Dutta and Talukdar (2004) were able to detect and locate a multiple numbers of damages in a simply supported bridge structure. For this purpose, they investigated the changes in curvature of mode shape. A finite element model of the bridge deck was developed, where they considered Standard Ahmed Shell elements and noticed the higher peaks in modal curvature changes at location of damage. The study was also able to detect the damage along the beam in transverse and longitudinal directions. They also showed that modal curvature corresponding to higher modes is less accurate than the lower modes.

2.4 Methods based on other modal parameters (damping, flexibility etc.)

The damping properties have not been utilized much as compared to both, the mode shape and the natural frequencies based methods for damage detection. The crack in a structure develops a nonlinearity and dissipative effects, these are very difficult to detect with help of mode shape and natural frequency. Whereas, these changes can be detected easily with the help of damping. This is one of the major advantages of damping based methods. The dynamically measured flexibility matrix is another classification of damage detection methods. The effect of both, natural frequency and mode shape are included in modal flexibility matrix. It is defined as a combination of participation from all mode shapes and its corresponding natural frequency.

Pandey and Biswas (1994) used damage detection methods based on the flexibility matrix measured dynamically, to evaluate changes in the behavior of structure statically. This is because the inverse of static stiffness matrix is referred to as flexibility matrix. The flexibility matrix is obtained from applied static force '*f*' and the resulting displacement of structure '*u*' with help of the following relation:

$$\{u\} = [\mathbf{F}]\{f\} \tag{2.11}$$

The expression of the flexibility matrix is written as:

$$[\mathbf{F}] = [\mathbf{\Phi}][\mathbf{\Omega}]^{-1}[\mathbf{\Phi}]^{T} = \sum_{i=1}^{n} \frac{1}{\boldsymbol{\omega}_i^2}\{\phi_i\}\{\phi_i\}^{T} \tag{2.12}$$

Where, $[\mathbf{\Phi}] = \left[\{\phi_1\}\{\phi_2\}.....\{\phi_n\}\right]$ is mode shape matrix, $\{\phi_i\}$ being the i-th mode shape. The diagonal matrix of rigidity $[\mathbf{\Omega}]$ corresponds to ω_i^2 where ω_i is the i-th natural frequency. Thus each column of flexibility matrix $\left[\mathbf{F}^*\right]$ represents the displacement pattern of the structure associated with a unit force applied at the associated degree of freedom. Measuring the flexibility matrices before and after damage, the variation matrix $[\mathbf{\Delta}]$ can be obtained as:

$$[\mathbf{\Delta}] = \left[\mathbf{F}^*\right] - [\mathbf{F}] \tag{2.13}$$

Where $[\mathbf{F}]$ and $\left[\mathbf{F}^*\right]$ are, respectively, flexibility matrices before and after damage.

Now, for each column of the matrix $[\mathbf{\Delta}]$, let $\boldsymbol{\delta}_\mathbf{j}$ be the absolute maximum value of the elements in the j-th column.

$$\boldsymbol{\delta}_j = \max\left|\delta_{ij}\right| \quad \text{i=1,2,....n} \tag{2.14}$$

where δ_{ij} are elements of the matrix $[\mathbf{\Delta}]$ and represent the flexibility changes in each degree of freedom. Corresponding to largest δ_{ij} the column of the flexibility matrix indicates the degree of freedom where the variation in flexibility is maximum or the location of damage. This method was applied to an actual spliced beam where the damage was linear in nature and also applied to several numerical examples. Results of the experimental and numerical

examples showed that identification and estimation of the damage condition and the damage location could be obtained with the help of only first two modes of the structure measured.

Panteliou et al. (2001) stated that when a structure is subjected to an extreme event, there are large instabilities of temperature throughout the volume of its material. These fluctuations are experienced in a structural material because of the thermo-elastic effect. This results in irreversible conduction of heat and randomness in the material, which in turn causes thermodynamic damping. An analytical study investigated the entropy and temperature instabilities for a vibration cycle resulting in changes of damping factor. They also showed that the factor of damping is directly proportional to the increase in depth of the crack. It was also found that the damage detection methods based on damping factor have the advantage that, it is very less sensitive to the boundary conditions in comparison with the natural frequencies.

Salehi et al. (2011) develop a method to localize damage, the proposed method is based on changes in flexibility shapes as well as its curvature. Differential Quadrature Method (DQM) has been implemented to obtain the curvatures of flexibility shape. Uniform beam structures were used as test-setup to implement the method successfully. The method was validated experimentally and numerically. They showed that the results in both cases are satisfactory and could be used for damage detection of real-life structures.

Yamaguchi et al. (2013) proposed a novel method based on the identification of changes in modal damping of concrete and steel bridges. They illustrated that the energy-based damping analysis can be a powerful tool for the detection of damage of bridges in the vibration-based "SHM". They also found that against corrosion-induced damage in the reinforced concrete beams the modal damping is a very sensitive indicator. Even at very minor damage level without any visible crack, it was possible to identify damage with help of damping measurements, indicating that the local corrosion level might be identifiable by measuring the ratio of modal damping of reinforced concrete structure.

The entire summary of literature review on vibration based methods is mentioned in

Table *2.1*

Table 2.1 Summary of literature review on vibration based methods

Technique	Reference	Methodology	Validation	Conclusion/Results
Natural frequency based methods	Penny et al. (1993)	Non-destructive testing	Numerical	Identified the location and size of crack
	Lee and Chung (2000)	Armon's rank-ordering method	Numerical and Experimental	Maximum error of determining crack size was 25%
	Patil and Maiti (2003)	Transfer matrix method	Numerical	Pinpoint location of crack were determined
	Zhong et al. (2008)	Spectral center correction method	Numerical	Auxiliary mass location versus frequency curve was plotted to identify damage
Mode shape based methods	Ko et al. (1994)	Coordinate modal assurance criterion and modal assurance criterion	Experimental	Determined which degree of freedom is damaged
	Hadjileontiadis et al. (2005)	Fractal dimension based crack detection	Numerical and analytical	Damage was determined by peak on the FD curve
	Pawar et al. (2007)	Artificial neural network	Numerical	Damage was identified using Fourier coefficients

(Contd.)

Technique	Reference	Methodology	Validation	Conclusion/Results
Mode shape curvature based methods	Pandey et al. (1991)	Change in mode shape curvature (CMSC)	Numerical	Severity of damage was correlated with CMSC
	Shi et al. (2000)	Modal strain energy	Numerical and Experimental	Proposed method is sensitive to noise
	Dutta and Talukdar (2004)	Absolute difference in mode shape curvature (ADMC)	Numerical	Can detect the damage in transverse and longitudinal directions
Damping and flexibility based methods	Pandey and Biswas (1994)	Based on variation in flexibility matrix	Numerical and Experimental	Damage could be identified with the help of first two modes only
	Panteliou et al. (2001)	Based on changes in damping ratio	Numerical	Less sensitive to the boundary conditions
	Salehi et al. (2011)	Differential quadrature method	Numerical and Experimental	Method was success-fully implemented on beam structures
	Yamaguchi et al. (2013)	Based on changes in damping	Experimental	Identified the corrosion induced damage

Limitations of modal parameters based methods:

- In field applications, the results of modal-based methods are severely affected by factors such as the presence of unwanted noise in the acquired data, less number of sensors, environmental changes such as temperature, humidity, etc. and operational influences. For example, the change in natural frequency due to damage can be

countered by the change in frequency due to temperature changes in the field, thus failing to detect the damage.

- Most of the modal methods mentioned above make use of mathematical or FE model to derive a relation between dynamic changes and damage induced in a system. The FE model requires an extensive computational cost causing a serious delay in the final outcome of health monitoring approaches.
- The modal based methods are dependent on the data from the reference or baseline state. These methods compare the data from the recent state of the structure against the baseline state to quantify the damage. Therefore, these methods cannot be applicable to the systems where baseline data or any past data is not available.
- The sensitivity of modal parameters to minor damage is very less, therefore the identification of such small magnitude of damage is a key challenge for modal based "SHM" approaches. Also, these methods show a lower sensitivity to local level damages and fail to identify any damage at the elemental level.
- The dynamic characteristic of any damaged system is nonlinear, whereas modal based methods idealize the response behavior to be linear. Therefore, in the case of nonlinear behavior of any system, these techniques are not reliable.

2.5 Time-domain based methods

In the last two decades, the time-domain based methods have evolved enormously as a structural health monitoring approach. These methods directly analyze the raw time history data of the dynamical system and are independent of modal information. The main reason for the popularity of these methods is that with recent advancements in technology, for any structure the raw data can be easily acquired with the help of various sensors. The time-domain approaches identify the damage by minimizing the error between acquired response and numerically obtained response or by comparing the dynamic characteristics of the damaged system with reference system (Lee et al., 2005, Sakellariou and Fassois, 2006). The main benefit of these methods is that they can identify damage at both global and local level

(Banks et al., 1996, Zou et al., 2000). The literature review of this thesis classify the time domain methods broadly in four categories as follows:

- ❖ Time series analysis and signal decomposition based methods
- ❖ Methods based on blind source separation
- ❖ Phase space-based methods
- ❖ Recursive methods for online "SHM"

2.5.1 Time series analysis and signal decomposition based methods

a) Time series analysis

Time series analysis is one of the most common methodologies to extract the sensitive damage features from dynamic response of a structural system. The commonly used time series based methods are Auto-regressive (AR) (Lu and Gao, 2005), extended Kalman filter (EKF) (Yang et al., 2006b), auto-regressive model with exogenous input (ARX) (Adams and Farrar, 2002), the particle filter (PF) (Namdeo and Manohar, 2007), auto-regressive moving average (ARMA) (Grenier, 1983), unscented Kalman filter (UKF) (Al-Hussein and Haldar, 2015), and the least square estimation (LSE) (Yang et al., 2006a). These methods have gained significant attention because of the ease in implementation and development of "SHM" framework, unlike modal based methods. Almost every method in this category aims to model a unique time series model to the dynamic response of a system and later extract damage sensitive features from these models (Mosavi et al., 2012, Yao and Pakzad, 2012). However, when nonstationary exists in dynamic response, traditional vibration based methods suffer. The cause of nonstationary sources can arise either due to the nonstationary input loading such as earthquakes/transient excitations or due to nonlinear behavior of system. For a particular time-series function of a random process, if the mean of signal is constant over time it is known as first order stationary time series and if the standard deviation is constant over time it is referred to as second order stationary.

Now, consider the multiple time series of a random process as shown in Figure 2.4. The strictly stationary time series is the one that possesses an identical probabilistic/statistical

characteristic for a set of values and its corresponding time shifted set, mathematically this can be represented as:

$$P\left\{X_{(t_0,\zeta_0)} \le c_1,....,X_{(t_0,\zeta_n)} \le c_k\right\} = P\left\{X_{(t_1,\zeta_0)} \le c_1,....,X_{(t_1,\zeta_n)} \le c_k\right\} \tag{2.15}$$

where, $X_{(t_0,\zeta_0)}$ and $X_{(t_1,\zeta_0)}$ are set of values corresponding to time series at time step t_0 and a shifted time $t_{0+h}=t_1$, $P\{X_{(t,\zeta)}\}=c_k$ is the probabilistic/statistical property corresponding to any time step t as shown in Figure 2.4 (Shumway and Stoffer, 2017).

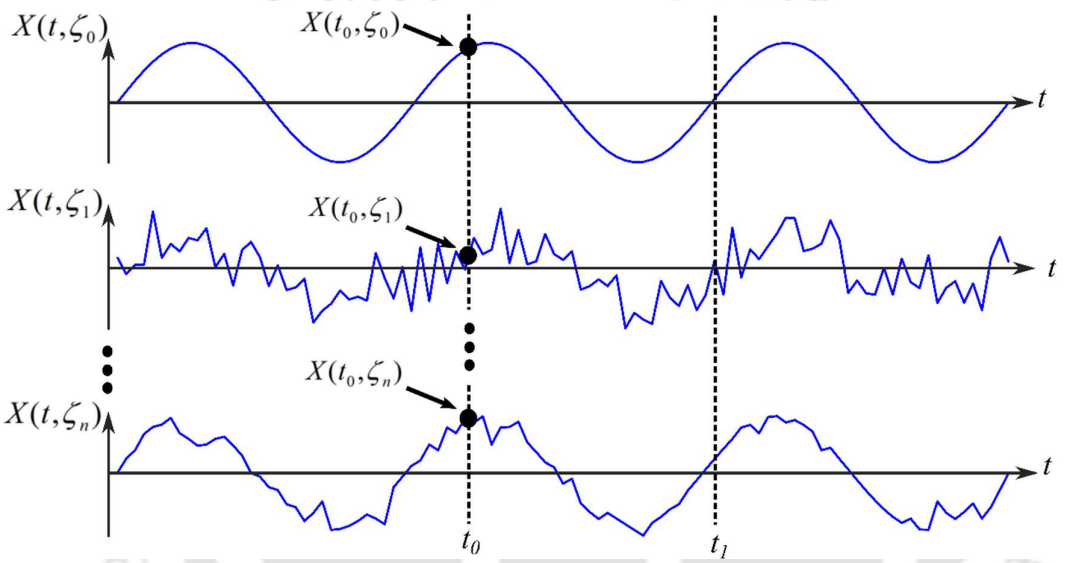

Figure 2.4 Set of time series function corresponding to a random process $X_{(t,\zeta)}$

Since the statistical and probabilistic characteristic of signal are constant over time for a stationary signal it is easier to draw valuable information from these signal. But, same is not the case for nonstationary signal, therefore it is difficult to process a nonstationary response of a damage system and detect damage. Some of the time series based methods do not use damage sensitive features, instead these methods compare the fitted model of test data with a model of training/reference data by evaluating the residual error between them (Adams and Farrar, 2002). Numerous researches proposed different form of time series models to develop a robust "SHM" framework. Some of the examples of these different form of time series approaches is briefly explained below.

Wang and Haldar (1997) proposed a novel time domain technique to identify the system's damping and stiffness parameters for each element. The important advantage of the proposed approach was: (i) no requirement of any information about input forces, and (ii) the response at all the degrees of freedoms is not necessary. The proposed approach is a unique combination of extended Kalman filter method with a weighted global iteration (KF-WGI) and an iterative least-squares procedure with unknown input excitations (ILS-UI). The presence of noise in acquired response is considered and the effect of noise on the accuracy of algorithm is analyzed. The efficacy of the proposed algorithm is tested and illustrated by a numerical example. The algorithm ILS-EKF-UI uses least information about the structure under investigation, therefore it requires longer measurements. To improve the efficiency and computation time, it was suggested to use shorter measurements for ILS-UI and longer measurements for KF-WGI. The accuracy of the proposed approach to identify system parameters would not be affected by considering different length measurements for ILS-UI and KF-WGI.

Sohn and Farrar (2001) proposed a novel damage localization technique based on "AR" and auto-regressive with exogenous inputs (ARX) time series modeling approaches. The input for the proposed approach is only the acceleration response of the structure under investigation. The approach developed here combined "AR" and "ARX" to formulate a two-stage prediction model. In proposed approach, the damage feature evaluated is based on residual error between measured and predicted time series model.

For a time series $x(t)$ corresponding to reference state, an AR model of order p can be formulated as:

$$x(t) = \sum_{j=1}^{p} \phi_{xj} x(t-j) + e_x(t) \tag{2.16}$$

In the same way, the AR model for all signals of reference and damage state was formed. The model order (p) for this work was select as 30, this was decided with help of a partial auto-

correlation method described by (Box et al., 1994) . The AR model for a damaged/unknown state was formulated as:

$$y(t) = \sum_{j=1}^{p} \phi_{yj} y(t-j) + e_y(t) \tag{2.17}$$

The "DSF" in the first stage of the proposed approach is formed by minimizing the difference between the AR model of reference state and damaged/unknown state.

$$\text{Difference} = \sum_{j=1}^{p} (\phi_{xj} - \phi_{yj})^2 \tag{2.18}$$

If the unknown state data does not possess damage, the value of difference will be zero, any value greater than zero depicts damage. Now in the second stage of the two-step prediction model, it was assumed that the error term in "AR" model is caused due to an unknown input loading. Based on this assumption, the "ARX" model was used to reconstruct the relation between output, input and the error term.

$$x(t) = \sum_{i=1}^{a} \alpha_i x(t-i) + \sum_{i=1}^{b} \beta_j e_x(t-j) + \varepsilon_x(t) \tag{2.19}$$

Where $\varepsilon_x(t)$ is the residual error of ARX(a,b) model fitted to $e_x(t)$ and $x(t)$ pair. The damage feature proposed from "ARX" model was based on the term $\varepsilon_x(t)$. Both the "DSF" were able to identify the occurrence of damage as its value increases. Further, the increase in "DSF" when maximized for sensors at each location can estimate the location of damage. The proposed damage localization approach is demonstrated for an eight degrees-of-freedom spring-mass system.

Nair et al. (2006) modeled the dynamic response obtained from a sensor with the help of autoregressive moving average (ARMA), a time series modeling approach. Based on the "AR" coefficients obtained by "ARMA", a novel "DSF" to identify the occurrence of damage is formulated considering the first three coefficients only.

Let $x_i(t)$ be the acceleration response from sensor *i*. The response data is then segmented into distinct streams $x_{ij}(t)$, where *i* represents the sensor location and *j* represents the j^{th} segment of data The formulation of an "ARMA" model used in this work is described below:

$$x_{ij}(t) = \sum_{k=1}^{p} \alpha_k x_{ij}(t-k) + \sum_{k=1}^{q} \beta_k e_{ij}(t-k) + \varepsilon_{ij}(t) \tag{2.20}$$

where $x_{ij}(t)$ is the normalized response signal, α_k and β_k are the k^{th} autoregressive (AR) and moving average (MA) coefficient respectively, $\varepsilon_{ij}(t)$ is the residual error term and the model order of "AR" and "MA" process are represented by *p* and *q* respectively. To localize the damage, two indices LI_1 and LI_2 are proposed as a function of the distance between clouds of "AR" coefficients and distance of clouds from the origin. For the response of sensor at the location of damage, the numerical estimate of LI_1 and LI_2 was observed to be higher with respect to undamaged response.

$$\mathrm{LI}_1 = \frac{d_{mean}}{d_{undam\ \ cloud}} \tag{2.21}$$

$$\mathrm{LI}_2 = \frac{d_{dam\ \ cloud}}{d_{undam\ \ cloud}} \tag{2.22}$$

Where $d_{undam\ \ cloud}$ is distance between origin and undamaged cloud, d_{mean} is distance between mean of undamaged and damaged clouds and $d_{dam\ \ cloud}$ is distance of damage cloud mean point from origin. The proposed damage identification and localization algorithm was validated for the linear system and for stationary response signals. The accuracy of proposed methodology was tested for experimental and analytical response data of ASCE benchmark model. The results obtained concluded that the proposed method was able to detect and localize damage accurately for the benchmark model.

Yang et al. (2006b) presented an adaptive technique based on the extended Kalman filter (EKF) approach. The proposed technique tracks the variations in the structure parameters to

identify the damage induced in structure. To quantify the damage this technique evaluates the relative changes of system parameters of damaged structure with respect to reference structure. A special criterion is proposed to evaluate an optimal solution to track the variation of structural parameters by means of constrained optimization procedures. The effectiveness of proposed method was proved by implementing it for linear and nonlinear structures, Phase I ASCE benchmark building (Johnson et al. 2004), and hysteretic structures.

Namdeo and Manohar (2007) identified the parameters of a nonlinear system using noisy response measurement and employing particle filter. The system parameters to be identified were treated as set of random variable that has finite and discrete states. The study developed a technique that conglomerates a self-learning particle filters and a global iteration strategy, the technique estimates the probability distribution of the parameters to be evaluated. The evolution of weights that are associated with system parameters is evaluated recursively. The accuracy and efficacy of developed method was demonstrated in a linear vibrating system, that can be solved by Kalman filter approach. Lastly, the examples on three nonlinear dynamic system excited by synthetic data was presented to demonstrate the accurate functioning of proposed method.

Gul and Catbas (2009) investigated the applicability of a statistical pattern recognition based "SHM" approaches on two distinct laboratory structures. The "SHM" approach is based on time series modeling where initial the model coefficients were obtained with help of an autoregressive modeling approach. An "AR" model is a data modeling approach that estimates the value of function at present time as a linear combination of its prior/past values. The basic formulation of an "AR" model is:

$$x(t) = \sum_{j=1}^{p} \psi_j x(t-j) + e(t) \tag{2.23}$$

where $x(t)$ is a time series, ψ is the set of model coefficients, and $e(t)$ is the error of "AR" process.

The obtained "AR" coefficient of a time series were processed by an outlier detection methodology that is based on Mahalanobis distance. The Mahalanobis distance of "AR" coefficients wers evaluated as follows:

$$Z_i = (x_i - \bar{x})^T \Sigma^{-1} (x_i - \bar{x}) \tag{2.24}$$

where x_i is the vector of potential outliers, $\bar{x}$is the sample mean of vector, Z_i is the index to identify the outliers, and Σ is the sample covariance matrix. With the help of above equation, the outliers were identified as the vectors whose Mahalanobis distance (Z_i) are higher than a threshold limit. If the threshold limit is decided too low, most of the healthy data will be recognized as outliers. Also, if the threshold limit decided is higher, the damaged data will be classified as inliers. Therefore, the efficacy of approach was checked for two different test structures. The two specimens were the steel grid structure and a simply supported beam. The acceleration response data was processed by the methodology and results were presented. Lastly, the advantages and shortcomings of the approach are discussed.

Zugasti et al. (2012) applied two damage identification techniques to monitor the health of a laboratory tower. The first one is NullSpace based identification method and the second one is based on AutoRegressive (AR) modeling of the time-history data. The methods were applied to a tower tested laboratory and were perfectly able to precisely detect and quantify the damage. The damage was manifested by loosening the bolts at some of the joints.

Null space method:

Consider a state space discrete model of a system in the form of

$$\begin{aligned} \{x_{k+1}\} &= [\mathbf{A}]\{x_k\} + \{w_k\} \\ \{y_k\} &= [\mathbf{C}]\{x_k\} + \{v_k\} \end{aligned} \tag{2.25}$$

where y_k is the output vector and x_{k+1} represents the state vector at time *'k'*. **A** and **C** are state matrix and output matrix. The Gaussian zero mean measurement noise and state noise are represented by v_k and w_k. Now, the next step is to perform singular value decomposition of weighted Hankel matrix ($\mathbf{H}_{p,q}$). The formulation of "SVD" is:

$$[\mathbf{H}]_{p,q} = [\mathbf{U}]_H [\mathbf{S}]_H [\mathbf{V}]_H^t \tag{2.26}$$

Now matrix $\mathbf{U}_{H0}$ was evaluated with the help of the following property

$$[\mathbf{U}]_{H0}^t [\mathbf{H}]_{p,q} = 0 \tag{2.27}$$

U_{H0}consists of a most number of independent vectors spanning the nullspace of the Hankel matrix. Now if damage is not present the unknown state signal, the multiplication between the nullspace $(\mathbf{U}_{H0})$and Hankel matrix corresponding to the unknown state will be zero. Thus a damage feature in the form of residue R was proposed in this work.

$$\mathbf{R} = [\mathbf{U}]_{H0}^t [\mathbf{H}]_{p,q}^t \tag{2.28}$$

The damage sensitive feature (**R**) used to quantify the damage had larger values in the case where damage is induced and smaller values for intact structure. The greater value of damage sensitive feature predicted the greater extent of the damage. Based on the results obtained, it was also concluded that the computational cost of the NullSpace based method is more than the "AR"-based method, whereas the efficiency of both for damage identification is almost same.

Yao and Pakzad (2012) reviewed two "AR" modeling based "SHM" approaches. The "AR" modeling was employed to extract damage features. One of the technique utilizes the Ljung-Box statistics of time series model as damage feature and the other one estimates the Cosh spectral distance of the estimated spectrum of "AR" model in order to identify damage. The two approaches were tested for various simulated and laboratory data; it was observed that the Ljung-Box based "SHM" method showed most number of false positive results. The data driven method that utilizes the Mahalanobis distance and Cosh spectral distance showed a better performance. To check the performance of both the approaches, the laboratory tests were conducted on a large scale bridge slab and on a truss.

Al-Hussein and Haldar (2015) proposed a novel unscented Kalman filter with unknown input (UKF-UI) approach for health assessment of nonlinear systems. A two-stage approach

is proposed by integrating iterative least square and unscented Kalman filter concepts. The method proposed here does not require information of input excitation and also it can identify the system parameters successfully by using limited response information of nonlinear system. The method considers response of sub-structure assembly instead of the entire structure. The accuracy of damage detection increases considerably if the damage is closer to the sub-assembly considered or is in the sub-assembly. The approach is verified for two examples, one with impulsive loading and other with seismic excitation as input loading. The proposed approach has high accuracy and can be used for monitoring the health of large structures.

b) Signal decomposition techniques:

The signal decomposition techniques deal with the extraction of the important information from the original signal in the form of multiple components. These multiple components are simple to understand, analyze them and are free from any unwanted data. The signal decomposition techniques are helpful in some of the above mentioned "SHM" approach where utilizing the raw data increases the computational cost. Also, the raw data often contains unwanted noise, mode mixing, and are of high model order. In such cases, the decomposed components of original data can be used to reduce the computation effort and also increase the efficiency of a "SHM" approach. The popular signal decomposition techniques are Empirical mode decomposition (EMD) (Huang et al., 1998) and wavelet analysis (Hou et al., 2000).

"EMD" method was developed by Huang et al. (1998), "EMD" decomposes a signal into its multiple intrinsic mode functions (IMF). The decomposed signal is considered as an "IMF" if it satisfies the two important conditions: (i) The number of zero crossing and number of maxima/minima is exactly same or at most differ by one; (ii) the mean of local minima envelope and local maxima envelope is zero. All the "IMFs" obtained from a signal with help of repetitive sifting process and are monocomponent. At the end of the "EMD" process, along with "IMFs" (c_k, k=1, 2, … n) a residue (r_n) is also obtained. For the success of "EMD"

stopping criteria of sifting must be satisfied. The commonly considered stopping criteria is the standard deviation. As soon as value of standard deviation reaches 0.2-0.3, sifting is terminated and first "IMF" is obtained.

$$SD=\sum_{t=0}^{T}\left[\frac{|\{h_k(t)-h_{k-1}(t)\}|^2}{\{h^2{}_k(t)\}}\right] \tag{2.29}$$

The same process of sifting is repeated for residue signal until residue becomes a monotonic function and no "IMFs" can be derived from it. The basic principle of "EMD" can be understood with the help of the following formulation:

$$\{x(t)\}=\sum_{i=1}^{n}\{c_i\}+\{r_n\} \tag{2.30}$$

Where x(t) is original signals, 'c_i' refers to i^{th} "IMF", the total number of "IMF" is represented by 'n' and 'r_n' is residue signal. Utilizing the "EMD" and wavelet transform, numerous research work has been carried out to develop a "SHM" approach. Some of these develop approaches are discussed below.

Yang et al. (2004a) proposed a novel method that serves as a reliable tool for the modal identification and damage detection of structures. They proposed two methods based on Empirical mode decomposition (EMD) and based on the amalgamation of "EMD" and Hilbert transform (Huang et al., 1998). The former method serves as an approach to extract damage spikes in the measured data, due to the sudden change in stiffness of the structure. The instant of spikes extracted from the raw acceleration data identifies the instant of damage and its location. The later one estimates the damage instants along with estimating modal parameters (natural frequency and damping) of the structure. The changes in the modal parameters help in estimating the damage. The methodology proposed was validated for an established benchmark problem of the ASCE task group on "SHM".

Loutridis (2004) developed a method to monitor the evolution of faults in the gear system, the proposed method is based on "EMD". An analytical model was developed to simulate the effect of tooth crack for gear also with help of "EMD", the experimental data were

decomposed into monocomponent signals referred to as intrinsic mode functions (IMFs). The Empirical relation between the energy of the "IMFs" and the crack magnitude was proposed in the study. It was observed that the modal energy of the second "IMF" increases as the relative magnitude of crack increases, thus this relation can be used for prediction of fault in gear pair. Moreover, it was also observed that the instantaneous information of time-domain vibration data in the frequency domain is a sensitive feature for the fault detection.

Huang et al. (2009) proposed a damage detection method based on a 2-dimensional wavelet transform. The numerical model was developed to simulate the response of damaged plate subjected to a static load, the healthy response for same load was assumed to be known. Now, by analyzing the variations in displacement response of healthy and damage plate with help of 2-d wavelet transform, multiple damage locations could be identified.

Hester and González (2012) stated that it is practically difficult to observe a difference in the deflection response of a healthy and a marginally damaged structure. Also, the structure may be subjected to a time-varying load and not necessarily a static load. Considering these limitations of past literature, they proposed a robust wavelet-based algorithm. The limitations were addressed by considering the acceleration signal instead of deflection data, by developing a FE model considering elemental interaction and thereby developing a damage detection approach utilizing wavelet energy of equally spaced bridge sections. The damage strip showed a higher level of energy compared to undamaged strip. The accuracy of detection of damage location was increased by considering the use of multiple sensors.

Amezquita-Sanchez and Adeli (2015) presented an adaptive methodology that is based on multiple signal classification (MUSIC) and Empirical wavelet transform (EWT). The MUSIC-EWT methodology uses MUSIC algorithm to evaluate the frequency components in the signal and form the suitable boundaries to generate the wavelet filter bank. Then, as per the evaluated frequency boundaries, EWT is used to decompose the time series into multiple frequency bands. Lastly, the advancement of calculated frequency bands over time is observed with help of Hilbert transform. The efficacy of proposed approach was validated

with help of an ECG signal acquired experimentally and two simulated signals. The results demonstrated the efficiency of approach even in presence of noise and the approach was also found to be helpful for closely-spaced frequencies.

The entire summary of literature review on time series and signal decomposition based methods is mentioned in Table 2.2

Table 2.2 Summary of literature on time series and signal decomposition based methods

Technique	Reference	Methodology	Validation	Conclusion/Results
Time series analysis based methods	Wang and Haldar (1997)	ILS-EKF-UI	Numerical	Do not require input information and response at all degree of freedom is not necessary
	Sohn and Farrar (2001)	Auto-regressive with exogenous inputs	Numerical	Proposed approach was demonstrated for an eight degree spring-mass system
	Nair et al. (2006)	Autoregressive moving average	Numerical and Experimental	Proposed method identi-fied damage accurately for ASCE model
	Yang et al. (2006) Yang et al. (2006b)	Extended Kalman filter	Numerical	Implemented successfu-lly for nonlinear, Phase I ASCE benchmark, and hysteretic structures
	Zugasti et al. (2012)	NullSpace	Experimental	Impleme-nted on a tower tested laboratory
	Yao and Pakzad (2012)	Ljung-box statistics	Numerical and Experimental	Tests were conducted on a large scale bridge slab and on a truss
	Al-Hussein and Haldar (2015)	Unscented Kalman filter with unknown input	Numerical	Approach is highly accurate to use for SHM of large structures

(*Contd.*)

Technique	Reference	Methodology	Validation	Conclusion/Results
Signal decomposition based methods	Yang et al. (2004a)	Empirical mode decomposition	ASCE "SHM" benchmark problem	Estimates the damage instants and modal parameters
	Loutridis (2004)	Empirical mode decomposition	Numerical	Empirical relation between "IMFs" energy and crack magnitude was proposed
	Huang et al. (2009)	2-dimensional wavelet transform	Numerical	Multiple damage locations could be identified.
	Hester and González (2012)	Wavelet	Numerical	Accuracy was increased by considering the use of multiple sensors rather than a single sensor
	Amezquita-Sanchez and Adeli (2015)	Multiple signal classification	Experimental	Approach is also helpful for closely spaced frequencies

Advantages and limitations of time series analysis and signal decomposition based methods:

Advantages:

- The time series methodologies are a form of unsupervised learning as during the training phase, these methods require the information from the healthy state structure only and not from the damaged state. This is one of the most important advantages of these methods.
- Signal decomposition techniques are helpful to get rid of unwanted noise from acquired data and thereby increasing the efficacy of "SHM" algorithms. These methods are also helpful in reducing the model order and thereby reducing the computational cost.

- The application of these methodologies for an automated health monitoring approach is more feasible in comparison to modal based methods.

Limitations:

- Though the time series based methodologies are most efficacious in detecting the manifestation of the damage, most of these methods often fail to determine the location of the damage.
- Most of these methods do not deal with exactly quantifying the extent of damage induced and also estimating the remaining strength or service life of any structure.
- For an online application of "SHM" approaches, these methods are not useful as they require some past information to identify the damage and most of them cannot be implemented in the recursive formulation.

2.5.2 Blind source separation based methods

In the late '90s, blind source separation (BSS) has developed as a robust signal processing methodology for de-mixing of the mixed audio recordings (Cardoso, 1998). "BSS" is a type of an inverse problem, as it deals with the extraction of primary source data from the obtained multiple recorded mixed signals. The basic formulation of "BSS" is represented as:

$$\{x(t)\} = [\mathbf{A}]\{s(t)\} \tag{2.31}$$

$$\{y(t)\} = [\mathbf{W}]\{x(t)\} \tag{2.32}$$

Where $x(t)$ is the recorded mixed signal, $\mathbf{A}$ is the mixing matrix, $s(t)$ is the primary source data, $\mathbf{W}$ is a demixing matrix, and $y(t)$ is obtained independent/primary sources.

Now, consider the equation of motion of undamped multiple degree of freedom system under external force $\{F\}$ is given as

$$[\mathbf{m}]\{\ddot{x}\} + [\mathbf{k}]\{x\} = \{F\} \tag{2.33}$$

The system response $\vec{x}$ is assumed to be dynamic mixtures of the sources as the response can be treated as convolution product of impulse response function and external force vector. The eigenvalue solution to determine natural frequency $\boldsymbol{\omega}^2$ and corresponding normal modes $\vec{X}$ is given by:

$$\boldsymbol{\omega}^2[\mathbf{m}]\{X\}=[\mathbf{k}]\{X\} \tag{2.34}$$

According to the expansion theorem, the solution vector is expressed by a linear combination of normal modes:

$$\{X(t)\}=\mathbf{q}_1(t)\{X^{(1)}\}+\mathbf{q}_2(t)\{X^{(2)}\}+.....+\mathbf{q}_n(t)\{X^{(n)}\} \tag{2.35}$$

Where, $\mathbf{q}_1(t),\mathbf{q}_2(t),.....,\mathbf{q}_n(t)$ time dependent natural coordinates also known as principal coordinates or modal participation coefficients. Equation 3 can be written in matrix form as

$$\{x(t)\}=[\mathbf{X}]\{q(t)\} \tag{2.36}$$

The time derivate function of $\vec{x}(t)$ is given by equation 5. The mode shape matrix **X** is independent of time.

$$\{\ddot{x}(t)\}=[\mathbf{X}]\{\ddot{q}(t)\} \tag{2.37}$$

Substituting equation (2.37) in equation (2.33) gives

$$[\mathbf{m}][\mathbf{X}]\{\ddot{q}(t)\}+[\mathbf{k}][\mathbf{X}]\{q(t)\}=\{F(t)\} \tag{2.38}$$

Pre-multiplying equation (2.38) with $[\mathbf{X}]^T$

$$[\mathbf{X}]^T[\mathbf{m}][\mathbf{X}]\{\ddot{q}(t)\}+[\mathbf{X}]^T[\mathbf{k}][\mathbf{X}]\{q(t)\}=[\mathbf{X}]^T\{F(t)\} \tag{2.39}$$

The normalization of modes yield

$$\begin{aligned}[\mathbf{X}]^T[\mathbf{m}][\mathbf{X}]&=[\mathbf{I}]\\ [\mathbf{X}]^T[\mathbf{k}][\mathbf{X}]&=[\boldsymbol{\omega}^2]\end{aligned} \tag{2.40}$$

The vector of generalized forces $Q(t)$ associated with generalized coordinates $q(t)$ as

$$\{Q(t)\}=[\mathbf{X}]^T\{F(t)\} \tag{2.41}$$

The equation (2.39) can be express in decouple form as:

$$\{\ddot{q}_i(t)\}+\omega_i^2\{q_i(t)\}=\{Q_i(t)\},i=1,2,.....n \tag{2.42}$$

Note that the equation 2.41 and 2.31 are similar. Therefore, the extraction of modal responses can be performed using “BSS” based approach such as independent component analysis, second order blind identification etc. The key goal of a “BSS” approach can be easily

illustrated with the most popular cocktail party example. The example is demonstrated in Figure 2.5 where several people are speaking together. The microphone installed in same room acquired the voice that was mixture of all the speech signals. The Figure 2.5 shows that three people are speaking at the identical time in a room, their voices are recorded using three distinct recording instruments. The recorded speech signals are mixtures of the individual voices. The main objective of any "BSS" approach is to obtain the demixing matrix accurately and thereby extracting the independent sources from the recorded mixed signals (Amezquita-Sanchez and Adeli, 2016).

Some of the popular "BSS" methods proposed in the literature are second-order blind identification (SOBI) (Poncelet et al., 2007), independent component analysis (ICA) (Hyvärinen and Oja, 2000), Algorithm for Multiple Unknown Signals Extraction (AMUSE) (Tong et al., 1990) etc.

The SOBI method assumes that the primary source signals are uncorrelated and uses the covariance matrices of the measured mixed signal to perform de-mixing of signals. Whereas, the "ICA" separates the multiple mixed signals into independent components by employing the statistical independence and non-gaussianity of the sources without considering the time structure (Cichocki and Amari, 2003). Some of the work carried out in "SHM" domain with the help of these techniques is mentioned below.

Zang et al. (2004) combined independent component analysis (ICA) for extraction of sources from a time history response and artificial neural network (ANN) to detect damages in structure. The advantage of the proposed approach is that raw measurements from sensors are only required, limitations being measurement noise, the quantum of data, lack of reliable feature extraction tool. To avoid the limitations, "ICA" is applied on the raw measurements and obtain the linear combination of independent sources along with a mixing matrix. The mixing matrix provides a simplified relationship between measurements and independent sources. With the help of this relationship, the neural network model is formed for identifying the damage. To demonstrate the efficacy of the approach, two examples are presented in this

study. The first one is a truss structure comprising of multiple elements is simulated and the response of truss was used to classify the damage at nine elements of the truss. The second example considers a bookshelf structure and the response is measured with the help of 24 piezoelectric accelerometers. The results of proposed approach, when applied on the second example, showed a successful identification of damaged and undamaged state with great accuracy.

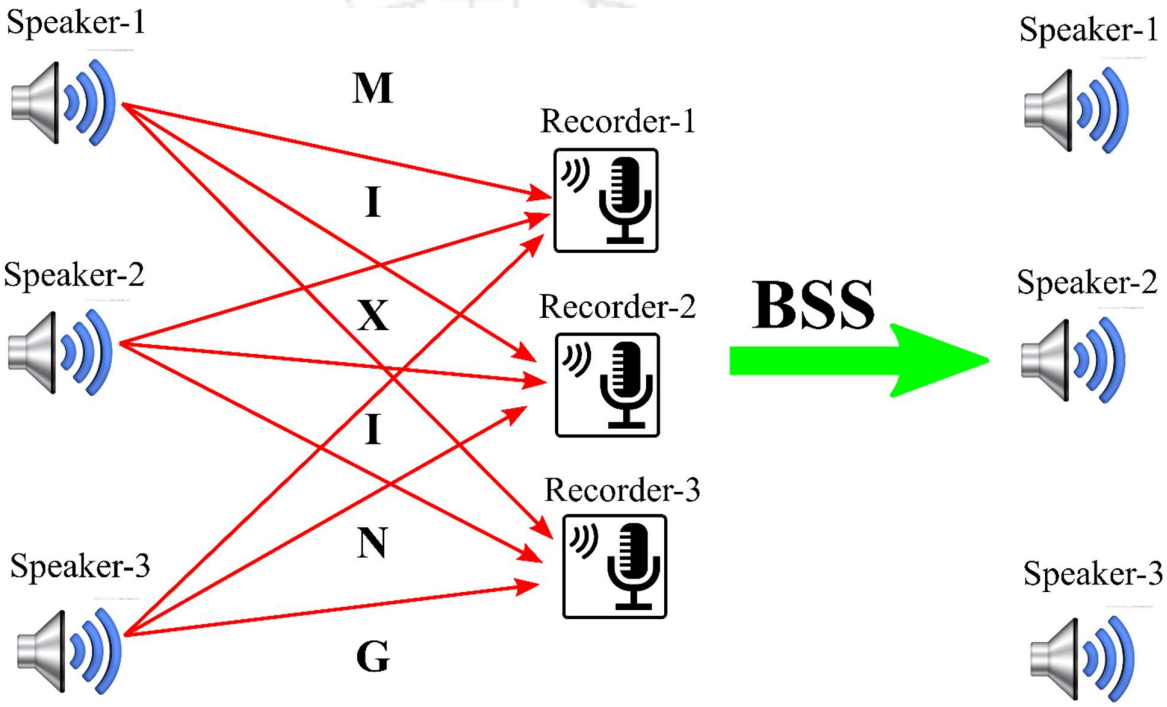

Figure 2.5 BSS implemented on the cocktail party example.

Zhou and Chelidze (2007) introduced a method based on blind source separation (BSS) to identify the linear normal mode. "BSS" is a novel and robust source separation technique that exploits the time coherence of the source data (Belouchrani et al., 1997). The modal properties of any structure are considered a special case of sources of time-history dynamic response. Therefore, it is possible to identify the modal properties with the help of "BSS" approaches. The study mentioned that approaches based on statistics of second-order are suitable for identifying linear normal mode of a structural system. In this work, two algorithms were considered; (i) algorithm for multiple unknown signals extraction (AMUSE)

and (ii) second-order blind identification (SOBI). The former one helps to illustrate its similarity with the Ibrahim time domain system identification approach (Ibrahim and Pappa, 1982). Whereas, the latter one is used to demonstrate its efficiency to identify mode shape even in the presence of noise. The study also presented the numerical and experiments validation of the "BSS" approaches and ITD algorithm.

Poncelet et al. (2007) applied "BSS" techniques to free vibrations of mechanical systems. The relationship between vibration modes and mixing matrix was presented for low and moderate damped systems. The technique developed was based on the independent component analysis (ICA) and is a simplified output-only modal analysis. For a case of free vibration, a robust criterion was developed to select the actual modes from the identified modes. The criterion was suitable for the case where a number of measurement sources are more than the excited modes and thus the standard complex stabilization charts were avoided. The numerical study was also demonstrated to prove the efficacy of approach and it was found that the method is insensitive to noise and holds strength to be applied for practical scenarios. The only limitation of proposed based on "ICA" is that the number of sensors must be greater than the number of excited modes.

Hazra et al. (2009) proposed a new method namely the modified cross-correlation (MCC) method based that is based on SOBI. They stated that, for a low damped system (i.e. damping ratio of < 1%), "ICA" can be implemented successfully. Whereas, for practical structural systems that are highly damped, methods based on SOBI have shown significant improvement over "ICA" methods. However, in the presence of nonstationary sources, the conventional SOBI methods suffer. In this paper, these limitations are addressed with help of MCC method. The key steps involved in MCC method are:

1. Evaluate the correlations of the acquired dynamic response and obtain the vector $\{r\}$.
2. Calculate the whitened vector as $\{\overline{r}(k)\} = [\mathbf{Q}]\{r(k)\}$.
3. Divided the whitened vector inot L nonoverlapping sets and estimate the covariance matrices as $[\hat{\mathbf{R}}_{\mathbf{r}}(T_i, p)]$ for i=1,...,L $\forall$ p.

4. Obtain an unitary matrices that diagonalized all the L matrices at every lag of p.
5. Last step is to compute the mixng matrix as $[\hat{\mathbf{H}}]=[\mathbf{Q}]^{-1}[\mathbf{V}]$.

This mixing matrix is the key to extract the modal information of a dynamical system from the measured responses. The circumstances for which the problem of structural system identification can be modelled as a "BSS" problem was also discussed. The numerical study of a 3-degree of freedom spring-mass-dashpot system and a tower structure were conducted to demonstrate the applicability of proposed method. The simulations were carried out for a case of wind loading and seismic excitations and results of natural frequencies, mode shapes, and damping ratios were extracted. The results of modal parameters showed that the proposed MCC method attains superior performance over conventional "ICA" and SOBI methods under both stationary and nonstationary excitations. The capability to extract modal parameters for a highly damped dynamical system proves that the MCC method holds substantial potential in the domain of system identification. Experimental results also obtained to demonstrate the applicability of the MCC method for system identification problems.

Sadhu et al. (2011) proposed an algorithm based on wavelet transform to identify the global mode of the structure with the help of sparse sensor information. The proposed method requires information from a few sensors only at a time, this the most important advantage of the proposed approach. The proposed method initially transforms the response acquired by sensors into a sparse representation by using a stationary wavelet packet transform (SWPT). The wavelet transform (WT) of a signal *y(t)* is mathematically represented as:

$$w_k^j(y) = \frac{1}{\sqrt{j}} \int_{-\infty}^{\infty} y(t)\ \psi_k^{j*}(t) dt \tag{2.43}$$

Where ψ is generally known as mother wavelet function and * refers complex conjugation. k and j denotes translational and scaling parameters, respectively. Whereas, the SWPT is an extension of WT and is implemented as a generalized form of pyramidal algorithm. The SWPT basis is mathematically define as:

$$\psi_k^{j,v}(t) = \frac{1}{2^j}\psi^v\left(\frac{t-k}{2^j}\right) \tag{2.44}$$

where $\psi^{1,0}(t) = \phi(t)$ and $\psi^{1,1}(t) = \psi(t)$ denotes the father (scaling) and mother (wavelet) function respectively. Now, as the wavelet transform is completed, principal component analysis (PCA) is performed on the coefficients obtained by wavelet transform.

"PCA" is a multivariate statistical technique used for dimension reduction and system identification that is closely related to Proper Orthogonal Decomposition (Chatterjee 2000) and Singular Value Decomposition (SVD) (Wall et al. 2003). "PCA" of *N* x *n* dimensional data separates dataset into *n* linear, mutually orthogonal sets by Eigen-analysis of the covariance matrix. "PCA" decomposes a matrix $\mathrm{A}_{N\,\mathrm{x}\,n}$, which contains *N* observations and *n* variables, into a transformed subspace of reduced dimension. The Eigenvector corresponding to highest Eigenvalue contains most relevant information and is called principal orthogonal component (POC) of corresponding data. Only dominant PC's are retained for transformation, and thus residual matrix E is formed. The mathematical representation of "PCA" on response matrix $\mathrm{A}_{N\,\mathrm{x}\,n}$ is given as follows:

$$[\mathbf{A}] = [\mathbf{Z}][\mathbf{Q}]^{\mathrm{T}} + [\mathbf{E}] \tag{2.45}$$

where [**Z**] is transformed data set, columns [**Q**] are eigenvectors and [**E**] is a residual error.

"PCA" algorithm:

Step-1: For n number of response variables, each comprising N number of samples forms a response matrix, $[\mathbf{A}]_{N\,\mathrm{x}\,n}$.

Step-2: Subtract mean from response matrix $[\mathbf{A}]_{N\,\mathrm{x}\,n}$ data to zero mean data $[\bar{\mathbf{A}}]_{N\,\mathrm{x}\,n}$.

Step-3: Calculate the covariance of the response matrix $[\bar{\mathbf{A}}]$

$$[\mathbf{C}_o] = \frac{1}{n-1}([\bar{\mathbf{A}}]^{\mathrm{T}} \times [\bar{\mathbf{A}}]) \tag{2.46}$$

Step-4: Calculate Eigenvalues (Ψ) and Eigenvectors (Q) of the covariance matrix $(\mathbf{C}_o)$

$$[\mathbf{C}_0]\{Q\} = \mathbf{\Psi}\{Q\} \tag{2.47}$$

Step-5: Transform matrix Z is obtained as

$$[\mathbf{Z}] = [\bar{\mathbf{A}}][\mathbf{Q}]^{\mathrm{T}} \tag{2.48}$$

The eigenvector corresponding to highest eigenvalue contains dominant information. "PCA" yields the transformed coefficient matrix from coefficients obtained by wavelet transform of few sensors. This is done multiple times for multiple groups of sensors. Lastly, the results obtained from each group are concatenated to obtain the global modal parameters of the structure under investigation. The study presented two examples and proved that the proposed method is efficient to identify the modal properties of frame structures.

Hazra et al. (2012) proposed a novel approach to address the issue of sparse measurements while identifying the modal parameters of a system. The other issues for an accurate system identification method are a noisy environment, closely spaced modes. These challenges were overcome in this study by integrating the "BSS" method with a time-frequency decomposition method. The hybrid method presented here, integrate wavelet and Empirical mode decomposition along with SOBI. The time-frequency decomposition is employed in two ways, one is by transforming the signal completely to time-frequency domain from time domain and other is by transforming a subset of all sources to the time-frequency domain. Both the techniques are integrated with "BSS" for identifying the modal properties. The proposed method addresses the issue of the sparse sensor and closely spaced modes. Lastly, the robustness of the proposed method was verified by extracting the modal parameters of an airport control tower structure.

Sadhu and Hazra (2013) developed a damage identification approach based on "BSS" in conjunction with time-series analysis. The proposed method initially identifies the modal response of the dynamic system by implementing "BSS" using the dynamic response. In the next step, the modal responses are characterized by time-series analysis and the resulting model were used for one-step-ahead prediction of mono-component modal response. Now, by comparing a variance based damage sensitive feature derive from initial measurements of

an intact system and newer measurements, the time instant of damage was identified. After the identification of damage instant, the modal parameters of healthy and damaged system are estimated. The proposed method was able to identify damage instant, localize damage and quantify its severity. The approach was validated by implanting it for an extensive numerical simulation and also by a full-scale study of UCLA Factor building under Parkfield ground motion.

Antoni and Chauhan (2013) focused on covering three important aspect of second-order "BSS" (SOBSS) application. Firstly, a mathematical analysis of "SOBSS" technique is conducted focusing on its applicability within the framework of operational modal analysis (OMA). Secondly, a new "SOBSS" method is proposed that overcomes the limitations of technique developed in first step. The novel technique estimates the complex mode shapes and can even extract more active modes than the number of available response. Also this technique shows a great performance in case of coupled modes and for a highly damped structure. Lastly, a theoretical link is established between "SOBSS" and stochastic subspace identification a popular OMA method. All the approaches are also compared with help of numerical study.

Chang et al. (2016) stated that independent component analysis (ICA) has a major limitation of not being able to identify modal parameters of structures with high damping. Therefore, to overcome this limitation a new technique based on "ICA" and inverse damping transfer (IDT) is proposed in this study. The "ICA+IDT" method initially obtains free vibration data from the response of structure under ambient vibrations. "IDT" is now employed on these highly damped free vibration response in order to get the low damped response without compromising the other modal characteristics. Now, with help of "ICA" and low damped response, the odal parameters are identified. Lastly, the evaluated damping ratios are corrected to eliminate the error due to "IDT". The effectiveness of proposed approach was validated on two numerical study- a mass spring dynamic system and a simply supported

beam. The approach was also tested on experimental study of a three storey steel frame and was found to be working satisfactorily even for highly damped structures.

The overview of various studies carried out with help of "BSS" methods is summarized in Table 2.3.

Table 2.3 Important details of "BSS" methods (Sadhu et al., 2017)

Model	Criteria	References	Issues addressed
Over determined system	Second order statistics	Brewick and Smyth (2014) Ghahari et al. (2013) Hazra et al. (2010) Sadhu et al. (2012)	Damping under traffic loading Non-classical damping Closely spaced modes Nonstationarity
	Higher order statistics	Yang and Nagarajaiah (2012) Yang and Nagarajaiah (2014b) Antoni (2005) Ghahari et al. (2013)	Highly-damped modes Data compression Basic challenges of "BSS" Non-proportional damping
Under determined system	Second order statistics	Hazra et al. (2011) Abazarsa et al. (2013) Abazarsa et al. (2015)	Limited sensor Non-proportional damping Spurious modes
	Time frequency methods	Sadhu and Narasimhan (2014) Yang and Nagarajaiah (2013b) Yu et al. (2014)	Narrowband excitation Limited sensors Time-varying parameters

Advantages and limitations of BSS based methods:

Advantages:

- The "BSS" methods are helpful for evaluation of modal responses from the mixed dynamic response of the structure. Modal responses are more sensitive to damage in comparison to raw response acquired. "BSS" are helpful in increasing the efficacy of "SHM" method by utilizing modal response for analysis instead of original mixed response.

- The "BSS" techniques perform with good accuracy in the presence of noise, and are also helpful to separate closely spaced modes.

Limitations:

- The "BSS" method fails to perform accurately for structures that have a high value of damping (greater than 5%).
- The current "BSS" method are heavily focused on identification of linear dynamic system and the focus for nonlinear system is very less as these methods do not perform adequately for nonlinear transient signals.
- The "BSS" method fails to extract modal responses if the number of sesnors is less than the number of modes excited.
- One more limitation of "BSS" method is that even in the presence of an optimal number of input data, the "BSS" method fails to extract modal responses corresponding to higher modes and low energy content. It only extracts modal responses for high energy content lower modes.

2.5.3 Phase space-based methods

Phase space is a multidimensional representation of all the possible dynamic states of a system (such as displacement, velocity, acceleration). Any unique point in phase space corresponds to a possible unique dynamic state of the system. This multidimensional space representation of dynamic state variables is a useful tool to capture the nonlinear dynamics of a system. For a *d*-dimensional phase space, the *'d'* number of state variable are represented as principal axes. For a system represented by one, two and three state variable are called a phase line, a phase plane, and a phase space respectively. The evolving path of state variables as a function of time forms a specific path in multidimensional phase space which is called as phase space trajectory (PST) (Zhang et al., 2015). In experimental study, it is not always possible to measure all the state variables of a dynamic system. Though all the variables cannot be measured, yet a phase space reconstruction can be successfully performed with the help of Takens' embedding theorem (Takens', 1981).

The embedded theorem states that one state variable of a nonlinear dynamic system contains enough information about remaining variables. The complete information of the dynamical system could be obtained by an individual measured variable, preserving the topology of the unknown attractor. For this purpose, the method of delays can be used where, the time series of a single measured variable is concatenated *m* times, each with a delay equivalent to τ . Hence at any time *n,* the attractor can be represented as,

$$X(n) = [x(n), x(n+\tau), ..., x(n+(m-1)\tau)] \tag{2.49}$$

where '*m'* is the embedding dimension and '$_\tau$' is the time lag. The four common types of attractor are briefly explained below and are represented in Figure 2.6:

1) *Point attractor*: If any system evolves to a fixed single point, it is said to be a point attractor. The single pendulum bob is an example of a point attractor.
2) *Limit cycle attractor*: For a cyclic system such as planetary motions, the position of system within the cycle can be predicted with help of its cyclic attractor. The attractor for such a system are commonly referred as limit cycle attractor.
3) *Limit torus attractor*: A system that can be represented by a limit torus attractor has same trajectories as that of limit cycle. The only difference is that for limit torus, the trajectories are bounded within a ring torus. For example, the rings of planet Jupiter consisting of dust particles in motions.
4) *Strange attractor*: For a system trajectories evolving in an irregular shape and has no repetition in time, the attractor for such a system is said to be a strange attractor. For example, the Lorentz attractor.

For nonlinear dynamical systems, the damage sensitive features (DSFs) extracted from phase space topology are superior to conventional modal features (Todd et al., 2001, Liu et al., 2016). Some of the popular "DSFs" that accommodate non-linearity in the structure are Phase Space Warping (PSW), Local Attractor Variance Ratio (LAVR) and Change of Phase Space Topology (CPST).

PSW refers to changes in the vector field of phase space of the damaged system and healthy system (Chelidze and Liu, 2006, Alwasel et al., 2017). Todd et al. (2001) proposed LAVR feature calculated as the variance ratio of the clusters corresponding to baseline data and damage data. Change of Phase Space Topology (CPST) is a prominent "DSFs" that identifies nonlinearity in the structure using the Euclidean distance between phase portrait of progressive damage states (Nie et al., 2012, Nie et al., 2013, Hao et al., 2018).

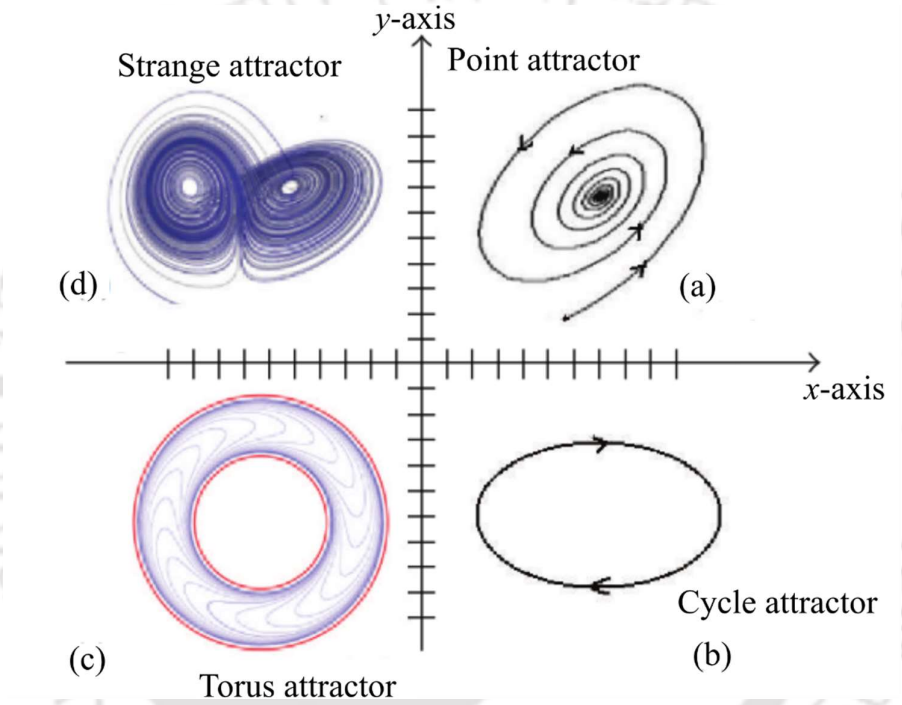

Figure 2.6 Types of attractors represented in 2-dimensional phase space; (a) point attractor, (b) cycle attractor, (c) torus attractor, (d) strange attractor (Adewumi et al., 2016)

In past literatures, for system excited using nonstationary excitations the applicability of phase space methodology is demonstrated (Nichols, 2003, Paul et al., 2017). However, these studies are limited to low-frequency excitation and lower dimension signals that can be embedded in phase space using Takens' theorem (Takens', 1981). The response of the structure excited using high-frequency loadings such as ground motion, impact loading, blast, and shock loading are difficult to represent in phase space due to high dimensionality. The brief description of some of the work carried out in this domain are described below.

Todd et al. (2001) presented a novel feature extraction method to detect damage of a nonlinear dynamic system. Numerical analysis of eight degree-of-freedom mass-spring-damper is carried out and the damage was introduced by reducing the stiffness of one spring. In numerical analysis, the system is excited by a chaotic input. The dimensionality of system is controlled with the help of Lyapunov exponents of excitation to Eigenvalues of the structure. The geometrical state space representation of input and output is used to analyze the effect of damage. The geometric properties of attractors alter at local level due to damage, which was captured by extracting the average local attractor variance ratio (ALAVR), the proposed feature. They also compared the modal-based features with the "ALAVR" and the proposed feature was found to be superior and robust for damage detection.

Chelidze and Liu (2006) developed a novel multidimensional damage detection approach and investigated it with the help of an experimental study. The experimental study of cantilever beam was carried out, where the beam vibrated under the influence of a magneto-elastic oscillator. The electromagnetic oscillator was activated by a power supply controlled by a computer. The entire experimental study was carried out within a chaotic regime. The damage was induced with the help of controlled electromagnets by changing the potential field of cantilever beam. The identification of damage is done by analyzing the response of a vibrating beam that was recorded with laser vibrometers and accelerometers. The damage features based on phase space warping were evaluated along with the implementation of a new phase space partitioning method. The new partitioning scheme helped to improve the damage identification capability of proposed approach in presence of noise. It was also demonstrated that the quality of damage identification for an experimental study improved as record length of data is increased.

Nie et al. (2012) proposed a novel phase space based algorithm to localize the damage. A damage indicator based on variation/changes in the phase space topology of dynamic response was proposed and was named as changes of phase space topology (CPST). The numerical and experimental study of an arch structure was carried out to investigate the

applicability of phase space based damage identification methodology. The dynamic response of the structure under impact loads was considered for reconstruction of "PST" and detect damage. The proposed method was able to detect damage for numerical and experimental study successfully. The approach was demonstrated to be more sensitive to damage in and least to noise as compared to conventional modal based approaches. The damage index being more sensitive to damage than modal parameters can be a good candidate for development of online structural health monitoring system.

Liu et al. (2016) proposed a damage detection method that is compatible with non-stationary input sources (e.g. ground motion). The proposed methodology is based on the geometrical alters of trajectories in phase space representation. The presented approach works on the assumption of zero-mean excitation and uses the extended random decrement technique to obtain free vibration response from the non-stationary response of system. To enrich the statistical analysis, the transient responses of system are reconstructed with the help of Takens' embedding theorem.

The reconstructed trajectories are mapped into phase space and the temporal prediction error of system dynamics is adopted as a damage sensitive feature. The damage was quantified statistically by evaluating the Bhattacharya distance and operating characteristic curves. The proposed approach was validated by numerical and experimental analysis of a structure subjected to non-stationary ground motion, hence can be used for scenarios such as wind, earthquake and traffic loadings.

The entire summary of literature review on phase space based methods is mentioned in Table 2.4.

Table 2.4 Summary of literature review on phase space based methods

Technique	Reference	Methodology	Validation	Conclusion/Results
Phase space based methods	Todd et al. (2001)	Average local attractor variance ratio	Numerical	The geometrical state space representation of input and output was used to analyze the effect of damage
	Chelidze and Liu (2006)	Phase space partitioning method	Experimental	The damage features based on phase space warping were evaluated to detect damage
	Nie et al. (2012)	Changes of phase space topology	Numerical and Experimental	The damage index is more sensitive to dam-age than to modal para-meters
	Liu et al. (2016)	Extended random decrement technique	Numerical and Experimental	The damage was quan-tified by evaluating the Bhattacharya distance and operating character-ristic curves

Advantages and limitations of phase space-based methods:

Advantages:

- The damage in any system subjected to extreme loading induces nonlinearity in its dynamic characteristics. This abrupt behavior of the system is complex to understand or capture with the help of conventional methods. Whereas, phase space-based methods can capture the nonlinear dynamics of any system accurately and later detect damage with the help of damage sensitive features.
- The damage sensitive features derived from phase space trajectories are a lot more sensitive to damage and shows low sensitivity to noise than the conventional modal-based

damage features. Even if the source of damage is far from the sensor, the measured data shows dissimilarity in "PST" and detects damage successfully.

Limitations:

- The phase space based methods are computationally expensive for system possessing large degree of freedom.
- The successful reconstruction of phase space-based methods is dependent on embedding parameters. The procedure for evaluating optimal embedding parameters is offline. Therefore, it restricts phase space-based methods to be applied in the recursive domain and use for online "SHM".

2.5.4 Online recursive methods for SHM

In the case where the immediate decision of damage is required to avoid catastrophic failure such as aerospace system, bridges, etc., the online methods hold great potential. The above mentioned "SHM" approaches perform on the basis of proper baseline data availability and are mostly implemented in offline manner; therefore, online methods are important to develop. The online "SHM" can be accomplished by formulating some of the offline methods are developed in the recursive domain (Yan and Yam, 2002, Krishnan et al., 2017). Some of the recursive algorithms developed for online "SHM" frameworks are discussed below.

Rajan and Rayner (1996) demonstrated a feature extraction methodology for a non-stationary time history signal. The time dependency of these signals makes it difficult to extract a robust and reliable feature from data. Therefore, to overcome this difficulty a finite small interval of signal was modeled by time-varying autoregressive (TVAR) processes. The feature considered in this work were time-dependent "AR" coefficients that can be represented by a group of basis vectors. A novel Bayesian formulation was developed that determines the exact model order of "AR" process and also specifies the form and number of basis vectors needed to model "AR" coefficients. It was concluded that the basis coefficients directly relate to the "TVAR" coefficients, are time-invariant and are suitable features for

segregation. Lastly, a simple comparison of proposed methods with an alternative feature extraction methods was demonstrated and the proposed method performed better.

Yan and Yam (2002) proposed an online damage detection method to detect small and initial defects in a composite structure. The propose method is based on changes in energy of dynamic response evaluated using wavelet analysis. The proposed method was sensitive enough to identify small cracks in a composite plate. The results presented proved that the proposed approach was capable of detecting small cracks of width 0.1 mm and length 2.3 mm. The area of the crack detected was only 0.06% of the total area of composite plate. The piezoelectric materials were embedded in composite plate to function as actuator and receiver. The proposed method is also suitable for structure that are inaccessible and are used under severe environments without need of any special facility. The method is also safe, reliable and affordable for inspection of structure during service.

Yu et al. (2007) propose an online damage identification approach for a laminated composite shells filled with fluid partially (LCSFF) . A finite element model was established to simulate the response of "LCSFF" for healthy as well as damage state. The FEM is validated with help of natural frequencies obtained experimentally. The damage index formulated was based on the variations in the energy content of decomposed signals obtained from wavelet analysis. A nonlinear relationship between various states of LCSFF and the damage index is established with help of an artificial neural network that was trained with help of numerical data. The results obtained in this study showed that the proposed approach was able to identify the damage states of LCSFF successfully and with good accuracy.

Musafere et al. (2015) proposed a technique by integrating "BSS" with "TVAR" modeling in order to detect damage. The integration of "BSS" and "TVAR" is done to overcome the limitation of each other. The SOBI is employed first and mono-harmonic components from the acquired response were being extracted.

Second-order blind identification (SOBI):

Generally, the dynamics of a structure can be assumed as linear system with lumped mass (*'n'*- degree of freedom) and is classically damped. The equation of motion for such a structure subjected to excitation *F(t)* is:

$$[\mathbf{M}]\{\ddot{x}(t)\}+[\mathbf{C}]\{\dot{x}(t)\}+[\mathbf{K}]\{x(t)\}=\{F(t)\} \tag{2.50}$$

where [**M**], [**C**] and [**K**] are mass, damping and stiffness matrices respectively. $x(t)$ is displacement vector containing displacement coordinated of each degree of freedom. The solution to the equation of motion can be considered as superposition of all the vibration modes and is written in matrix form as:

$$\{x(n)\}=[\mathbf{A}]\{s(n)\} \tag{2.51}$$

where $x(n)$ is a measurement matrix consisting of the dynamic response at each degree of freedom, $s(n)$ is a matrix consisting of modal responses and [**A**] is the modal mixing matrix. The SOBI method aims to find the unknown modal mixing matrix and thereby obtain the modal responses with help of response measurements. For a damaged system, the obtained modal responses will contain response from both undamaged and damage states. To separate damaged response from undamaged, "TVAR" model was implemented subsequently.

Time-varying autoregressive modeling (TVAR):

The AR model of modal response *y(n)* with zero-mean measurement noise *v(n)* and model order of *p* can be written as:

$$y(n)=\sum_{k=1}^{p}a_k y(n-k)+v(n) \tag{2.52}$$

where a_k represents the "AR" coefficients. Since the nature of modal response was observed to be non-stationary, therefore a recursive "TVAR" modeling approach was implemented. For "TVAR" approach, a_k becomes $a_k(t)$ and Kalman filter was used to obtained the time varying "AR" coefficients. The discrete representation of these coefficients is represented in following equation:

$$x(n) = \Gamma(n-1)x(n-1) + w(n)$$
$$y(n) = C(n)x(n) + v(n) \tag{2.53}$$

where $x(n)$ is the unknown vector containing time varying coefficients, $w(n)$ and $v(n)$ are uncorrelated process and measurement noise. The matrix $\Gamma(n-1)$ was assumed as identity matrix and $C(n)$ is the discrete observation data. The Kalman filter utilizes the time update and measurement update processes to evaluated the time varying "AR" coefficients.

Now, with help of "TVAR" modeling process, damage instant is obtained by observing trend of time varying "AR" coefficients. The obtained damage instant is further used to segregate damage and undamaged modal response. These segregated mono-harmonic responses depict changes in damaged and undamaged natural frequencies, which is used to quantify the damage. The proposed novel algorithm was validated by both numerical and experimental study. Lastly, a full-scale study of UCLA factor building is also demonstrated to validate the performance of the algorithm for a realistic application. The presented work primarily focused on quantify damage and identify the instant of damage.

Santos et al. (2016) presented a paper that addresses the issue of damage detection in initial stage and is not reliant on baseline/reference data. The proposed strategy is based on the combination of two statistical methods. The neural networks were utilized in order to estimate the dynamic response of structure, and the clustering methods were implemented for an automatic classification of the neural network errors. The proposed approach was implemented in a moving window process in order to ensure its on-line applicability. The numerical and experimental study of a cable-stayed bridge was carried out in order to validate and test the applicability of proposed approach. Though the approach is sensitive to small reduction in stiffness, it is also robust enough to avoid false detection.

Krishnan et al. (2017) developed a novel non-baseline approach for online damage identification of a "MDOF" system. The proposed approach is an amalgamation of recursive principal component analysis (RPCA) and recursive condition indicators. The method uses

the acceleration response of system to obtain recursive proper orthogonal modes with help of rank-one perturbation approaches.

The basic formulation of "RPCA" is:

$$[\mathbf{R}]_k = \frac{k-1}{k}[\mathbf{R}]_{k-1} + \frac{1}{k}[\mathbf{X}]_k[\mathbf{X}]_k^T \tag{2.54}$$

where X_k and R_k are the data points matrix and the covariance matrix at *k*th time step respectively.

The covariance matrix R_k can be written as an Eigen decomposition as mentioned:

$$[\mathbf{R}]_k = [\mathbf{W}]_k[\mathbf{\Omega}]_k[\mathbf{W}]_k^T \tag{2.55}$$

where W_k denotes the proper orthogonal modes. The projection of data matrix/response in the principal orthogonal modes" subspace can be obtained as:

$$[\mathbf{X}^*(\mathbf{k})] = [\mathbf{W}]_{k-1}^{1} * [\mathbf{W}]_k^{1^T} * [\mathbf{X(k)}] \tag{2.56}$$

where $\mathbf{X}^*(\mathbf{k}) = [x_1^*(k), x_2^*(k), ..., x_m^*(k)]^T$ is the projection of data matrix $\mathbf{X(k)} = [x_1(k), x_2(k), ..., x_m(k)]^T$, '*m*' represents total degree of freedom and '*k*' represents a time step.

The projected modes are used to detect the sudden variations in the dynamic characteristic of the vibrating system with respect to pristine state and identify damage. The condition indicator $(\varepsilon_{RR} - Y_i)$ proposed was based on the Euclidean distance of error between the projected response (obtained by "RPCA") and the actual response.

$$\boldsymbol{\varepsilon}_{\mathbf{RR}} - \mathbf{Y_i} = | x_i^{*^2}(k) - x_i^2(k) | \tag{2.57}$$

This recursive condition indicator facilitated the approach to work in an online fashion. The proposed approach was also demonstrated successfully for spatio-temporal detection with help of a numerical study of a five-degree of freedom nonlinear system and an experimental study of a cantilever beam. The real life and reference free applicability of proposed algorithm was demonstrated by analysis of UCLA Factor building.

The summary of literature review on online recursive methods for "SHM" is mentioned in Table 2.5.

Table 2.5 Summary of literature review on online recursive methods for SHM

Technique	Reference	Methodology	Validation	Conclusion/Results
Online recursive methods for "SHM"	Rajan and Rayner (1996)	Time-varying autoregressive	Synthetic time-varying AR data	A novel Bayesian formulation was developed to determine the model order of AR process
	Yan and Yam (2002)	Wavelet analysis	Numerical	Suitable for structures that are inaccessible and are used under severe environments
	Yu et al. (2007)	Artificial neural network	Numerical	Damage index was based on the variations in e energy content of signals decomposed by wavelet analysis
	Musafere et al. (2015)	Time-varying autoregressive	Numerical and Experimental	Primarily focused on quantify damage and identify its instant
	Santos et al. (2016)	Artificial neural network	Numerical and Experimental	Approach is sensitive to small reduction in stiff-ness and also robust enough to avoid false detection
	Krishnan et al. (2017)	Recursive principal component analysis	Numerical and Experimental	The real life applicability of proposed algorithm was demonstrated by analysis of UCLA Factor building

Advantages and limitations of Recursive methods for online SHM:

Advantages:

- The recursive methods even work for the case of sparse sensors which is clearly an important advantage over conventional batch mode or windowed methods. This also helps in reducing the monetary cost of implementation of the "SHM" approach in real life scenarios.
- The recursive methods are able to track nonlinearity changes in the response of the system at each time interval and thus identify the damage. These methods do not require past data and works on the initial data that is used for buffering/convergence of recursive approaches.

Limitations:

- Most of the recursive methods work for multiple output case and fail to work for the case where information from the only a single sensor is available. The development of online "SHM" methods for single output case holds great potential.
- The recursive methods provides lot of reduntant information therefor data mining is also needed for accurated monitoring, these methods are also computationaly slow and expensive.

2.5.5 Brief review on damage sensitive features (DSFs):

The above mentioned "SHM" techniques detect damage with the help of a unique geometrical, statistical or modal feature of a system. These feature shows significant changes as damage are induced in the system, hence are selected as damage sensitive features (DSF). For successful implementation of "SHM" approach, it is important to select a "DSF" that is sensitive to minor damages and also works for nonlinear case. The "DSFs" explored and proposed in some of the past literatures are based on Euclidean distance (Ying et al., 2012), Mahalanobis distance (De Maesschalck et al., 2000), Bhattacharya distance (Liu and Sohn, 2016), Cepstral distance (Zheng and Mita, 2009) and Itakura distance (Kong et al., 1995b).

The Euclidean distance is a geometric measure that simply calculates the squared difference in each dimension and later evaluates the square root of their sum. Whereas, Mahalanobis distance (MD) is a multidimensional statistical measure that exploits the statistical information of all the sensitive feature in a unified manner to quantify the distance between two clusters using covariance between the states vectors. Nair and Kiremidjian (2007) have utilized the MD to measure the extent of damage using damage sensitive feature. Mathematically, Mahalanobis distance (D_M) between a matrix X and point *v* is defined as:

$$D_M = \sqrt{(v-\bar{x})C^{-1}(v-\bar{x})^T} \tag{2.58}$$

where C is the covariance matrix of X, and $\bar{x}$ is the mean vector of X

The Euclidean distance shows improper results for the case where the variance in each principal direction is different, but the Mahalanobis distance is an accurate measure for this case (De Maesschalck et al., 2000). This is because MD takes into account the covariance of the variables to evaluate the distance between two data points. Now, if the dimension of variables under consideration is different, the Euclidean distance may give more weight to one of the dimensions that might lead to poor interpretation. Euclidean distance also leads to a wrong interpretation of data for which the variables are correlated, whereas the MD takes covariance between variables under consideration and thus resolves the problems arising due to correlated variables.

The Bhattacharyya distance (BD) in its simplest form can be defined as the distance between two classes that has normal distribution. The BD can be evaluated by obtaining the mean and variances of two distinct distributions (Coleman and Andrews, 1979). Liu and Sohn (2016) evaluated a damage feature with help of Bhattacharyya Distance (BD). The damage feature used in this study was calculated to indicate the geometric variations among the attractors due to crack-induced. The attractors considered here were attained from the two measurement points close to the crack.

$$BD_{(a,b)} = \frac{1}{4}\ln\left(\frac{1}{4}\left(\frac{\sigma_a^2}{\sigma_b^2}+\frac{\sigma_b^2}{\sigma_a^2}+2\right)\right)+\frac{1}{4}\left(\frac{(\mu_a-\mu_b)^2}{\sigma_a^2+\sigma_b^2}\right) \tag{2.59}$$

Where,

BD is the Bhattacharya distance between *a* and *b* classes or distribution

σ_i^2 represents the variance of the *i*-th class

μ_i represents the mean of the *i*-th class

a, b are two distinct distributions or classes

In time series analysis, the similarity of the "AR" coefficients for segmented data is determined using Itakura distance (ID) and Cepstral distance. The ID is a parameter that measures the distance between two sets of auto-regressive coefficients and is widely used in signal and speech processing applications. ID tests how optimally the "AR" parameter of known state/ baseline state (ϕ_1) signal fits the signal of the unknown state (ϕ_2) and is mathematically defined as:

$$d'(\phi_1,\phi_2) = \log\frac{\phi_2^T R_x \phi_2}{\phi_1^T R_x \phi_1}$$
$$d''(\phi_1,\phi_2) = \log\frac{\phi_1^T R_y \phi_1}{\phi_2^T R_y \phi_2} \quad (2.60)$$

$$ID = \frac{1}{2}\left(d'(\phi_1,\phi_2) + d''(\phi_1,\phi_2)\right) \quad (2.61)$$

where R_x and R_y are the autocorrelation matrix of known state and unknown state signal respectively, and *ID* is the Itakura distance. The Cepstral distance between two distinct "AR" models is obtained by evaluating the Cepstral distance between autoregressive moving-average (ARMA) models, the evaluation procedure of Cepstral distance is proposed by Martin (2000). The formulation of an "ARMA" model is given in equation (2.20). The Cepstral distance is mathematically formulated as:

$$CD(X,Y)^2 = \sum_{n=1}^{\infty} n\,|c_x(n) - c_y(n)|^2 \quad (2.62)$$

where $c_x(n)$ and $c_y(n)$ are Cepstral coefficients of two "ARMA" models *X* and *Y* respectively.

Zheng and Mita (2009) have utilized "AR" coefficients to quantify the damage using ID and Cepstral distance in the five-storey model building. To study the proposed approach, numerical and experimental study were conducted. Based on the results obtained it was concluded that, by utilizing the pre-whitening filter, the damage detection capability of the proposed features ID and Cepstral distance got improved considerably, particularly for damage localization. The ID and Cepstral distance were observed to follow a monotonically increasing trend as the severity of damage increase, which proves them to be potential feature for damage quantification.

2.6 Gap Areas

Although extensive work has been already carried out on "SHM" in past literature, yet there are few gap areas which are needed to be resolved. Some of these gap areas are:

- Though the time series based "SHM" methodologies are mostly efficacious in detecting the damage, most of these methods often fail to determine the location of the damage, quantify the damage and also estimating the remaining strength or service life of any structure. Also, most of these methods fail to identify and quantify the damage induced due to extreme events such as blast, shock, and earthquake, etc.
- The "SHM" method often fails to perform accurately for structures that possess high value of damping (> 5%). The "SHM" methodology works on the assumption that the noise present in the acquired data is zero mean Gaussian white noise, therefore it fails to work in the presence of measurement noise that is uncorrelated spectral noise.
- The structure that undergoes damage induces nonlinearity and behaves in a complex manner. The damaged structure exhibits a nonlinear structural mode of vibration. The nonlinear structural modes of vibration are not fully understood. Therefore, an adaptive "SHM" technique needs to be developed that is capable of detecting and quantifying damage induced in the nonlinear system.
- "SHM" methodology requires an optimal number of sensors on the system for efficient damage detection. Most of these techniques fail to perform satisfactorily for

sparse sensor conditions. In field application, it is quite likely that all the installed sensors may not be functional at a given time. In such conditions, there must be an efficient "SHM" methodology that works for sparse sensor condition.

- ❖ Damage in any system often induces non-stationarity responses in the dynamic characteristics of the system. This results in dramatical changes in spectral and statistical characteristics of the system at different time instants. Generally, signal decomposition and extraction of dominant features are easier for stationary signals. Whereas, for non-stationary signals to derive any information of damage is difficult and many "SHM" methodologies fail in such conditions.
- ❖ Most of the existing "SHM" techniques are not suitable for online system identification and damage detection. Existing technique demands availability of benchmark data that is seldom available. Therefore, real-time damage detection framework using time recursive formation is not within the current realm of "SHM" tools.
- ❖ The key aspect of any "SHM" framework is to detect and quantify the damage instance, evolution and its severity with help of "DSF". The "DSF" should be sensitive and robust to successfully identify major damage in a structure. However, in most structural damage remains undetected and damages keep incubating and evolved causing dramatic failure of the system. Therefore, efficient DST are needed for damage detection in the structure irrespective of loading and boundary conditions.

To demonstrate the efficacy of all the proposed "SHM" approaches in current work, the experimental study is carried out on two different simplified models of a building. The first model is a shear building and second one is moment resisting frame.

Shear building:

The shear building model is a simplest idealization of a multiple degree of freedom (MDOF) system. The shear building idealization is based on assumptions as:

i) *Rigid floors*: All the floors of a "MDOF" system are considered to be rigid and incompressible. Due to rigid floor assumption, the floor displacement is equally transferred to all the columns, there is no floor rotation and base excitation is applied to all columns equally.

ii) *Lumped mass at each floor level*: The mass of all the floors is assumed to be lumped at centre of mass and the columns are considered as a massless supporting elements.

iii) *Symmetric buildings:* This assumption consider the centre of stiffness and centre of mass to be coincident for each floor. This assumption restricts the change in orientation or position of columns for all the floors of entire building.

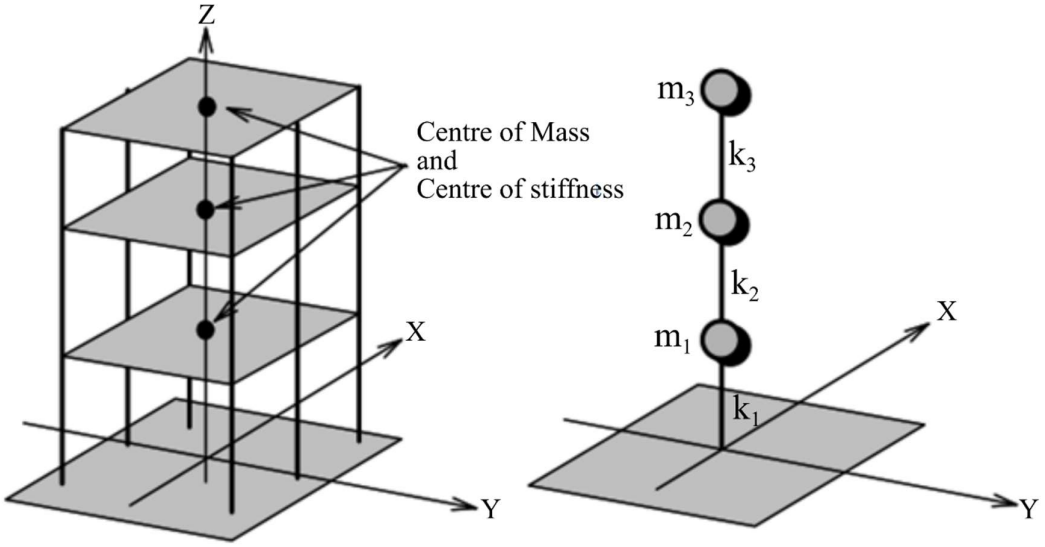

Figure 2.7 Multiple degree of freedom shear building idealization (Winkel, 2017)

iv) *Decoupling of motion in x,y, and z directions, small linear deflections:* Due to no torsional effect and small linear deflection assumption, the motion of a shear building in three perpendicular directions can be analyzed separately. Therefore, a building is idealized as a single column with mass lumped on it (Figure 2.7).

All the above mentioned assumptions, restrict the type of buildings that can be idealized as shear building. However most "MDOF" building's analysis can be idealized as shear building (Chopra, 2001). The equation of motion for a shear building is given below:

$$[\mathbf{M}]\{\ddot{u}\} + [\mathbf{K}]\{u\} = \{F\} \tag{1.1}$$

Moment resisting frames:

The moment frame also known as moment resisting frames (MRF) are the rectilinear assembly of columns and beams. The beams of "MRF" are rigidly connected to columns. The "MRF" provides resistance to lateral loads by developing shear force and bending moments in members and also at joints, this is known as rigid frame action. As the "MRF" resists load as a rigid frame action, therefore without bending the columns and beams, the frame cannot have lateral displacement. Therefore, the strength of entire "MRF" is solely dependent on strength of frame members and their bending stiffness. In many seismic zones, the steel "MRF" (SMRF) have been popular due to its ductile behavior and due to its versatility from architectural point of view.

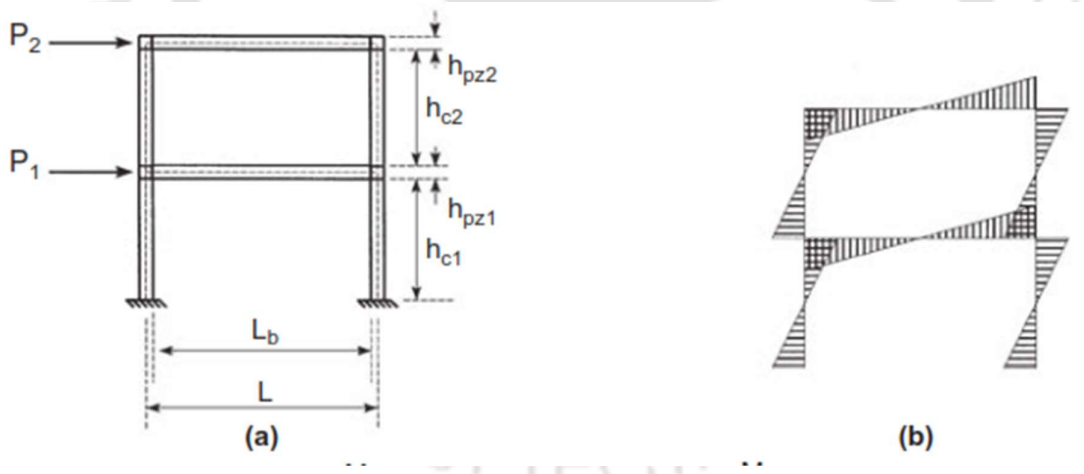

Figure 2.8 Moment resisting frame (a) geometric sketch, and (b) bending moment diagram under lateral loading (Bruneau et al., 2011)

Chapter 3

Principal component analysis based damage quantification approach for shear building subjected to base excitation

3.1 Introduction

Structural health monitoring (SHM) has gathered significant attention of researchers as structure with large damage will eventually lead to collapse resulting in the loss of life. Various events of catastrophic failure have triggered a paradigm shift in the development and practical implementation of health monitoring systems. “SHM” is a process that analyzes the dynamic response of system to identifying the damage, localize it and quantify the severity of damage. “SHM” deals with the prognosis and diagnosis of damage at global and local level. The evolution and progression of damage at local level is quantified with the help of guided wave based approaches (Shelke et al., 2011, Wandowski et al., 2011). Local level “SHM” for a large structure is time consuming and inconvenient due to inaccessibility of each members of structure. Recently, with the advancement in the technology, it is economically convenient to install a smart sensory system on a structure to acquire its dynamic response induced due to natural hazards such as an earthquake.

In the last two decades, vibration-based methods (VBM) for “SHM” have evolved as a reliable tool for damage detection in structures. The extensive literature on vibration-based health monitoring approaches is discussed by many researchers (Doebling et al., 1998, Sohn et al., 2002, Farrar and Worden, 2007). The success of “SHM” approaches using “VBM” is uncertain in presence of noise, for structural systems possessing closely spaced structural modes of vibration. Due to these limitations, they are not suitable for application in realistic scenarios. These limitations of “VBM” operating in spectral domain are overcomed by time domain techniques (Sohn and Farrar, 2001). Time domain “SHM” techniques are sensitive to local damage, therefore can localized the damage and identity the instant of damage

successfully. These methods are broadly categorized as non-parametric and parametric approaches. The time domain methods in conjunction with signal processing techniques extract the modal parameters for system identification (Hayes, 2009).

Some of the popular time domain approaches to extract the modal parameters from acquired response are Wavelet Transform (Taha et al., 2006), Empirical Mode Decomposition (Huang et al., 1998), Auto-Regressive (AR) Model (Lu and Gao, 2005), Hilbert Huang Transform (Yang et al., 2004a), Auto-Regressive Moving Average Model (ARMA) (Bodeux and Golinval, 2001), and Singular Spectrum Analysis (Lakshmi et al., 2017). In presence of uncertainties in "SHM" approaches, the methods such as outlier analysis, Bayesian modal updating , control chart methods are employed to increase the efficacy of damage identification (Beck and Katafygiotis, 1998, Worden et al., 2000, Kullaa, 2003). To model non-stationary signals autoregressive modeling is a commonly accepted tool.

The strictly stationary time series is the one that possesses an identical probabilistic/statistical characteristic for a set of values and its corresponding time shifted set Generally, processing the stationary signal is easier as its probabilistic/statistical characteristic are constant at each time instant. Therefore, with help of entire data the statistics of signal at any time can be evaluated and this information can be used to derive conclusion. Whereas, for non-stationary signals to derive any information, algorithms that are adaptive/ recursive should be used to get information at each time step. Sohn et al. (2000), Bodeux and Golinval (2001), Sohn et al. (2001), and Yao and Pakzad (2012) have developed adaptive feature extraction approach based on the Autoregressive with exogenous input/Autoregressive/Autoregressive with moving average for damage identification in dynamical systems. These approaches assume behavior of structure to be linear and detect the damage with help of changes in extracted feature or the proposed novel damage index derived from these features (Worden et al., 2008).

The above mentioned techniques process the raw data or its decomposed form in order to detect damage. The raw data acquired by the sensors behave as a cryptic signal which does not provide a direct measure of damage. Hence, it is extremely important to extract and evaluate sensitive features from the signals for quantification of damage. The selection of appropriate and sensitive features is determined by the structure under investigation, its magnitude, and type of damage. The commonly used features are a change in the Eigenfrequencies, change in the mode shape, and reduction in the damping of the system (Yang et al., 2004a). The statistical damage sensitive features in terms of statistical distance measures are Mahalanobis distance and Itakura distance between response of healthy and damage state (Kong et al., 1995b, Mosavi et al., 2012). The Time series analysis methods such as Auto-Regressive and Auto-Regressive with exogenous input models are popular methodologies for damage detection (Omenzetter and Brownjohn, 2006, Yao and Pakzad, 2012). The main advantage of these methods is the reliance on data from existing state and not on the reference state. The efficient system identification (SI) techniques utilize features derived from wavelet transform (Hou et al., 2000, Huang et al., 2009, Xin et al., 2019), Hilbert-Huang transform (Huang et al., 1999, Yang et al., 2004a, Roveri and Carcaterra, 2012), Empirical mode decomposition (EMD) (Loutridis, 2004, Li et al., 2007, Tang et al., 2012), and principal component analysis (PCA) (Shlens, 2003, Wall et al., 2003), time-varying autoregressive modelling etc. SI is challenging in a noisy environment and it works on the assumption that the effect of damage on any system is linear, which is not the actual case (Worden et al., 2008).

The current work discusses the development and implementation of health monitoring algorithm on a three storey shear building that is damaged due to repetitive application of base excitation. The proposed approach is based on two popular time domain methods namely “EMD” and “PCA”. In the first step of proposed approach the “EMD” of acquired responses gives the decomposed monocomponent signal known as “IMFs”. Now, the “IMF” possessing maximum energy or correlation is selected as dominant “IMF” for further

analysis. The dominant "IMFs" contains most of the important information and is free of noise and any redundant information (Tang et al., 2012). This step is important for success of proposed approach because any noise or vague information if present, may alter the damage sensitive feature even if no damage is induced in structure. In the next step, the condition indicator based on principal components is evaluated to quantify the change in Eigen structure of signal. The condition indicator is successfully able to identify and quantify the damage induced in shear building. The novelty of the proposed work is that a new algorithm is proposed based on the amalgamation of "EMD" and "PCA" technique. The proposed method initially performs signal decomposition and later on by extracting dominant features, the damage in the shear building is detected and quantified effectively.

3.2 Experimental investigation

The experimental studies related to the application of extreme loadings such as earthquake on a structure and its health monitoring are limited. The current work presents an experimental investigation on one bay, three-storey shear building subjected to repetitive base excitation. The experimental investigation also demonstrates the effectiveness and robustness of the proposed health monitoring algorithm. The algorithm proposed in current work deals with quantification of damage in a shear building whose members are plasticized due to repetitive application of base excitation.

Dimensions of shear building:

The slab, columns, and beams of the shear building consist of aluminum angle-section and steel rectangular plate respectively, the dimension of which are presented in Table 3.1. The total height of the structure was 1.5 m with each storey height being 0.5 m. The entire frame was rigidly mounted on a rigid platform to attain fixity condition at the base.

Table 3.1 Dimension of structural components of shear building

Structural component	Dimension	Material and Section
Slab	300 mm x 300 mm x 16 mm	Steel rectangular plate
Column	19 mm x 19 mm x 2 mm	Aluminum angle section
Beam	19 mm x 19 mm x 2 mm	Aluminum angle section

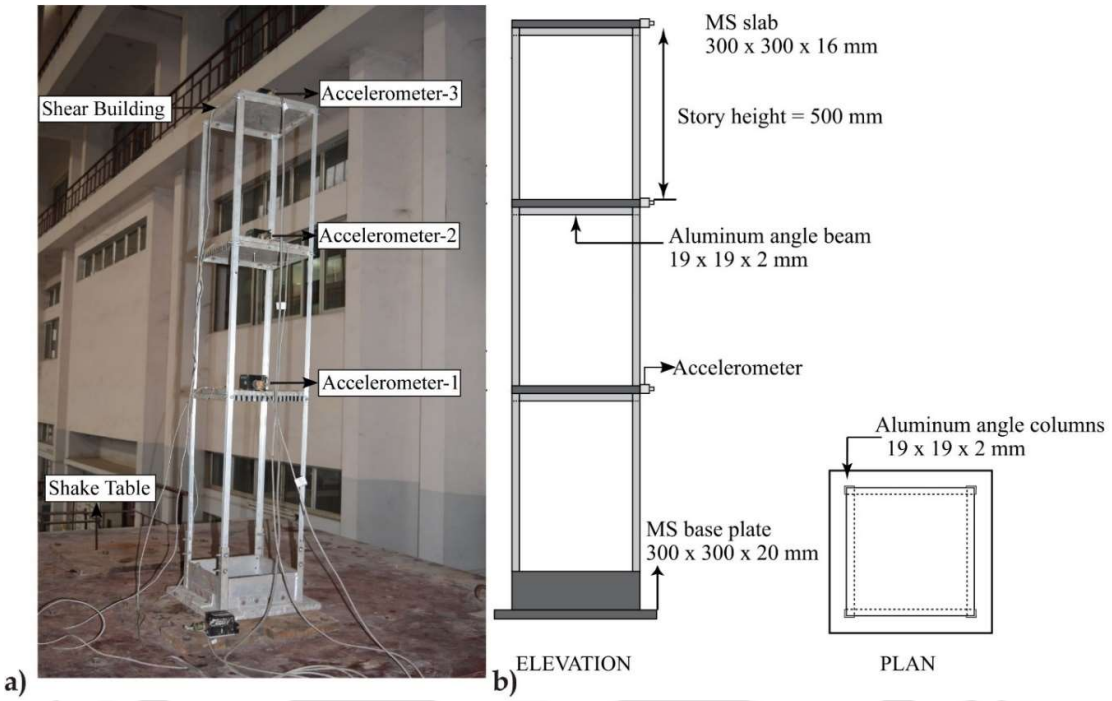

Figure 3.1 (a) Experimental setup and; (b) schematic sketch of steel frame

Shake table experimental setup and instrumentation:

The image of the shear building mounted on a shake table along with its schematic diagram are shown in Figure 3.1. The shear building was rigidly mounted on a uniaxial shake table (model no. Bi-00-300). The base excitation applied on the shear building was a white noise possessing frequency bandwidth ranging from 0.01 Hz to 3 Hz and 45 mm as maximum amplitude (Figure 3.2). The detailed technical specifications of the shake table equipped with a control hydraulic actuator are mentioned in Table 3.2.

Table 3.2 Detailed specifications of the shake table

Load capacity	5000 kg
Dimension	150 cm x 150 cm
Acceleration	-2.0g to +2.0g
Maximum velocity	153 cm/sec
Linear displacement	-500 to +500 mm

The repetitive application of white noise base excitation (WNBE) was imparted for four times; each time the same WNBE was applied. Repetitive loading is a realistic scenario in

some earthquake-prone areas where tectonic movements are often expected to occur that may lead to maximum devastation. Progressive degradation to the system and nonlinearity was induced in the shear building due to repetitive application of WNBE. The image of damaged specimen at the end of experimental investigation is shown in Figure 3.3.

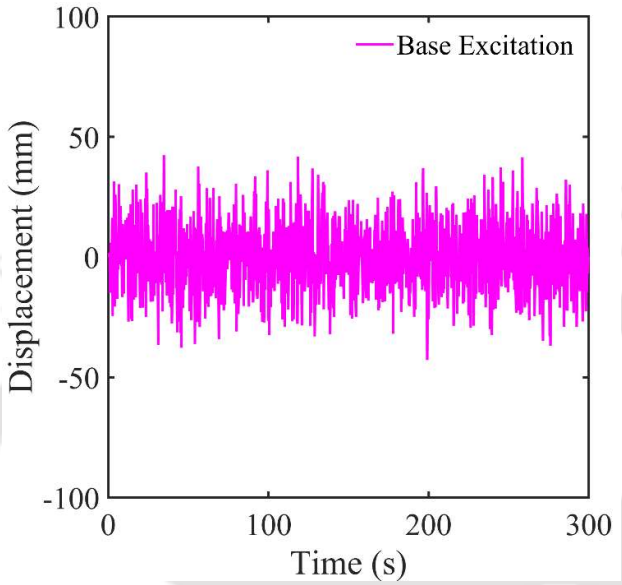

Figure 3.2 Time history plot of WNBE applied on three storey shear building

To acquire the dynamic response of the shear building, it was instrumented with three number of Honeywell accelerometers '*TEDS* by *HBM*^{TM}' that are used to acquire the acceleration response of all the floors in the direction of loading. The Honeywell accelerometers can measure acceleration amplitudes in between the range of -5g to +5g. The response acceleration data was acquired using the Data Acquisition System namely: QuantumX MX410 *HBM*^{TM}. The sampling frequency for all the experiments was kept fixed at 100 Hz. Thus in this way, the shear building was excited with a WNBE. The shake table was displacement controlled, therefore the WNBE was a displacement time history.

Figure 3.3 Image of damaged shear building at the end of experimental investigation

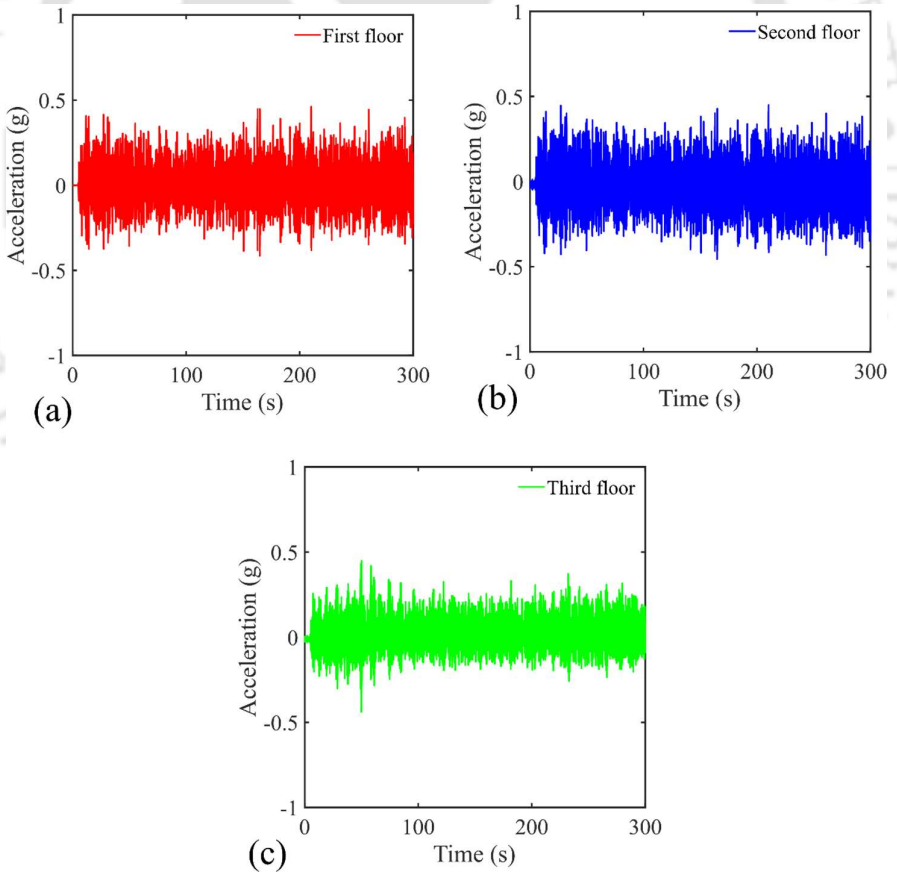

Figure 3.4 Dynamic response of shear building subjected to WNBE for a) first floor, b) second floor and c) third floor

The subsequent sections concentrate on the building blocks of the proposed damage detection approach for separating pristine and healthy responses and later on presenting the results of proposed approach along with quantifying the extent of damage. The shear building was instrumented with three accelerometers at each floor level to acquire the dynamic response. The time history of the acceleration response at all the three floors of the shear building are shown in Figure 3.4. The Fourier analysis of the acceleration response was performed to evaluate the dominant excited frequency of shear building after each experiment.

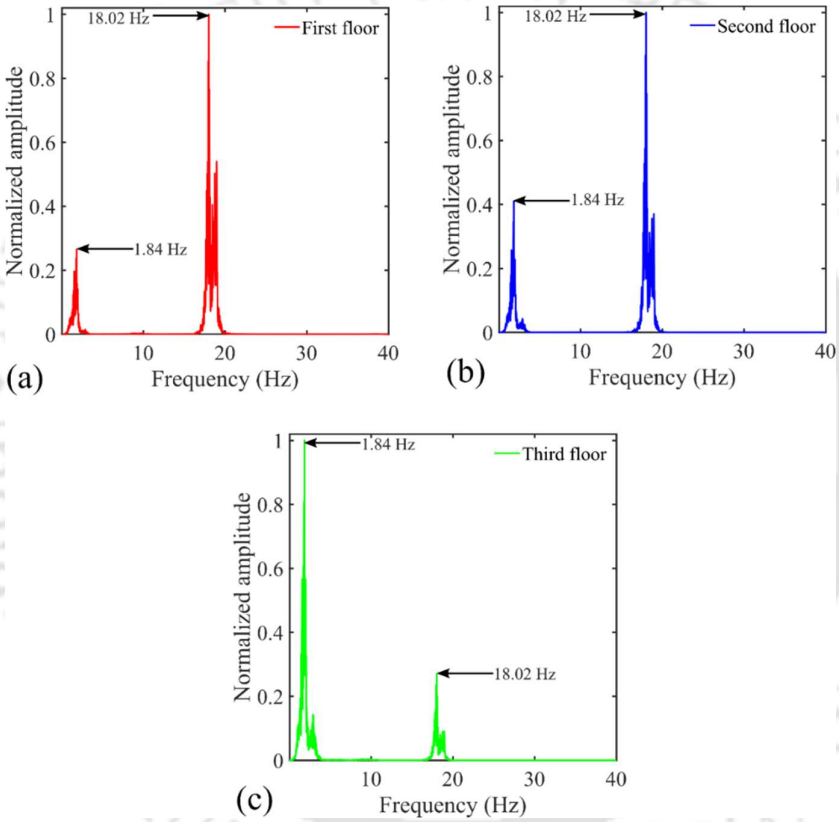

Figure 3.5 Frequency spectra of shear building subjected to WNBE for a) first floor, b) second floor and c) third floor

The dominant frequencies for all the experiments of shear building were evaluated and it was observed that the changes in dominant frequencies demonstrates negligible changes. Therefore, the frequency domain approach fails to evaluate the component level damages in the structure. The inefficiency of the spectral domain method is due to the fact that response in frequency domain is modeled considering only lower order linear dynamic modes. Thus,

inefficiency of spectral domain emphasized the need for a robust time-domain algorithm that can quantify the damage induced in the shear building.

3.3 Building blocks of the proposed algorithm for damage detection

3.3.1 Principal component analysis

Principal Component Analysis (PCA) is a statistical approach that finds the combinations of variables to describe important information in the data. "PCA" is closely interrelated to Singular Value Decomposition (SVD) and Proper Orthogonal Decomposition (Chatterjee, 2000, Wall et al., 2003). In batch-wise "PCA", the dataset $Y \in R^{n \times m}$ is initially altered to a zero-mean dataset $\overline{Y} \in R^{n \times m}$, where $\overline{Y} = Y - E(Y)$, n is number of samples, m is number of variables and $E(X)$ is the mean of the dataset Y. Then after the covariance matrix C_o of the zero mean data is obtained as:

$$[\mathbf{C_o}]_{m \times m} = \frac{1}{n-1}[\overline{\mathbf{Y}}]^T_{m \times n}[\overline{\mathbf{Y}}]_{n \times m} \tag{3.1}$$

Now the Eigen analysis of the covariance matrix is done (equation (3.2)), the output of Eigen analysis is matrix Q where columns of $Q = [q_1, q_2, q_3 \ldots q_m]$ are eigenvectors of C_o and the diagonal matrix λ consists of the eigenvalues of C_o.

$$[\mathbf{C_o}]_{m \times m}[\mathbf{Q}]_{m \times m} = [\boldsymbol{\lambda}]_{m \times m}[\mathbf{Q}]_{m \times m} \tag{3.2}$$

The eigenvectors that corresponds to the smaller eigenvalues (i.e. the Eigen-values with magnitude lower than the 25% of maximum Eigen-value) contains least information, hence are eliminated (Mujica et al., 2008). The eigenvectors corresponding to dominant Eigen-values are designated as principal components (PCs). The transformed data set X after projection in new Eigen space will be *p*-dimensional:

$$[\overline{\mathbf{Y}}]_{n \times m} = [\mathbf{X}]_{n \times p}[\mathbf{Q}]^T_{m \times p} \tag{3.3}$$

where '*p*' is the number of dominant principal components.

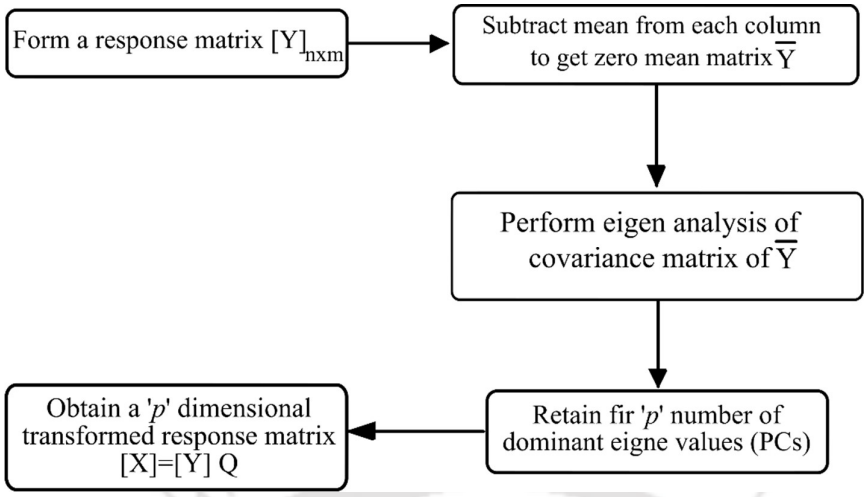

Figure 3.6 Block diagram of "PCA" algorithm

The transformed dataset is of reduced dimension; therefore, the computational effort is reduced without compromising the important information. Now, the projection of X back to the original data set is $\mathbf{X}\mathbf{Q}^{\mathrm{T}}$. In procedure of "PCA", some of the least dominant eigenvectors are eliminated, this introduces a residual error matrix [E]:

$$[\mathbf{E}]_{n \times m} = [\bar{\mathbf{Y}}]_{n \times m} - [\mathbf{X}]_{n \times p}[\mathbf{Q}]^{\mathrm{T}}_{p \times m} \tag{3.4}$$

The block diagram explaining the procedure of "PCA" algorithm is presented in Figure 3.6.

3.3.2 Empirical mode decomposition:

Any acquired response signal X(t) will always consists of an unavoidable part, known as noise. Hence the acquired signal will always consist of original signal $s(t)$ mixed with nonlinear noise $n(t)$:

$$\{\mathrm{X}(t)\} = \{s(t)\} + \{n(t)\} \tag{3.5}$$

In case of non-stationary and non-linear processes it is very difficult to separate noise with help of conventional filters even though the frequency and time-scale of signal and noise are distinct. For such case, Empirical mode decomposition (EMD) proves to be a helpful tool for noise deduction and signal decomposition. "EMD" decomposes an acquired response signal into mono-component intrinsic mode functions (IMFs). An "IMF" possess single local frequency content, no two different "IMFs" have same frequency content at a particular time instant and "IMF" is always symmetric.

The procedure to get the "IMFs" is as follows: Foremost with help of cubic spline fitting of entire signal over all local minima is done to obtain a lower envelop of signal; in the same way an upper envelope is also obtained. These envelopes must cover the entire signal and mean of both the envelope is μ_1. The difference between mean and signal is $g_1 = X(t) - \mu_1$. The signal g_1 is most commonly referred to as a proto-mode function (PMF). The PMF is treated further as signal and same process is repeated. This repetitive process to get true "IMF" is known as 'sifting', at the end of first sifting g_2 is obtained as:

$$\{g_2\} = \{g_1\} - \boldsymbol{\mu}_2 \tag{3.6}$$

The accuracy and success of "EMD" is dependent on stopping criteria of sifting. One of the common stopping criteria for sifting is with help of standard deviation (equation (3.7)) between two successive sifted events.

The termination criterion is reached when value of standard deviation reaches between 0.2-0.3.

$$\mathrm{SD} = \sum_{t=0}^{T} \left[\frac{|\{ g_k(t) - g_{k-1}(t) \}|^2}{\{g_k^2(t)\}} \right] \tag{3.7}$$

As soon as value of standard deviation is close to the stopping criterion, the process of sifting is terminated and if sifting ends after '*k*' repetition then the first "IMF" is:

$$\{a_1\} = \{g_k\} \tag{3.8}$$

Now, the obtained "IMF" is deducted from the original signal to obtain a residue as $R_1 = X(t) - a_1$. The entire procedure of obtaining "IMFs" is repeated till R_n becomes a monotonic function from which no "IMF" can be obtained.

$$\begin{aligned} \{R_1\} - \{a_2\} &= \{R_2\}, \\ &\vdots \\ \{R_{n-1}\} - \{a_n\} &= \{R_n\} \end{aligned} \tag{3.9}$$

The final residue can be different than null vector, even if the mean of original data is zero. In order to obtain original signal from "IMFs" following relation must be used:

$$\{X(t)\} = \sum_{i=1}^{n} \{a_i\} + \{R_n\} \tag{3.10}$$

The entire process of "EMD" is represented in a flowchart presented in Figure 3.7.

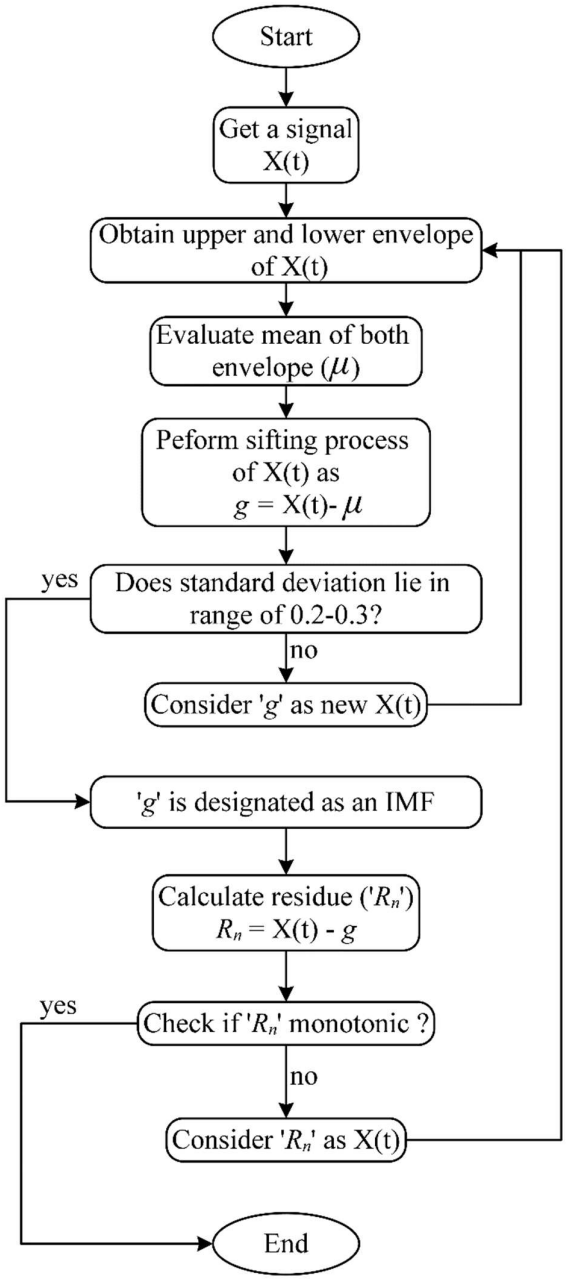

Figure 3.7 Flowchart representing the steps of Empirical mode decomposition

3.4 Algorithm for damage detection in shear building

The proposed algorithm is described in detail considering the idealized structure presented in current work:

Step-1: Acquire the response signal and construct a response matrix

The shear building is subjected to white noise base excitation and the acceleration response is acquired at each storey. The acquired acceleration response forms a response matrix [A] of size N x 3, where numeric 3 denotes the total number of accelerometers and N denotes the total number of acquried data points

$$[\mathbf{A}]=\begin{bmatrix} x(t)_1 & y(t)_1 & z_1 \\ \vdots & \vdots & \vdots \\ x(t)_N & y(t)_N & z(t)_N \end{bmatrix}_{N\,\mathrm{x}\,3}$$

Step-2: Perform "EMD" of response matrix.

The "EMD" of response matrix is mathematically represented as:

$$\{A(\mathrm{t})\} = \sum_{\mathrm{i}=1}^{\mathrm{n}} \{\mathrm{c_i}\} + \{\mathrm{r_n}\}$$

where $\{A(\mathrm{t})\}$ represents a column vector of response matrix, c_i represents ith "IMF" of $\{A(\mathrm{t})\}$, and r_n is the residue signal.

The "EMD" of any column vector of [A] will result in numerous "IMFs".

$$EMD\big(x(t)\big)=\big[\{IMF_{1x}\} \quad \cdots \quad \{IMF_{mx}\}\big]$$

where '*m*' is the total number of "IMFs" in which the original signal is decomposed by "EMD" and $\{IMF_{1x}\}$ represents the first "IMF".

In the next step the correlation or energy of each mono-component "IMF" is evaluated and the "IMF" that corresponds to maximum correlation or energy is considered as the dominant "IMF".

$$\mathbf{E}(\{x_j(t)\})=\frac{\sum_{i=1}^{N}\left|\{x_j(t_i)\}\right|^2}{\mathbf{T}}$$

For e.g. if, $E\{IMF_{ix}\}>E\{IMF_{jx}\}>E\{IMF_{kx}\}>\cdots>E\{IMF_{lx}\}$ then i^{th} "IMF" is considered as most dominating "IMF" and is processed further.

Step-3: Perform "PCA" of all combinations of "IMFs".

This step, deals with "PCA" of all the possible two-dimensional combination of response matrix.

$$[\mathbf{X}]_{n \times p} = [\overline{\mathbf{Y}}]_{n \times m} \; [\mathbf{Q}]_{m \times p}$$

where columns of $[\mathbf{Q}] = [q_1, q_2, q_3 \ldots q_m]$ are principal components.

In current work, the total number of variables are three that will lead to at most three 2-dimensional combinations as:

$$[\mathbf{C-1}] = \begin{bmatrix} x(t)_1 & y(t)_1 \\ \vdots & \vdots \\ x(t)_N & y(t)_N \end{bmatrix}, [\mathbf{C-2}] = \begin{bmatrix} y(t)_1 & z(t)_1 \\ \vdots & \vdots \\ y(t)_N & z(t)_N \end{bmatrix}, [\mathbf{C-3}] = \begin{bmatrix} z(t)_1 & x(t)_1 \\ \vdots & \vdots \\ z(t)_N & x(t)_N \end{bmatrix}$$

where, C-1, C-2 and C-3 represent combination-1, combination-2, and combination-3.

The "PCA" give a unique set of principal components and principal angles corresponding to a specific combination. The comprehensive description of "PCA" is given in section 3.3.1. The principal angles corresponding to a damage case and healthy (reference) case are denoted by θ_d and θ_{ref} respectively.

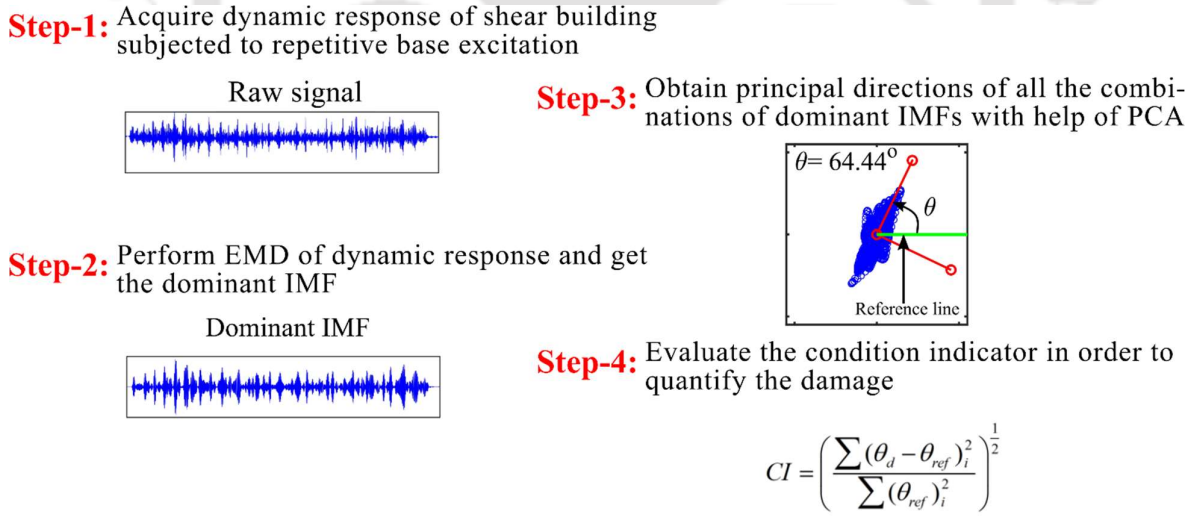

Figure 3.8 Important steps of the proposed damage detection algorithm

Step-4: Evaluation of condition indicator to quantify the damage.

The condition indicator (CI) proposed in current work is based on the value of the principal angle for reference and damage case. This step deal with evaluation of CI for each damage state.

$$\mathbf{CI} = \left(\frac{\sum (\boldsymbol{\theta}_d - \boldsymbol{\theta}_{ref})_i^2}{\sum (\boldsymbol{\theta}_{ref})_i^2} \right)^{\frac{1}{2}}$$

where *i* is number of all the possible combinations of response matrix. As mentioned in step-3 the value of i for present case is 'three'.

The entire process of algorithm is also presented in Figure 3.8.

3.5 Results and discussion

The response signals acquired by accelerometers are collected for different states, i.e. pristine state and the damaged states. The current section explains the results and conclusions for damage detection with help of the proposed approach. Initially, the procedure of selecting the dominant "IMF" with help of two different approach is discussed. Further, the procedure to evaluate the principal components with help of "PCA" is presented along with the results. Lastly, to quantify the damage induced, a condition indicator is formulated. The condition indicator quantifies the damage by numerically evaluating the magnitude of change in angle between PCs of healthy and damaged state.

3.5.1 Empirical mode decomposition of response signals

The response signals acquired are decomposed into monocomponent Intrinsic Mode Functions (IMFs) with the help of "EMD" (section 3.3.2). Each of the "IMF" obtained represents an integral timescale characteristic of the original signal and are mono-component. The "IMFs" of a signal received by a sensor for pristine state are shown in Figure 3.9. In order to precisely quantify the damage in the shear building, the response signals are examined through their dominant "IMFs". The "IMF" that has a maximum correlation with the original signal is the dominant one, also it has no vague data (e.g. high-frequency noise).

The commonly adopted approach for selection of dominant "IMF" are correlation-based approach and energy-based approach.

3.5.1.1 Energy based approach

The first approach uses the maximum/average energy content of the "IMF", which can be evaluated as:

$$\mathbf{E}(\{x_j(t)\}) = \frac{\sum_{i=1}^{N} \left|\{x_j(t_i)\}\right|^2}{\mathbf{T}} \tag{3.11}$$

where $x_j(t)$ represents the j^{th} "IMF" of the measured signal $x(t)$, T is the total duration of the signal and N is the total number of samples. The contribution of an "IMF" towards the original signal is directly proportional to the energy content.

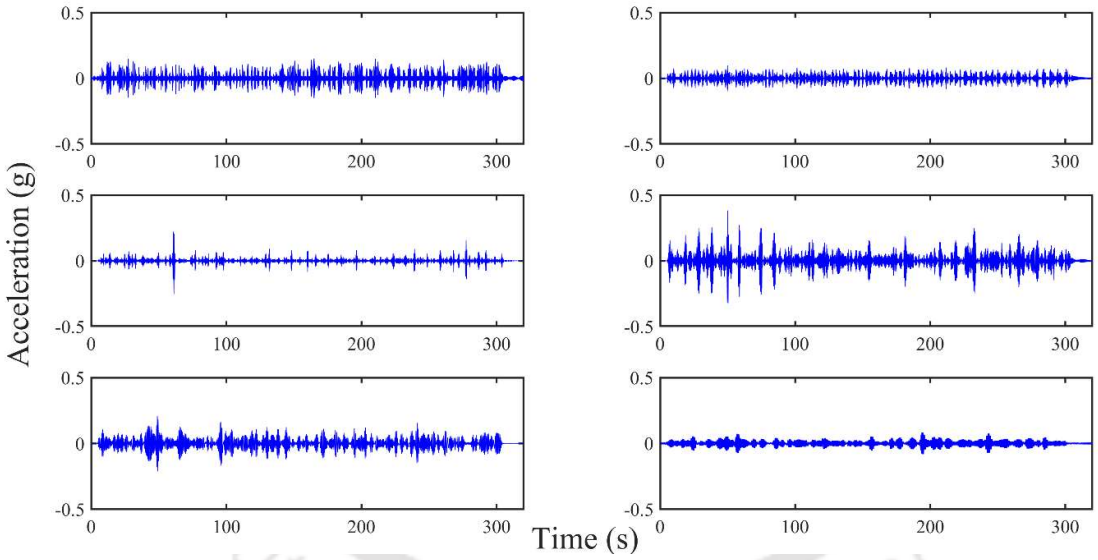

Figure 3.9 "IMFs" corresponding to pristine state signal received by a sensor for baseline state of system

3.5.1.2 Correlation-based approach

The second approach estimates the correlation among the "IMFs" and original signal. The "IMF" that correlates maximum with the original signal is the most dominant "IMF". The correlation coefficient is calculated as

$$\Lambda(x(t), x_j(t)) = \frac{C_{x(t)x_j(t)}}{\sigma_{x(t)}\sigma_{x_j(t)}} \tag{3.12}$$

where $x(t)$ and $x_j(t)$ represent the original signal and its j^{th} "IMF", $C_{x(t)x_j(t)}$ is the covariance between $x(t)$ and $x_j(t)$, and $\sigma_{x(t)}$ and $\sigma_{x_j(t)}$ are the standard deviations.

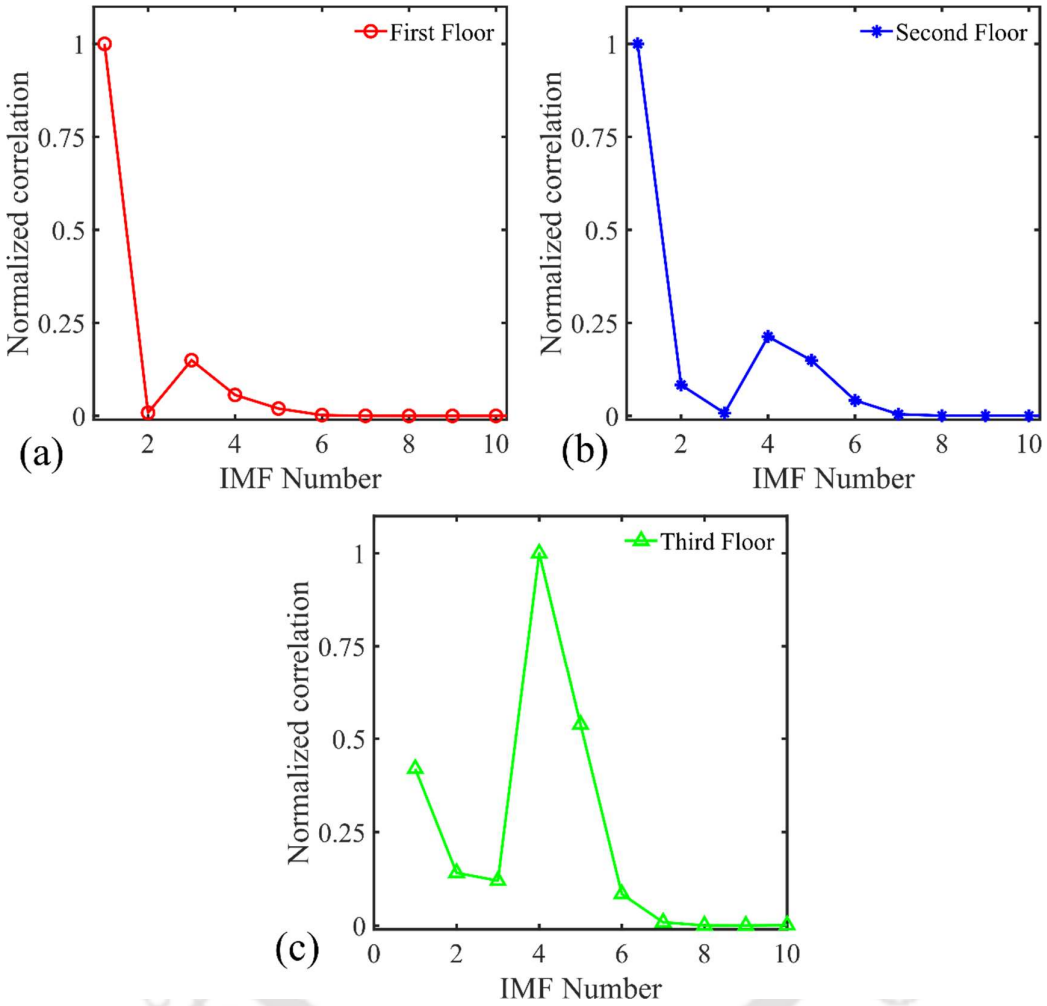

Figure 3.10 Normalized correlation of all "IMFs" corresponding to response acquired by accelerometers of both the floors in direction of loading for reference state

In current work, correlation-based approach is implemented and the correlation of each "IMF" is calculated. The normalized value of correlation with respect to the maximum value is shown in Figure 3.10. The dominant or the most contributing "IMF" is the one that have a maximum correlation. For further examination, the dominant "IMFs" are considered instead of the original signal. This step also takes care of de-noising of the signal and enabling elimination of ambient instabilities. Once the dominant "IMFs" are selected for reference and

damage states. They are used to quantify damage using Principal Component Analysis as explained in the following section.

3.5.2 Principal component analysis of dominant intrinsic mode functions

The arrangement of accelerometers for presented experimental investigation provides three response signals, from sensors in direction of loading. Assuming [**X**] to be the response matrix for a given state of the shear building (i.e. reference or damaged state). The columns of matrix [**X**] consists of the response signal received by all the accelerometers. For "PCA" instead of the acquired response matrix, another matrix [$\mathbf{X}_{IMF}$] is considered. The columns of [$\mathbf{X}_{IMF}$] contains the dominant "IMFs" corresponding to columns of the response matrix [**X**]. In the present study, there is one pristine and three damage state response leading to four distinct [$\mathbf{X}_{IMF}$] matrix. The damage is induced in the shear building due to multiple implications of base excitation. The presented study offers a quantitative demonstration of the damaged states with respect to the pristine state using "PCA". Principal component analysis is a tool for realizing a given set of data in a transformed set of coordinates which reduces the redundancy in the dataset. The transformed coordinates are a unique grouping of the original coordinates and are uncorrelated. "PCA" helps to evaluate the principal structure of data that can be explored as a damage quantification tool.

As explained in section 3.3.1, to obtain the PCs, the Eigen analysis of covariance matrix ($[\mathbf{C}]_{m\ x\ m}$) of $[\mathbf{X}_{IMF}]_{n\ x\ m}$ is done where n is the number of observations and m is the number of observed data (dimension of "PCA).

The PCs obtained using "PCA" are an essential indicator of the fundamental Eigen-structure of the data. In the present case, the alterations in the Eigen-structure of the matrix [$\mathbf{X}_{IMF}$] corresponding to pristine and damage states are examined. This step is followed on the reasoning that any change in the state of the shear building will alter the Eigen-structure of the response data. The alteration in the Eigen-structure of the data is measured by the variations in the angle of the PCs. Let $\boldsymbol{\theta}_{ref}, \boldsymbol{\theta}_{d_1}, \boldsymbol{\theta}_{d_2}$ and $\boldsymbol{\theta}_{d_3}$ be the angle of PCs w.r.t to reference axis corresponding to pristine and three damage states respectively (Figure 3.11).

3.5.3 Evaluation of CI

In the current study as the total number of accelerometer instrumented on structure are three. Therefore, the potential combinations for "PCA" are: combination-1) first floor acceleration and second floor acceleration, combination-2) second floor acceleration and third floor acceleration, and, combination-3) third floor acceleration and first floor acceleration in direction of loading. These combinations are plotted in Figure 3.11 to form a Eigen space. For all the combinations of the acquired response matrix, $\theta_{ref}, \theta_{d_1}, \theta_{d_2}$ and θ_{d_3} are calculated. Based on the measurements of $\theta_{ref}, \theta_{d_1}, \theta_{d_2}$ and θ_{d_3} a condition indicator (CI) is proposed as follows:

$$\mathbf{CI} = \left(\frac{\sum (\boldsymbol{\theta}_d - \boldsymbol{\theta}_{ref})_i^2}{\sum (\boldsymbol{\theta}_{ref})_i^2} \right)^{\frac{1}{2}} \tag{3.13}$$

where *i* is number of combinations. The values of the CI have been tabulated in Table 3.3.

Table 3.3 Quantitative alterations in condition indicator for different damage states of shear building subjected to repetitive base excitation

Damage Cases	Damage 1	Damage 2	Damage 3
CI values	0.03	0.1	0.24

From the results of CI, it can be evidently stated that the Damage 3 case reflect more severe damage than Damage-1 and Damage-2. The proposed CI helps to quantify the progressive damage induced in the shear building for the various damage states of current experimental investigation. It should be noted that for any damage case, even if the magnitude of loading is different, the proposed CI can quantify the progressive damage. Therefore, the magnitude of loading does not affect the robustness of the proposed damage detection algorithm.

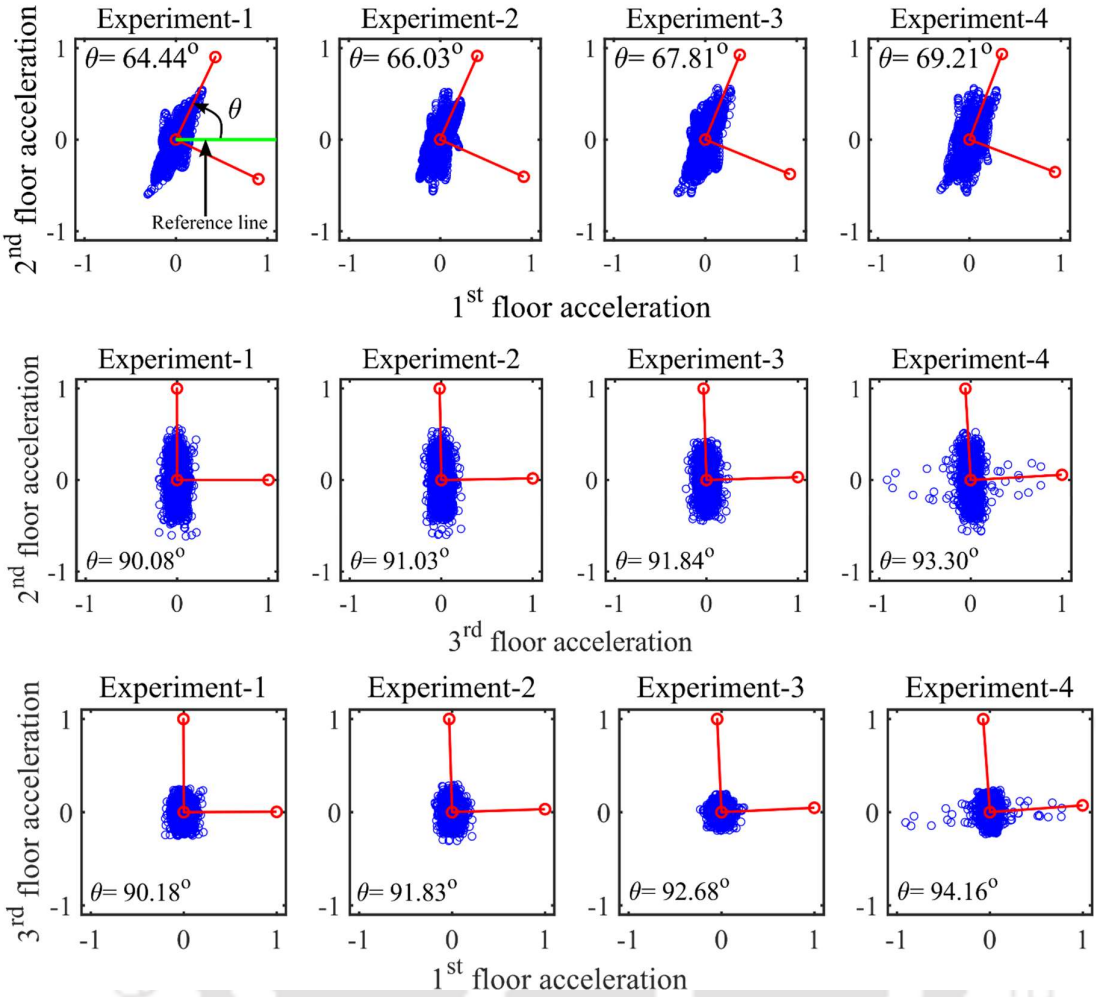

Figure 3.11 Principal components corresponding to pristine and damage states for all the combinations (Note: experiment-1 corresponds to pristine state, experiment-2, experiment-3, and experiment-4 corresponds to damage-1, damage-2, and damage-3 respectively)

3.6 Conclusion

The outcome of the work presented in the current study is to quantify the progressive damage induced in the shear building using "EMD" and "PCA". The damage is induced in the shear building by application of multiple white noise base excitation. By repetitive application of base excitation, an attempt has been made to replicate a realistic scenario of a structure being subjected to natural earthquakes multiple times in its life span. Any structure being subjected to multiple base excitation is expected to accumulate damage progressively. To detect the progressive damage, the proposed algorithm implements "EMD" on the acquired dynamic

response and separates dominant modes as the dominant "IMFs". Subsequently, the "IMF" is analyzed by the proposed damage detection algorithm to estimate condition indicator. The occurrence of damage and its progression is quantified with the help of the alteration in the value of condition indicator (CI). The value of CI corresponding to damage states of present work are 0.03, 0.1, and 0.24. Instead, of determining the location of damage, the magnitude of the damage is quantified with the help of CI. The relative change in magnitude of CI reflects the manifestation and severity of damage. Instead of processing raw data, "IMFs" are processed for evaluation of CI because due to "EMD" noise and redundant information is suppressed. The noise if present may alter the value of CI significantly, but "EMD" helps to avoid the false interpretation. The use of "EMD" along with "PCA" makes the algorithm more robust and accurate. The proposed approach is capable of quantifying the damage with the help of a condition indicator that could be appropriate for various "SHM" framework.

Chapter 4

Damage detection using dissimilarity in phase space topology of shear-building subjected to shock wave loading

4.1 Introduction

Structural health monitoring (SHM) involves detection, localization, and quantification of damage using dynamic response. "SHM" technique includes diagnosis and prognosis of damage and cracks evolution at local and global level. At the local level, the spatial-temporal evolution of damage feature is quantified using guided wave techniques (Shelke et al., 2011, Wandowski et al., 2011). For a large dynamical system, local damage detection technique is infeasible due to inaccessibility of structural members.

Vibration-based methods (VBM) in conjunction with statistical novelty detection analysis have evolved as a reliable tool for damage detection. The detailed literature review on vibration-based "SHM" is presented by many researchers (Doebling et al., 1998, Sohn et al., 2002, Farrar and Worden, 2007). System identification (SI) using VB technique is challenging in a noisy environment and for closely spaced linear normal modes. Vibration-based techniques have low resolution in detection of small-scale damage, which makes it unattractive in practical scenarios. To a certain extent, these limitations are overcome by statistical pattern recognition and time series analysis that has broader applicability compared to "VBM" (Sohn and Farrar, 2001). Various time series approaches such as wavelet analysis, Hilbert-Huang transform, auto-regressive models, autoregressive moving average models are used to detect damage (Bodeux and Golinval, 2001, Yang et al., 2004a, Lu and Gao, 2005, Taha et al., 2006). Methods such as control chart methods, outlier analysis, and Bayesian model updating are employed for improving the accuracy of damage detection in the presence of uncertainties in "SHM" methodology (Beck and Katafygiotis, 1998, Worden et al., 2000, Kullaa, 2003). Statistical damage detection techniques involve measurement of damage

sensitive features in terms of statistical distance measures namely Mahalanobis distance (MD) (Gul and Catbas, 2009, Figueiredo et al., 2011, Mosavi et al., 2012, Yeager et al., 2018), Bhattacharya distance (Guorong et al., 1996), and Rao's distance (McLachlan, 1999, Liu et al., 2014).

Most of the aforementioned techniques work on the assumption that the effect of damage on the system is linear, whereas the process of evolution of damage in the system is essentially non-linear (Worden et al., 2008). The mild nonlinearity in the structural system is addressed by linearizing the nonlinear models and applying recursive time domain SI techniques (Peeters et al., 2009). Katkhuda and Haldar (2008) have developed a technique using Extended Kalman Filter Weighted Global Iteration (EKF-WGI) for nonlinear system identification using sparse sensors in the presence of noise. Recently, SI has been extended to separate the closely spaced linear and nonlinear modes of vibration from noisy output data using principal component analysis (PCA), blind source separation (BSS) and second-order blind identification (SOBI) (Belouchrani et al., 1997, Shlens, 2003, Cichocki and Amari, 2003, Antoni, 2005). The data-driven model based on phase space reconstruction of the response topography has gained significant research interest in nonlinear damage identification. Phase space is a graphical representation of measured state variables of a system in the multidimensional orthogonal coordinate system. Phase space reconstruction (PSR) relies on the development of nonlinear attractor model of system dynamics and quantifying the geometrical and statistical predictor distance between the response of pristine state and damage state (Nichols et al., 2003, Zhang et al., 2017).

For nonlinear dynamical systems, the damage sensitive features (DSFs) extracted from phase space topology are superior to conventional modal features (Todd et al., 2001, Liu et al., 2016). The response of the structure excited using high-frequency loadings such as ground motion, impact loading, blast, and shock loading are difficult to represent in phase space due to high dimensionality. Therefore, in this study, a damage detection algorithm is proposed that is based on representation of high dimensional response in phase space and

thereby detect damage with help of "DSFs" evaluated from phase portrait. In order to improve the detectability and reduce the computational effort, the algorithm is categorized into two phases. In the first phase, "PCA" is used to reduce the dimension of the multivariate dynamic system response by retaining dominant features. The changes in principal orthogonal components (POC) of reduced data set is used to detect the migration of linear normal modes to nonlinear modes and segregating minor damages from perturbative damages. In the second phase, the embedded dimension of the highly nonlinear and non-stationary dominant response is reduced using Empirical mode decomposition (EMD). The dominant "IMF" obtain by "EMD" are graphically represented in a phase space diagram. Changes in geometrical properties of phase space topology are used to derive "DSFs" such as "CPST" and "MDPST" to predict local damage.

In order to demonstrate the applicability and strength of the proposed methodology, "SHM" of a three-storey shear structure was performed that is damaged through shock wave loading. In literature, "SHM" using phase space approach is limited to the stochastic random process of slow modulation of amplitude and frequency. Limited studies exist in time and frequency domain to detect damage under extreme loading condition. Shock-induced damage detection in the structure is challenging, as the plastification of the structural component occurs in time scale equivalent to the duration of shock wave loading (i.e. few milliseconds). Shock loading induces nonlinear plastic deformation in the structure resulting in an exhibition of non-normal dynamic modes of vibration. The phase space approach is not explored to detect damage in the structure subjected to extreme loading. Two robust "DSFs" namely change in phase space topology (CPST) and Mahalanobis distance between phase space topology (MDPST) are utilized to detect a defect in the structure damage through shock loading. In the following sections, a detailed discussion of the formulation of the algorithm is presented.

4.2 Principal component analysis

To reduce the computation time and enhance the detectability of damage, the algorithm classifies the response in two distinct class. The principal component analysis (PCA) is conducted on the response data to obtain changes in "POCs" for progressive damage state. Damage arising from a minor perturbation in material properties are segregated from minor scale damage by setting a threshold limit on the changes in "POCs". "PCA" is a multivariate statistical technique used for dimension reduction and system identification that is closely related to Proper Orthogonal Decomposition and Singular Value Decomposition (SVD) (Chatterjee, 2000, Wall et al., 2003). "PCA" of N x n dimensional data separates dataset into n linear, mutually orthogonal sets by Eigen-analysis of the covariance matrix (Shlens, 2003). "PCA" decomposes a matrix $\mathrm{A}_{N\mathrm{x}n}$, which contains N observations and n variables, into a transformed subspace of reduced dimension. The Eigenvector corresponding to highest Eigenvalue contains most relevant information and is called principal orthogonal component (POC) of corresponding data. Only dominant PC's are retained for transformation, and thus residual matrix E is formed. The mathematical representation of "PCA" on response matrix $[\mathbf{A}]_{N\mathrm{x}n}$ is given as follows:

$$[\mathbf{A}] = [\mathbf{Z}][\mathbf{Q}]^{\mathrm{T}} + [\mathbf{E}] \tag{4.1}$$

where [**Z**] is transformed data set, columns [**Q**] are eigenvectors and [**E**] is a residual error. In this chapter, "PCA" of acceleration response $[\mathbf{A}]_{N\mathrm{x}n}$ is evaluated to obtain the changes in "POCs" that manifest the progressive evolution of damage. The details of the "PCA" algorithm are discussed in section 3.3.1

4.3 Empirical mode decomposition

Empirical Mode Decomposition (EMD) is a technique to decompose a time history signal $X(t)$ into a set of mono-component signals (Huang et al., 1998, Huang et al., 1999). The process of "EMD" decomposes a signal into elemental signals called "intrinsic mode

functions" (IMFs). The "IMFs" are symmetric and mono-component (Li et al., 2007). The details regarding procedure of "EMD" are discussed in section 3.3.2

4.4 Phase space reconstruction

The multi-dimensional phase-space trajectory (PST) is a useful tool to represent the dynamic of state variables. A unique point in the "PST" provides the information of all the dynamic state variables at a given time instant. The dynamic response of a d-dimension system can be represented mathematically by the first-order differential equation:

$$\dot{x} = T(x,t) \tag{4.2}$$

where $\dot{x}$ is the first derivative of state variable and T is a nonlinear function of time t and state variables (x). In a real-world scenario, it is difficult to measure all the state variables such as displacement, velocity, and acceleration through experiments. However, this limitation is overcome by applying embedding theorems proposed by Takens' (Takens', 1981). The embedded theorem states that the complete information of dynamical system could be numerically reconstructed by only one state variable measured accurately. In order to reconstruct the trajectories, the time series of a single measured variable is concatenated m times, each with a delay equivalent to τ. Hence at any time n, the attractor can be represented as,

$$[\mathbf{X}(n)] = [x(n), x(n+\boldsymbol{\tau}), ..., x(n+(m-1)\boldsymbol{\tau})] \tag{4.3}$$

Where 'm' is the embedding dimension and 'τ' is the time lag, this method of reconstruction is called the method of delays.

4.4.1 Average mutual information function to obtain time delay

The reconstruction of linearly uncorrelated phase space depends on the appropriate selection of time lag $(\boldsymbol{\tau})$. A common method for selection of a proper lag is through autocorrelation function (Abarbanel and Gollub, 1996). The time corresponding to first zero crossing of the autocorrelation function is selected as a time lag.

The expression of normalized autocorrelation function, $c_{xx}(t)$ is

$$c_{xx}(t) = \frac{\sum_{n=0}^{N-1}[x(n)-\bar{x}][x(n+t)-\bar{x}]}{\sum_{n=0}^{N-1}[x(n)-\bar{x}]^2} \tag{4.4}$$

where $\bar{x}$ is the mean value of any time series (x). An autocorrelation function fails for the system described by nonlinear mathematical models. Therefore, average mutual information function (AMIF) is adopted that is suitable for nonlinear systems. The time lag corresponding to first minima of "AMIF" is selected as lag for reconstruction. The "AMIF" is a probability-based method proposed by Fraser and Swinney (1986) and is calculated as

$$I(t) = \sum_{n} p(x(n), x(n+t)) \log_2 \frac{p(x(n), x(n+t))}{p(x(n))\, p(x(n+t))} \tag{4.5}$$

Where, $p(x(n),x(n+t))$ are the joint probability density function, I is the "AMIF" of *t*, $p(x(n))$ and $p(x(n+t))$ are the estimated marginal probability density of $x(n)$ and $x(n+t)$ respectively. The theoretical probabilities in Equation (4.5) can be estimated using histograms on $x(n)$ and $x(n+t)$ and jointly $x(n), x(n+t)$ in which the range $[-\max(x(n)), \max(x(n))]$ is divided into $N_{x(n)}$ intervals and range $[-\max(x(n+t)), \max(x(n+t))]$ is divided into $N_{x(n+t)}$ intervals. Now the three probabilities in Equation (4.5) are estimated by tallying the counts of $x(n)$ and $x(n+t)$ and joint $x(n)$, $x(n+t)$ within the intervals $N_{x(n)}$, $N_{x(n+t)}$ and $N_{x(n)}$ $N_{x(n+t)}$, lastly dividing the counts by total number of observation yielding $p(x(n))$, $p(x(n+t))$ and $p(x(n), x(n+t))$ respectively.

4.4.2 Singular value decomposition to obtain embedding dimension

The proper selection of embedding dimension $(\mathbf{m})$ is important for a successful reconstruction of "PST". Singular system analysis (SSA) and false nearest neighbor (FNN) methods are commonly used methods to obtain optimal embedding dimension (Broomhead and King, 1986, Kennel et al., 1992). The "SSA" method performs singular value

decomposition (SVD) of the measured state variable vector (x) as represented in equation (4.6).

$$[\mathbf{X}]_{N \text{ x } q} = [\mathbf{U}]_{N \text{ x } q} [\mathbf{\Lambda}]_{q \text{ x } q} [\mathbf{V}]^{\mathrm{T}}_{q \text{ x } q} \tag{4.6}$$

where $[\mathbf{X}]_{N \text{ x } q}$ is matrix formed by concatenating $q-1$ unit delayed copies of vector x with N time points. $[\mathbf{\Lambda}]_{q \text{ x } q}$ is a diagonal matrix with elements as singular values of the system, $[\mathbf{U}]_{N \text{ x } q}$ is the left singular vector matrix, and each column vector of [**U**] represents the projection of [**X**] in one singular subspace and $[\mathbf{V}]^{\mathrm{T}}_{q \text{ x } q}$ is the right singular matrix, and each column vector of [**V**] represnts a basis that describes a signal subspace. The reconstructed attractor matrix $[\mathbf{X}]$ is formed with a delay of τ=1.

$$[\mathbf{X}] = \begin{bmatrix} x(1) & x(2) & \cdots & x(\mathbf{q}) \\ x(2) & x(3) & \cdots & x(\mathbf{q}+1) \\ \vdots & \vdots & \ddots & \vdots \\ x(N-\mathbf{q}) & x(N-\mathbf{q}+1) & \cdots & x(N) \end{bmatrix} \tag{4.7}$$

where q is time window $(q = F_s \eta)$ evaluated as the product of sampling frequency (F_s) of acquired signal and a parameter $\boldsymbol{\eta}$ that is related to the maximum frequency content present in the signal $(\mathbf{f})$ of the signal as proposed by Broomhead and King (1986).

$$\boldsymbol{\eta} \leq 1/\mathbf{f} \tag{4.8}$$

To get the appropriate embedding dimension (m), initially, the elements of diagonal matrix $[\mathbf{\Lambda}]_{q \text{ x } q}$ are normalized by their sum as

$$\hat{\mathbf{\Lambda}}_i = \frac{\mathbf{\Lambda}_{i \text{ x } i}}{\sum_{i=1}^{q} \mathbf{\Lambda}_{i \text{ x } i}} \tag{4.9}$$

Secondly, the vector $\{\hat{\Lambda}\}_{q \text{ x } 1}$ is plotted as a function of their indices, and the number of indices at which the graph suddenly drops to a value close to zero is selected as the proper value of 'm' for embedding.

4.4.3 Stepwise procedure for development of phase-space topology

Step-1: Consider a time series data $x(t) = \{x(1), x(2), ..., x(N)\}$.

Step-2: Evaluate the optimal time delay for reconstruction of PST from measured time series $x(t)$. The optimal time delay $\boldsymbol{\tau}$ is selected as first minima of AMIF evaluated for $x(t)$ (refer equation 4.5).

Step-3: Evaluate the optimal embedding dimension for reconstruction of PST from measured time series $x(t)$. The optimal embedding dimension $\mathbf{m}$ is obtained with help of SVD of $x(t)$ (refer equation 4.7). The singular values obtained by SVD are plotted as a function of their indices, and the point at which the graph reaches close to zero is selected as optimal embedding dimension.

Step-4: With help of optimal time delay and embedding dimension, the phase space matrix $[\mathbf{X}]$ is reconstructed as follows:

$$[\mathbf{X}] = \begin{bmatrix} x(1) & x(2) & \cdots & x(\mathbf{m}) \\ x(2) & x(3) & \cdots & x(\mathbf{m}+1) \\ \vdots & \vdots & \ddots & \vdots \\ x(N-\mathbf{m}) & x(N-\mathbf{m}+1) & \cdots & x(N) \end{bmatrix}$$

Now, for better understanding let us assume time series $x(t)$ to comprise of 1000 points. Therefore, $x(t) = \{x(1), x(2), ..., x(1000)\}$. Also assume optimal time lag as $\boldsymbol{\tau} = 1$ and an optimal embedding dimension as $\mathbf{m} = 3$. For such a case, the phase space matrix would be reconstructed as follows:

$$[\mathbf{X}] = \begin{bmatrix} x(1) & x(2) & x(3) \\ x(2) & x(3) & x(4) \\ \vdots & \vdots & \vdots \\ x(997) & x(998) & x(1000) \end{bmatrix}$$

4.5 Damage sensitive feature

The geometry of "PST" is strongly correlated to the dynamic response of the system. The evolution of damage causes changes in the dynamic response of the system. These changes

are manifested in the topology of the "PST". This behavior provides us an opportunity to detect damage by quantifying the dissimilarity in the "PST". The two damage sensitive features proposed in current work namely, "CPST" and "MDPST" are sensitive and accurate in determining the dissimilarity of the phase portrait.

To illustrate the evaluation of "DSFs", consider two attractors corresponding to the response of pristine $X(n)$ and damaged $Y(n)$ state where:

$$[\mathbf{Y}(n)] = [y(n), y(n+\mathbf{t}), \ldots\ldots, y(n+(\mathbf{m}-1)\mathbf{t})] \tag{4.10}$$

Here, **m** and **t** are the optimal value of embedding dimension and lag, respectively.

A fiducial point $Y(k)$ with time index k is selected on a damaged trajectory. Minimizing the Euclidean distance between the fiducial point and the baseline "PST", the nearest neighbors to the fiducial point are selected on baseline "PST" as:

$$[\mathbf{NN}_f(n_j)] = \min \| \mathbf{X}(n_j) - \mathbf{Y}(k) \| \quad j = 1, \ldots, P \tag{4.11}$$

where, P is total number of neighborhood points, operator $\|.\|$ evaluates the Euclidean norm, $[\mathbf{NN}_f]$ denotes the set of nearest neighbor points to fiducial point $Y(k)$. The set of nearest neighbors is formed without considering the time instant corresponding to any point, as the process is entirely based on minimizing the Euclidean norm. The selected neighborhood points are used to describe dissimilarity in the dynamic state of baseline and damaged trajectory. Hence, the total number of neighborhood points (**P**) are important and is generally selected in the range of 10^{-4} N to 10^{-3} N, where N is total number of points in the reconstructed trajectory (Nichols, 2003).

The future value of $Y(k)$ at '**s**' number of time steps are selected in the baseline trajectory as

$$\hat{\mathbf{Y}}(k+\mathbf{s}) = \frac{1}{\mathbf{P}} \sum_{j=1}^{P} \mathbf{X}(n_j + \mathbf{s}), \quad j = 1, \ldots, P \tag{4.12}$$

where $\hat{\mathbf{Y}}(k+\mathbf{s})$ is the predicted average value of all the evolved future points, corresponding to set $[\mathbf{NN}_f]$ for time step '**s**'. To maintain the correlation between an evolved neighborhood in time, the value of time interval '**s**' (prediction horizon) is selected in such

a way that $1 \le \mathbf{s} \le 0.5t$ (Torkamani et al., 2012). Now, the evolved values on the damaged trajectory corresponding to time step '$\mathbf{s}$' is selected as $\mathbf{Y}(k+\mathbf{s})$ as shown in Figure 4.1.

Two main "DSFs" are adapted in the present study namely change in phase space topology (CPST) and Mahalanobis distance between phase space topology (MDPST). Both the "DSFs" can be calculated either in the signal subspace or reduced subspace. Both, Euclidean and statistical distance measure is evaluated to quantify the evolution of progressive damage. Details of both the damage features are discussed below.

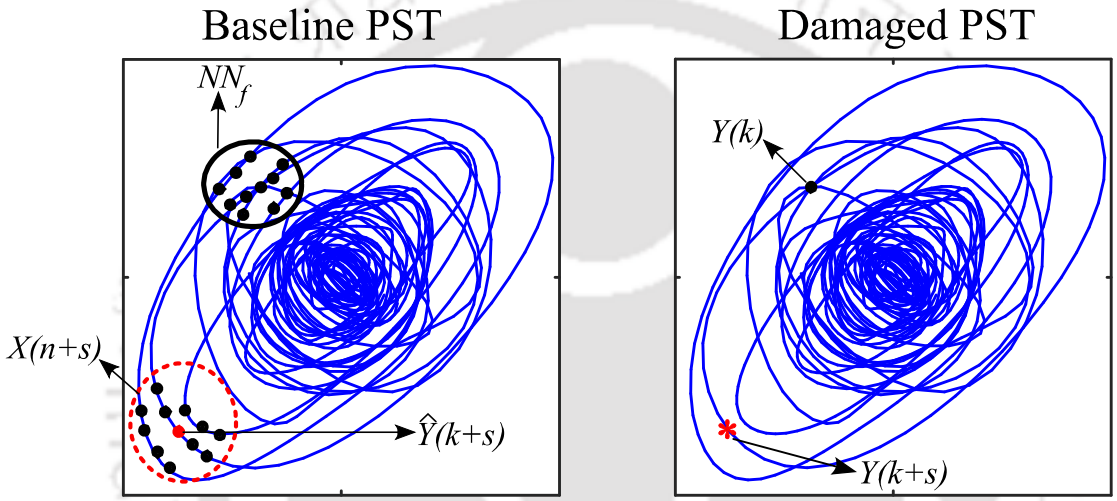

Figure 4.1 Schematic diagram of phase space trajectory for pristine state and damage state to evaluate damage sensitive feature

4.5.1 Change in phase space topology

The damage feature based on changes in phase space topology (CPST) is defined as:

$$\mathrm{CPST}(\mathbf{i}) = \frac{1}{P} \| \hat{\mathbf{Y}}(k+\mathbf{s}) - \mathbf{Y}(k+\mathbf{s}) \| \tag{4.13}$$

where $\hat{\mathbf{Y}}(k+\mathbf{s})$ and $\mathbf{Y}(k+\mathbf{s})$ is shown in Figure 4.1 as a red dot $(\bullet)$ and red asterisk $(*)$ respectively. This calculation has to be repeated for the choice of numerous Fiducial points to attain the best and stable estimate. The appropriate number of Fiducial points to be selected are minimum 5% of the total number of points in the reconstructed trajectory to get a reasonable estimate of "CPST".

The acceptable estimate of damage feature is adapted based on the average value of evaluated "CPST" at each Fiducial points and is given as:

$$\text{CPST} = \sum_{i=1}^{nt} CPST(i) / nt \tag{4.14}$$

There is a possibility that when an undamaged attractor is analyzed by itself to evaluate the value of "CPST", a non-zero value may be obtained. This value is considered as an error and must be subtracted from "CPST" value evaluated by analyzing the undamaged and damaged attractor. The error subtraction will result in a better estimate of the change in "CPST" value due to induced damage.

4.5.2 Mahalanobis distance between phase space

In the multi-dimensional statistical analysis, Mahalanobis distance (MD) is referred to a measure of a distance in the scale of standard deviation between an observation and reference sample (Mahalanobis, 1936, De Maesschalck et al., 2000). Mahalanobis metric considers direction dependent variance and accounts for covariance between the samples. The basic algorithm to determine the MD is similar to the calculation of "CPST". A fiducial point $Y(k)$ with time index k is selected on a baseline trajectory, nearest cluster of neighborhood points $[\mathbf{NN}_f]$ are selected on the damage trajectory with respect to fiducial point $Y(k)$. Based on the neighborhood points, a multivariate system dynamic matrix $[\mathbf{X}(n+\mathbf{s})]_{NN_f \times m}$ is evolved at $k$time instant, where NN_f represents number of neighborhood points and m is embedded dimension. Further, the covariance matrix $\Sigma(\mathbf{k})$ is constructed as that is non-singular and positive definite :

$$[\mathbf{\Sigma(k)}]_{m\times m} = \frac{1}{n-1}[\mathbf{X}(n+\mathbf{s})_{NN_f \times m}]^T[\mathbf{X}(n+\mathbf{s})_{NN_f \times m}] \tag{4.15}$$

The MD between a fiducial point and cluster of neighborhood points at k time instant is given as:

$$\mathbf{d}_{mahal}(k) = \sqrt{(\mathbf{Y}(k+\mathbf{s}) - \overline{\mathbf{Y}})^T[\mathbf{\Sigma(k)}]^{-1}(\mathbf{Y}(k+\mathbf{s}) - \overline{\mathbf{Y}})} \tag{4.16}$$

where $X(n+\mathbf{s})$ and $Y(k+\mathbf{s})$ are shown in Figure 4.1 as a red dotted cluster and red asterisk $(*)$ respectively. For large embedded dimension, $[\mathbf{X}(n+\mathbf{s})]_{NN_f \times m}$ might contain redundant and correlated variables. Multi-collinearity in the $[\mathbf{X}(n+\mathbf{s})]_{NN_f \times m}$ leads to the nearly singular $[\mathbf{\Sigma}(k)]$ matrix that cannot be inverted. Also, feature reduction using principal component analysis is needed for $Y(k)$ to ensure $NN_f > m$. If the $[\mathbf{X}(n+\mathbf{s})]_{NN_f \times m}$ is uncorrelated random vector and has unit variance, $\mathbf{\Sigma}(k)_{\mathbf{m\times m}} = \mathbf{I}$ and Mahalanobis distance will correspond to the square of the L2 norm $\| \ . \ \|^2$ of $Y(k+\mathbf{s})$ and $X(n+\mathbf{s})$ (De Maesschalck et al., 2000). The future values of $Y(k)$ at '**s**' number of time steps are evaluated using equation (4.12). Similar, procedure is repeated for various choices of fiducial points approximately equal to 5% of the total number of points $(n\,t)$ for time-varying steps from $k=1$ to '**s**'. For the given fiducial points at a selected time instant, a vector of MD $d_{mahal}(k)_{k\to 1:s}$ is computed. The reliable estimate of MD is evaluated for a number of selected fiducial points (nt) given as:

$$\mathbf{d}_{mahal} = \sum_{i=1}^{nt} \mathbf{d}_{mahal}(i) / nt \tag{4.17}$$

For uncorrelated variables of nearest neighborhood points having unit variance, "CPST" and MDSPT will converge to the same metric.

4.6 Proposed damage detection algorithm

The two-phase damage detection algorithm proposed in the current study is summarized below and represented in Figure 4.2.

Phase-1

Step-1: Reduce the dimension of response matrix with the help of principal component analysis

Step-2: Segregate minor damages from small perturbative changes with help of rotation in

proper orthogonal components for reduced dimension response matrix.

Phase-2

Step-3: Decompose high embedding dimensional response data into low embedding dimension data with the help of Empirical mode decomposition.

Step-4: Select dominant "IMF" out of multiple number of "IMFs" obtained in step-3. Also, select optimal values of embedding dimension and lag for reconstruction of "PST" with help of singular value decomposition and average mutual information function.

Step-5: Reconstruction of "PST".

Step-6: Evaluation of "DSFs" to detect and quantify the evolution of damage.

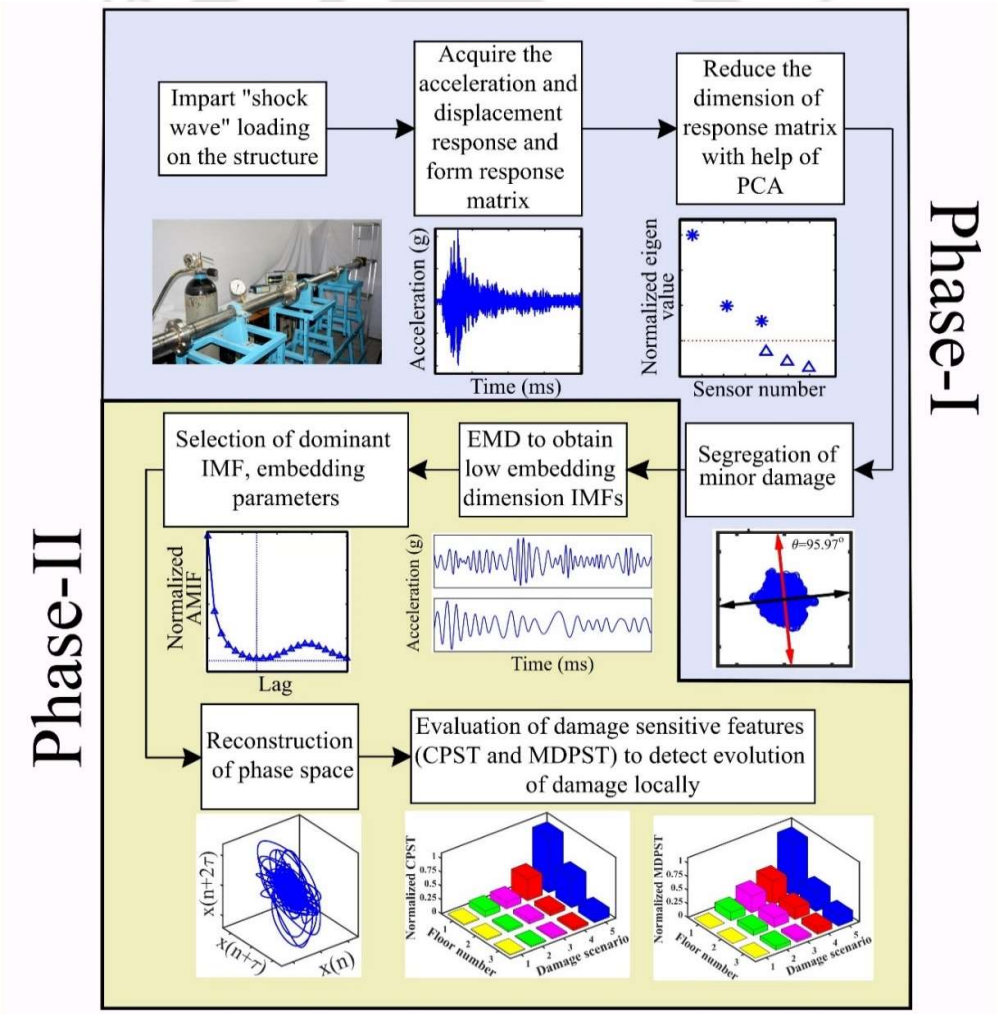

Figure 4.2 Flowchart of the proposed damage detection algorithm that explores dissimilarity in phase space trajectory

4.7 Experimental investigation

As mentioned earlier, limited experimental studies are available for damage detection in the structure subjected to extreme loadings such as shock, blast, and impact. To demonstrate the efficiency and robustness of the proposed damage detection algorithm, an experimental investigation on a three-storey, one bay shear building was conducted. The efficacy of the proposed algorithm is demonstrated for damage detection in the structure whose members are plasticized due to shock loading.

The beams and columns of the shear building consist of aluminum angle-section of dimension 19 mm x 19mm x 2mm. The slab consists of a steel rectangular plate having dimensions as 300mm x 300mm x 16mm. The total height of the structure was 1.5 m with each storey height being 0.5 m. The entire frame was rigidly mounted on a rigid platform to attain fixity condition at the base.

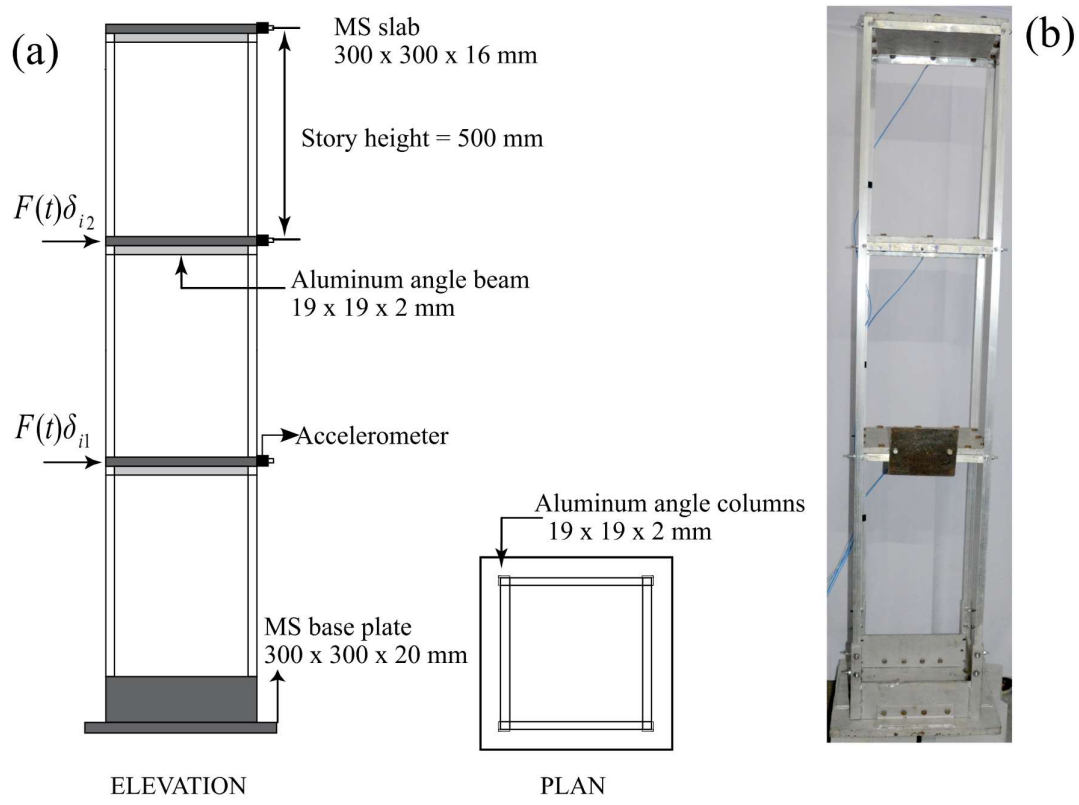

Figure 4.3 a) Schematic diagram and b) experimental model of frame structure

The schematic diagram and image of the structure are shown in Figure 4.3. The experiments were planned and performed in two stages. In Figure 4.3, δ_{ij} represents Kronecker delta function. The dynamic responses of all the floors were acquired for each set of experiments.

Stage-I:

As shown in Figure 4.3 (a) the shock loading was applied at 'first floor' of the three storey building. Maximum damage is supposed to incurred on the first floor and progressively enhanced for repetitive loading.

Stage-II:

In this stage, as shown in Figure 4.3 (a) (for i=2), the shock loading was applied at 'second floor' of the three storey building.

In both the stages, repetitive shock load was imparted for five times at constant standoff distance and intensity. Each unique set of experiments were repeated twice to ensure repeatability. Repetitive loading is a realistic scenario in a conflict zone where explosives are detonated in continuous series for maximum devastation. Repetitive controlled shock loading will cause progressive degradation to the system and induces systematic nonlinearity in the building. The detailed explanation of both the stage is given below:

Stage-I

Experiment-1: Shock loading was applied 'once' on the first floor of the healthy shear building. The data collected in this stage is considered as baseline data.

Experiment-2: Shock loading was applied 'twice' on the first floor of the healthy shear building. The data collected in this stage is considered as damaged data. The same step is repeated in Experiment-3, Experiment-4, and Experiment-5, where shock loading is applied thrice, four times and five times respectively.

Stage-II

The stage-II is exactly same as stage-I, the only change is that shock loading is applied on second floor instead of first floor. For both the stages, the data acquired during experiment-1

was considered as baseline data. So out of five experiments, data acquired during experiment-1 is considered as baseline data and rest are the damaged data.

The shock tube test setup was utilized as a source to generate controlled shock wave loading. The details of shock tube design and shock characterization can be found at Kore et al. (2016). The shock wave loading was imparted on frame structure at the first and second floor level to induce damage. The frame structure was subjected to repeated shock loading and the dynamic responses were acquired. The displacement of each floor is measured using LVDT sensors. Two accelerometers were attached to each floor, one in north-south (N-S) direction and other at east-west (E-W) direction. The acceleration response at each degree of freedom of the frame structure was measured with piezo-electronics accelerometers having a sensitivity of 100 mV/g. The shear building was kept at a standoff distance of 1 m. The overburden pressure on the shear structure was measured with high-resolution pressure probe (PCB-112A21). The reflected pressure on the shear structure is shown in Figure 4.4.

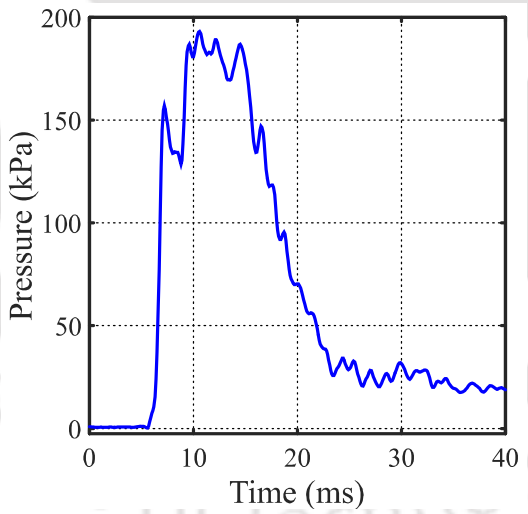

Figure 4.4 Reflected shock pressure profile from frame structure at standoff distance of 1 m

4.8 Results and discussion

4.8.1 Structural response due to shock loading

Acceleration response and evaluation of frequency:

The shear building was excited with maximum shock load of 190 KPa. The design of experiments is followed as mentioned in stage I and stage II. The acceleration time history of

each floor is shown in Figure 4.5 and Figure 4.6. When the shock wave loading was applied to a multi-storey shear building, high-frequency vibration modes were excited. To evaluate the excited frequency, Fast Fourier Transform (FFT) of the acceleration response data was performed. Figure 4.7 and Figure 4.8 show the dominant frequency component of the acceleration for stage-I and stage-II experiments respectively. It is observed that the changes in frequency is least sensitive to detect major progressive degradation of the structure under the application of shock wave loading. Therefore, frequency domain techniques do not hold much promise in damage detection. This provides us the motivation to explore the change in the "PST" approach in the time domain for damage detection.

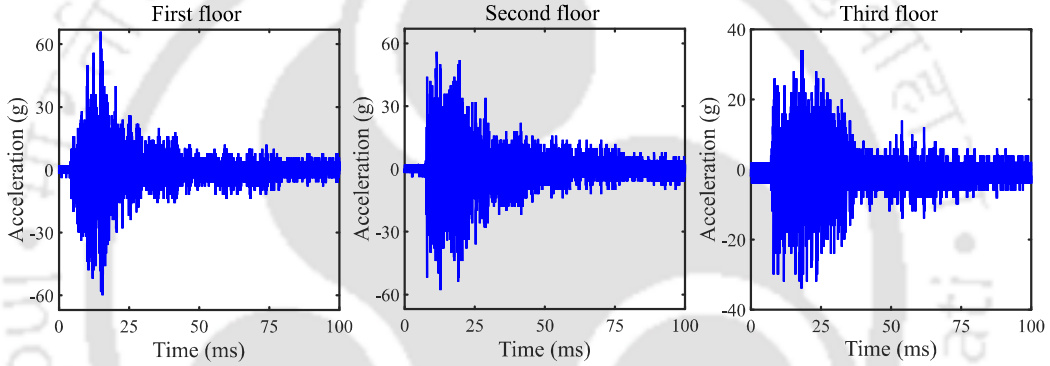

Figure 4.5 Acceleration time history of shear building for stage I shock loading

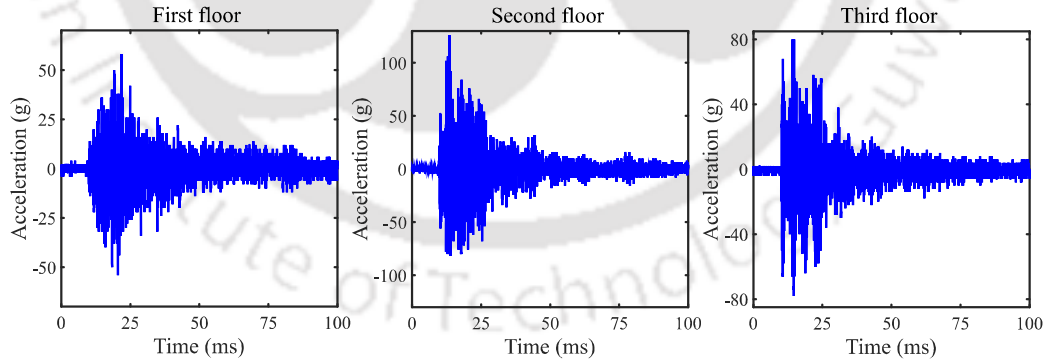

Figure 4.6 Acceleration time history of shear building for stage II shock loading

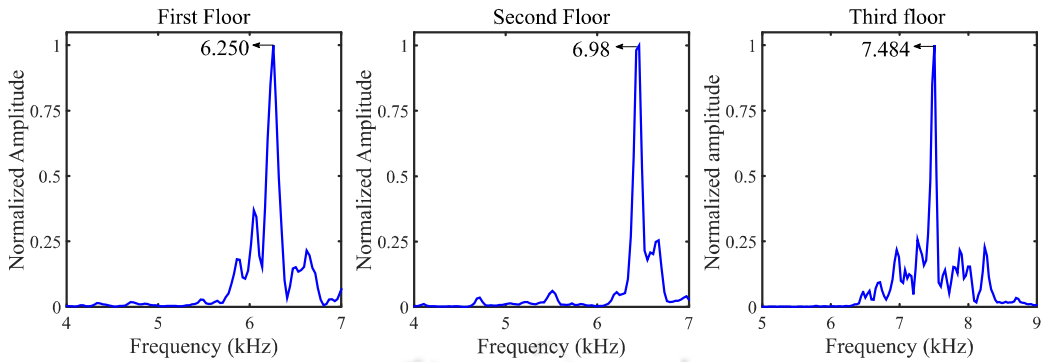

Figure 4.7 Frequency spectra of dynamic response of the shear building subjected to stage-I shock loading

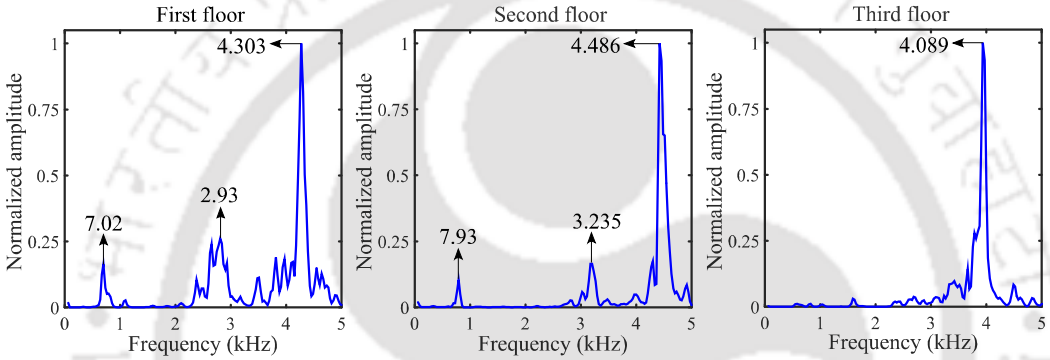

Figure 4.8 Frequency spectra of dynamic response of the shear building subjected to stage-II shock loading

Displacement response:

Repetitive shock loading on the rigid slab causes progressive permanent deformation in the structural system. The permanent deformation is related to the accumulation of the damage in the structural member. The shock induced permanently deformed the shape of the shear building for stage I and stage II loading are shown in Figure 4.9. The experimental deformed shape shows plastification and excessive deformation of the column members.

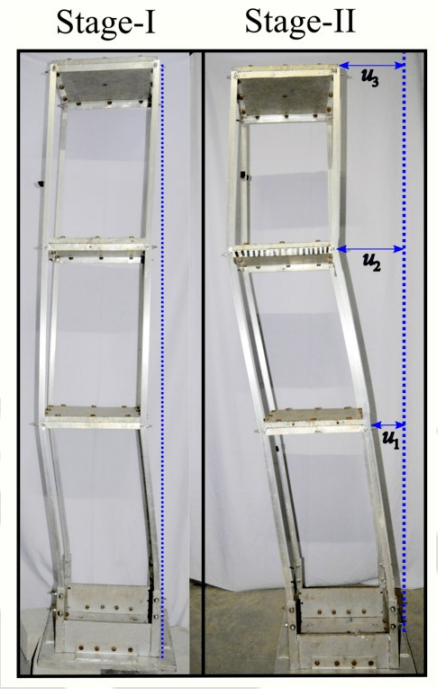

Figure 4.9 Plastic deformed shape of shear structure after experiment-5 of stage-I and stage-II

Figure 4.10 shows the deformation profile along the height of the structure at the time instant (t) for which the displacement at the shock location is maximum.

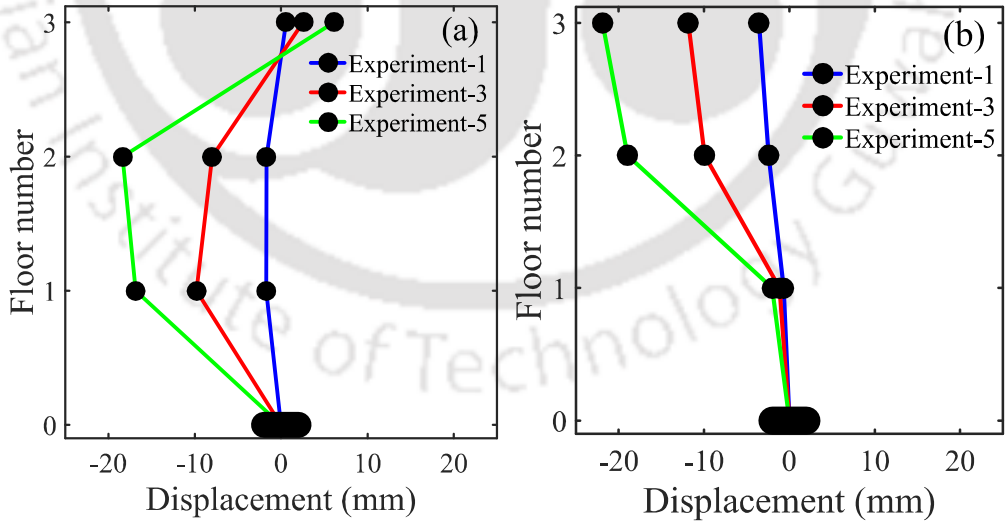

Figure 4.10 Maximum displacement profile along the height of a structure for a) stage-I and b) stage-II shock loading experiment

An interesting observation is seen for Experiment-5, stage I loading. At the time instant when the first floor has a maximum displacement, second-floor experiences even higher displacement. In stage II loading, the third-floor experiences maximum displacement compared to other floors. The structural dynamic modes migrated from linear normal mode to nonlinear dynamic modes upon excessive deformation. Under the influence of nonlinearity, the displacement profile for stage I and stage II remotely resembles second and the first mode of vibration respectively.

Therefore, linear system identification techniques are not suitable for quantifying the damage induced in the system. Time domain novelty detection techniques based on parametric signal modeling are better suited for quantification of progressive damage evolution.

4.8.2 PCA of response data to identify non-linearity induced in the structure

Dimension reduction of response data

Principal orthogonal decomposition provides the Eigenvector of the covariance matrix of the dynamic response that corresponds to linear normal modes of vibration (Feeny and Liang, 2003, Yan et al., 2005). The Eigenvectors and Eigenvalues obtain from the response covariance matrix are referred to principal orthogonal modes and principal orthogonal values. The acceleration in both N-S and E-W direction is acquired at each lumped mass when subjected to shock wave loading. The "PCA" is conducted on the n dimension response data set $A_k \in \Re^{n\times N}$, at time $t_{k(k=1,2,\ldots N)}$, where N is number of samples. "PCA" is performed by linear mapping the data from the original dimension n to lower dimension m as [**Z**]=[**Q**][**A**]. Here, $Z \in \Re^{m\times N}$ is referred as score matrix and $Q \in \Re^{m\times n}$ as loading matrix. The mathematical representation of singular value decomposition (SVD) is:

$$[\mathbf{A}][\mathbf{A}]^T = [\mathbf{U}][\mathbf{\Sigma}]^2[\mathbf{U}]^T = [\mathbf{U}]\begin{bmatrix} \sigma_1^2 & & \\ & \ddots & \\ & & \sigma_n^2 \end{bmatrix}[\mathbf{U}]^T \text{, with } [\mathbf{U}][\mathbf{U}]^T = [\mathbf{I}] \quad (4.18)$$

The column of the U is orthonormal matrix represents principal components. The $\boldsymbol{\Sigma}^2$ is a diagonal matrix and containing singular values. These singular values are arranged in decreasing order as, $diag(\sigma_1 > \sigma_2 > .... \sigma_m > \sigma_{m+1} .... > \sigma_n), \sigma_n \to 0$. The dimension of the response data is reduced by retaining the dominating singular values having maximum energy and projecting back into original signal subspace. The interesting dynamic of the system is retained and further used for evaluating the information of linear normal mode of vibrations. The feature reduction is also needed to avoid singularity of the covariance matrix to avoid computation complexity in the evaluation of Mahalanobis distance. The singular values of the response in N-S direction were highly dominating compared to E-W direction as shown in Figure 4.11.

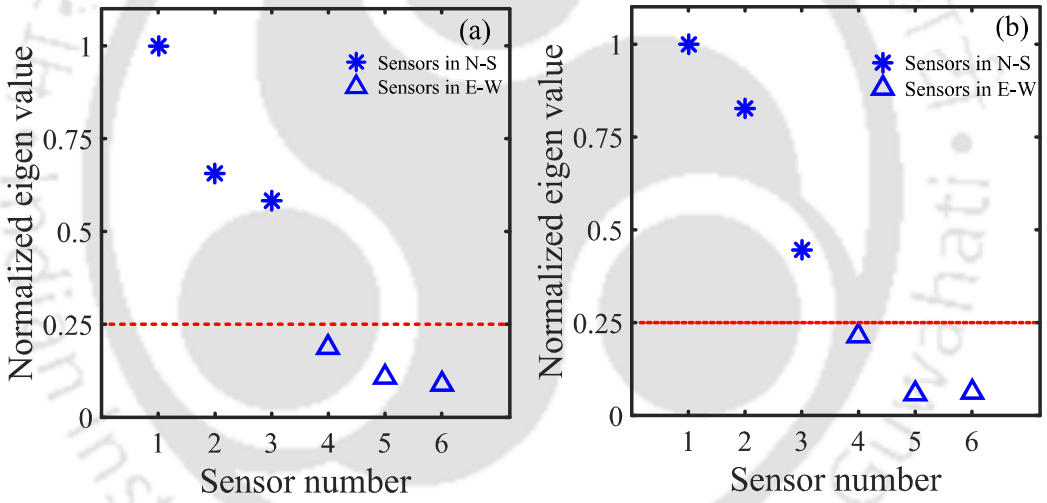

Figure 4.11 Eigenvalues of dynamic response of the structure in E-W and N-S direction for a) stage-I and b) stage-II shock loading experiment

The normalized singular values below 0.25 (i.e. 75% lesser than maximum singular value) are considered to have the least energy. The original data was back projected to a reduced subspace by retaining dominant singular values. This reduced dimension data contains most of the information and is processed further for segregating minor damage from perturbative damage, as explained below.

Principal component analysis and linear normal modes

Feeny and Liang (2003) have shown the relationship between the principal orthogonal modes and linear normal mode for free vibration of the lumped mass system. Considering, an undamped linear multiple degree of freedom (MDOF) system whose equation of motion is given as $[\mathbf{M}]\{\ddot{Y}\}+[\mathbf{K}]\{Y\}=0$. Here, M and K are symmetric and positive definite representing mass and stiffness matrix. By assuming displacement vector (Y) as $[\mathbf{M}]^{-1/2}\{X\}$, the equation of motion is transformed to:

$$\{\ddot{X}\}+[\mathbf{M}]^{-1/2}[\mathbf{K}][\mathbf{M}]^{-1/2}\{X\}=0 \tag{4.19}$$

The transformed physical response $\{X\}=\{x_1,x_2,....x_M\}^{\mathrm{T}}$ is related to Eigenvector of linear normal mode $\{V\}=\{v_1,....,v_M\}^T$ and vector of modal coordinate $\{Q\}=\{\mathrm{q}_1,\mathrm{q}_2,....\mathrm{q}_\mathrm{N}\}$ using following expression:

$$[\mathbf{X}]=\{V\}\{Q\} \tag{4.20}$$

$[\mathbf{X}]_{\mathrm{M\&N}}$ is physical response matrix, where M,N indicates number of degree of freedom and number of time samples, respectively. The covariance matrix of the large samples of model response is diagonal for moderately low damping and is given as $[\mathbf{R}]_{\mathrm{Q}}=\frac{1}{\mathbf{N}}[\mathbf{Q}][\mathbf{Q}]^{\mathrm{T}}$. Krishnan et al. (2017) have demonstrated that systems with moderate modal damping and finite sample size, the principal orthogonal component (POC) approximates to linear normal mode of vibration.

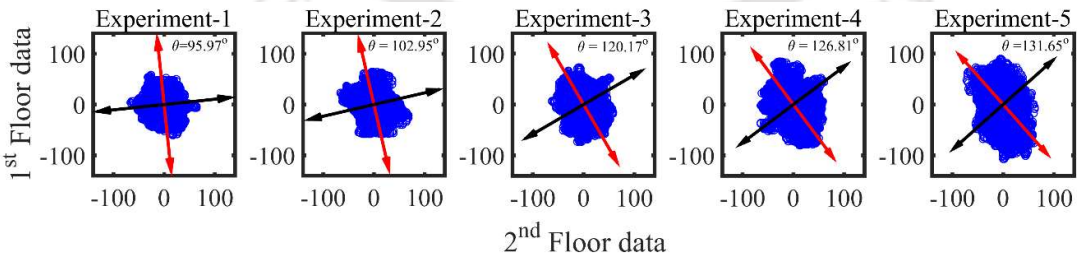

Figure 4.12 Progressive changes in the direction of "POC" for stage-I shock loading

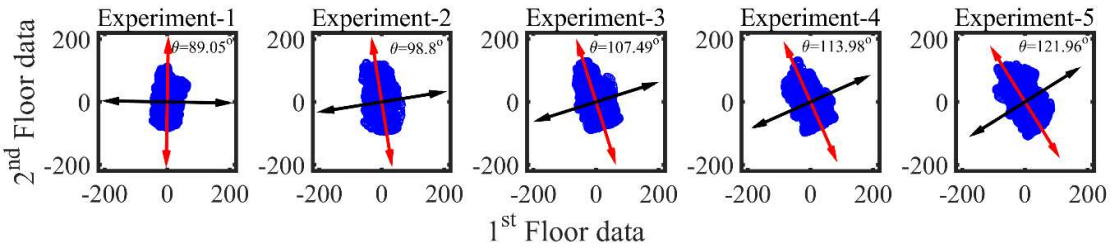

Figure 4.13 Progressive changes in the direction of "POC" for stage-II shock loading

As the structural properties progressively deteriorate from linear to the non-linear stage under extreme loading events, the "POC" vector will change dramatically. Hence, the changes in the "POC" indicate the initiation and evolution of damage induced due to non-linearity in the structure. In the current work, "PCA" is utilized to identify the changes in-state of the structure by quantifying the rotation of "POC" of the dynamic responses. Figure 4.12 and Figure 4.13 represents the direction of Eigenvectors (principal components) obtained by "PCA" for both stages of loading. As shown in Figure 4.12 and Figure 4.13, the angle between the principal components rotates due to progressive damage evolution. Rotations of the PC beyond certain threshold limit indicates minor damage has been induced in the structure. The threshold limit depends on the problem-specific application and adjusted based on heuristic techniques. The main purpose of "PCA" is to identify minor damages using the rotation of "POC".

Further, utilizing the "PSR" methodology "DSFs" are evaluated namely "CPST" and "MDPST" (will be discussed in section 4.8.4). The computational effort for evaluating rotation of "POC" is much less compared to evaluation of "DSFs". "PST" approach and "DSFs", will be implemented only if changes in the "POC" are beyond calibrated threshold limits (i.e. 5^{o} in the present case). "PCA" serves as an early alarm feature that helps in identifying minor damages. The next step is to localize and quantify the damage with help of "PST" and "DSFs". For appropriate reconstruction of "PST", the signal should be of low dimension. This is not satisfied for the measured response data, so signals are converted to mono-component with reduced dimensionality using Empirical mode decomposition (EMD).

4.8.3 Selection of dominant IMF and embedding parameters for phase space reconstruction

The representation of the dynamic response to "PST" demands mono-component and lower dimensional signals. The dynamic response is multiple components and high dimensional data. "EMD" is performed on the dynamics response to obtain n number of "IMFs" to extract a mono-component signal with reduced dimensionality (Figure 4.14). Appropriate reconstruction of "PST" requires proper selection of the dominant "IMF", embedding dimension and the lag.

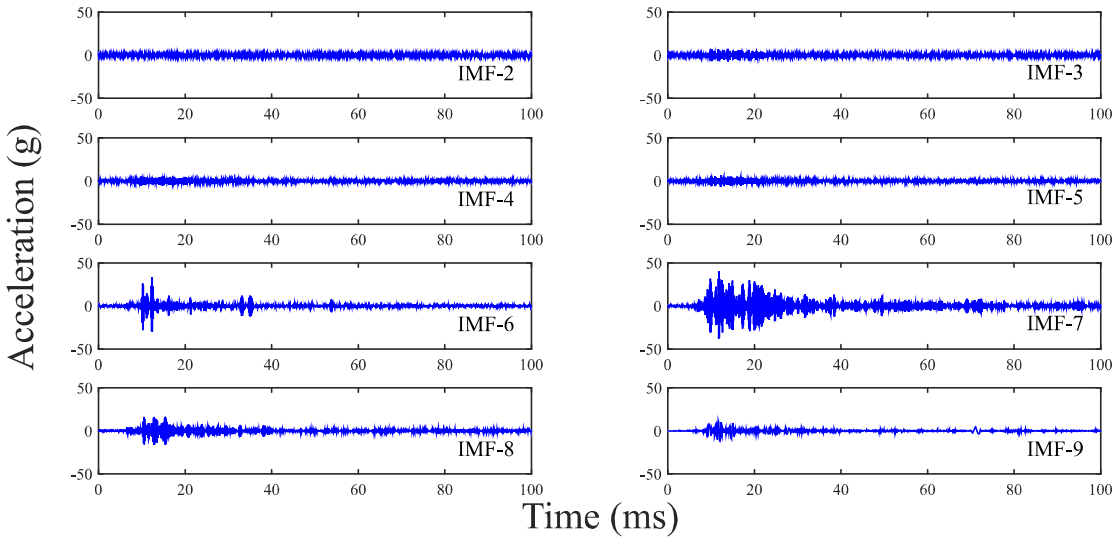

Figure 4.14 Intrinsic mode function (IMF) obtained by "EMD" of first floor's acceleration response for the stage-I shock loading

Cross-correlation is a technique to measure the similarity between two signals. The dominant "IMF" is selected based on the measure of maximum cross-correlation between "IMF" and the original signal. The cross-correlation between the original signal (x_1) and an "IMF" is calculated by equation (4.21).

$$R(\tau) = \frac{1}{T}\int_0^T x(t)IMF(t+\tau)dt \tag{4.21}$$

The cross-correlation between all the "IMFs" and the original signal is calculated and shown in Figure 4.15. The process is repeated for all the "IMFs" corresponding to each degree of

freedom. In general, first few "IMFs" have low correlation with the original signal which corresponds to high-frequency noise in the signal. For stage I, "IMF" number '6' has maximum correlation and selected as dominant "IMF". Similarly, for stage II, "IMF" number '7' is selected as dominant "IMF" (Figure 4.15). The "PST" of dominant "IMF" requires appropriate selection of time lag and embedding dimension. The appropriate embedding dimension for dominant "IMFs" is obtained with the help "SVD" method as discussed in section 4.4.2. Figure 4.16 shows that the singular value tends to zero for dimension '*m*' equal to 3.

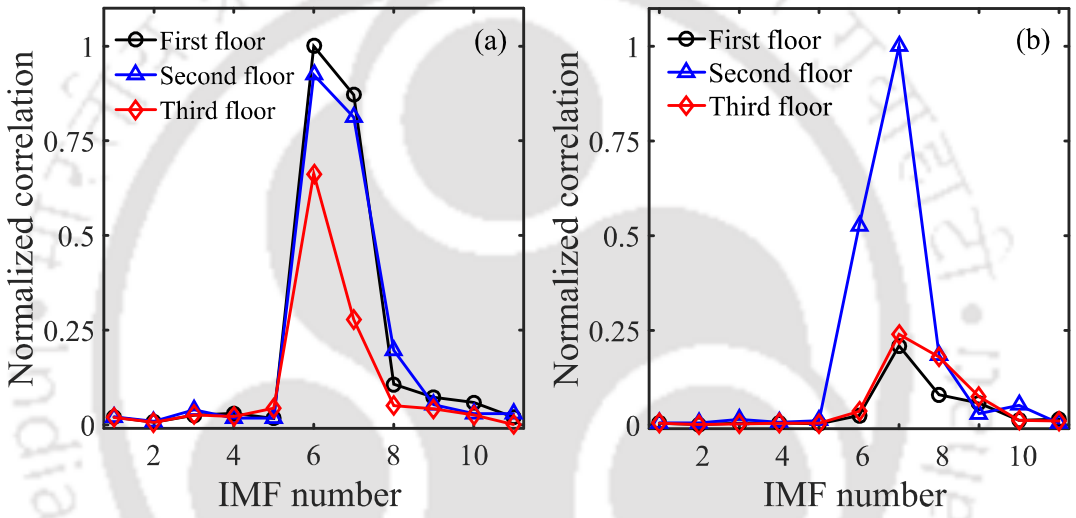

Figure 4.15 Correlation between "IMFs" and its corresponding dynamic response for (a) stage-I experiment and (b) stage-II shock loading experiment

This indicates that selecting dimension '*m*' greater than 3 will lead to the high computational effort without any improvement in performance of the algorithm. The appropriate delay in reconstruction is selected with the help of "AMIF" as explained in section 4.4.1. The first minima of the "AMIF" plot with lag correspond to the optimal choice of the delay. These values of lag corresponding to first minima indicates a weak statistical independence of "IMF" and is selected as appropriate lag. Figure 4.17 shows the "AMIF" plot corresponding to dominant "IMF" for all degree of freedoms. The lag factor for the stage-I and stage II experiments is 33 and 28, respectively.

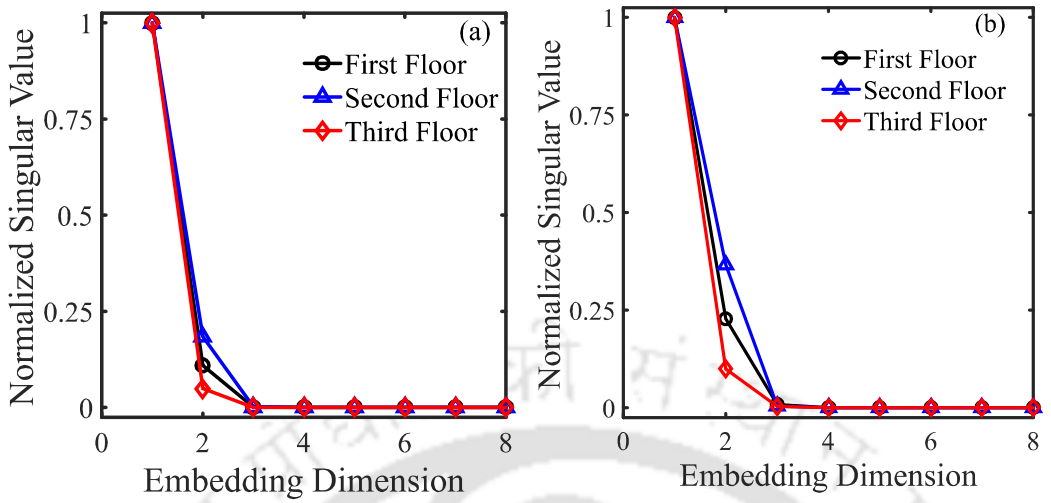

Figure 4.16 Normalized singular values with respect to embedded dimension of dynamic response for a) stage-I and b) stage-II shock loading

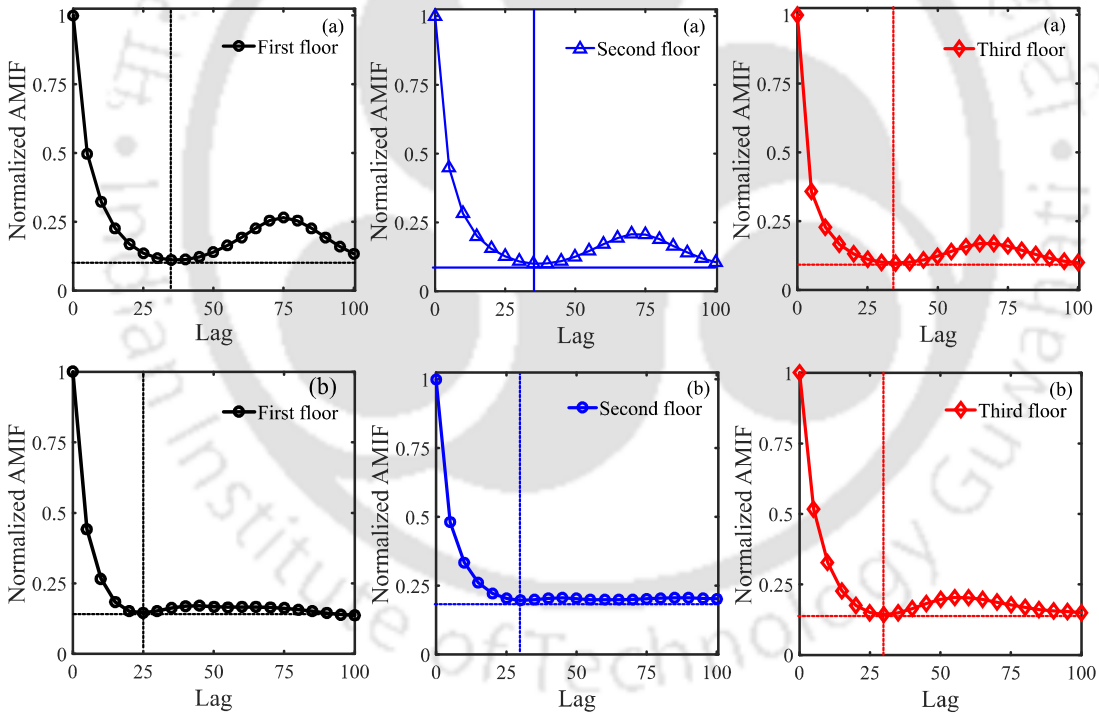

Figure 4.17 Variation of "AMIF" with lag for the dynamic response of a shear building for (a) stage-I and (b) stage-II shock loading experiments

4.8.4 Phase space reconstruction and evaluation of damage sensitive features

The "PSR" of the dominant "IMF" is performed in accordance with the procedure explained in section 4.4. The procedure to determine the appropriate choice of the time delay and

embedding dimension for dominant "IMF" is discussed in section 4.4. For instance, in Stage I experiments, the dominating "IMF" is 7 having embedded dimension 3 and lag factor 38. Using dominating and influential parameters, the "PSR" is performed. Figure 4.18 and Figure 4.19 shows the "PST" plot for stage I and II experiments. After successful "PSR" of all the experiment, "PST" corresponding to experiment-1 is selected as baseline data. The damage sensitive features measure the change in "PST" between the benchmark and progressive damaged states. Figure 4.20 and Figure 4.21 shows the normalized "CPST" and "MDPST" value depicting progressive damage evolution for stage I and stage II loading, respectively.

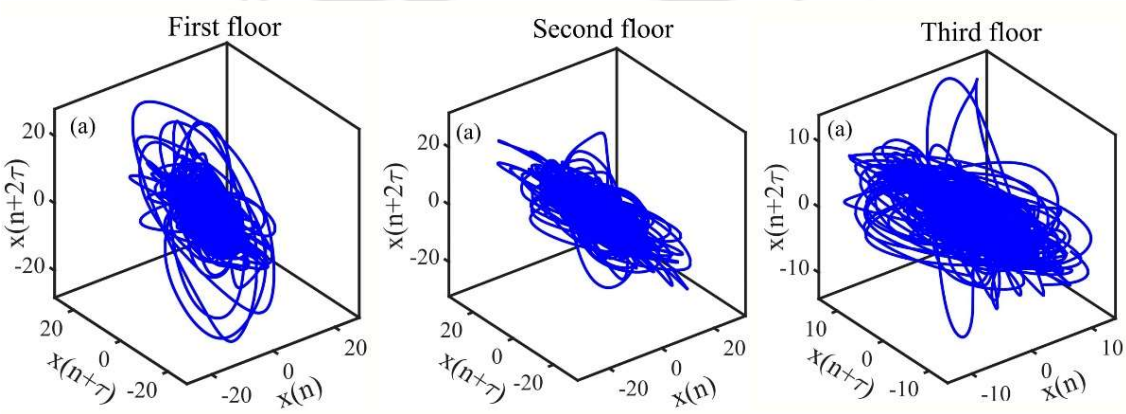

Figure 4.18 "PST" of dominant "IMF" for all degree of freedom for stage-I shock loading experiment

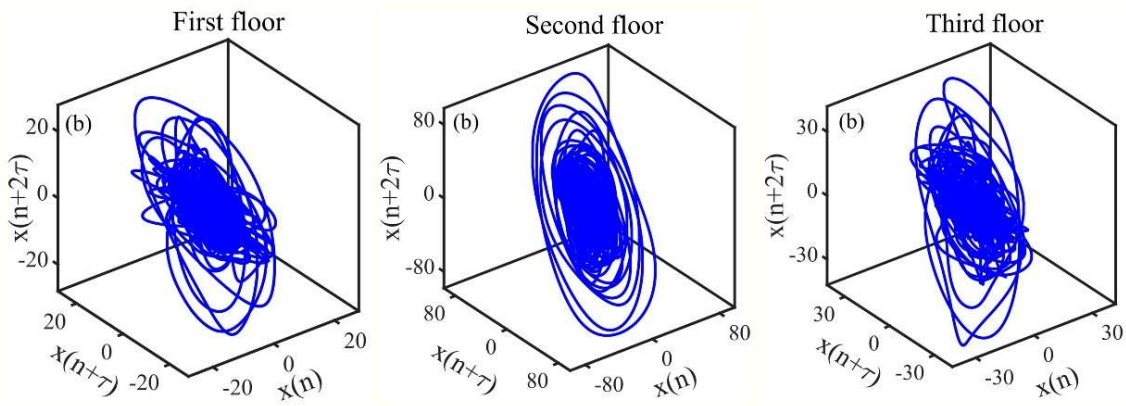

Figure 4.19 "PST" of dominant "IMF" for all degree of freedom for stage-II shock loading experiment

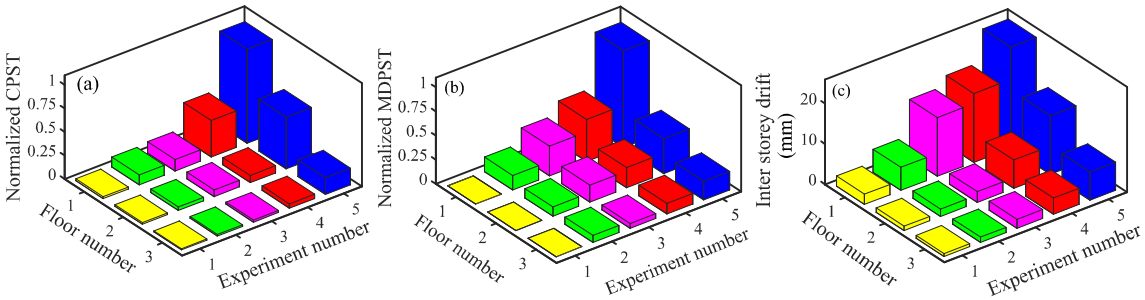

Figure 4.20 Three-dimension bar chart showing the variation of a) normalized "CPST", b) normalized "MDPST" and c) drift ratio with respect to various experiments and location of damage for stage I experiments (Note: The experiment-1 corresponds to baseline (pristine) data)

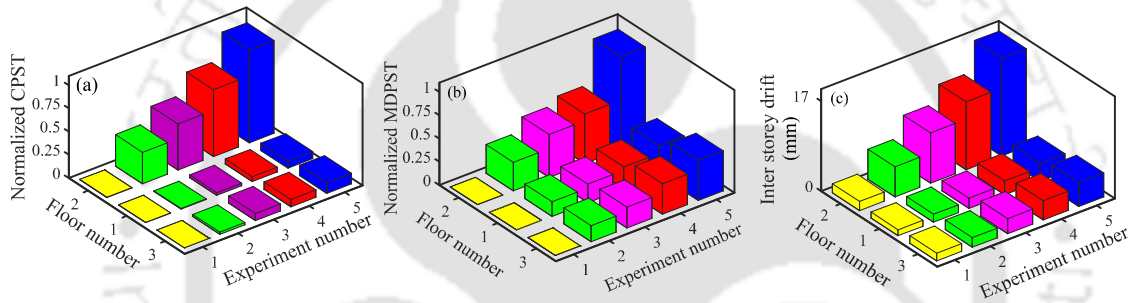

Figure 4.21 Three-dimension bar chart showing the variation of a) normalized "CPST", b) normalized "MDPST" and c) drift ratio with respect to various experiments and location of damage for stage II experiments

For stage I loading, "DSFs" values are maximum at first floor that experiences direct shock loading. It is observed that the magnitude of damage reduces as the distance from loading increases (Figure 4.20). For Stage-II experiments, the "DSFs" value are maximum at a second-floor level that experiences direct shock loading. The loading at second floor has also induced lower magnitude damage in remaining two floors. The third floor has damage more compared to the first floor as observed from Figure 4.21. It is obvious to note that both the "DSFs" are largest for the floor that experiences direct shock load. The numerical value of both the damage feature increases after each experiment, indicating the progressive evolution of damage after each experiment. The algorithm was able to parametrically quantify the magnitude and location of the progressive evolution of damage. The changes in "DSF" must

corroborate with behavioral changes in the primary response variables such as displacement or strain.

In the present study, the changes in the drift between each floor is investigated for successive damage evolution. The temporal displacement at each floor was measured for successive shock wave loading. The maximum temporal displacement $u(i)$ was used to evaluate the inter-storey drift of the shear structure, where i is floor number. Inter-storey drift (δ_i) is defined as relative translation displacement between two consecutive floors $(\delta_i = u_i - u_{i-1})$. The inter-storey drift is induced primarily by shear drift and flexural drift. The drift due to shear effect causes local failure, whereas the drift governed by flexural causes plastification and excessive bending of the members. In general, the inter-storey drift provides an indirect measure to evaluate the location and magnitude of damage. Figure 4.20 and Figure 4.21 show the three-dimension variation of inter-storey drift with respect to storey height and various experiments. It is observed, that the variation of inter-storey drift and "DSFs" are similar. The change in inter-storey drift is an indicative measure of damage that is used to enhance the confidence in the "DSFs".

4.9 Conclusion

The current chapter describes a novel technique for structural health monitoring and damage detection. The shockwave loading was applied on a shear building and progressive damage was induced in the structure. The structural response was analyzed through the proposed damage detection algorithm.

The proposed algorithm was divided into two segments that segregate perturbative damages and microscale damages. In the first segment, principal component analysis (PCA) was used for dimension reduction and evaluation of changes in principal orthogonal components (POC). In the second segment, the response was decomposed in mono-component signals (IMFs) using Empirical mode decomposition (EMD). The appropriate embedding parameters were calculated using singular system analysis and average mutual

information function, respectively. The dominant "IMF" using embedding parameters was represented in the phase space trajectory (PST). The proposed study leverages the dissimilarity of the "PST" to derive damage sensitive features (DSFs). The "DSFs" quantifies the dissimilarity between the "PSTs" corresponding to progressive damage states through Euclidean and Mahalanobis distance. The "DSFs" are potential indicators of occurrence, localization and progressive evolution of damages. The efficacy of the algorithm was demonstrated on a shear building that was progressively damaged through shock loads. Systematic experimental investigations were conducted to introduce localized and progressive damage in the structure. High-intensity shocks caused large deformation and plastification of the structural members. It was observed that "CPST" and "MDPST" were robust sensitive features that were able to quantify the damage initiation and evolution. The estimate of "DSFs" were compared with inter-storey drift that corroborates the evolution of damage. The algorithm was able to quantify the damage arising due to material nonlinearity.

Chapter 5

Damage classification in steel moment resisting frame using time-varying autoregressive modelling

5.1 Introduction

Health monitoring of structures under the post-earthquake scenario is one of the crucial aspects towards ensuring the future safety of people and infrastructure. The decision capabilities of municipal authorities are often paralyzed due to inadequate and unreliable certified assurances of the health assessment of the structures (Bruneau and MacRae, 2017). For instance, Tohoku earthquake in Japan, 2011 has resulted in 20,896 casualties and induced severe distress to 95,000 residential and commercial buildings (Japan Building Disaster Prevention Association, 2001). The 1994 Northridge (Los Angeles) earthquake in the USA and 1995 Kobe earthquake in Japan has a significant impact on the health of moment resisting steel structure (Bruneau et al., 1998). The structural damage to the steel moment resisting (MRF) buildings was significant and widespread but was unnoticed during structural damage assessment. The beam-to-column moment connections of "MRF", prior to 1994 Northridge experience brittle fracture due to excessive stress concentration near full penetration welds of the beam. These dramatic events have triggered a paradigm shift in the design philosophy, which has led to capacity based ductile designing of the steel structure that avoids brittle failure of beam-to-column connections (Bruneau et al., 1998). The efforts towards ductile designing of steel structure have resulted in design provisions and standards in North America namely; Specifications for Structural Steel Buildings (AISC, 1999), Seismic Provisions for Structural Steel Buildings (AISC, 2010b), and Prequalified Connections for Special and Intermediate Steel Moment Frames for Seismic Applications (AISC, 2010a). As per ASCE-7's, Design Basis Earthquake (DBE), the plastic hinge will form hierarchical at the predefined location in the steel moment resisting frame (SMRF) (ASCE-7). However, under the

influence of prolonging ambient vibration, the beam-to-column connection of "MRF" will undergo fatigue resulting in loosing of bolts causing the reduction in stiffness (Amezquita-Sanchez and Adeli, 2016). Additionally, under extreme loadings such as earthquake, blast and impact loading, the "MRF" connections undergo excessive magnitude of vibration (Krauthammer, 1999). These extreme vibrations can lead to catastrophic failure if the health of structure is left unmonitored. With the recent advancement in the technology of health monitoring systems, it is feasible to install smart sensory system economically and efficiently to acquire and process real-time data (Kundu, 2016). Notable applications of "SHM" framework towards damage detection in large structures are Tsing Ma Bridge in Hong Kong (Wong, 2004), Commodore Barry Bridge in the United States (Aktan et al., 2002), Golden gate bridge, San Francisco (Pakzad, 2010) and Jindo Bridge, South Korea (Nagayama et al., 2010).

The health monitoring of the structure is conventionally classified as global and local system identification (SI) of the system. The SI techniques are further divided into the spectral domain and temporal domain. Frequency domain SI techniques model the global response of the structure but are incapable to evaluate the elemental level information failing to detect local level damages (Wang and Haldar, 1997, Doebling et al., 1998, Farrar and Worden, 2007). Time domain SI techniques are sensitive to local level perturbation and can localize the damage in the temporal and spatial domain. The time domain methods are mainly categorized as parametric and non-parametric approaches. The parametric approaches extract the modal parameters in the time domain using advanced signal processing techniques (Hayes, 2009). Empirical Mode Decomposition (Huang et al., 1998), Wavelet Transform (Taha et al., 2006), Hilbert Huang Transform (Yang et al., 2004a), and Singular Spectrum Analysis (Lakshmi et al., 2017), Auto-Regressive (AR) Model (Lu and Gao, 2005), Auto-Regressive Moving Average Model (ARMA) (Bodeux and Golinval, 2001) are the popular approaches to evaluate modal parameters from the dynamic response. "AR" modeling is a widely accepted tool to model non-stationary signal using time-invariant coefficients. In

"AR" modeling, the physical response is assumed to be an auto-regressive process in the sense that the current state depends on the linear combination of past observations. The model error for an "AR" process is a zero mean, stationary Gaussian white noise. Bodeux and Golinval (2001), Sohn et al. (2000), Yao and Pakzad (2012) and Sohn et al. (2001) have proposed feature extraction algorithm based on the Autoregressive/Autoregressive with exogenous input/Autoregressive with moving average for damage detection in civil structures. These approaches assume linearity of the structural response and identify the damage by changes in the system modal parameters and novel damage index (Worden et al., 2008). Time series approaches in conjunction with statistical pattern recognition have evolved as a promising tool in "SHM" domain (Hayes, 2009, Farrar and Worden, 2012). Notable contributions of nonlinear damage detection using time domain methods are least-squares (LS) methods (Smyth et al., 2002, Yang and Huang, 2007), the iterative least squares with unknown input (ILS-UI) (Wang and Haldar, 1994, Ling and Haldar, 2004), the particle filter (PF) method (Namdeo and Manohar, 2007, Chatzi and Smyth, 2009).

In the current chapter, a feature extraction and damage classification in steel "SMRF" are performed using Time-Varying Autoregressive (TVAR) modeling excited using white noise process. Most of the local and global damage detection techniques based on the system identification tools inherently assume stationary response (Farrar and Worden, 2012). It implies that the model parameters and underlying statistics are independent of time. This assumption is often erroneous for responses arising from physical phenomena such as seismic excitation, aerodynamic loading and wave loading. There exists no generalized accepted signal modeling technique for non-stationary responses. The complexities associated with time dependency is circumvented by presuming the response as locally stationary for short and finite duration but globally non-stationary for the entire event (Rajan and Rayner, 1996). The local stationarity assumption facilitates in adapting standard stationary time series modeling using batch mode or sliding window technique. The width of the sliding window dictates the resolution of time localization of damage. The parametric modeling of the time

varying non-stationary response leads to extraction of time varying essential features manifesting the damage localized in time (Kopsaftopoulos and Fassois, 2013, Musafere et al., 2016, Krishnan et al., 2018).

These time varying auto regressive coefficient forms the damage sensitive features defined as feature vectors. The dominant feature vectors are extracted based on the model order of the "TVAR" model. The essential damage sensitive features are plotted in a hyperspace to form a damage sensitive cluster. The migration of the feature vector in the hyperspace manifests the evolution of the damage. The data clustering of the feature vector is further used to discover a set of patterns using statistical classification technique to judge the existence of the individual feature in different group or class of data (Jain, 2010). Data clustering is used for discovering underlying data structure, natural classification, and data compression. The clustering algorithm is classified as hierarchical and partitioned clustering. Hierarchical clustering recursively finds the nested cluster in agglomerative mode or divisive mode. Partitioned clustering technique finds simultaneous clusters without imposing any hierarchical restrictions. K-means clustering is a partitioned technique that minimizes the sum of squared error between the clustered mean and feature vector using a greedy optimization algorithm. Clustering and outlier detection is inherently coupled for high dimensional data set. Chawla and Gionis (2013) have presented a unified approach by formulating K means - - clustering that in conjunction with clustering of data detects and removes the outliers simultaneously. The clustering of the damage sensitive features in the hyperspace is utilized for classification and detection of damage using migration of clusters (Nair and Kiremidjian, 2007). The distance between the health state cluster and damage state cluster is evaluated using various metric defined as damage sensitive feature index (Nair and Kiremidjian, 2007, Gul and Catbas, 2011). Krishnan et al. (2018) have utilized the recursive statistic of the individual "TVAR" coefficient as a metric to quantify the damage in UCLA factored building. The damage induced in the structure is quantified using the statistical metric of the feature clusters.

In the current work, a novel damage detection algorithm is proposed for assessing the condition of the beam-column joint periodically to avoid catastrophic failure of steel structures. The algorithm is based on "TVAR" approaches of time series modeling in amalgamation with the K-means -- clustering (Chawla and Gionis, 2013). In past, the individual coefficients of "AR" and "TVAR" have been explored for spatial-temporal damage detection (Musafere et al., 2015, Krishnan et al., 2018). The current work claims that it is effective to consider the influence of all the "TVARC" in form of cluster instead of an individual coefficient to quantify the damage. This is because there could be contradictory conclusions if all the coefficients are tracked individually leading to inaccurate health assessment. In order to develop an efficient health assessment approach, the current work considers removal of an outlier from clusters. The presence of outliers affects the accuracy and efficiency of the proposed health assessment approach. The robustness of the proposed algorithm is further increased by exploring two damage sensitive features, this also reduces the possibility of false alarms. The "DSF" explored are namely; Mahalanobis distance and Itakura distance that quantifies the damage of deteriorating beam-column joints with help of "TVAR" coefficients, respectively. The following sections will discuss the essential building blocks of the proposed approach along with an experimental study and finally the results and conclusion derived from current work.

5.2 Time-varying autoregressive (TVAR) modelling

The proposed work emphasizes the health monitoring of the structural system using time series modeling of the response data and utilizes the time-varying coefficients to quantify the damage. Time-varying autoregressive (TVAR) modeling approach is used to model the nonstationary structural response of the structure excited using white noise (Musafere et al., 2015).

Let the signal $y(n)$ represent the acquired nonstationary structural response and $n \in [1;N]$ be the discrete time index where N is the number of discretely sampled data points in the acquired signal, the "AR" model of order p over the time $t \in [0;T]$ can then be represented as:

$$y(n) = \sum_{k=1}^{p} a_k y(n-k) + v(n) \tag{5.1}$$

where *v(n)* represents zero mean Gaussian white noise with variance σ_v^2 . In traditional "AR" process, the coefficients a_k are considered to as time invariant (Nguyen et al., 2009). However, in the present case, it is important to note that the "AR" coefficients $a_k(t)$ evolves with time owing to the non-stationary nature of the acquired responses. To estimate these time-varying "AR" coefficients, the Kalman filter (KF) an adaptive technique have been adopted, given the incremental observation data (Grenier, 1983). The KF framework of "TVAR" can be thought of by writing the "AR" model in a discrete state-space representation for the formulation of the adaptive filter. The following equations are a discrete state-space representation of AR coefficients.

$$\mathbf{x}(n) = \Gamma(n\text{-}1)\mathbf{x}(n\text{-}1) + \mathbf{w}(n) \tag{5.2}$$

$$y(\mathrm{n}) = \mathbf{C}(\mathrm{n})\mathbf{x}(\mathrm{n}) + \mathbf{v}(\mathrm{n}) \tag{5.3}$$

where $\mathbf{x}(n) = [a_1(n), a_2(n), ..., a_p(n)]$ is the unknown state variable analogous to AR coefficients, $\mathbf{w}(n)$ is the state transition noise with covariance σ_w^2, $\mathbf{v}(n)$ is the observation noise with covariance σ_v^2, $\mathbf{C}(n) = [y(n-1), ..., y(n-p)]$ is the system observation matrix with discrete *n* steps and $\Gamma(n-1)$ is assumed as an identity matrix $(I_{p\,\mathrm{x}\,p})$. The KF equations at each step can be written as a.) time update process and b.) measurement update process:

a.) Time update (prediction) process:

$$\mathbf{x}(n|n-1) = \mathbf{x}(n-1|n-1) \tag{5.4}$$

$$\sum_x (n|n-1) = \sum_x (n-1|n-1) + \mathbf{I}\sigma_w^2 \tag{5.5}$$

$$y(n|n-1) = \mathbf{C}(n)\mathbf{x}(n|n-1) \tag{5.6}$$

$$\sigma_y^2(n|n-1) = \mathbf{C}(n)\sum_x (n|n-1)\mathbf{C}(n)^T + \sigma_v^2 \tag{5.7}$$

b.) Measurement update (correction) process:

$$\mathbf{K}(n) = \sum_x (n|n-1)\mathbf{C}(n)^T \sigma_y^2 (n|n-1)^{-1} \tag{5.8}$$

$$\mathbf{x}(n|n) = \mathbf{x}(n|n-1) + \mathbf{K}(n)(y(n) - y(n|n-1)) \tag{5.9}$$

$$\sum_x (n|n) = \sum_x (n|n-1)[\mathbf{I} - \mathbf{K}(n)\mathbf{C}(n)] \tag{5.10}$$

where, $\mathbf{I}$ is the identity matrix of dimension $p \times p$, the posteriori $\mathbf{x}(n|n)$ is evaluated by a linear combination of priori estimate $\mathbf{x}(n|n-1)$. The Kalman gain matrix $K(n)$ makes an optimal prediction of $\mathbf{x}(n|n)$ by laying emphasis on the difference between the actual observational data and the predicted data. (Musafere et al., 2015). $\sum_x (n|n)$ and $\sum_x (n|n-1)$ represents the priori and posteriori error covariance estimates respectively.

In the current work, the emphasis is to obtain the coefficients matrix for healthy and damage scenario. The coefficient matrix is mathematically represented as:

$$[\mathbf{X}] = \begin{bmatrix} x(1|1) \\ \vdots \\ x(N|N) \end{bmatrix} \tag{5.11}$$

where N is the total number of sample in the response matrix and $x(N|N) = [a_1(N|N), ..., a_p(N|N)]$

The time varying "AR" coefficient are evaluated for healthy and damages state non-stationary structural response. The existence and evolution of damage is quantified by evaluating statistical property of the "TVAR" coefficients and is explained in later sections.

5.3 Clustering techniques and outlier detection

The "TVAR" coefficient forms the feature vector containing the damage sensitive feature used for health monitoring. The time varying feature vectors were arranged in a multi-dimensional hyperspace (X_c) to identify and track the evolution of the damage. The hyperspace matrix X_c is mathematically represented as:

$$[\mathbf{X}]_c = \begin{bmatrix} X_h \\ X_d \end{bmatrix}$$

$$[\mathbf{X}]_h = \begin{bmatrix} x_h(1|1) \\ \vdots \\ x_h(N|N) \end{bmatrix} = \begin{bmatrix} \{a_{1h}(1|1),...,a_{ph}(1|1)\} \\ \vdots \\ \{a_{1h}(N|N),...,a_{ph}(N|N)\} \end{bmatrix} \tag{5.12}$$

$$[\mathbf{X}]_d = \begin{bmatrix} x_d(1|1) \\ \vdots \\ x_d(N|N) \end{bmatrix} = \begin{bmatrix} \{a_{1d}(1|1),...,a_{pd}(1|1)\} \\ \vdots \\ \{a_{1d}(N|N),...,a_{pd}(N|N)\} \end{bmatrix}$$

where X_h and X_d are the coefficient vectors corresponding to healthy and damage states respectively. The matrix X_c contains information of both, healthy and damage state. To classify the extent and magnitude of the damage, a clustering technique is essential to label the state clusters separately in the matrix X_c. The dimension of the feature vector depends on the model order (p) of "TVAR" process. The clustering of the reference feature vectors in the hyperspace X_h provides the information of initial state referred to as "healthy/reference state". The changes in the orientation, translation, and expansion of the cluster implies the change of states. Change of state does not essentially imply the existence of damage unless its magnitude is quantified using damage sensitive index and corroborate with independent metrics.

As the damage will evolve in the structure, the state cluster will exhibit the topological and statistical changes. As the evolution of damage is rather slow under the ambient vibration, the migration of the state cluster in the hyperplane will lead to issues associated with overlapping and interweaving of the feature vectors in hyperspace X_c. These feature vectors present in hyperspace X_c may contain aberrations that can lead to wrong interpretation of the statistical properties. Therefore, a partitioning clustering and simultaneous outlier removal technique is needed to segregate the clusters. The K-means -- algorithm is used in current work for clustering and simultaneous removal of the aberrations.

5.3.1 K-means clustering

K-means is a partitional iterative clustering method that is widely used for finding the statistical structures in the data (Linde et al., 1980). Data matrix $A=\{x_i, i=1,...,k\}$ and a desired k no. of clusters are input variables in the K-means algorithm. K-means algorithm segments the data such that the sum of the square of the Euclidean distance between the mean of the cluster and points in the cluster is locally minimized. Hence, the goal is to minimize the objective function $J_{K-means}$ given by:

$$J_{K-means} = \sum_{i=1}^{k} \sum_{x_i \in \chi_k} || x_i - \mu_k ||^2 \tag{5.13}$$

Where, χ_k denotes the set of data points having mean μ_k (Jain, 2010)

The main steps of the **K-means algorithm** are as follows:

Step 1: Randomly select initial cluster centers $(\mu_i, i=1,...,k)$ from the data points in the input data matrix A.

Step 2: Each data point from A is assigned to the closest cluster centers $(\mu_i, i=1,...,k)$.

Step 3: New cluster center $(\mu_j, j=1,...,k)$ is updated to the mean of its constituent data points.

Step 2 and 3 are iterated until there is no further change in the assignment of each data point to the respective clusters.

5.3.2 K-means-- clustering

K-means is observed to be very sensitive to the presence of aberrations due to the fact that it utilizes the squared Euclidean distance as convergence criteria. The presence of even a few of the outliers can alter the actual cluster centers that may lead to inefficient clustering. Unlike K-means clustering, the outliers are not a by-product and are explicitly distinguished in K-means-- clustering: a unified approach to clustering and outlier detection (Chawla and Gionis, 2013).

K-means -- algorithm:

Step 1: Randomly select initial cluster centers $(\mu_i, i = 1,...,k)$ from the data points in the input matrix A.

Step 2: Each data point from A is assigned to the closest cluster center $(\mu_i, i = 1,...,k)$.

Step 3: Find the top n most distant points from their corresponding cluster centers.

Step 4: Recompute the cluster centers $(\mu_j, j = 1,...,k)$ excluding the computed anomalies.

Step 5: Iterate from step 2 to step 4 until the algorithm converges i.e. no further change in data point assignment.

The pictorial representation of K-means -- clustering is shown in Figure 5.1. Figure 5.1(a) shows three different clusters with only one label assigned (i.e. blue color). The value of k for dataset represented in Figure 5.1(a) is k=3. Therefore, in the first step of K-means --, three initial cluster centers/ seed points are selected. These seed points are marked as 'x' in Figure 5.1(b). Each point of the data set is now assigned to the closest seed point and is assigned a label (i.e. A, B and C) as shown in Figure 5.1(b).

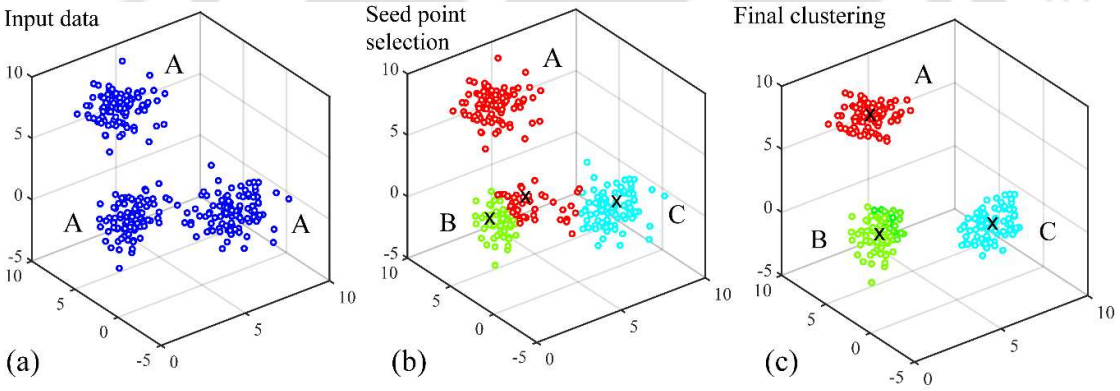

Figure 5.1 Pictorial representation of K-means -- clustering approach (For typical representation only)

Based on data points present in three clusters, the cluster centers are recomputed with the simultaneous exclusion of anomalies. These steps are continued until the algorithm converges

to three unique clusters excluding anomalies (Figure 5.1(c)). In current work, the coefficient matrix X_c is the input matrix of the K-means -- algorithm.

The Figure 5.2 (a) and (b) shows the output of clustering on simulated data using K-means and K-means -- approach, respectively. Figure 5.2a shows inefficient clustering using K-means clustering due to the presence of outliers. A tight bounded efficient cluster is obtained using K means -- algorithm. The center of clusters obtained after K-means deviates a lot in the presence of outliers. This problem of large deviation of the center of the cluster in presence of outlier is not observed in the case of K-means -- approach due to the elimination of the outlier and anomalies. Therefore in the current work, the K-means -- approach is adopted, since inaccurate clustering will risk the efficient quantification of damage severity by affecting the cluster center and thereby the results of "DSF".

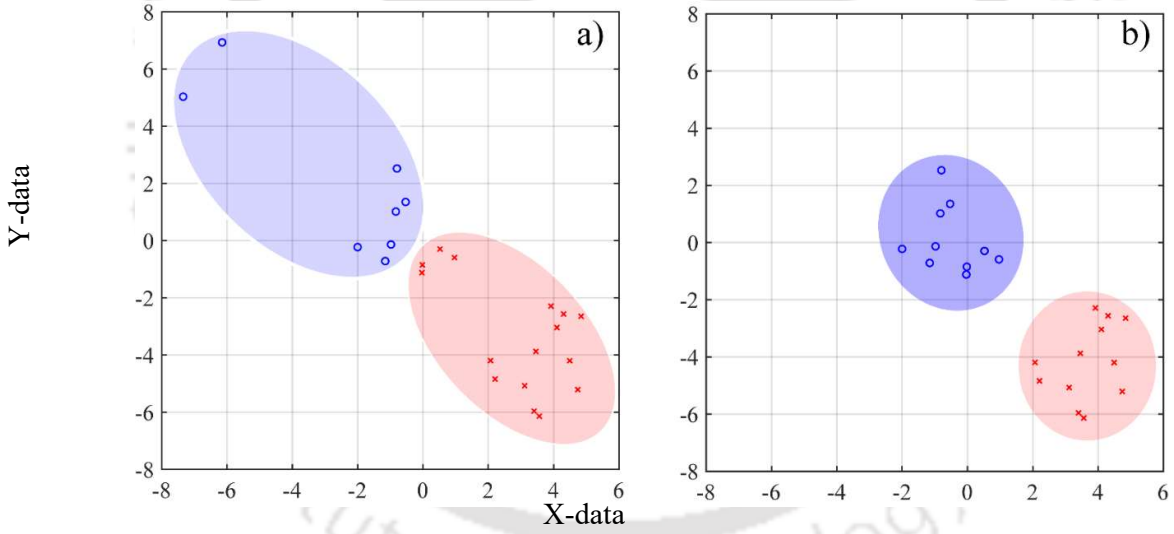

Figure 5.2 (a) Demonstrates inefficient clustering while adopting the K-means approach due to the presence of outliers and; (b) tighter clusters are obtained as outliers are removed while adopting the K-means -- approach (For typical representation only)

The next step of the proposed algorithm is to evaluate a statistical property correlating the healthy and damage clusters in order to quantify the severity of damage.

5.4 Damage sensitive features (DSF)

The attempt here is to develop a damage sensitive feature index using statistical metrics to quantify the relative magnitude of the damage using a topological representation of the health and damage state clusters. Two damage sensitive features are proposed based on the statistical properties of the "TVAR" coefficient namely, Mahalanobis distance (MD) and Itakura Distance (ID). The damage sensitive feature should be able to effectively distinguish between pristine and damage states and furthermore be able to quantify the magnitude of the damage.

5.4.1 Mahalanobis distance (MD)

In the current study, the healthy and damage clusters of "TVAR" coefficients are categorized using K-means – algorithm. In order to numerically quantify the segregation and separation of these clusters, Mahalanobis distance was calculated between healthy and damage coefficient clusters. Mathematically, Mahalanobis distance D_M between a matrix X and vector v is defined as:

$$D_M = \sqrt{(v-\bar{x})C^{-1}(v-\bar{x})^T} \tag{5.14}$$

Where C is the covariance matrix of X and $\bar{x}$ is the mean vector of X (De Maesschalck et al., 2000).

In current work, X is the damage cluster and v is the mean of the healthy cluster in "TVARC" hyperspace. It was expected that as the severity of damage increases, the Mahalanobis distance should escalate monotonically. The proposed "DSF" (D_M) is robust and capable of measuring the magnitude of damage in the structural system as explained in the next sections.

5.4.2 Itakura distance (ID)

Itakura Distance (ID) is a parameter that measures the distance between two sets of auto-regressive coefficients and is widely used in signal and speech processing applications (Muthuswamy and Thakor, 1998). ID is based on the model coefficients of the "AR" process

and the autocorrelation matrix of the response signal. In other words, ID tests the optimality of "AR" coefficients corresponding to an unknown state response if it is used to model the known state response.

Let $h(n)$ and $d(n)$ be the output response of steel frame corresponding to pristine and damage state respectively. The "AR" model for both the state can be mathematically represented as:

$$\begin{aligned} h(n) &= \sum_{i=1}^{p} a_h(i)h(n-i) + \varepsilon_h(n) \\ d(n) &= \sum_{i=1}^{p} a_d(i)d(n-i) + \varepsilon_d(n) \end{aligned} \tag{5.15}$$

where $a_h(i)$ and $a_d(i)$ are the parameters describing the acceleration response of the experimental system, $\varepsilon_h(n)$ and $\varepsilon_d(n)$ are white noise that corresponds to unpredicted data of the response signal. Now, for the optimal model order for the structural system p, the model coefficients for both the response signals can be written as:

$$\begin{aligned} \{\phi_1\} &= \{1 \; -a_h(1) \; -a_h(2) \; \cdots \; -a_h(p)\}^T \\ \{\phi_2\} &= \{1 \; -a_d(1) \; -a_d(2) \; \cdots \; -a_d(p)\}^T \end{aligned} \tag{5.16}$$

The mean square error (MSE) for the baseline process can be defined as follows:

$$\xi_1 = \{\phi\}_1^T [\mathbf{R}]_h \{\phi\}_1 \tag{5.17}$$

where $[\mathbf{R}]_h$ is the autocorrelation matrix of $h(n)$

$$[\mathbf{R}]_h = \begin{bmatrix} r_h(0) & r_h(1) & r_h(2) & \cdots & r_h(p) \\ r_h(1) & r_h(0) & r_h(1) & \cdots & r_h(p-1) \\ \vdots & \vdots & \vdots & \cdots & \vdots \\ r_h(p) & r_h(p-1) & r_h(p-2) & \cdots & r_h(0) \end{bmatrix} \tag{5.18}$$

The individual element in the matrix $r_h(k)$ is the autocorrelation of the signal $h(n)$ at different numbers of lag (m), which is given by:

$$r_h(m) = \frac{1}{N} \sum_{n=1}^{N-m} h(n)h(n+m), \; m = 0,1,2,...,p \tag{5.19}$$

where *N* represents the total number of samples in the response data $h(n)$.

The "MSE" for response signal $h(n)$ passing through the "AR" model of damage or unknown state signal $d(n)$ will be:

$$\xi_2 = \{\phi\}_2^T [\mathbf{R}]_h \{\phi\}_2 \tag{5.20}$$

Now for a particular case where the data $h(n)$ and $d(n)$ corresponds to the identical state, i.e. both corresponds to a healthy state, the relationship $\xi_1 = \xi_2$ holds true. In the case where the unidentified state is not the same as the healthy state, the "MSE" ξ_1 will be smaller than "MSE" ξ_2. Thus, the Itakura distance assesses how far the parameter of the unknown state (ϕ_2) is from the parameter of the known state (ϕ_1) and is mathematically defined as:

$$\mathbf{d}'(\phi_1, \phi_2) = \log \frac{\{\phi\}_2^T [\mathbf{R}]_h \{\phi\}_2}{\{\phi\}_1^T [\mathbf{R}]_h \{\phi\}_1} \tag{5.21}$$

Similarly, the ID tests how optimally the parameter of the baseline state fits the response signal of the unknown/damage state can be determined as:

$$\mathbf{d}''(\phi_1, \phi_2) = \log \frac{\{\phi\}_1^T [\mathbf{R}]_d \{\phi\}_1}{\{\phi\}_2^T [\mathbf{R}]_d \{\phi\}_2} \tag{5.22}$$

where $[\mathbf{R}]_d$ is the autocorrelation matrix of the signal $d(n)$. Now, by combining two ID measure represented in equation (5.21) and (5.22), a symmetric measure can be evaluated as:

$$\mathbf{ID} = \frac{1}{2}\left(\mathbf{d}'(\phi_1, \phi_2) + \mathbf{d}''(\phi_1, \phi_2)\right) \tag{5.23}$$

The assumption to get an ID is that the healthy and damage/unknown state signals consists of the same number of samples *N*. The sensitivity of the ID to the order of "AR" process is rather low, as pointed out in an experimental study carried out by Kong et al. (1995a). In current work, a low order of "AR" and "TVAR" process is adopted in order to avoid heavy computation. Therefore, this distance measure is suitable to be used as a damage sensitive feature in order to identify and quantify the damage.

5.5 Proposed algorithm

The current work is based on an algorithm that is an amalgamation of two different methodologies, namely: "TVAR" (section 5.2) and K-means -- clustering (section 5.3). The "TVAR" is used for fitting a non-stationary time series of the response data and eventually obtain time-varying model coefficients. Later on, K-means-- approach is applied on the "TVAR" coefficients represented in a hyperspace to categories the clusters.

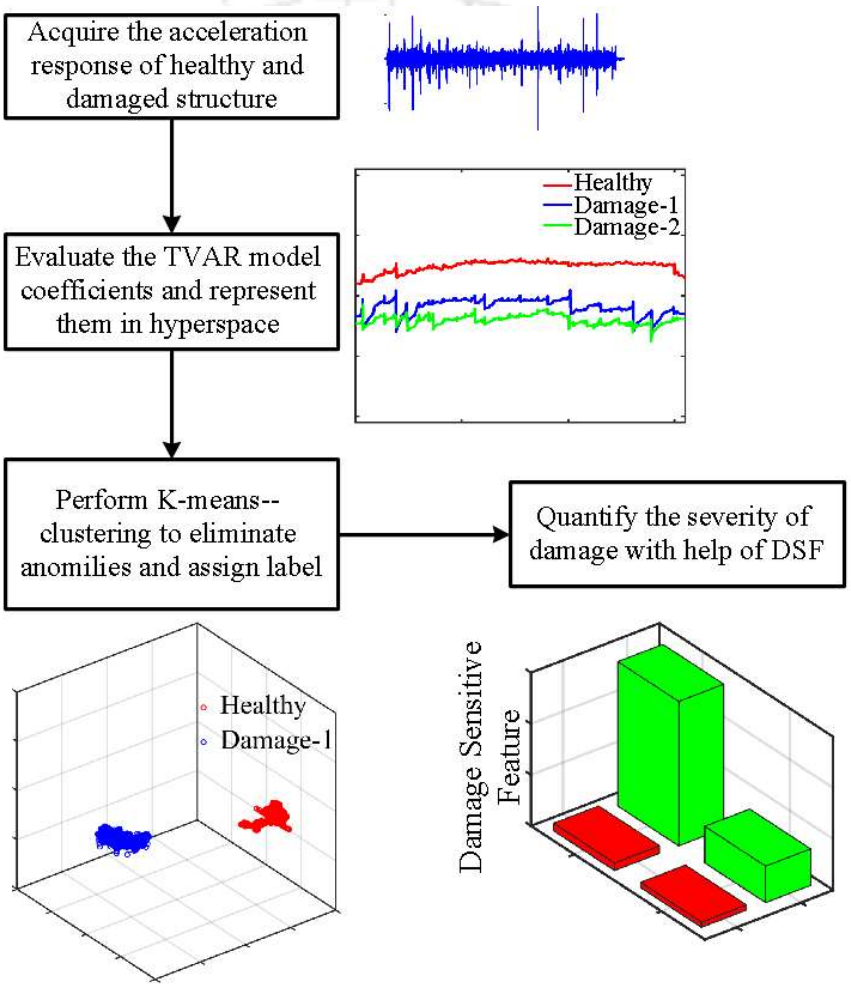

Figure 5.3 Block diagram of the steps involved in the novel damage detection algorithm using "TVARC"

The basic steps of the algorithm are as follows:

1) Initially, the non-stationary response of the steel frame subjected to white noise base excitation is acquired for healthy and damage case and response matrix is constructed.

2) The "TVAR" model is implemented on the response matrix to obtain "TVAR" coefficients matrix $[\mathbf{X}_h]$ and $[\mathbf{X}_d]$ corresponding to healthy and damage state, respectively (section-5.2).
3) K-means-- algorithm is performed on the coefficient matrix $[\mathbf{X}_c]=[\mathbf{X}_h \quad \mathbf{X}_d]$ to remove the outliers and data clustering is achieved (section-5.3).
4) Damage sensitive feature is proposed to quantify the severity of damage in the structure (section 5.4)

The schematic representation of the damage detecting algorithm for the non-stationary response is shown in Figure 5.3.

5.6 Experiment investigation

To demonstrate the efficiency, accuracy, and sensitivity of the proposed algorithm, an experimental study was conducted to detect the damage induced in the "SMRF" due to loosing of the beam-to-column moment connection.

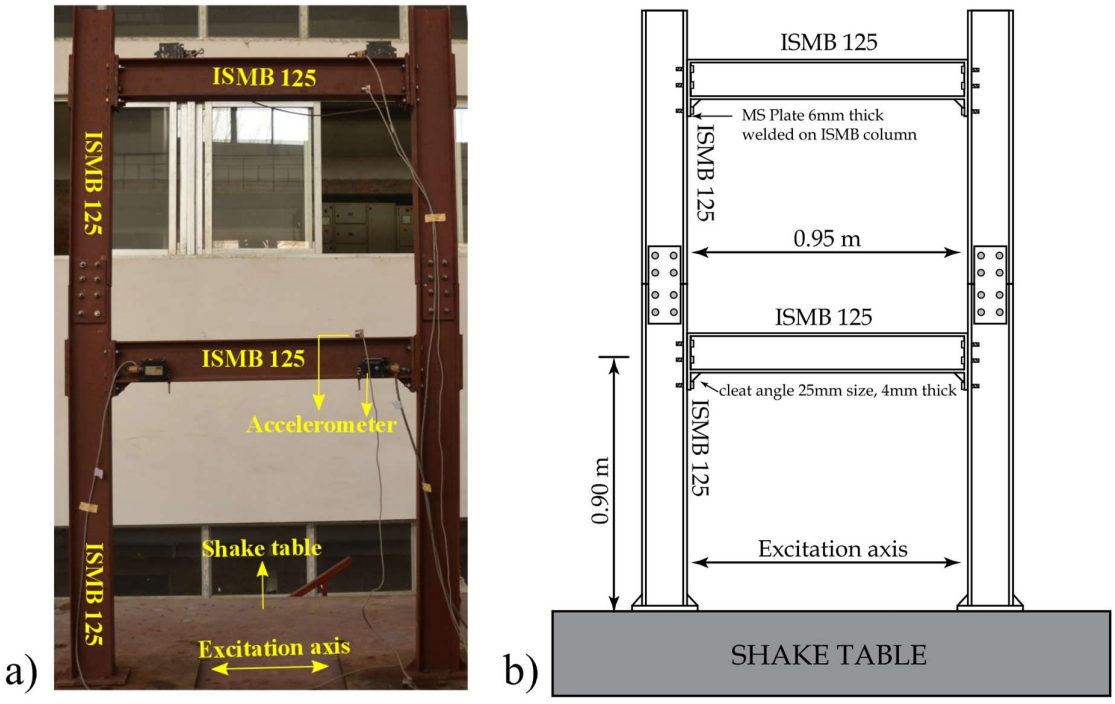

Figure 5.4 (a) Experimental setup and, (b) schematic sketch of steel frame

The beams and columns of the "SMRF" were designed as per the half-scale model consisting of the India Standard Medium Weight Beam (ISMB) of depth 125 mm. The total height of the structure was 1.8 m with each story height being 0.9 m and bay width of 0.95 m. The image and schematic diagram of the structure is shown in Figure 5.4 (a and b). The structural detailing of the moment resistant beam-to-column bolted connection is shown in Figure 5.5. Total of two set of three bolts of 10 mm diameter was used on either side to connect beam-to-column joint.

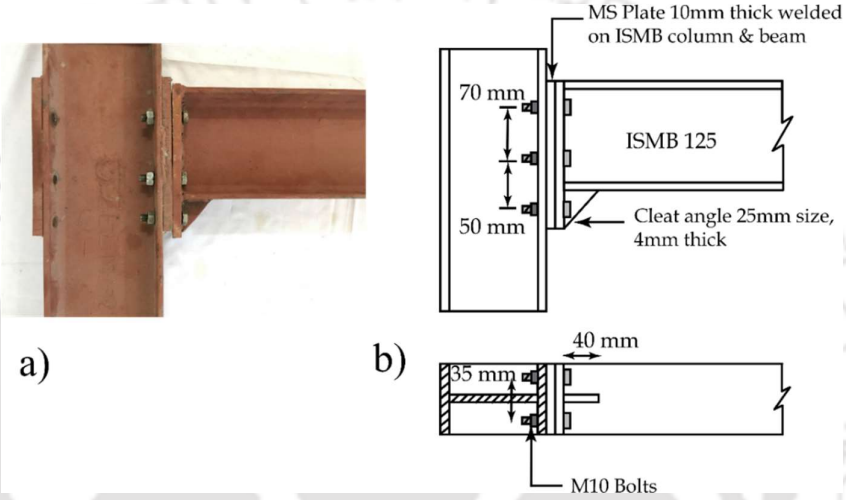

Figure 5.5 (a) Enhanced image of the moment connection of "SMRF" and; (b) schematic structural detailing of the beam-to-column connection

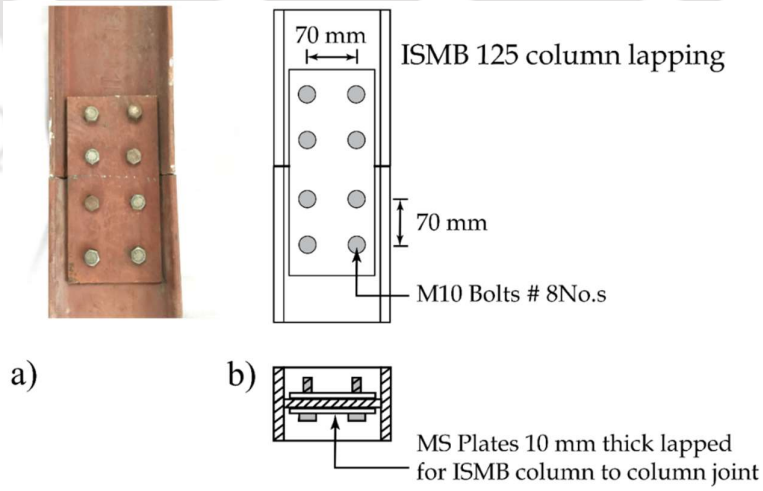

Figure 5.6 (a) Enhanced image of the column web splice connection and; (b) schematic structural detailing of the splice connecting column web

The structural detailing of the column web splice is shown in Figure 5.6 (a and b). Two 10 mm thick mild steel plates were used on either side of the column web as a splice plate. Total of eight bolts of 10 mm diameter was used to connect web splice plate.

The steel frame setup is instrumented with six numbers of accelerometers. Two number of Honeywell accelerometers *TEDS* by *HBM*^{TM} are used to instrument the two beams of steel "MRF" to measure the longitudinal acceleration. The Honeywell accelerometers can measure acceleration amplitudes from ambient noise level to a maximum of ±5g. The response acceleration data are collected using QuantumX MX410 *HBM*^{TM} Data Acquisition System at a sampling frequency of 200 Hz. The acceleration response of the beams in the vertical and transversal direction of both the floors was measured using four number of uniaxial force balance accelerometer (Model: ES-U2, Make: Kinematics Inc., USA). The Kinematics accelerometers can measure acceleration amplitudes from ambient noise level to a maximum of ±2g. The accelerometers are capable to signal conditioning and amplify the measured responses. The data from accelerometers is directly acquired with the help of a dynamic data acquisition system manufactured by M/s HBM GmBH, Germany (Model: MGC plus). The sampling rate of acquisition for all the experiments was 200 Hz.

The experiments were planned and performed in four stages. The four stages of experiments are mentioned below:

(i) Stage I- The "MRF" is in the reference/ pristine state and considered as healthy with all the connections rigidly tightened. This stage is also referred as the healthy/pristine/reference state.

(ii) Stage II- In this stage, the damage was induced at the second floor level of the beam-to-column connection by releasing one bolt of the joint. This is also referred to as damage-1 state.

(iii) Stage III- This stage is also referred to as damage-2 state. After completion of stage II experiment, the progressive damage was introduced by loosing of one bolt of the beam to column connection of the first floor.

(iv) Stage IV- This stage is also referred to as damage-3 state. After completion of stage III experiment, the progressive damage was introduced by loosing of one bolt of the splice plate connecting the column to column connection.

In this manner, progressive damage was introduced at the connections in the steel frame. The current work focuses on detecting damage in dynamic system irrespective of the damage sequence, therefore even if the damage is induced in any random pattern, the algorithm will still work. In each case, the response of steel frame subjected to white-noise excitation was acquired and analyzed. The response for each experiment is acquired after some transient period has passed (approximately 15-20 seconds).

5.7 Results and discussion

5.7.1 Acceleration response and Fourier analysis

The steel frame structure was excited with a white noise base excitation. The shake table was displacement controlled, therefore the white noise excitation was converted to displacement time history. Figure 5.7 shows the time history of the acceleration acquired at the base of the shake table. The acceleration response at the first floor and second-floor beam are shown in Figure 5.8 (a and b).

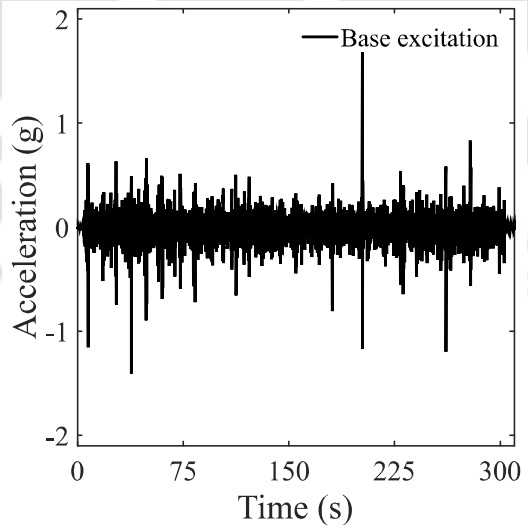

Figure 5.7 Acceleration time history of the base excitation subjected to the frame structure

The dominant excited frequency of healthy and damage structure was evaluated from the acceleration response and the results are shown in Figure 5.9. The dominant excited

frequencies of healthy frame structure under white noise excitation were 2 Hz and 17 Hz (refer to Figure 5.9).

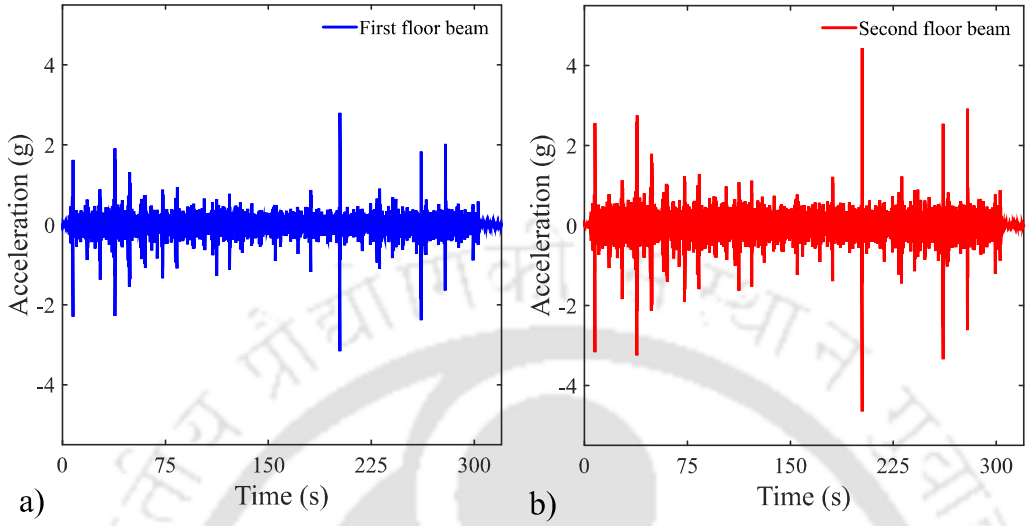

Figure 5.8 Acceleration time history of (a) first-floor and; (b) second-floor of two storey frame structure

Table 5.1 summarizes the dominant modal frequencies of steel frame depicting marginal changes in frequency content for healthy and damage state. In the frequency domain approach, the response is modeled globally considering only fewer lower order linear dynamics modes. Thus, spectral domain methods fail to evaluate the component level damages in the structure. The inefficiency of the spectral domain method demands for development of a robust time-domain algorithm that can segregate and quantify the magnitude of damage. The following section focuses on the proposed algorithm for segregating damage and healthy responses and later on quantifying the severity of damage.

Table 5.1 Frequency content of the steel frame structure under healthy and damage scenario

	First frequency (Hz)	**Second frequency (Hz)**
Healthy scenario	2	17
Damage scenario-1	1.8	12.18
Damage scenario-2	1.73	9.47
Damage scenario-3	1.5	9.22

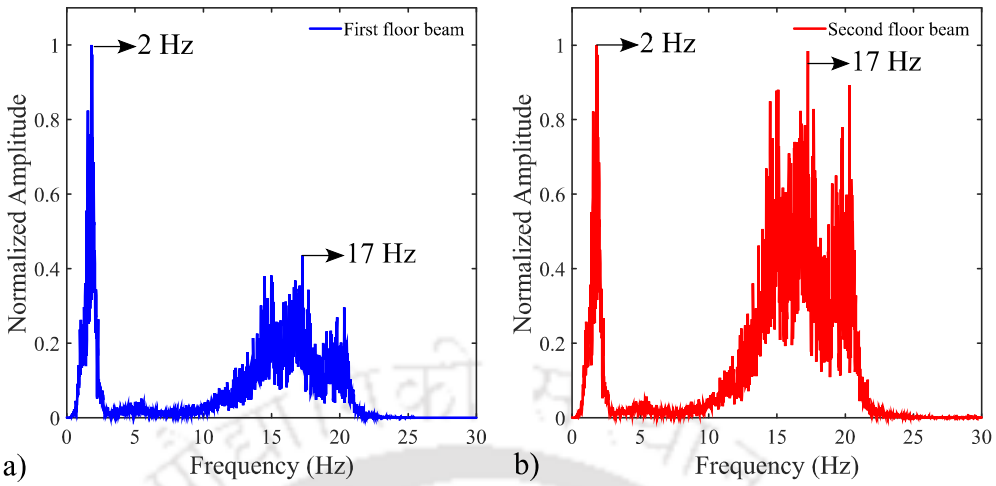

Figure 5.9 Frequency spectra of dynamic response at (a) first-floor beam and, (b) second-floor beam of the steel frame subjected to white noise base excitation

5.7.2 TVAR modelling of acceleration response

As discussed in section 5.6, a total of three progressive damage cases are induced in the structure. The first step of the proposed algorithm is to evaluate the "TVAR" coefficient of the time history response of the structure as explained in section 5.2.

Let the acquired data for healthy or any damage case be represented as $y_i(n)$, where 'i' is to distinguish healthy and damaged states and $n \in [1; N]$ is the discrete time index with $N = 64000$ in the healthy and damage cases. The AR model of order p for $y_i(n)$ is:

$$y_i(n) = \sum_{k=1}^{p} a_{ik} y_i(n-k) + v(n) \tag{5.24}$$

As mentioned in section 5.2, the non-stationary structural response is model with "TVAR" and its time-varying "AR" coefficient that are changing from a_k to $a_k(t)$ need to be evaluated. To estimate these time-varying "AR" coefficients, the Kalman filter (KF) an adaptive technique has been adopted. For a model order of p, tracking changes in the coefficients obtained by "TVAR" of response data indicate the possibility of the damage. In the present case, the model order is evaluated as p=3, leading to three time-varying sets of coefficients. The low model order selection for "TVAR" is due to save computational time. Figure 5.10

shows the time-varying coefficients series of all three coefficients corresponding to the healthy, damage-1 and damage-2 cases.

In the present case, the deviation of the coefficient $a_1(t)$ for the damage-2 state, w.r.t $a_1(t)$ corresponding to the healthy case is more when compared with the damage-1 state (Figure 5.10a). From this observation, it can be inferred that damage-2 state is more severe than damage-1, a true interpretation. Now, it is interesting to note that the deviation of the coefficient $a_2(t)$ for the damage-2 state, w.r.t $a_2(t)$ corresponding to the healthy case is less when compared with the damage-1 state (Figure 5.10b). This observation can lead to the conclusion that damage-1 state is more severe than the damage-2 state, a false interpretation. Also, due to arbitrary results of $a_3(t)$ for damage-1 and damage-2, no conclusion can be derived. Therefore, only tracking the changes in any one of the "TVAR" coefficients does not guarantee the detection, classification, and evaluation of the damage. For a successful "SHM", the proposed algorithm must be robust enough to quantify the damage considering all the three coefficients. For this purpose, the proposed algorithm evaluated a statistical "DSF" considering all the three coefficients in hyperspace as explained in next sections.

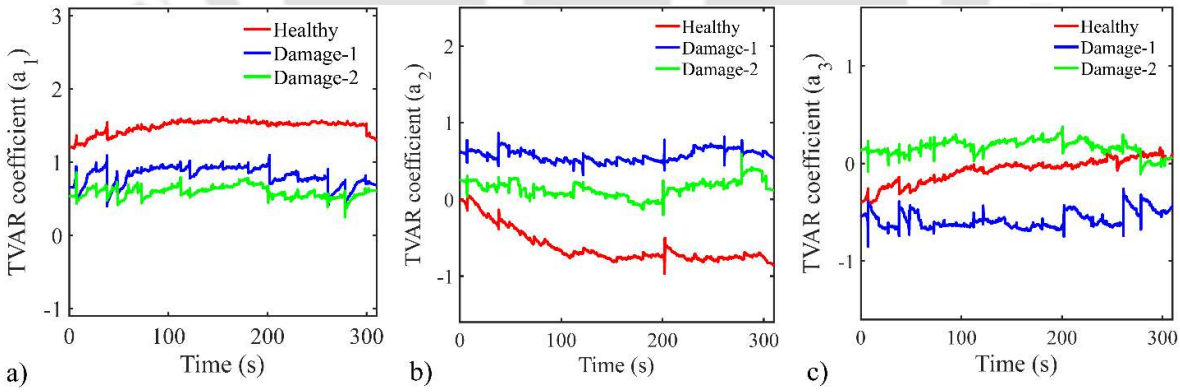

Figure 5.10 Time history representation of time series coefficients (a) "TVAR" coefficient (a_1), (b) "TVAR" coefficient (a_2) and; (c) "TVAR" coefficient (a_3)

5.7.3 Eigenanalysis of coefficient cluster

For a model order of *p,* the Eigen parameters of the *p*-dimension cluster formed by "TVAR" coefficients will alter significantly as the structure is damaged. In the present case, the model order is *p*=3, leading to Eigenanalysis of a three-dimensional coefficient cluster $[\mathbf{X}_c]$. The Eigenvector corresponding to the highest Eigenvalue is represented:

$$\{v\} = \begin{Bmatrix} v_1 \\ v_2 \\ v_3 \end{Bmatrix} \tag{5.25}$$

To identify a change in the state of the structure, a damage feature (α) is derived from $\{v\}$ as follows:

$$\boldsymbol{\alpha}_{12} = \tan^{-1}\left(\frac{v_2}{v_1}\right),\ \boldsymbol{\alpha}_{23} = \tan^{-1}\left(\frac{v_3}{v_2}\right),\ \boldsymbol{\alpha}_{31} = \tan^{-1}\left(\frac{v_1}{v_3}\right) \tag{5.26}$$

The proposed algorithm is initialized by buffering the 400 initial data samples from the coefficient cluster $[\mathbf{X}_c]$ and damage feature $(\boldsymbol{\alpha})$ is evaluated. As the new sample is acquired, the coefficient matrix $[\mathbf{X}_c]$ is populated and damage feature $\boldsymbol{\alpha}$ is updated in real-time.

The polar plot of damage feature $\boldsymbol{\alpha}$ (representing $\boldsymbol{\alpha}_{12}$) w.r.t time is shown in Figure 5.11. The orientation and the phase of the damage sensitive parameter α reverts its direction with any significant change in the state of the structure. In the present case, the orientation of the health state vector is in anti-clockwise that changes to clockwise direction as damage is evolved in the structure. From Figure 5.11, it can be concluded that two distinct states are present in the coefficient cluster $[\mathbf{X}_c]$. Therefore, by tracking the damage feature $(\boldsymbol{\alpha})$, the damage and healthy data are segregated. The results presented in this section proves that the damage feature $(\boldsymbol{\alpha})$ derived with the help of "TVAR" coefficients is a potential indicator to segregate two different states. To perform K-means - - clustering successfully it is must to specify the number of states present in the input matrix. Therefore, the results obtained in this section will serve as an input for K-means -- clustering.

It should be noted that eigenvectors are computed about the mean of the coefficient cluster $[\mathbf{X}_c]$. Therefore, because of the different mean of coefficient clusters $[\mathbf{X}_{c_1}]=\begin{bmatrix}\mathbf{X}_h & \mathbf{X}_{d_1}\end{bmatrix}$ and $[\mathbf{X}_{c_2}]=\begin{bmatrix}\mathbf{X}_h & \mathbf{X}_{d_2}\end{bmatrix}$ a difference in curves for the healthy states in Fig. 10 (a) and Fig. 10 (b) is observed.

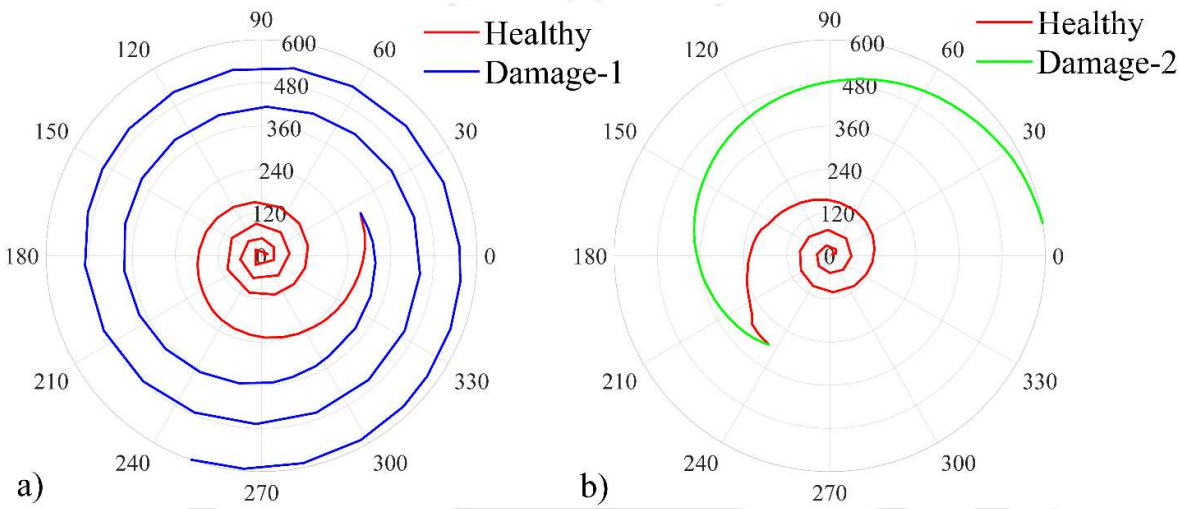

Figure 5.11 Polar plot of damage feature (α) for (a) coefficient cluster $X_{c_1}=\begin{bmatrix}X_h & X_{d_1}\end{bmatrix}$ and; (b) coefficient cluster $X_{c_2}=\begin{bmatrix}X_h & X_{d_2}\end{bmatrix}$

5.7.4 K-means -- clustering of coefficient cluster

The time history profile of "TVAR" coefficients is not a reliable option to quantify the damage as explained in section 5.7.2. Therefore, the coefficient matrix $[\mathbf{X}_c]$is represented in the $'n'$ dimensional hyperspace instead of time domain representation. The clusters formed using a modified representation of coefficients for healthy and damage case are well separated as shown in Figure 5.12. The separation of the cluster can be numerically quantified with the help of Mahalanobis distance and Itakura distance, as discussed in section 5.4.

The "TVAR" coefficient for damage-1 and damage-2 state as represented in Figure 5.10 (a) shows no conclusive evidence of the presence of the significant damage. Also, in Figure 5.10 (b), due to the decreasing trend of "TVAR" coefficient corresponding of damage-1 and

damage-2, it may be concluded that damage-2 is less severe than damage-1, which is not true. Therefore, the representation of the "TVAR" coefficients as a cluster in hyperspace has an inherent advantage over time-history representation. Figure 5.12 (a) and Figure 5.12 (b) represents the "TVAR" coefficients in hyperspace for coefficient cluster $[\mathbf{X}_{c_1}]=\begin{bmatrix}\mathbf{X}_h & \mathbf{X}_{d_1}\end{bmatrix}$ corresponding to damage-1 state and coefficient cluster $[\mathbf{X}_{c_2}]=\begin{bmatrix}\mathbf{X}_h & \mathbf{X}_{d_2}\end{bmatrix}$ corresponding to damage-2 state respectively. (Note: The total number of samples in an acquired response for each experiment is 64000 and for initialization of "TVAR" modeling 800 points are used therefore the size of the clusters $[\mathbf{X}_h]$, $[\mathbf{X}_{d_1}]$, and $[\mathbf{X}_{d_2}]$ is 63200 leading to the size of $[\mathbf{X}_{c_1}]$ and $[\mathbf{X}_{c_2}]$ as 126400).

In this study, the "TVAR" coefficients are observed to have high Kurtosis value indicating a heavy tail distribution. The heavy tail represents the initialization of the "TVAR" coefficients and hence do not represent any structural property of the frame structure. These initial "TVAR" coefficients are confidently designated as outliers and removed from coefficient matric using K-means -- algorithm. Figure 5.13 demonstrates simultaneous clustering with outlier removal and assigning the labels to the clusters using K-means -- clustering for coefficient cluster corresponding to both the damage case. The square marked points in Figure 5.13 indicate the presence of the outliers. In the present work, 10 percent of the total coefficient data points are designated as outliers. Such a high percent of outliers is due to the extremely dynamic and random nature of applied ground motion. The final outcome after application of the K-means -- clustering technique, for which the input is coefficient clusters $[\mathbf{X}_{c_1}]$ and $[\mathbf{X}_{c_2}]$ is presented in Figure 5.14. The clustering helps to label the coefficient clusters $[\mathbf{X}_{c_1}]$ and $[\mathbf{X}_{c_2}]$ into different states. As shown in Figure 5.14(a) and Figure 5.14(b), the healthy state cluster is labeled as circle (o) shaped data points which are marked as 'H', the damage-1 state cluster is labeled as triangle (Δ) also marked as D-1, the damage-2 state

cluster is labeled as a cross $(\times)$ and marked as D-2. The total number of states present in any coefficient cluster is obtained based on the formulation explained in section 5.7.3.

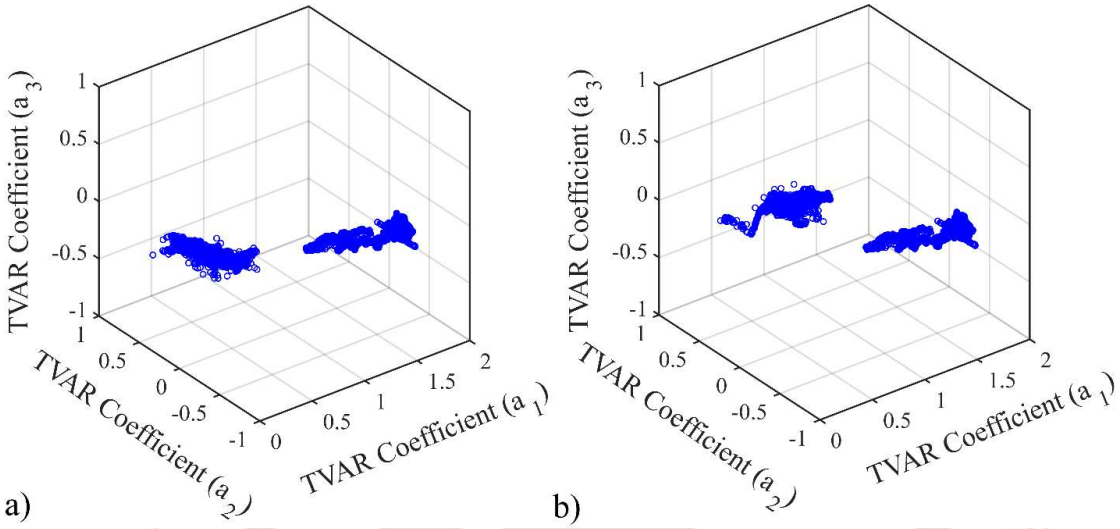

Figure 5.12 Representation of model coefficients in "TVARC" subspace for (a) coefficient cluster $[\mathbf{X}_{c_1}]=\left[\mathbf{X}_h \quad \mathbf{X}_{d_1}\right]$ corresponding to damage-1 and; (b) coefficient cluster $[\mathbf{X}_{c_2}]=\left[\mathbf{X}_h \quad \mathbf{X}_{d_2}\right]$ corresponding to damage-2

From Figure 5.14 it can be seen that after K-means -- clustering, the clusters corresponding to damage and healthy case are well parted and the outliers are separately designated. The distance of outliers from the mean of the cluster is greater for damage-2 state than that in damage-1 state. This is because as damage progresses the system vibrates in a much abrupt manner. This structural behavior is also reflected in the "TVAR" coefficient cluster, indicating the sensitivity of the proposed algorithm. The "DSF" is evaluated to measure the separation of the clusters to evaluate the magnitude of damage.

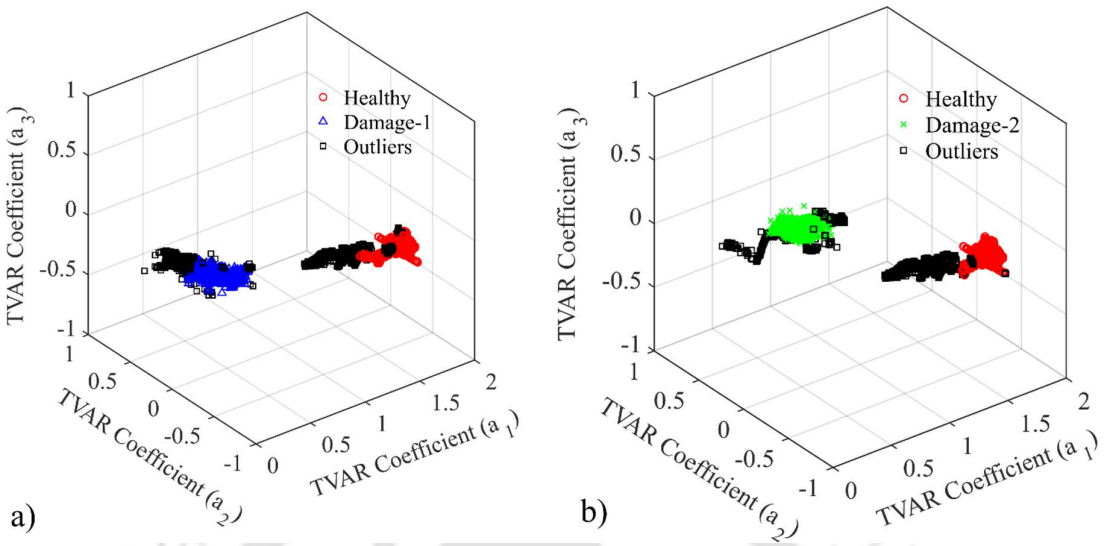

Figure 5.13 The K-means -- clustering approach assigned labels to the clusters for (a) damage-1 case and; (b) damage-2 case

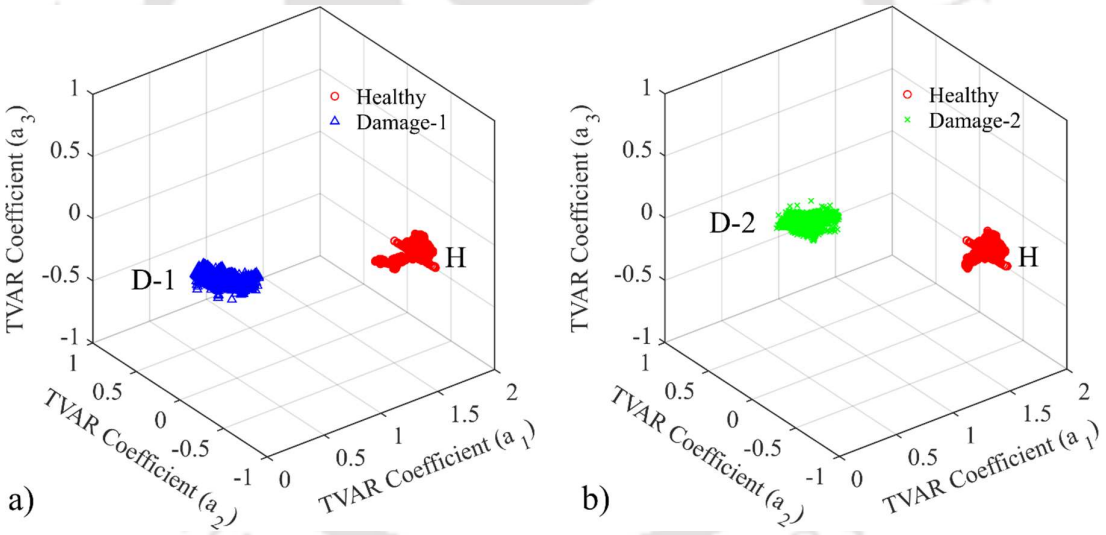

Figure 5.14 The final output after the clusters are processed by K-means -- approach for (a) damage-1 case and; (b) damage-2 case

5.7.5 Damage sensitive feature (DSF)

"DSF" using Mahalanobis distance ("MD-DSF"):

In order to numerically quantify the segregation and separation of these clusters, a "DSF" based on Mahalanobis distance was calculated. The damage sensitive features namely "MD-DSF" measures the Mahalanobis distance between "TVAR" coefficient cluster

corresponding to pristine state and damage state. The mathematical formulation of "MD-DSF" is:

$$MD\text{-}DSF_i = \sqrt{(\mu_h - \overline{\mu_{d_i}})Cov(X_{d_i})(\mu_h - \overline{\mu_{d_i}})^T} \tag{5.27}$$

where $Cov(X_{d_i})$ is the covariance matrix of damage cluster (X_{d_i}), μ_h is mean of the healthy cluster (X_h) and μ_{d_i} is mean of damage cluster (X_{d_i}). The damage states considered in current work are three, therefore we calculated "*MD-DSF"* for damage states as follows:

$$MD\text{-}DSF_1 = \sqrt{(\mu_h - \overline{\mu_{d_1}})Cov(X_{d_1})(\mu_h - \overline{\mu_{d_1}})^T} \tag{5.28}$$

$$MD\text{-}DSF_2 = \sqrt{(\mu_h - \overline{\mu_{d_2}})Cov(X_{d_2})(\mu_h - \overline{\mu_{d_2}})^T} \tag{5.29}$$

where $\mu_h, \overline{\mu_{d_1}}, \overline{\mu_{d_2}}$ are the mean of healthy, damage-1 state, and damage-2 state clusters respectively and are marked as h, d-1, and d-2 in Figure 5.14. Similarly for damage-3 state, $MD\text{-}DSF_3$ was evaluated. The damage sensitive feature "*MD-DSF"* was evaluated for the first floor and the second floor for all the damage cases, the results for which are presented in Figure 5.15. The "DSF" value is greater for damage-2 state compared to damage-1 state, due to accumulative and progressive damage evolution in the structure. The magnitude of the "DSF" increases for stage-2 and stage-3 experiment, indicating the progressive evolution of damage. From Figure 5.15 it can be observed that both, the Mahalanobis distance between the mean of healthy and cluster of damage corroborates with the magnitude of damage. The algorithm proposed in the current work was efficient enough to parametrically quantify the extent of the damage.

"DSF" using Itakura distance (ID-DSF):

In order to numerically quantify the damage, another "DSF" based on Itakura distance was calculated. The damage sensitive features namely "ID-DSF" measure the ID between pristine state and damage state. The mathematical formulation of "ID-DSF" is presented in section 5.4.2, where ID was explained as a batch mode analysis. Whereas, in current work, ID is

calculated as windowed analysis The entire signal is divided into '*ns*' sample size '*q*' number of windows and ID for each window is calculated to get a vector of ID. The actual values of '*ns*' and '*q*' for the current study are 800 and 80 respectively.

$$\overline{ID\text{-}DSF} = \begin{Bmatrix} ID_1 \\ ID_2 \\ \vdots \\ ID_q \end{Bmatrix} \tag{5.30}$$

where, ID_q is Itakura distance for healthy and a damage state corresponding to q numbered window. In current work, the number of samples for all the experiments is the same leading to the same number of windows for fixed window size. Therefore, a particularly numbered window corresponding to healthy state response can be tested with the same numbered window of damage state response. The fourth moment of the vector represented in equation 5.30 was further calculated to obtain a scalar damage sensitive feature $(\overline{ID\text{-}DSF})$.

$$ID\text{-}DSF = Kurtosis(\overline{ID\text{-}DSF}) = E\left[\left(\frac{\overline{ID\text{-}DSF} - \mu_{\overline{ID\text{-}DSF}}}{\sigma_{\overline{ID\text{-}DSF}}}\right)^4\right] \tag{5.31}$$

Where, $\mu_{\overline{ID\text{-}DSF}}$ and $\sigma_{\overline{ID\text{-}DSF}}$ are mean and standard deviation of the vector $\overline{ID\text{-}DSF}$ (equation 5.30). The results of "ID-DSF" (equation 5.31) are shown in Figure 5.15(b) for all the damage state.

For the damage-1 state, where damage is only manifested at the second floor, "ID-DSF" shows a large value at both the floors, unlike "MD-DSF". This indicates the sensitivity of "ID-DSF" to be higher than "MD-DSF", therefore even in case of the sparse sensor, "ID-DSF" can be used to get the information regarding the evolution of damage in structure globally. In the case where sensors mounted in a structure are adequate in number and present at a critical position, "MD-DSF" and "ID-DSF" both can be used to localize damage accurately and avoid any false alarm.

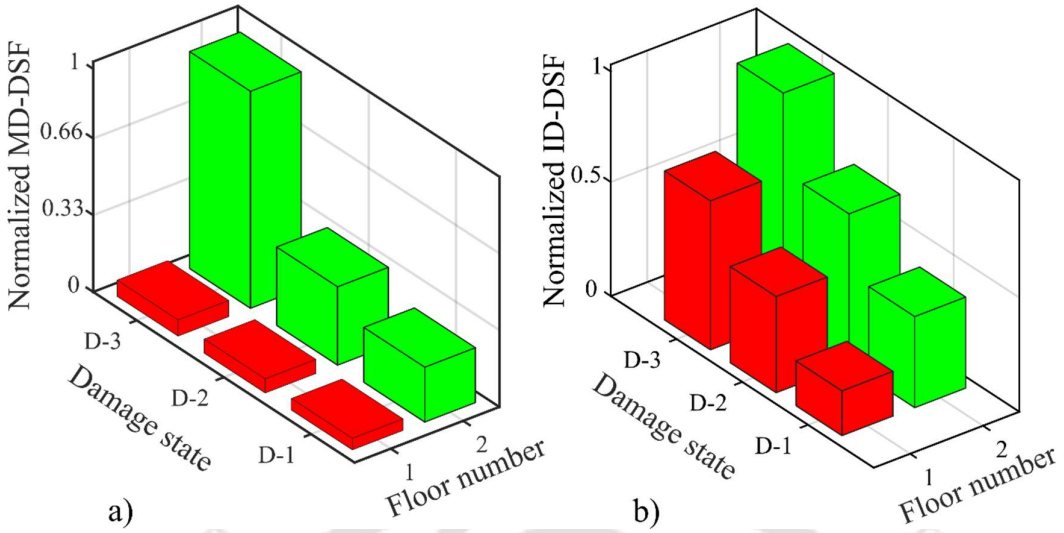

Figure 5.15 Graphical representation of the (a) "DSF" based on Mahalanobis distance and; (b) "DSF" based on Itakura distance evaluated for all the damage states

5.8 Conclusion

The current chapter proposes a robust damage detection technique using time series modelling integrated with clustering techniques. To demonstrate the efficacy of the proposed novel algorithm, a two storey steel frame was excited with white noise base excitation. The damage was manifested in steel frame progressively by loosening bolt/bolts of beam-column joint and column-to-column splice plate.

The non-stationary response of the structure subjected to white noise excitation was modelled using time-varying autoregressive modelling The model order of the structural response subjected to ambient vibration was low (i.e. p=3) that eliminated high computational resources. An adaptive Kalman filter (KF) technique was utilized to evaluate the time-varying "AR" coefficients (TVARC). The "TVARC" encompasses the information of initiation and progression of damage in its time series that is used to evaluate the damage. It was observed that only dominant "TVARC" depicts the changes in the coefficient progressively. Whereas, the remaining two coefficients exhibit random behavior and had no correlation with the actual damage case. Hence, a better alternative was to combine all these coefficients and represent in "TVARC" subspace that showed enhanced capabilities to segregate and classify the damage.

The "TVARC" representation showed distinctly and spatially resolved healthy and the damage clusters in the hyperspace. The segregation and separation of the clusters in the "TVARC" subspace was numerically quantified by two damage sensitive features using Mahalanobis distance and Itakura distance. Both the "DSF" exhibits larger numerically magnitude for the damage-2 case in comparison to damage-1 and corroborated with the progressive evolution of damage successfully. The "DSFs" are potential and sensitive indicators to detect initiation and progressive evolution of damage state. The developed algorithm was able to successfully quantify the damage arising due to loosing of the bolt in the beam-to-column connection and column-to-column connection by splice pate. The algorithm demonstrates its capability to detect slow and gradual evolution of damage in the structure under nonstationary ambient vibration excitation

Chapter 6

Damage quantification in moment resisting frame using phase space reconstructed from independent component sources

6.1 Introduction

Monitoring the health of structure is of paramount importance to ascertain the safety and security of people and infrastructure upon the occurrence of extreme loading events such as earthquake, hurricane, and tornado. Several earthquakes in the past, have exposed the vulnerability of beam-column joints in the steel moment resisting frames (SMRF). In the literature, several structural health monitoring (SHM) techniques have evolved to detect the local and global damage in the structure. The popular and widely accepted "SHM" techniques in the time domain are Hilbert Huang Transform (Yang et al., 2004a), Empirical Mode Decomposition (Huang et al., 1998), Wavelet Transform (Taha et al., 2006), and Singular Spectrum Analysis (Lakshmi et al., 2017), Frequency domain decomposition (FDD) (Brincker et al., 2000), Auto-Regressive (AR) Model (Lu and Gao, 2005), Auto-Regressive Moving Average Model (ARMA) (Bodeux and Golinval, 2001) and Extended Kalman Filter Weighted Global Iteration techniques (Katkhuda and Haldar, 2008). These techniques perform satisfactorily for the linear dynamic system to identify the system parameters. However, the occurrence of damage often introduces nonlinearity in the structure that possesses severe challenge in system identification. To address the complexities involved in the nonlinear damage detection, a novel approach based on phase space trajectories of the system response have been explored (Todd et al., 2004). The damage detection and quantification is performed by evaluating the geometrical and statistical changes between the phase space trajectory (PST) of the baseline and damaged structure (Nichols et al., 2003).

The statistical distance between "PSTs" is quantified using Rao's distance(Atkinson and Mitchell, 1981), Mahalanobis distance (Figueiredo et al., 2011, Mosavi et al., 2012) and Bhattacharya distance (Liu et al., 2014) to derive damage sensitive features (DSFs).

In nonlinear damage detection, efficient "DSFs" are Local Attractor Variance Ratio (LAVR) (Todd et al., 2001), Phase Space Warping (PSW) (Alwasel et al., 2017), and Change of Phase Space Topology (CPST) (Paul et al., 2017) . The "PST" for any dynamic system can be reconstructed with the help of Takens' theorem (Takens', 1981). The constraints being excitation should be of low-frequency resulting in low dimension response. The mono-component response signal of low dimension helps to identify the system parameters easily and accurately. In past studies, these limitations have been addressed to detect damage using phase space methodology (Nichols, 2003, Paul et al., 2017). In the real scenario, the excitation is often high-frequency and the response also is of higher dimension. Therefore, the phase space based methodology cannot be directly applied for successful damage identification. In order to get a lower dimensional mono-component signal from the measured response, the methodology such as Empirical mode decomposition (EMD) (Huang et al., 1998), Independent component analysis (ICA) (Fraser and Swinney, 1986), Principal component analysis (Shlens, 2003), Wavelet decomposition (Hou et al., 2000) have been used. Linear system identification has been successfully achieved using Principal component analysis (PCA), Independent component analysis (ICA) (Yang and Nagarajaiah, 2012), Wavelet transform (Hazra and Narasimhan, 2009), Eigensystem realization algorithm (Juang and Pappa, 1985), Stochastic subspace iteration (SSI) (Van Overschee and De Moor, 1996), algorithm for multiple unknown signals extraction (AMUSE) (Tong et al., 1990), Ibrahim time domain (ITD) (Ibrahim and Pappa, 1982), Natural excitation technique (NExT) (James et al., 1995) and Second-order blind identification (SOBI) (Belouchrani et al., 1997, Cichocki and Amari, 2003, Antoni, 2005, Poncelet et al., 2007). However, nonlinear system identification is still a largely unexplored topic in structural dynamics.

Independent component analysis aims to retrieve the set of independent sources from the physical measurements without relying on the information of the underlying mixing process (Belouchrani et al., 1997, Hyvärinen and Oja, 2000). Blind source separation techniques based on independent component analysis is gaining wide acceptance in the structural modal analysis (Hazra et al., 2012), structural damage detection (Sadhu and Hazra, 2013, Yang and Nagarajaiah, 2014a), condition monitoring (Gelle et al., 2003), and mode separation (Tang et al., 2012, Sadhu et al., 2017). "ICA" seeks to recover the component of the signal that is statistically as independent as possible. Kerschen et al. 2007 demonstrated that the modal responses act as virtual independent sources and could be retrieved from the structure responses with a low level of damping (less than 1 %). Several authors have exploited the second order statistic of the temporal signal using SOBI to extract model features of highly damped structures subjected to seismic and wind-induced excitation (Poncelet et al., 2007, Zhou and Chelidze, 2007, Hazra et al., 2010, Yang and Nagarajaiah, 2013a).

In the presented study, a damage detection algorithm based on the amalgamation of "ICA" and phase space methodology is proposed. The experimental study on the steel moment resisting frame (SMRF) was carried out to validate the proposed algorithm. The steel "SMRF" was subjected to base excitation and damage was induced by loosening bolts at the joint connections. Initially, "ICA" on the response was performed to separate mode mixing and extract mono-component modal responses. The motivation to implement "ICA" algorithm is to extract virtual independent source information that may closely represent modal response for the lightly damped system. The presence of damage has a strong influence on the modal responses that might get suppress during the mixing process. In the next step, phase space topology of the modal response was reconstructed in order to capture the dynamical behavior of "SMRF". The phase space reconstruction technique is limited to a signal of low dimension. The current work deals with the health monitoring of "SMRF" frame subjected to random base excitation, resulting in a response of high dimension. Considering

the acquired raw response for reconstruction of "PST" and thereby evaluating damage sensitive feature (DSF) for damage detection will result in an inaccurate detection. Therefore, a lower dimension and independent modal responses obtained with the help of "ICA" are considered for reconstruction of "PST". The Phase space reconstruction of virtual independent sources rather than observed response provides a unique opportunity to detect damage from modal system dynamics. Later, the dissimilarity between "PST" of healthy and damaged state is evaluated to quantify damage using "DSFs". To the best of authors knowledge, the novel algorithm based on the amalgamation of "ICA" and phase space has not been explored in the literature. The following sections will explain the independent component analysis, procedure of reconstructing "PST", an experimental investigation carried out in the presented study and lastly results, discussion and derived conclusions are also discussed.

6.2 Independent component analysis

Principal component analysis (PCA) is a dimension reduction technique that utilizes orthogonal transformation to convert correlated responses to linearly uncorrelated responses using Eigenvalue decomposition (Shlens, 2003). For example, in case of strongly correlated data sets having a joint probability density function as an ellipse, the "PCA" will lead to uncorrelated variables and orients the principal vectors along its major and minor axis. "PCA" is used to transform the data from higher dimension subspace to lower dimension subspace by retaining the variance present in the original data. "PCA" of the data $x(t)$ having dimension $n \times m$ performs the orthogonal transformation of the basic vector obtain from Eigenanalysis of the data covariance matrix and projected back on the subspace corresponding to the largest Eigenvalues. The transformed data retain the dominant features of the original data. The overall variance of the transformed data is the same as that of the original data (Shlens, 2003).

From the structural dynamics perspectives, in case of undamped free vibration, the principal orthogonal decomposition of structural response yields principal orthogonal modes that

closely resembles linear normal modes (Feeny and Kappagantu, 1998, Kerschen and Golinval, 2002). However, for uncorrelated random variables (RVs) having non-Gaussian probability density function, the principal components (PCs) are not statistically independent, this arises serious challenges in modal identification of highly damped structural vibration system. Statistical independence is a stronger property than uncorrelated random variables (RV). The uncorrelated RV does not strictly imply statistical independent event. The structural modes of vibration are statistically independent that motivates to explore independent component analysis (ICA) rather than "PCA" for system identification (Kerschen et al., 2007).

"ICA" is a multivariate statistical analysis that assumes the dynamic responses are a linear combination of statistically independent sources. The "ICA" model with two independent sources and two acquired dynamic response is represented as follows:

$$\begin{aligned} \{x_1(t)\} &= \mathbf{a}_{11}\{s_1(t)\} + \mathbf{a}_{12}\{s_2(t)\} \\ \{x_2(t)\} &= \mathbf{a}_{21}\{s_1(t)\} + \mathbf{a}_{22}\{s_2(t)\} \end{aligned} \tag{6.1}$$

The generic model can also be represented as $\{x(t)\} = [\mathbf{A}]\{s(t)\}$. Here, $x(t)$ is the vector of dynamic responses acquired from the vibration of a structure subjected to white noise. The dynamic response emanates from the linear combination of the source components $s(t)$. The linear relationship between the response $x(t)$ and the source components $s(t)$ is given by linear combination represented in the mixing matrix $[\mathbf{A}]$. The main challenge in the generic formulation of the "ICA" is neither the mixing matrix $[\mathbf{A}]$ or source component $s(t)$ is known a prior. The extracted sources $s(t)$ are the independent components and the basis vectors of the mixing matrix $[\mathbf{A}]$ are referred to as "ICA" modes. "ICA" modes extracted from the mixing matrix are essentially linearly independent. These "ICA" modes are achieved by maximizing the non-Gaussianity of the response data. Therefore, "ICA" is irrelevant for the data possessing Gaussian distribution as the higher order statistic are zero.

"ICA" assumes that the sources are statistically independent at each time instant (t). "ICA" seeks to estimate demixing matrix $[\mathbf{W}]$, such that possibly the independent components are recovered as:

$$\{Y(t)\} = [\mathbf{W}]^T \{x(t)\} \tag{6.2}$$

Where $Y(t)$ is as independent as possible and are approximately the source vector $s(t)$ and the W is approximately inverse of the mixing matrix A. From equation (6.2),

$$\{Y(t)\} = [\mathbf{W}]^T [\mathbf{A}]\{s(t)\} = [\mathbf{Z}]^T \{s(t)\} \tag{6.3}$$

Equation (6.3) implies that the $[\mathbf{Z}]^T \{s(t)\}$ will be more Gaussian than the source $s(t)$ itself. The central limit theorem states that for the large numbers, the sum of two independent RV is more Gaussian than the original RV. The maximization of non-Gaussianity of the $[\mathbf{Z}]^T \{s(t)\}$ guarantees the convergence of $Y(t)$ towards independent components. The statistical indicator for quantifying the non-Gaussianity is the Kurtosis. The Kurtosis of the Gaussian RV is zero. "ICA" treat the dynamic response as RV and extract the time-independent component equivalent to standing modes of vibration.

The "ICA" extract linearly independent modes, whereas "PCA" extracts orthogonal modes by un-correlating the data. "ICA" has an advantage over "PCA" as the structural vibrations modes are linearly independent and not essentially orthogonal is practical sense. However, "ICA" also requires the data to be non-Gaussian, which is not the case with standing wave modes. In the current work, "ICA" algorithm proposed by Bell-Sejnowski "ICA" (Bell and Sejnowski, 1995) and Stone (2004) is implemented.

6.3 Phase space representation

The mathematical representation of the dynamic response of a d -dimension system is the first-order differential equation:

$$\dot{x} = T(x,t) \tag{6.4}$$

where T represents a nonlinear function of both time (t) and state variables (x), the term $\dot{x}$ represents the first derivative of the state variable. In order to study the system dynamics, the state variables are represented in a multi-dimensional phase-space trajectory (PST). At any given time instant, each and every point of the "PST" provides the information regarding the dynamics of the state variables. From the dynamic equation of motion, it is possible to get information about all the state variables such as acceleration, velocity, and displacement. Whereas, same is difficult for data acquired from laboratory or field investigations. However, this limitation can be relaxed by applying Takens' embedding theorems (Takens', 1981). The embedding theorem proposed by Takens' states that with the help of an accurate measurement of an individual state variable, information of the dynamical system can be reconstructed numerically. Implementing Takens' embedding theorem the successful reconstruction of the trajectories is done by concatenating the time series of an individual measured variable m times, each corresponding to a delay of τ. Hence at any time n, the attractor can be represented as:

$$[\mathbf{X}(n)] = [x(n), x(n+\boldsymbol{\tau}), ..., x(n+(\mathbf{m}-1)\boldsymbol{\tau})] \tag{6.5}$$

Where 'τ' is the time lag and 'm' is the embedding dimension, this procedure or method of reconstruction is called the method of delays.

6.3.1 Average mutual information function to obtain time delay

The time lag $(\boldsymbol{\tau})$ is a key parameter for the reconstruction of linearly uncorrelated phase space, therefore the appropriate selection of time lag $(\boldsymbol{\tau})$ is of utmost importance. The most common method for selection of an optimal value of time lag is with the help of autocorrelation function (Abarbanel and Gollub, 1996). The first most time instant for which the autocorrelation function corresponds zero value is selected as an optimal value of time lag.

The normalized autocorrelation function '$c_{xx}(t)$' is represented as:

$$c_{xx}(t) = \frac{\sum_{n=0}^{N-1}[x(n)-\bar{x}][x(n+t)-\bar{x}]}{\sum_{n=0}^{N-1}[x(n)-\bar{x}]^2} \tag{6.6}$$

where $\bar{x}$ represents the mean value of any time series (x).

The optimal time lag for the dynamical systems described by nonlinear mathematical models cannot be evaluated by autocorrelation function. For this purpose, average mutual information function (AMIF) is adopted for nonlinear systems. Fraser and Swinney (1986) proposed the "AMIF", that is a probability-based function and is calculated as:

$$I(t) = \sum_{n} p(x(n), x(n+t))\log_2 \frac{p(x(n), x(n+t))}{p(x(n))\,p(x(n+t))} \tag{6.7}$$

where, I is the "AMIF" of t, $p(x(n),x(n+t))$ are the joint probability density function, and $p(x(n+t))$ are the estimated probability density of $x(n)$ and $x(n+t)$ respectively. The time lag selected as lag for reconstruction is the one that corresponds to the first minima of "AMIF".

6.3.2 Singular value decomposition to obtain embedding dimension

To obtain the optimal embedding dimension for reconstruction of "PST", Broomhead and King (1986) and Kennel et al. (1992) proposed method namely Singular System Analysis (SSA) and false nearest neighbor (FNN) respectively. The appropriate choice of embedding dimension (m) is of prime importance for the proper reconstruction of "PST". For this purpose, the current work adopts the "SSA" method, where singular value decomposition (SVD) of a state variable vector (x) is performed that is mathematically represented in the equation (6.8)

$$[\mathbf{S}]_{N\,x\,q} = [\mathbf{U}]_{N\,x\,q}\,[\mathbf{\Lambda}_s]_{q\,x\,q}\,[\mathbf{V}]^{\mathrm{T}}_{q\,x\,q} \tag{6.8}$$

where $[\mathbf{S}]_{N\,x\,q}$ is a matrix that is formed by concatenating $q-1$ delayed replicas of vector x containing N time points. The elements of diagonal matrix $[\mathbf{\Lambda}_s]_{q\,x\,q}$ represent the singular

values of the system. The attractor matrix $[\mathbf{S}]$ represented in equation (6.9) is formed by considering a unit delay or lag factor $(\tau = 1)$.

$$[\mathbf{S}] = \begin{bmatrix} x(1) & x(2) & \cdots & x(\mathbf{q}) \\ x(2) & x(3) & \cdots & x(\mathbf{q}+1) \\ \vdots & \vdots & \ddots & \vdots \\ x(N-\mathbf{q}) & x(N-\mathbf{q}+1) & \cdots & x(N) \end{bmatrix} \tag{6.9}$$

where q is time window $(\mathbf{q} = \mathbf{F}_s \boldsymbol{\psi})$ estimated as the multiplication of a parameter ψ that is related to the maximum frequency content $(\mathbf{f}_{max})$ and sampling frequency ($\boldsymbol{F}_s$) of the acquired signal as proposed by Broomhead and King (1986).

$$\boldsymbol{\psi} \leq 1/\mathbf{f}_{max} \tag{6.10}$$

The appropriate embedding dimension (m) is obtained with the help of diagonal matrix $[\boldsymbol{\Lambda}_s]_{q \times q}$. The foremost step is to normalize the elements of diagonal matrix $[\boldsymbol{\Lambda}_s]_{q \times q}$ by their sum as represented in equation (6.11).

$$\hat{\Lambda}_{s_i} = \frac{\Lambda_{s_{i \times i}}}{\sum_{i=1}^{q} \Lambda_{s_{i \times i}}} \tag{6.11}$$

Now, the vector $\{\hat{\Lambda}_s\}_{q \times 1}$ is represented graphically in a two-dimensional plot, where one axis corresponds to the indices of the vector, and the remaining axis is the value of the element corresponding to each index. Finally, the number of indices at which the two-dimension plot approaches to a value that is approximately equal to zero is designated as the optimal value of embedding dimension 'm'.

6.4 Damage sensitive feature

6.4.1 Mahalanobis distance between phase space trajectories (MDPST)

The occurrence and evolution of damage in the structural system cause topological changes in reconstructed "PST". This is because the initiation and evolution of damage alter the dynamic response of the system, which changes the geometry of "PST" as it is strongly

correlated with the response of the system. The sensitivity of "PST" to damage provides an opportunity to quantify the damage by evaluating the geometrical changes of the "PST".

The damage sensitive features (DSFs) proposed in the present work are referred to as, Change in Phase Space Topology (CPST) and Mahalanobis Distance between Phase Space Topology (MDPST). The "CPST" is a Euclidean distance based approach to evaluate the dissimilarity in "PST" between pristine and damage state. Whereas, "MDPST" is a sensitive statistical distance measure that can determine the geometrical changes between the phase portrait of pristine and damage state.

Consider two attractors $[\mathbf{X}(n)]$ and $[\mathbf{Y}(n)]$corresponding to the dynamic response of healthy and damage state respectively as shown in Figure 6.1.

$$[\mathbf{Y}(n)] = [y(n), y(n+\boldsymbol{\tau}), ..., y(n+(\mathbf{m}-1)\boldsymbol{\tau})] \tag{6.12}$$

where, $\boldsymbol{\tau}$ and $\mathbf{m}$ are the ideal value of lag and embedding dimension, respectively.

The "MDPST" is evaluated by a procedure explained in the following steps:

Step-1: Evaluation of nearest neighborhood points to fiducial point

In this step, initially a point $\mathbf{Y}(K)$ corresponding to the time index K is selected on the damaged trajectory. The randomly selected point $\mathbf{Y}(K)$ is referred to as a fiducial point. Now, the nearest neighbors $[NNE]$ corresponding to the fiducial point are selected on pristine "PST" by minimizing the Euclidean distance between the point and "PST".

$$[\mathbf{NNE}(n_i)] = \min \| \mathbf{X}(n_i) - \mathbf{Y}(K) \| \quad i = 1, \ldots, p \tag{6.13}$$

where, operator ||.|| estimates the Euclidean norm, *'p'* is the number of the nearest neighbor, and $[\mathbf{NNE}]$ represents the set of nearest neighbor points to $Y(K)$, a fiducial point.

The set of neighborhood points [**NNE**] are used to quantify the dissimilarity between the "PSTs". Hence, it is important to decide criteria regarding selection of *NNE*. Generally, the total number of points (p) in [**NNE**] are in the range of 10^{-4} N to 10^{-3} N, where N is the total number of data points in the reconstructed "PST" (Nichols, 2003). While collecting the set

of [**NNE**], the time instant corresponding to fiducial points is not considered, as the entire process of forming [**NNE**] is established on minimizing the Euclidean norm.

Step-2: Evaluating the fiducial point and NNE at future time step

The value of $Y(K)$ at future time step of $'K+f'$ are evolved in the pristine trajectory as

$$[\mathbf{X}(K+\mathbf{f})_{j\times m}] = \mathbf{X}(n_j+\mathbf{f}), \quad j=1, \ldots, p \tag{6.14}$$

$$\tilde{\mathbf{Y}}(K+f) = \frac{1}{p}\sum_{j=1}^{p}\mathbf{X}(n_j+\mathbf{f}), \quad j=1, \ldots, p \tag{6.15}$$

where $[\mathbf{X}(K+\mathbf{f})]_{p\times m}$ (Figure 6.1 (a)) represents all the evolved points corresponding to set NNE at a future time step $'K+\mathbf{f}'$, $\mathbf{m}$ is embedded dimension and $\tilde{\mathbf{Y}}(K+\mathbf{f})$ (Figure 6.1 (a)) is the fiducial point at future time step in the baseline "PST".

The evolved value of fiducial point corresponding to time step $'K+\mathbf{f}'$ on the damaged "PST" is selected as $\mathbf{Y}(K+\mathbf{f})$ as shown Figure 6.1 (b). The correlation between all the evolved neighborhood in time is maintained by selecting the value of $'\mathbf{f}'$ (prediction horizon) in such a way that $1\le\mathbf{f}\le 0.5t$ (Torkamani et al., 2012).

Step-3: Evaluation of "CPST" and "MDPST"

"CPST": The damage feature "CPST" evaluates the changes in "PST" of reference and damage state with help of Euclidean distance and is defined as:

$$\mathrm{CPST(i)} = \frac{1}{p}\| \tilde{\mathbf{Y}}(K+\mathbf{f}) - \mathbf{Y}(K+\mathbf{f}) \| \tag{6.16}$$

where $\tilde{\mathbf{Y}}(K+\mathbf{f})$ and $\mathbf{Y}(K+\mathbf{f})$ are shown in Figure 6.1 as a green cross mark $(\times)$, this calculation has to be repeated for all the fiducial points.

The acceptable estimate of damage feature is adapted based on the average value of evaluated "CPST" at each Fiducial points and is given as:

$$\mathrm{CPST} = \sum_{i=1}^{nt} CPST(i)/nt \tag{6.17}$$

"MDPST": The "DSF" namely "MDPST" a statistical distance measure is evaluated to quantify the advancement of progressive damage in the system. In the n-dimensional

statistical analysis, the distance between the reference sample and observation in the scale of standard deviation is referred to as Mahalanobis distance (Mahalanobis, 1936, De Maesschalck et al., 2000). To evaluate "MDPST", the covariance matrix Σ is evaluated as a positive definite and non-singular:

$$[\mathbf{\Sigma}(\mathbf{k})]_{m\times m} = \frac{1}{p-1}[\mathbf{X}(K+\mathbf{f})^{T}_{p\ \mathrm{x}\ m}][\mathbf{X}(K+\mathbf{f})_{p\ \mathrm{x}\ m}] \tag{6.18}$$

The MD between the neighborhood cluster at a particular time instant *K* and a fiducial point is given as:

$$\mathbf{d}_{mahal}(K) = \sqrt{(\mathbf{Y}(K+\mathbf{f}) - \tilde{\mathbf{Y}}(K+\mathbf{f}))^{T}[\mathbf{\Sigma}(\mathbf{k})]^{-1}(\mathbf{Y}(K+\mathbf{f}) - \tilde{\mathbf{Y}}(K+\mathbf{f}))} \tag{6.19}$$

where $\mathbf{Y}(K+f)$ and $\mathbf{X}(K+f)$ are represented in Figure 6.1 (b) as a cross marked point $(\times)$ and yellow cluster respectively. In case, where the optimal embedding dimension for reconstruction of "PST" is a large value, there is a high possibility that $[\mathbf{X}(K+\mathbf{f})]_{p\times m}$ might possess correlated and redundant variables. Therefore, dimensionality reduction using independent component analysis is required to ensure $p > m$. For a particular case where the $[\mathbf{X}(K+f)]_{p\times m}$ is an uncorrelated matrix of unit variance, then the covariance $[\mathbf{\Sigma}(\mathbf{k})]_{m\times m}$ will lead to an identity matrix and Mahalanobis distance will correspond to the square of the L2 norm $\|\ .\ \|^2$ of $\mathbf{X}(K+\mathbf{f})$ and $\mathbf{Y}(K+\mathbf{f})$ (De Maesschalck et al., 2000). In order to attain the best estimate, the above mentioned procedure has to be reiterated for the several choices of Fiducial points. The most suitable number of Fiducial points to be considered are a minimum of 5% of the total data samples in the reconstructed "PST" to get a reasonable estimate of dissimilarity between two "PST" (Nichols, 2003). The most suitable estimate of MD is calculated for all the selected fiducial points (nt) and later on, the average of all the estimate gives:

$$MDPST = \sum_{i=1}^{nt} d_{mahal}(i)/nt \tag{6.20}$$

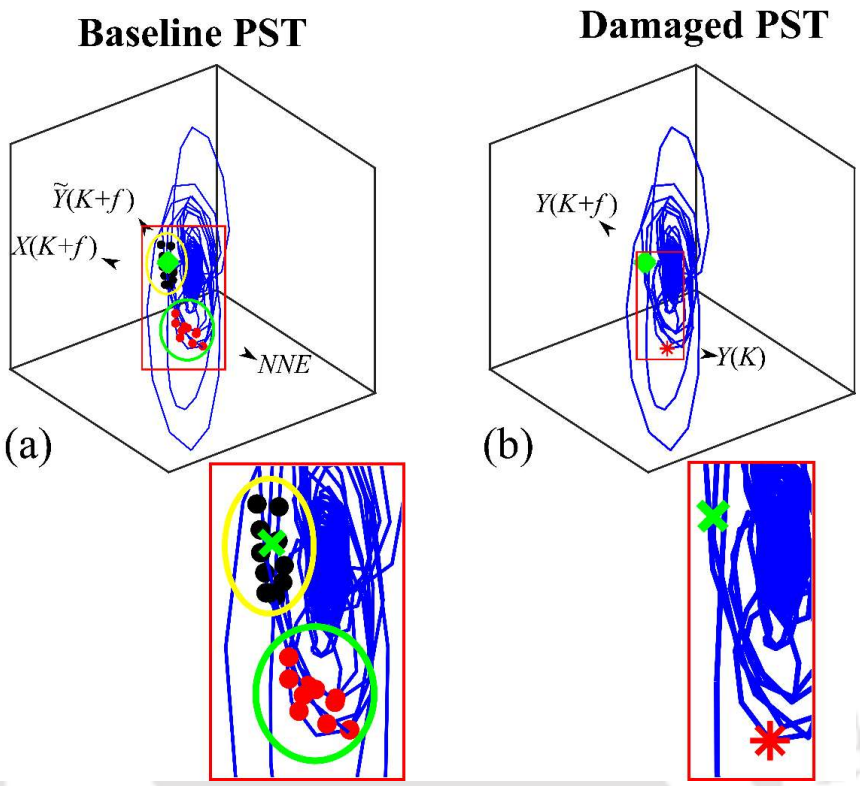

Figure 6.1 Schematic diagram of phase space trajectory for (a) pristine state and; (b) damage state to evaluate damage sensitive feature

Now, when two identical attractors corresponding to the pristine state are analyzed to calculate the value of "MDPST" and "CPST" between them, a non-zero value may be obtained. The non-zero value thus obtained is designated as an error and has to be subtracted from all the values of "MDPST" and "CPST" evaluated for damage states The deduction of error from the estimates of "DSFs" for any damage state will result in precise quantification of damage.

6.4.2 Itakura distance

Itakura Distance (ID) is a numerical index that is generally used in speech processing and signal processing applications to evaluate the dissimilarity between two sets of auto-regressive coefficients (Muthuswamy and Thakor, 1998). ID parameter is based on the autocorrelation matrix and "AR" model coefficients of the time-history. In other words, the ID parameter examines how accurately the "AR" coefficients of an unknown state response

can fit the time-history signal corresponding to known state response. For detailed explanation and procedure to evaluate ID is mentioned in section 5.4.2.

6.5 Proposed algorithm

The proposed damage detection algorithm is based on the amalgamation of "ICA" and "PST". The proposed novel algorithm consists of two segments, the brief description of each segment is mentioned below:

Algorithm: Phase Space Reconstructed from Independent Component Sources

---

A) First segment:

Step-1: Acquire the acceleration response $x(t)$ of the structural system

Step-2: Perform "ICA" on the response $x(t)$ using generic model $x(t) = As(t)$ to get the independent modal response $Y(t) = W^T x(t)$; using demixing matrix W

Step-3: Get the embedding parameters of the responses using "AMIF" $I(t)$ and "SSA" $[S]$

$I(t) = \sum_n p(x(n), x(n+t)) \log_2 \frac{p(x(n), x(n+t))}{p(x(n))\, p(x(n+t))}$ and; $[S]_{N \times q} = [U]_{N \times q} [\Lambda_s]_{q \times q} [V]^{\mathrm{T}}_{q \times q}$

$p(x(n), x(n+t))$ are the joint probability density function, and $[S]$ is "SVD" of response.

B) Second segment:

Step-4: Reconstruct the "PST" of modal responses with help of the "AMIF" $I(t)$ and "SSA" $[S]$

Step-5: Evaluate the "DSFs" namely $\mathrm{CPST(i)} = \frac{1}{p} \| \tilde{Y}(K+f) - Y(K+f) \|$ and

$d_{mahal}(K) = \sqrt{(Y(K+f) - \tilde{Y}(K+f))^T \Sigma(k)^{-1} (Y(K+f) - \tilde{Y}(K+f))}$

where $Y(K+f)$ and $\tilde{Y}(K+f)$ are evolved fiducial point corresponding to time step $'K+f'$ on the damaged "PST" and baseline "PST" respectively. $\Sigma(k)$ is the covariance matrix of the evolved cluster at time step $'K+f'$ on the baseline "PST" (refer Figure 6.1).

Output: "DSF" based on "CPST" and "MDPST" to quantify the initiation and progression of damage

---

The step-by-step representation of the proposed algorithm is shown in Figure 6.2.

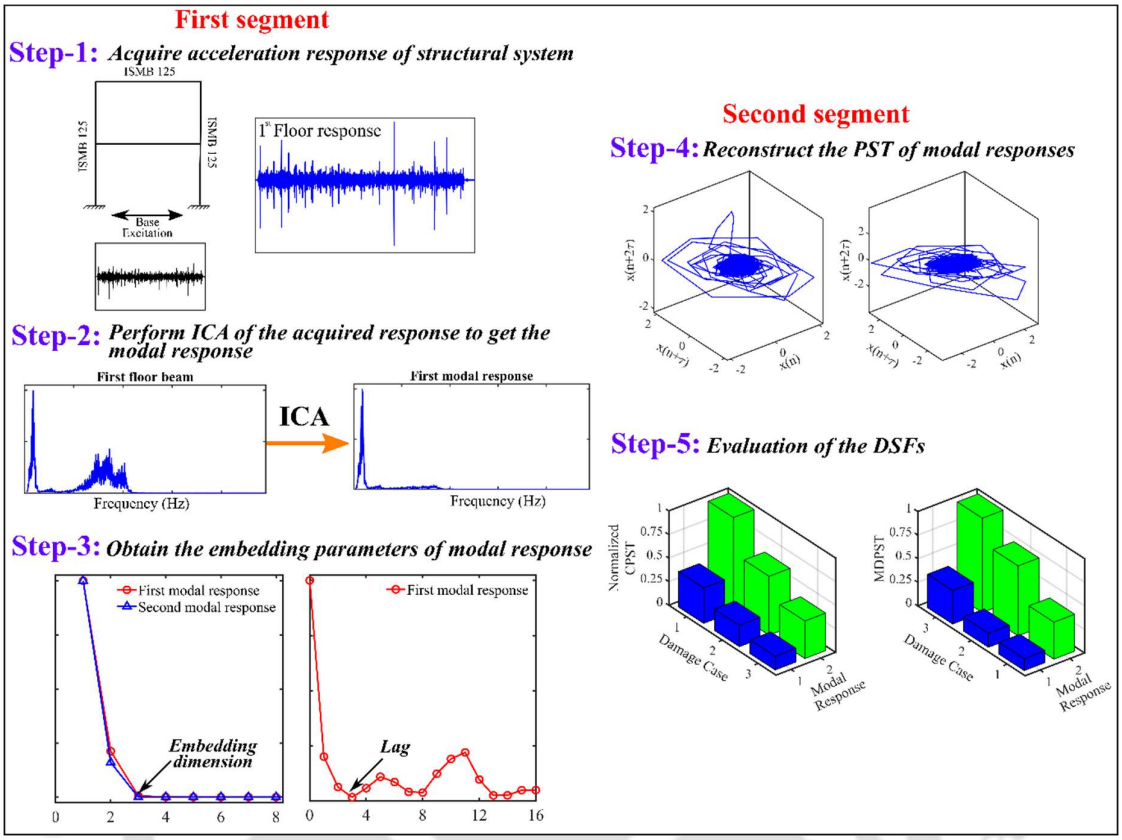

Figure 6.2 Representation of the proposed damage detection algorithm

6.6 Experimental investigations

Dynamic analysis of the two storey, steel moment resisting frame (SMRF) was conducted to demonstrate the performance of the proposed algorithm. The steel moment resisting frame was designed as per the half-scale model. The beams and columns are the India Standard Medium Weight Beam (ISMB) section of depth 125 mm. The total height of the entire "SMRF" was 1.8 m with bay width of 0.95 m and story height is 0.9 m. The detailed explanation of the experimental investigation can be found in section 5.6. In each stage of the experimental investigation, the dynamic response of "SMRF" subjected to white-noise base excitation (WNBE) was acquired and further analyzed for detecting the damage. It is also important to note that no bolts were tightened throughout the experimental investigation.

6.7 Results and discussion

6.7.1 Dynamic response of "SMRF" subjected to white noise

The "SMRF" structure was mounted on a shake table and excited with displacement controlled white noise. The acceleration time history acquired at the base of shake table is shown in Figure 5.7. The structural responses of the "SMRF" at the first floor and second-floor beam are shown in Figure 5.8 (a and b). The frequency domain response of the acquired signal for the stage-I experiments are shown in Figure 5.9. Also, the dominant frequency of all the experimental stages is tabulated in *Table 5.1*. The modal frequencies of healthy and damage states differ marginally and hence, provide inconclusive information to detect and quantify the damage. The inefficiency of spectral domain methods demands for a novel approach for damage quantification. The section 6.7.2 onwards focuses on the proposed algorithm for segregating modal responses from the acquired responses and later on quantifying the severity of damage.

6.7.2 Independent component sources

For a linear multiple-degree-of-freedom (MDOF) system, the equation of motion is mathematically represented as:

$$[\mathbf{M}]\{\ddot{y}(t)\}+[\mathbf{C}]\{\dot{y}(t)\}+[\mathbf{K}]\{y(t)\}=\{F(t)\} \tag{6.21}$$

Where **[M]**, **[K]**, and **[C]** are mass, stiffness, and damping matrices of the system respectively; $F(t)$ represents the force vector that is applied to the "MDOF" system. Assuming the modes of "MDOF" system as normal modes, the dynamic response can also be evaluated as:

$$\{y(t)\}=\mathbf{\Omega}\{q(t)\}=\sum_{i=1}^{n}\mathbf{\Omega}_i q_i(t) \tag{6.22}$$

Therefore;

$$\{q(t)\}=\mathbf{\Omega}^{-1}\{y(t)\} \tag{6.23}$$

where, $\{q(t)\}=\{q_1(t),q_2(t),...,q_n(t)\}^T$ and $\{y(t)\}=\{y_1(t),y_2(t),...,y_n(t)\}^T$ are the modal responses and displacement responses, respectively; $\mathbf{\Omega}$ represents the normal mode matrix.

Note that the equation (6.2) and equation (6.23) are similar. According to Kerschen et al. (2007), the modal response are independent, for the case where the frequencies corresponding to the modal responses are incommensurable. Therefore, the extraction of modal responses can be performed using "ICA".

In the current work, the modal responses were evaluated by performing "ICA" on the response acquired from "SMRF" subjected to WNBE. Figure 6.3 (a and b) shows the acquired responses and the frequency spectrum of the structural system subjected to white noise. Independent component analysis was performed on the response signal to obtain as independent component as possible to retrieve modal responses. Figure 6.4 shows the modal responses obtained from "ICA" and its frequency spectrum.

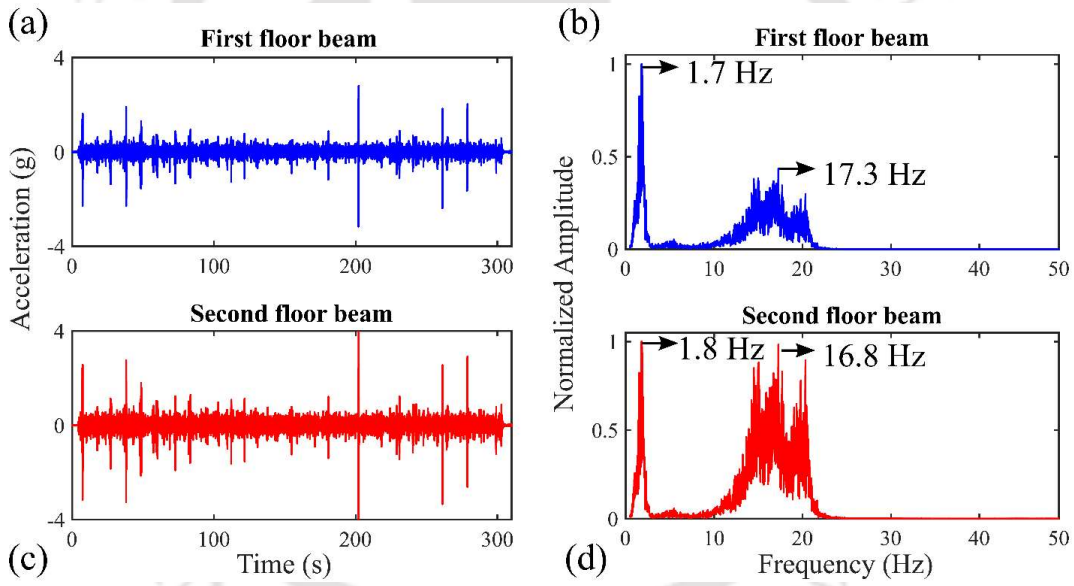

Figure 6.3 (a-c) Time-history plot of acceleration responses and; (b-d) corresponding frequency spectrum acquired from "SMRF"

Figure 6.3 (b and d) shows multiple frequency content in the acceleration time history due to coupled structural response. It is observed that the fundament modal response exhibits monotone frequency at 1.7 Hz that demonstrate effective recovery through "ICA" (Figure 6.4 (b)). However, Figure 6.4 (d) shows a marginal energy leakage at a frequency of 17 Hz which is contributed from the first modal coupling. "ICA" essentially recovers characteristic

modal information that is hidden/mix in the response. However, it is difficult to completely separate the modal components with low participation from the mixture. The "ICA" recovery of the second mode from the mixture is not seriously affected by the first modal coupling due to low energy participation. For the system with high proportional damping, the coupling modes possess severe challenge due to significant participation in the mixing process. For the structural system under consideration, the modal responses obtained are mono-component and also have low dimension enabling an appropriate reconstruction of the "PST". The results obtained for embedding parameters and the reconstruction of "PST" is explained in the next sections.

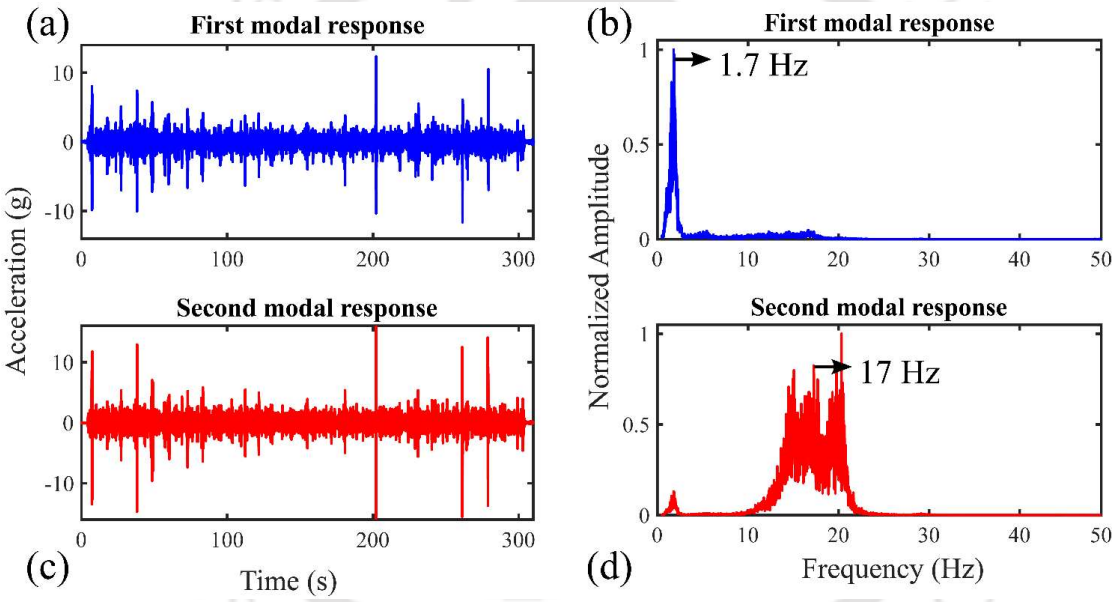

Figure 6.4 (a-c) Modal response recovered from "ICA" and; (b-d) corresponding frequency spectrum

6.7.3 Embedded parameters for phase space reconstruction

The successful and appropriate reconstruction of "PST" solely depends on the selection of optimal embedding parameters. These embedding parameters include time delay/lag and embedding dimension. The method to select optimal embedding parameters is discussed in section 6.3.1 and 6.3.2.

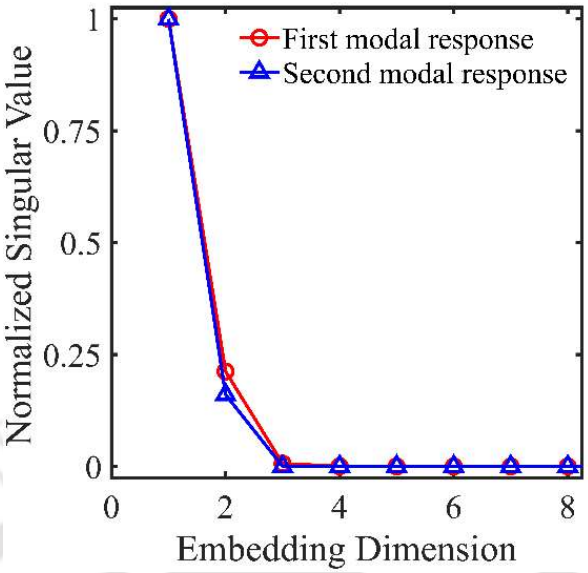

Figure 6.5 Selection of optimal embedding dimension from the variation of singular value and embedding dimension

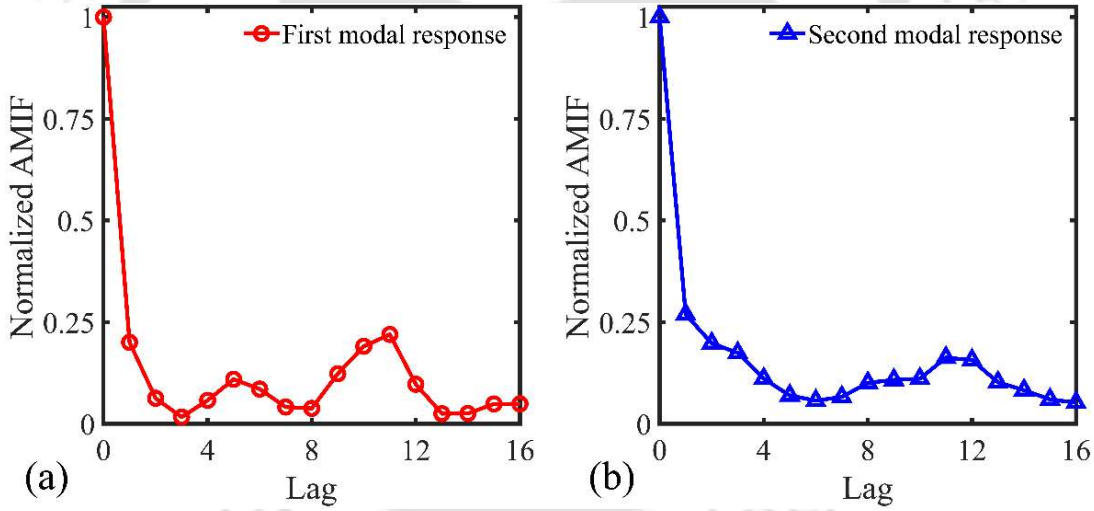

Figure 6.6 (a) The first minima of curve between "AMIF" and; (b) Lag corresponds to the optimal time delay/lag for first and second modal response

The optimal embedding dimension is selected at a point when singular value approaches zero (Figure 6.5). A higher value of embedding dimension causes loss in efficiency of the algorithm due to high computational effort. Figure 6.5 shows that the embedding dimension of 'three' is optimal for reconstruction of "PST" from the modal responses. For the effective reconstruction of "PST", the curve of "AMIF" and lag is plotted and the first absolute minima

is selected as the optimal value of time delay/lag (refer Figure 6.6). The optimal value of delay ensures the weak statistical independence of the modal response. The optimal delay factor for all the experiments is evaluated in a similar manner.

6.7.4 Reconstruction of "PST" and quantification of damage using "DSF"

The phase portrait was successfully reconstructed using modal responses and optimal embedding parameters using the methodology explained in section 6.3. ICA was employed to selectively separate the closely spaced modes from the response before implementing PSR algorithm. The extraction of modal responses and the evaluation of optimal embedding parameters from the acceleration response of the structure is discussed in sections 6.7.2 and 6.7.3 respectively. The phase space reconstruction is performed for the modal responses obtain from all the experimental stages and is presented in Figure 6.7.

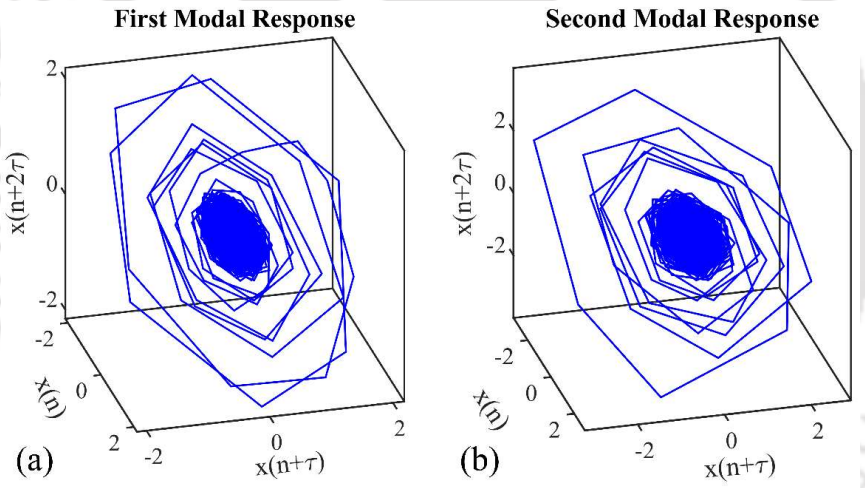

Figure 6.7 Phase portrait of (a) first modal responses and; (b) second modal response of the "SMRF" subjected to WNBE

The stage-I experiment "PST" is designated as a reference or pristine state and its discrepancy with the damaged "PST" is considered as a feature to quantify the damage. The discrepancy between the reference and damaged "PST" is numerically quantified by evaluating two "DSFs" (CPST and MDPST), as explained in section 6.4. The normalized numerical value of these "DSFs" for progressive damage states are represented in Figure 6.8. In the current experimental investigation, the "SMRF" was damaged progressively, therefore the results of

"DSF" are expected to have a monotonically increasing or decreasing trend. Figure 6.8 shows that both the "DSFs" (CPST and MDPST) exhibit an increasing trend. Therefore, it is concluded that the "DSFs" derived from the "PSTs" are efficient in the quantification of progressive damages.

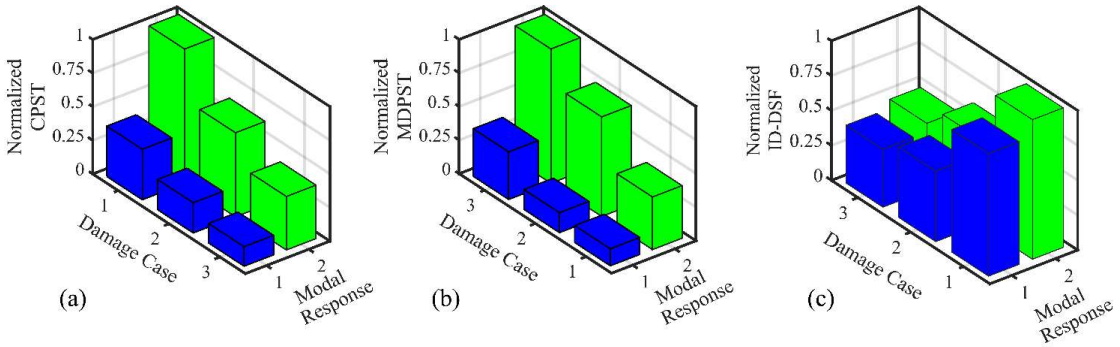

Figure 6.8 Damage sensitive features representation of (a) normalized "CPST", (b) normalized "MDPST" and; (c) normalized ID for progressive damage stages in "SMRF"

To corroborate the accuracy and efficiency of the proposed algorithm, an independent "DSF" is proposed based on the dissimilarity of the modal response of healthy and damage states. section 6.4.2 discusses the evaluation of ID in a batch mode that has been extended to windowed analysis. For windowed analysis, the modal response is divided into 'k' number of windows, each window being of 'N' sample size. The ID for each window is evaluated and a vector $\overline{ID\text{-}DSF}$ is obtained.

$$\overline{ID\text{-}DSF} = \{ID_1, ID_2, ..., ID_k\}^T \tag{6.24}$$

where, ID_k corresponds to the Itakura distance between reference and damage state corresponding to k^{th} window. As the number of samples for each experiment are same in current experimental investigation, therefore the number of windows are also same for 'N' sample sized window. Therefore, any k^{th} window corresponding to reference state response can be tested with the same numbered window of damage state response. Now, to obtain a scalar "DSF" $(ID\text{-}DSF)$ from the vector represented in the equation (6.24), Kurtosis (i.e. the fourth moment) of the vector was evaluated.

$$ID\text{-}DSF = Kurtosis(\overline{ID\text{-}DSF}) = E\left[\left(\frac{\overline{ID\text{-}DSF} - \mu_{\overline{ID\text{-}DSF}}}{\sigma_{\overline{ID\text{-}DSF}}}\right)^4\right] \quad (6.25)$$

Where, $\sigma_{\overline{ID\text{-}DSF}}$ and $\mu_{\overline{ID\text{-}DSF}}$ are standard deviation and mean of the vector $\overline{ID\text{-}DSF}$. The results of "ID-DSF" (equation (6.25)) are represented in Figure 6.8 (c).

The evaluated "DSFs" namely "CPST", "MDPST", and "ID-DSF" shows a monotonic trend. The "ID-DSF" shows a decreasing trend, whereas "MDPST" and "CPST" shows an increasing trend. The relative change in the magnitude of "DSF" is large for "CPST" and "MDPST" whereas small for "ID-DSF", indicating higher sensitivity and accuracy of the former two. The behavior of "DSFs" concludes that the discrepancy in the "PST" of modal response is an accurate and highly sensitive measure for damage detection compared to the evaluation of dissimilarity of "AR" coefficients of modal response. Now, to further enhances the accuracy and robustness of the algorithm, all three "DSFs" should be used simultaneously to avoid any false alarm and detect damage successfully.

6.8 Conclusion

The current chapter proposes a novel technique based on "ICA" and Phase space reconstruction of structural response for structural health monitoring. Given that the "ICA" is limited to lightly damped structure and "PSR" is inefficient for higher dimensional data, the proposed algorithm leverages the virtues of both techniques sequentially by exploring the modal responses achieved from "ICA" and representing in "PSR" for damage quantification. The efficacy of the proposed algorithm is validated with the help on experimental investigation of a two storey steel frame was carried out. The steel frame was excited with a white noise base excitation for different damage stages. The initiation and progressive damage were manifested in steel frame by loosening bolt/bolts of beam-to-column and column-to-column connection.

The proposed approach consists of two segments, in the first segment, the modal responses were obtained using "ICA" of the acquired response. Now, for reconstruction of "PST", the

optimal embedding parameter was evaluated with the help of "AMIF" and "SSA". In the second segment, the lower dimensional modal responses were represented in the phase space trajectory (PST) with the help of embedding parameters. The modal responses obtained in the first segment are of lower embedding dimension, which is required for appropriate reconstruction of "PST". Since the proposed approach leverages the dissimilarity of the "PST" to quantify damage, "ICA" is the most important for robustness of the proposed approach. The "DSFs" namely "CPST", "MDPST" quantifies the dissimilarity between the "PSTs" corresponding to progressive damage states through Euclidean and Mahalanobis distance. Whereas, Itakura distance measures the dissimilarity between auto-regressive coefficients of healthy and damaged state. Both "MDPST" and "CPST" are potential indicators of occurrence and progressive evolution of damages excited under nonstationary ambient vibration. The proposed algorithm is capable of detecting damage induced due to loosening of bolted connections which is of relatively small magnitude. The results of "MDPST" and "CPST" exhibited a numerically increasing trend and corroborated with progressive damage evolution in successive stages of the experimental study.

Chapter 7

Summary and Conclusions

7.1 Summary and conclusions

The present study deals with the development and implementation of health monitoring algorithms to monitor the health of different structural systems subjected to an extreme scenario such as shock, earthquake etc. Overall four novel health monitoring approaches were proposed. To verify all the proposed approaches, various experimental studies were carried out on a three storey shear building and a two storey moment resisting frame.

The first approach develops an algorithm based on a combination of Empirical mode decomposition (EMD) and principal component analysis (PCA) to monitor the health of three storey shear building subjected to repetitive seismic excitation of high return period. Under the influence of repetitive base excitation, an extreme loading scenario, the shear building is expected to incur a reduction in its service life (i.e. damage is induced). The process of "EMD" gives the dominant intrinsic mode function that has no noise and redundant information. This step helps to avoid false alarm, as any redundant information if present, will alter the Eigen-structure of signal even in case of no damage. Later, with the help of "PCA", the change in the Eigen-structure is evaluated and a sensitive condition indicator (CI) was proposed. The proposed CI quantifies damage by evaluating the normalized Euclidean norm of the change in principal angles, corresponding to pristine and damage state. The proposed algorithm implements "EMD" on the received wave and segregates dominant modes as the dominant "IMFs". Subsequently, the "IMF" is processed by the proposed damage detection algorithm to evaluate condition indicator. The manifestation of damage and its evolution is quantified with the help of the change in the value of condition indicator (CI). The value of CI corresponding to damage cases of present work are 0.39, 0.40, and 0.58. The relative change in magnitude of CI reflects the manifestation and severity of damage. The

proposed framework is capable of quantifying the damage in shear building with the help of a condition indicator that could be applicable for various "SHM" framework.

The second approach deals with another case of extreme loading, that is shockwave loading, high pressure, and short duration pulse. The shock loading can induce significant damage in any structure and can be identified with the help of the second approach. The proposed approach was divided into two segments that segregate perturbative damages and microscale damages. In the first segment, principal component analysis (PCA) was used for dimension reduction and evaluation of changes in principal orthogonal components (POC). In the second segment, the response was decomposed in mono-component signals (IMFs) using Empirical mode decomposition (EMD). The appropriate embedding parameters were calculated using singular system analysis and average mutual information function, respectively. The dominant "IMF" using embedding parameters was represented in the phase space trajectory (PST). The proposed study leverages the dissimilarity of the "PST" to derive damage sensitive features (DSFs). The "DSFs" quantifies the dissimilarity between the "PSTs" corresponding to progressive damage states through Euclidean and Mahalanobis distance. The "DSFs" are potential indicators of occurrence, localization and progressive evolution of damages. The efficacy of the algorithm was demonstrated on a shear building that was progressively damaged through shock loads. Systematic experimental investigations were conducted to introduce localized and progressive damage in the structure. High-intensity shocks caused large deformation and plastification of the structural members. It was observed that "CPST" and "MDPST" were robust sensitive features that were able to quantify the damage initiation and evolution. The estimate of "DSFs" were compared with inter-storey drift that corroborates the evolution of damage. The algorithm was able to quantify the damage arising due to material nonlinearity.

The third approach is a robust damage detection technique using time series modeling integrated with clustering techniques. To demonstrate the efficacy of the proposed novel algorithm, a two storey steel frame was excited with white noise base excitation. The damage

was manifested in steel frame progressively by loosening bolt/bolts of beam-column joint and column-to-column splice plate. The non-stationary response of the structure subjected to white noise excitation was modeled using time-varying autoregressive modeling The model order of the structural response subjected to ambient vibration was low (i.e. p=3) that eliminated high computational resources. An adaptive Kalman filter (KF) technique was utilized to evaluate the time-varying "AR" coefficients (TVARC). The "TVARC" encompasses the information of initiation and progression of damage in its time series that is used to evaluate the damage. It was observed that only dominant "TVARC" depicts the changes in the coefficient progressively. Whereas, the remaining two "TVARC" exhibits random behavior and had no correlation with the actual damage case. Hence, a better alternative was to represent all three coefficients in "TVARC" subspace that showed enhanced capabilities to segregate and classify the damage. The "TVARC" representation showed distinctly and spatially resolved healthy and the damage clusters in the hyperspace. The segregation and separation of the clusters in the "TVARC" subspace was numerically quantified by two damage sensitive features using Mahalanobis distance and Itakura distance. Both the "DSF" exhibits larger numerically magnitude for damage-2 case than damage-1 and corroborated with the progressive evolution of damage successfully. The "DSFs" are potential and sensitive indicators to detect initiation and progressive evolution of damage state. The developed algorithm was able to successfully quantify the damage arising due to loosening of the bolt in the beam-to-column connection and column-to-column connection by splice pate. The algorithm demonstrates its capability to detect slow and gradual evolution of damage in the structure under nonstationary ambient vibration excitation.

The fourth and last approach proposes a novel technique based on "ICA" and Phase space reconstruction of structural response for structural health monitoring. Given that the "ICA" is limited to lightly damped structure and "PSR" is inefficient for higher dimensional data, the proposed algorithm leverages the virtues of both techniques sequentially by exploring the modal responses achieved from "ICA" and representing in "PSR" for damage

quantification. The efficacy of the proposed algorithm is validated with the help on experimental investigation of a two storey steel frame was carried out. The steel frame was excited with a white noise base excitation for different damage stages. The initiation and progressive damage were manifested in steel frame by loosening bolt/bolts of beam-to-column and column-to-column connection. The proposed approach consists of two segments, in the first segment, the modal responses were obtained using "ICA" of the acquired response. Now, for reconstruction of "PST", the optimal embedding parameter was evaluated with the help of "AMIF" and "SSA". In the second segment, the lower dimensional modal responses were represented in the phase space trajectory (PST) with the help of embedding parameters. The modal responses obtained in the first segment are of lower embedding dimension, which is required for appropriate reconstruction of "PST". Since the proposed approach leverages the dissimilarity of the "PST" to quantify damage, "ICA" is the most important for robustness of the proposed approach. The "DSFs" namely "CPST", "MDPST" quantifies the dissimilarity between the "PSTs" corresponding to progressive damage states through Euclidean and Mahalanobis distance. Whereas, Itakura distance measures the dissimilarity between auto-regressive coefficients of healthy and damaged state. Both "MDPST" and "CPST" are potential indicators of occurrence and progressive evolution of damages excited under nonstationary ambient vibration. The proposed algorithm is capable of detecting damage induced due to loosening of bolted connections which is of relatively small magnitude. The results of "MDPST" and "CPST" exhibited a numerically increasing trend and corroborated with progressive damage evolution in successive stages of the experimental study.

The summary of actual work is tabulated in Table 7.1 that described the strengths and limitation and practical applicability for SHM of real life structure. Based on the strengths and limitations of algorithm, it is most preferable to use ICA and PSR based algorithm mentioned in chapter-6. The remaining algorithms fail for reasons such as nonlinearity in system, closely spaced modes, nonstationary response etc. Whereas, ICA and PSR based

algorithm works in presence of nonlinearity, nonstationary response and also works for closely spaced modes.

Table 7.1 Strengths, limitation and practical applicability of proposed SHM approaches

Strengths/ Limitations	Principal component analysis	Phase space reconstruction (PSR)	Time varying autoregressive modeling	Independent component analysis+PSR
Low computation cost	Yes	No	Yes	Yes
Spatial damage detection	Yes	Yes	Yes	Yes
Applicable in online fashion	No	No	Yes	No
Modal information can be obtained	Yes	No	No	Yes
Works for non-linear systems	No	Yes	No	Yes

7.2 Limitations of proposed approaches

1. The first approach proposed in current work is based on "PCA" and "EMD", where "EMD" decomposes the original signal into monocomponent "IMFs" that do not possess any unwanted noise. But "EMD" is an offline process, hence the proposed approach cannot be implemented in real time. Further, as the number of sensors increases the combinations to be used for evaluation of CI increases.
2. The second approach is based on phase space based methodology that identifies the magnitude and location of damage in a three storey shear building. The damage is localized at storey level with the help of proposed approach successfully and accurately. But, the proposed method does not deal with localization of damage at a particular column or beam.

3. The third approach is based on time-varying autoregressive modeling, where damage is identified with the help of "TVAR" coefficients projected in a hyperspace. An offline clustering technique is also used to eliminate the outliers present in "TVARC" clusters. Due to the application of offline clustering technique, the proposed appraoch cannot be applied in online application.
4. The fourth approach deals with the identification and quantification of damage by analyzing the modal responses of the system. To obtain the modal responses "ICA" is used as a tool and is later represented in phase portrait. "ICA" based methods do not work for nonlinear case.
5. All the developed algorithms can located damage ar storey level and not at exact location of damage. This limitation could be removed if more sensors are used. In this work, the sensors are placed at slab only and not at any columns, so the damage can be localized at floor level only. However, if the response of columns is also available, the algorithm can detect the column member that is damaged. Moreover, in order to specify exact location in a column member, further wave propagation techniques could be adopted.
6. All the methodologies developed and implemented cannot identify the remaining service life of the structure.
7. The proposed approaches are highly dependent on the baseline or reference information of the system under investigation.

7.3 Scope of future work

Based on the research work carried out in this thesis, the following objectives holds a great scope in future work to be carried out in a structural health monitoring area.

1. The extensive scope as future work is the online application of the "PCA" and "TVAR" based approach with the help of a real-time signal decomposition technique and real-time clustering techniques, respectively.

2. To develop novel damage localization framework that can localize the damage at elemental level instead of floor/slab level.
3. To extend the proposed methodologies in order to carry out prognosis of structural system and estimate the remaining service life. The estimated strength/service life would be helpful for taking decision regarding retrofitting or rehabilitation of structural system.
4. The sensitivity analysis of all the proposed approach for the smallest size of damage that can be detected accurately can be carried out in future research work.
5. Lastly, in order to broaden the applicability of all the approaches, it would be interesting to apply them on different types of systems such as plate-like structures, mechanical systems etc.

List of Journal Publications

1. Pamwani, L., Habib, A., Melandsø, F., Ahluwalia, B. and Shelke, A., 2018. Single-input and multiple-output surface acoustic wave sensing for damage quantification in piezoelectric sensors. *Sensors*, *18*(7), p.2017.
2. Pamwani, L. and Shelke, A., 2018. Damage detection using dissimilarity in phase space topology of dynamic response of structure subjected to shock wave loading. *Journal of Nondestructive Evaluation, Diagnostics and Prognostics of Engineering Systems*-ASME, *1*(4), p.041004.
3. Pamwani, L., Agarwal, V., & Shelke, A., 2019. Damage Classification and Feature Extraction in Steel Moment-Resisting Frame Using Time-Varying Autoregressive Model. *Journal of Nondestructive Evaluation, Diagnostics and Prognostics of Engineering Systems*, *2*(2), 021002.
4. Pamwani, L., & Shelke, A., 2019. Damage quantification in moment resisting frame using phase space reconstructed from independent component sources. *Structural Control and Health Monitoring*, e2438.

References

1. Abarbanel, H. D., & Gollub, J. P. (1996). Analysis of observed chaotic data. *Physics Today, 49*(11), 81-86.
2. Abazarsa, F., Nateghi, F., Ghahari, S., & Taciroglu, E. (2015). Extended blind modal identification technique for nonstationary excitations and its verification and validation. *Journal of Engineering Mechanics, 142*(2), 04015078.
3. Abazarsa, F., Nateghi, F., Ghahari, S. F., & Taciroglu, E. (2013). Blind modal identification of non-classically damped systems from free or ambient vibration records. *Earthquake Spectra, 29*(4), 1137-1157.
4. Adams, D. E., & Farrar, C. R. (2002). Application of frequency domain ARX features for linear and nonlinear structural damage identification. *Smart Nondestructive Evaluation for Health Monitoring of Structural and Biological Systems, 4702*, 134-148.
5. Adewumi, A., Kagamba, J., & Alochukwu, A. (2016). Application of chaos theory in the prediction of motorised traffic flows on urban networks. *Mathematical Problems in Engineering, 2016*, 15.
6. AISC. (1999). Specification for structural steel buildings. *AISC*, December. 1999, 27.
7. AISC. (2010a). Prequalified connections for special and intermediate steel moment frames for seismic applications. *American Institute of Steel Construction Chicago*.
8. AISC. (2010b). Seismic provisions for structural steel buildings. *American Institute of Steel Construction Chicago*.
9. Aktan, A. E., Catbas, F. N., Grimmelsman, K. A., & Pervizpour, M. (2002). Development of a model health monitoring guide for major bridges. *Report Submitted to Federal Highway Adminstration Research and Devlopment*.
10. Al-Hussein, A., & Haldar, A. (2015). Novel unscented Kalman filter for health assessment of structural systems with unknown input. *Journal of Engineering Mechanics, 141*(7), 04015012.

11. Alwasel, A., Yung, M., Abdel-Rahman, E. M., Wells, R. P., & Haas, C. T. (2017). Fatigue Detection Using Phase-Space Warping. *Journal of Biomechanical Engineering, 139*(3), 031001.
12. Amezquita-Sanchez, J. P., & Adeli, H. (2015). A new music-Empirical wavelet transform methodology for time–frequency analysis of noisy nonlinear and non-stationary signals. *Digital Signal Processing, 45*, 55-68.
13. Amezquita-Sanchez, J. P., & Adeli, H. (2016). Signal processing techniques for vibration-based health monitoring of smart structures. *Archives of Computational Methods in Engineering, 23*(1), 1-15.
14. Antoni, J. (2005). Blind separation of vibration components: Principles and demonstrations. *Mechanical Systems and Signal Processing, 19*(6), 1166-1180.
15. Antoni, J., & Chauhan, S. (2013). A study and extension of second-order blind source separation to operational modal analysis. *Journal of Sound and Vibration, 332*(4), 1079-1106.
16. ASCE. (2010). Minimum Design Loads for Buildings and Other Structures, Standard ASCE/SEI 7-10, Reston, VA: *American Society of Civil Engineers*.
17. Atkinson, C., & Mitchell, A. F. (1981). Rao's distance measure. *Sankhyā: The Indian Journal of Statistics, Series, 43*(A), 345-365.
18. Balageas, D., Fritzen, C.-P., & Güemes, A. (2010). Structural Health Monitoring (Vol. 90): *John Wiley & Sons.*
19. Banks, H., Inman, D., Leo, D., & Wang, Y. (1996). An experimentally validated damage detection theory in smart structures. *Journal of Sound and Vibration, 191*(5), 859-880.
20. Beck, J. L., & Katafygiotis, L. S. (1998). Updating models and their uncertainties. I: Bayesian statistical framework. *Journal of Engineering Mechanics, 124*(4), 455-461.
21. Bell, A. J., & Sejnowski, T. J. (1995). An information-maximization approach to blind separation and blind deconvolution. *Neural Computation, 7*(6), 1129-1159.

22. Belouchrani, A., Abed-meraim, K., Cardoso, J.-F., & Moulines, E. (1997). A blind source separation technique using second-order statistics. *IEEE Transactions on Signal Processing, 45*(2), 434-444.
23. Bodeux, J.-B., & Golinval, J.-C. (2001). Application of ARMAV models to the identification and damage detection of mechanical and civil engineering structures. *Smart Materials and Structures, 10*(3), 479.
24. Box, G., Jenkins, G., & Reinsel, G. (1994). Time series analysis, forecasting and control. *Englewood Clifs, San Francisco, CA, USA*.
25. Brewick, P., & Smyth, A. (2014). On the application of blind source separation for damping estimation of bridges under traffic loading. *Journal of Sound and Vibration, 333*(26), 7333-7351.
26. Brincker, R., Zhang, L., & Andersen, P. (2000). Modal identification from ambient responses using frequency domain decomposition. *Proceedings of the 18 'International Modal Analysis Conference (IMAC), San Antonio, Texas*.
27. Broomhead, D. S., & King, G. P. (1986). Extracting qualitative dynamics from experimental data. *Physica D: Nonlinear Phenomena, 20*(2-3), 217-236.
28. Bruneau, M., & MacRae, G. (2017). Reconstructing Christchurch: a seismic shift in building structural systems. *The Quake Centre, University of Canterbury, Christchurch*.
29. Bruneau, M., Uang, C.-M., & Whittaker, A. (1998). Ductile design of steel structures (Vol. 389): *McGraw-Hill New York.*
30. Cardoso, J.-F. (1998). Blind signal separation: statistical principles. *Proceedings of the IEEE, 86*(10), 2009-2025.
31. Catbas, F. N., Gul, M., & Burkett, J. L. (2008). Conceptual damage-sensitive features for structural health monitoring: laboratory and field demonstrations. *Mechanical Systems and Signal Processing, 22*(7), 1650-1669.

32. Chang, J., Liu, W., Hu, H., & Nagarajaiah, S. (2016). Improved independent component analysis based modal identification of higher damping structures. *Measurement,88,* 402-416.

33. Chatterjee, A. (2000). An introduction to the proper orthogonal decomposition. *Current Science, 78*(7), 808-817.

34. Chatzi, E. N., & Smyth, A. W. (2009). The unscented Kalman filter and particle filter methods for nonlinear structural system identification with non-collocated heterogeneous sensing. *Structural Control and Health Monitoring, 16*(1), 99-123.

35. Chawla, S., & Gionis, A. (2013). k-means–: A unified approach to clustering and outlier detection. *Proceedings of the 2013 SIAM International Conference on Data Mining, Texas, USA.*

36. Chelidze, D., & Liu, M. (2006). Multidimensional damage identification based on phase space warping: an experimental study. *Nonlinear Dynamics, 46*(1), 61-72.

37. Cichocki, A., & Amari, S. i. (2003). Adaptive Blind Signal and Image Processing (new revised and improved edition). *John Wiley, New York*.

38. Coleman, G. B., & Andrews, H. C. (1979). Image segmentation by clustering. *Proceedings of the IEEE, 67*(5), 773-785.

39. De Maesschalck, R., Jouan-Rimbaud, D., & Massart, D. L. (2000). The mahalanobis distance. *Chemometrics and Intelligent Laboratory Systems, 50*(1), 1-18.

40. Doebling, S. W., Farrar, C. R., & Prime, M. B. (1998). A summary review of vibration-based damage identification methods. *Shock and Vibration Digest, 30*(2), 91-105.

41. Doebling, S. W., Farrar, C. R., Prime, M. B., & Shevitz, D. W. (1996). Damage identification and health monitoring of structural and mechanical systems from changes in their vibration characteristics: a literature review. *Los Alamos National Lab., United States*.

42. Doyle, D., Zagrai, A., Arritt, B., & Çakan, H. (2010). Damage detection in bolted space structures. *Journal of Intelligent Material Systems and Structures, 21*(3), 251-264.

43. Dutta, A., & Talukdar, S. (2004). Damage detection in bridges using accurate modal parameters. *Finite Elements in Analysis and Design, 40*(3), 287-304.

44. Elkholy, S., & Meguro, K. (2004). Numerical simulation of high-rise steel buildings using improved applied element method. *13th World Conference on Earthquake Engineering. Vancouver, BC, Canada.*

45. Farrar, C., & James III, G. (1997). System identification from ambient vibration measurements on a bridge. *Journal of Sound and Vibration, 205*(1), 1-18.

46. Farrar, C. R., Doebling, S. W., & Nix, D. A. (2001). Vibration–based structural damage identification. *Philosophical Transactions of the Royal Society of London A: Mathematical, Physical and Engineering Sciences, 359*(1778), 131-149.

47. Farrar, C. R., & Worden, K. (2007). An introduction to structural health monitoring. *Philosophical Transactions of the Royal Society of London A: Mathematical, Physical and Engineering Sciences, 365*(1851), 303-315.

48. Farrar, C. R., & Worden, K. (2012). Structural health monitoring: a machine learning perspective: *John Wiley & Sons.*

49. Feeny, B., & Kappagantu, R. (1998). On the physical interpretation of proper orthogonal modes in vibrations. *Journal of Sound and Vibration, 211*(4), 607-616.

50. Feeny, B., & Liang, Y. (2003). Interpreting proper orthogonal modes of randomly excited vibration systems. *Journal of Sound and Vibration, 265*(5), 953-966.

51. Figueiredo, E., Park, G., Farrar, C. R., Worden, K., & Figueiras, J. (2011). Machine learning algorithms for damage detection under operational and environmental variability. *Structural Health Monitoring, 10*(6), 559-572.

52. Fraser, A. M., & Swinney, H. L. (1986). Independent coordinates for strange attractors from mutual information. *Physical Review A, 33*(2), 1134.

53. Fugate, M. L., Sohn, H., & Farrar, C. R. (2001). Vibration-based damage detection using statistical process control. *Mechanical Systems and Signal Processing, 15*(4), 707-721.

54. Gelle, G., Colas, M., Servière, C., & Measurement. (2003). Blind source separation: A new pre-processing tool for rotating machines monitoring *IEEE Transactions on Instrumentation and Measurement, 52*(3), 790-795.
55. Ghahari, S., Ghannad, M., & Taciroglu, E. (2013). Blind identification of soil–structure systems. *Soil Dynamics and Earthquake Engineering, 45*, 56-69.
56. Giurgiutiu, V., Reynolds, A., & Rogers, C. A. (1999). Experimental investigation of E/M impedance health monitoring for spot-welded structural joints. *Journal of Intelligent Material Systems and Structures, 10*(10), 802-812.
57. Grenier, Y. (1983). Time-dependent ARMA modeling of nonstationary signals. *IEEE Transactions on Acoustics, Speech, and Signal Processing, 31*(4), 899-911.
58. Gul, M., & Catbas, F. N. (2009). Statistical pattern recognition for structural health monitoring using time series modeling: Theory and experimental verifications. *Mechanical Systems and Signal Processing, 23*(7), 2192-2204.
59. Gul, M., & Catbas, F. N. (2011). Structural health monitoring and damage assessment using a novel time series analysis methodology with sensor clustering. *Journal of Sound and Vibration, 330*(6), 1196-1210.
60. Guorong, X., Peiqi, C., & Minhui, W. (1996). Bhattacharyya distance feature selection. *Proceedings of 13th International Conference on Pattern Recognition*. *Vienna, Austria, 2*, 195-199.
61. Hadjileontiadis, L., Douka, E., & Trochidis, A. (2005). Fractal dimension analysis for crack identification in beam structures. *Mechanical Systems and Signal Processing, 19*(3), 659-674.
62. Hao, H., Zhang, W., Li, J., & Ma, H. (2018). Bridge Condition Assessment Under Moving Loads Using Multi-sensor Measurements and Vibration Phase Technology. *Engineering Asset Management 2016,* 73-84.
63. Hayes, M. H. (2009). Statistical digital signal processing and modeling: *John Wiley & Sons*.

64. Hazra, B., & Narasimhan, S. (2009). Wavelet-based blind identification of the UCLA Factor building using ambient and earthquake responses. *Smart Materials and Structures, 19*(2), 025005.

65. Hazra, B., Roffel, A. J., Narasimhan, S., & Pandey, M. D. (2009). Modified cross-correlation method for the blind identification of structures. *Journal of Engineering Mechanics*, *136*(7), 889-897.

66. Hazra, B., Sadhu, A., Lourenco, R., & Narasimhan, S. (2010). Re-tuning tuned mass dampers using ambient vibration measurements. *Smart Materials and Structures, 19*(11), 115002.

67. Hazra, B., Sadhu, A., Roffel, A., Paquet, P., & Narasimhan, S. (2011). Underdetermined blind identification of structures by using the modified cross-correlation method. *Journal of Engineering Mechanics, 138*(4), 327-337.

68. Hazra, B., Sadhu, A., Roffel, A. J., & Narasimhan, S. (2012). Hybrid time-frequency blind source separation towards ambient system identification of structures. *Computer-Aided Civil and Infrastructure Engineering, 27*(5), 314-332.

69. Hester, D., & González, A. (2012). A wavelet-based damage detection algorithm based on bridge acceleration response to a vehicle. *Mechanical Systems and Signal Processing, 28*, 145-166.

70. Hou, Z., Noori, M., & Amand, R. S. (2000). Wavelet-based approach for structural damage detection. *Journal of Engineering Mechanics, 126*(7), 677-683.

71. Hua, X. (2006). Structural health monitoring and condition assessment of bridge structures. Doctoral dissertation, *The Hong Kong Polytechnic University.*

72. Huang, N. E., Shen, Z., & Long, S. R. (1999). A new view of nonlinear water waves: the Hilbert Spectrum 1. *Annual Review of Fluid Mechanics, 31*(1), 417-457.

73. Huang, N. E., Shen, Z., Long, S. R., Wu, M. C., Shih, H. H., Zheng, Q., Liu, H. H. (1998). The Empirical mode decomposition and the Hilbert spectrum for nonlinear and non-

stationary time series analysis. *Proceedings of the Royal Society of London A: Mathematical, Physical and Engineering Sciences, 454*(1971), 903-995.

74. Huang, Y., Meyer, D., & Nemat-Nasser, S. (2009). Damage detection with spatially distributed 2D continuous wavelet transform. *Mechanics of Materials, 41*(10), 1096-1107.
75. Huth, O., Feltrin, G., Maeck, J., Kilic, N., & Motavalli, M. (2005). Damage identification using modal data: Experiences on a prestressed concrete bridge. *Journal of Structural Engineering, 131*(12), 1898-1910.
76. Hyvärinen, A., & Oja, E. (2000). Independent component analysis: algorithms and applications. *Neural Networks, 13*(4-5), 411-430.
77. Ibrahim, S. R., & Pappa, R. S. (1982). Large modal survey testing using the Ibrahim time domain identification technique. *Journal of Spacecraft and Rockets, 19*(5), 459-465.
78. Ismail, M., Ikhouane, F., & Rodellar, J. (2009). The hysteresis Bouc-Wen model, a survey. *Archives of Computational Methods in Engineering, 16*(2), 161-188.
79. I-35W St. Anthony Falls Bridge Mississippi River Crossing in Downtown Minneapolis (2008). *Minnesota Department of Transportation*.
80. Jain, A. K. (2010). Data clustering: 50 years beyond K-means. *Pattern Recognition Letters, 31*(8), 651-666.
81. James, G., Carne, T. G., & Lauffer, J. P. (1995). The natural excitation technique (NExT) for modal parameter extraction from operating structures. *Modal Analysis-the International Journal of Analytical and Experimental Modal Analysis, 10*(4), 260.
82. Japan Building Disaster Prevention Association (JBDPA), "Guideline for Post-Earthquake Damage Evaluation and Rehabilitation", 1991 (revised in 2001).
83. Juang, J.-N., & Pappa, R. S. (1985). An eigensystem realization algorithm for modal parameter identification and model reduction. *Journal of Guidance, Control, and Dynamics, 8*(5), 620-627.

84. Johnson EA, Lam HF, Katafygiotis LS, Beck JL. (2004). The phase I IASC-ASCE structural health monitoring benchmark problem using simulated data. *Journal of Engineering Mechanics (ASCE) 130*(1), 3–15.
85. Katkhuda, H., & Haldar, A. (2008). A novel health assessment technique with minimum information. *Structural Control and Health Monitoring, 15*(6), 821-838.
86. Kennel, M. B., Brown, R., & Abarbanel, H. D. (1992). Determining embedding dimension for phase-space reconstruction using a geometrical construction. *Physical Review A, 45*(6), 3403.
87. Kerschen, G., & Golinval, J.-C. (2002). Physical interpretation of the proper orthogonal modes using the singular value decomposition. *Journal of Sound and Vibration, 249*(5), 849-865.
88. Kerschen, G., Poncelet, F., & Golinval, J.-C. (2007). Physical interpretation of independent component analysis in structural dynamics. *Mechanical Systems and Signal Processing, 21*(4), 1561-1575.
89. Kim, J.-T., Na, W.-B., Hong, D.-S., & Park, J.-H. (2006). Global and local health monitoring of plate-girder bridges under uncertain temperature conditions. *International Journal of Steel Structures, 6*(5), 369-376.
90. Ko, J., Wong, C., & Lam, H. (1994). Damage detection in steel framed structures by vibration measurement approach. *Proceedings-SPIE the International Society For Optical Engineering*, *Bellingham, USA.*
91. Kong, X., Goel, V., & Thakor, N. (1995). Quantification of injury-related EEG signal changes using Itakura distance measure. *International Conference on Acoustics, Speech, and Signal Processing, Detroit, MI, USA*
92. Kong, X., Thakor, N., & Goel, V. (1995). Characterization of EEG signal changes via Itakura distance. *17th Annual Conference of the Engineering in Medicine and Biology Society, Montreal, Canada.*

93. Kopsaftopoulos, F., & Fassois, S. (2013). A functional model based statistical time series method for vibration based damage detection, localization, and magnitude estimation. *Mechanical Systems and Signal Processing, 39*(1-2), 143-161.

94. Kore, R., Waychal, A., Agarwal, S., Yadav, P., Uddin, A., Sahoo, N., & Shelke, A. (2016). Impact induced solitary wave propagation through a woodpile structure. *Smart Materials and Structures, 25*(2), 025027.

95. Kovacic, I., & Brennan, M. J. (2011). The Duffing equation: nonlinear oscillators and their behaviour: *John Wiley & Sons*.

96. Krauthammer, T. (1999). Blast-resistant structural concrete and steel connections. *International Journal of Impact Engineering, 22*(9-10), 887-910.

97. Krishnan, M., Bhowmik, B., Hazra, B., & Pakrashi, V. (2018). Real time damage detection using recursive principal components and time-varying autoregressive modeling. *Mechanical Systems and Signal Processing, 101*, 549-574.

98. Krishnan, M., Bhowmik, B., Tiwari, A., & Hazra, B. (2017). Online damage detection using Recursive Principal Component Analysis and Recursive Condition Indicators. *Smart Materials and Structures, 26*(8), 085017.

99. Kullaa, J. (2003). Damage detection of the Z24 bridge using control charts. *Mechanical Systems and Signal Processing, 17*(1), 163-170.

100. Kundu, T. (2016). Ultrasonic and Electromagnetic NDE for Structure and Material Characterization: Engineering and Biomedical Applications, *Taylor & Francis, CRC Press*.

101. Kurata, M., Li, X., Fujita, K., & Yamaguchi, M. (2013). Piezoelectric dynamic strain monitoring for detecting local seismic damage in steel buildings. *Smart Materials and Structures, 22*(11), 115002.

102. Lakshmi, K., Rao, A. R. M., & Gopalakrishnan, N. (2017). Singular spectrum analysis combined with ARMAX model for structural damage detection. *Structural Control and Health Monitoring, 24*(9), e1960.

103. Lee, J. J., Lee, J. W., Yi, J. H., Yun, C. B., & Jung, H. Y. (2005). Neural networks-based damage detection for bridges considering errors in baseline finite element models. *Journal of Sound and Vibration, 280*(3-5), 555-578.

104. Lee, Y.-S., & Chung, M.-J. (2000). A study on crack detection using eigenfrequency test data. *Computers & Structures, 77*(3), 327-342.

105. Li, H., Deng, X., & Dai, H. (2007). Structural damage detection using the combination method of EMD and wavelet analysis. *Mechanical Systems and Signal Processing, 21*(1), 298-306.

106. Li, X., Kurata, M., & Nakashima, M. (2015). Evaluating damage extent of fractured beams in steel moment-resisting frames using dynamic strain responses. *Earthquake Engineering & Structural Dynamics, 44*(4), 563-581.

107. Linde, Y., Buzo, A., & Gray, R. (1980). An algorithm for vector quantizer design. *IEEE Transactions on Communications, 28*(1), 84-95.

108. Ling, X., & Haldar, A. (2004). Element level system identification with unknown input with Rayleigh damping. *Journal of Engineering Mechanics, 130*(8), 877-885.

109. Liu, G., Mao, Z., & Todd, M. (2016). Damage detection using transient trajectories in phase-space with extended random decrement technique under non-stationary excitations. *Smart Materials and Structures, 25*(11), 115014.

110. Liu, G., Mao, Z., Todd, M., & Huang, Z. (2014). Localization of nonlinear damage using state-space-based predictions under stochastic excitation. *Smart Materials and Structures, 23*(2), 025036.

111. Liu, P., & Sohn, H. (2016). Numerical simulation of damage detection using laser-generated ultrasound. *Ultrasonics, 69*, 248-258.

112. Loutridis, S. (2004). Damage detection in gear systems using Empirical mode decomposition. *Engineering Structures, 26*(12), 1833-1841.

113. Lu, Y., & Gao, F. (2005). A novel time-domain auto-regressive model for structural damage diagnosis. *Journal of Sound and Vibration, 283*(3), 1031-1049.

114. Mahalanobis, P. C. (1936). On the generalised distance in statistics. *National Institute of Sciences of India, 2*(1), 49-55.

115. Martin, R. J. (2000). A metric for ARMA processes. *IEEE Transactions on Signal Processing, 48*(4), 1164-1170.

116. Martinez-Flores, R. (2005). Damage assessment potential of a novel system identification technique-experimental verification, *Ph.D Dissertation, The University of Arizona*.

117. McLachlan, G. J. (1999). Mahalanobis distance. *Resonance, 4*(6), 20-26.

118. Mosavi, A. A., Dickey, D., Seracino, R., & Rizkalla, S. (2012). Identifying damage locations under ambient vibrations utilizing vector autoregressive models and Mahalanobis distances. *Mechanical Systems and Signal Processing., 26*, 254-267.

119. Mujica, L. E., Vehí, J., Ruiz, M., Verleysen, M., Staszewski, W., & Worden, K. (2008). Multivariate statistics process control for dimensionality reduction in structural assessment. *Mechanical Systems and Signal Processing., 22*(1), 155-171.

120. Musafere, F., Sadhu, A., & Liu, K. (2015). Towards damage detection using blind source separation integrated with time-varying autoregressive modeling. *Smart Materials and Structures, 25*(1), 015013.

121. Musafere, F., Sadhu, A., & Liu, K. (2016). Time-Varying System Identification Using a Hybrid Blind Source Separation Method. *Structural Health Monitoring, Damage Detection & Mechatronics,* 7, 99-104

122. Muthuswamy, J., & Thakor, N. V. (1998). Spectral analysis methods for neurological signals. *Journal of Neuroscience Methods, 83*(1), 1-14.

123. Nagayama, T., Jung, H., Spencer, B., Jang, S., Mechitov, K., Cho, S., Fujino, Y. (2010). International collaboration to develop a structural health monitoring system utilizing wireless smart sensor network and its deployment on a cable-stayed bridge. *5th World Conference on Structural Control and Monitoring, Shinjuku, Tokyo.*

124. Nair, K. K., & Kiremidjian, A. S. (2007). Time series based structural damage detection algorithm using Gaussian mixtures modeling. *Journal of Dynamic Systems, Measurement, and Control, 129*(3), 285-293.

125. Nair, K. K., Kiremidjian, A. S., & Law, K. H. (2006). Time series-based damage detection and localization algorithm with application to the ASCE benchmark structure. *Journal of Sound and Vibration, 291*(1-2), 349-368.

126. Namdeo, V., & Manohar, C. (2007). Nonlinear structural dynamical system identification using adaptive particle filters. *Journal of Sound and Vibration, 306*(3-5), 524-563.

127. Nguyen, D. P., Wilson, M. A., Brown, E. N., & Barbieri, R. (2009). Measuring instantaneous frequency of local field potential oscillations using the Kalman smoother. *Journal of Neuroscience Methods, 184*(2), 365-374.

128. Nichols, J. (2003). Structural health monitoring of offshore structures using ambient excitation. *Applied Ocean Research, 25*(3), 101-114.

129. Nichols, J., Todd, M., Seaver, M., & Virgin, L. (2003). Use of chaotic excitation and attractor property analysis in structural health monitoring. *Physical Review Research, 67*(1), 016209.

130. Nie, Z., Hao, H., & Ma, H. (2012). Using vibration phase space topology changes for structural damage detection. *Structural Health Monitoring, 11*(5), 538-557.

131. Nie, Z., Hao, H., & Ma, H. (2013). Structural damage detection based on the reconstructed phase space for reinforced concrete slab: Experimental study. *Journal of Sound and Vibration, 332*(4), 1061-1078.

132. Omenzetter, P., & Brownjohn, J. M. W. (2006). Application of time series analysis for bridge monitoring. *Smart Materials and Structures., 15*(1), 129.

133. Pakzad, S. N. (2010). Development and deployment of large scale wireless sensor network on a long-span bridge. *Smart Structures and Systems, 6*(5-6), 525-543.

134. Pandey, A., & Biswas, M. (1994). Damage detection in structures using changes in flexibility. *Journal of Sound and Vibration, 169*(1), 3-17.

135. Pandey, A., Biswas, M., & Samman, M. (1991). Damage detection from changes in curvature mode shapes. *Journal of Sound and Vibration, 145*(2), 321-332.

136. Panteliou, S. D., Chondros, T. G., Argyrakis, V., & Dimarogonas, A. (2001). Damping factor as an indicator of crack severity. *Journal of Sound and Vibration, 241*(2), 235-245.

137. Park, J.-H., Kim, J.-T., Hong, D.-S., Mascarenas, D., & Lynch, J. P. (2010). Autonomous smart sensor nodes for global and local damage detection of prestressed concrete bridges based on accelerations and impedance measurements. *Smart Structures and Systems, 6*(5-6), 711-730.

138. Patil, D., & Maiti, S. (2003). Detection of multiple cracks using frequency measurements. *Engineering Fracture Mechanics, 70*(12), 1553-1572.

139. Paul, B., George, R. C., & Mishra, S. K. (2017). Phase space interrogation of the Empirical response modes for seismically excited structures. *Mechanical Systems and Signal Processing, 91*, 250-265.

140. Paultre, P., Proulx, J., & Talbot, M. (1995). Dynamic testing procedures for highway bridges using traffic loads. *Journal of Structural Engineering, 121*(2), 362-376.

141. Pawar, P. M., Venkatesulu Reddy, K., & Ganguli, R. (2007). Damage detection in beams using spatial Fourier analysis and neural networks. *Journal of Intelligent Material Systems and Structures, 18*(4), 347-359.

142. Peeters, M., Viguié, R., Sérandour, G., Kerschen, G., & Golinval, J.-C. (2009). Nonlinear normal modes, Part II: Toward a practical computation using numerical continuation techniques. *Mechanical Systems and Signal Processing, 23*(1), 195-216.

143. Penny, J., Wilson, D., & Friswell, M. (1993). Damage location in structures using vibration data. *Proceedings-Spie The International Society For Optical Engineering*, *Bellingham, USA.*

144. Poncelet, F., Kerschen, G., Golinval, J.-C., & Marin, F. (2007). Second-order blind identification for operational modal analysis. *ASME 2007 International Design Engineering Technical Conferences and Computers and Information in Engineering Conference, Las Vegas, USA.*

145. Rajan, J. J., & Rayner, P. J. (1996). Generalized feature extraction for time-varying autoregressive models. *IEEE Transactions on signal processing, 44*(10), 2498-2507.

146. Roveri, N., & Carcaterra, A. (2012). Damage detection in structures under traveling loads by Hilbert–Huang transform. *Mechanical Systems and Signal Processing, 28*, 128-144.

147. Sadhu, A., & Hazra, B. (2013). A novel damage detection algorithm using time-series analysis-based blind source separation. *Shock and Vibration, 20*(3), 423-438.

148. Sadhu, A., Hazra, B., & Narasimhan, S. (2012). Blind identification of earthquake-excited structures. *Smart Materials and Structures, 21*(4), 045019.

149. Sadhu, A., Hazra, B., Narasimhan, S., & Pandey, M. (2011). Decentralized modal identification using sparse blind source separation. *Smart Materials and Structures, 20*(12), 125009.

150. Sadhu, A., & Narasimhan, S. (2014). A decentralized blind source separation algorithm for ambient modal identification in the presence of narrowband disturbances. *Structural Control and Health Monitoring, 21*(3), 282-302.

151. Sadhu, A., Narasimhan, S., & Antoni, J. (2017). A review of output-only structural mode identification literature employing blind source separation methods. *Mechanical Systems and Signal Processing, 94*, 415-431.

152. Sakellariou, J., & Fassois, S. (2006). Stochastic output error vibration-based damage detection and assessment in structures under earthquake excitation. *Journal of Sound and Vibration, 297*(3-5), 1048-1067.

153. Salehi, M., Rad, S. Z., Ghayour, M., & Vaziry, M. (2011). A non model-based damage detection technique using dynamically measured flexibility matrix. *Iranian Journal of Science and Technology. Transactions of Mechanical Engineering, 35*(M1), 1.

154. Santos, J. P., Crémona, C., Calado, L., Silveira, P., & Orcesi, A. D. (2016). On-line unsupervised detection of early damage. *Structural Control and Health Monitoring, 23*(7), 1047-1069.

155. Shelke, A., Kundu, T., Amjad, U., Hahn, K., & Grill, W. (2011). Mode-selective excitation and detection of ultrasonic guided waves for delamination detection in laminated aluminum plates. *IEEE Transactions on Ultrasonics, Ferroelectrics, and Frequency Control, 58*(3), 567-577.

156. Shi, Z., Law, S., & Zhang, L. M. (2000). Structural damage detection from modal strain energy change. *Journal of Engineering Mechanics, 126*(12), 1216-1223.

157. Shlens, J. (2003). A tutorial on Principal Component Analysis: Derivation, Discussion and Singular Value Decomposition. *https://www.cs.princeton.edu/picasso /mats/PCA-Tutorial-Intuition_jp.pdf.*

158. Shumway, R. H., & Stoffer, D. S. (2017). Time series analysis and its applications: with R examples: *Springer*.

159. Smyth, A. W., Masri, S. F., Kosmatopoulos, E. B., Chassiakos, A. G., & Caughey, T. K. (2002). Development of adaptive modeling techniques for non-linear hysteretic systems. *International Journal of Nonlinear Mechanics, 37*(8), 1435-1451.

160. Sohn, H., Czarnecki, J. A., & Farrar, C. R. (2000). Structural health monitoring using statistical process control. *Journal of Structural Engineering, 126*(11), 1356-1363.

161. Sohn, H., & Farrar, C. R. (2001). Damage diagnosis using time series analysis of vibration signals. *Smart Materials and Structures, 10*(3), 446.

162. Sohn, H., Farrar, C. R., Hemez, F. M., & Czarnecki, J. J. (2002). A review of structural health review of structural health monitoring literature 1996-2001. *Los Alamos National Laboratory. Report No. LA-UR-02-2095.*

163. Sohn, H., Farrar, C. R., Hemez, F. M., Shunk, D. D., Stinemates, D. W., Nadler, B. R., & Czarnecki, J. J. (2003). A review of structural health monitoring literature: 1996–2001. *Los Alamos National Laboratory. Report No. LA-UR-02-2095.*

164. Sohn, H., Farrar, C. R., Hunter, N. F., & Worden, K. (2001). Structural health monitoring using statistical pattern recognition techniques. *Journal of Dynamic Systems, Measurement, and Control, 123*(4), 706-711.

165. Stone, J. V. (2004). Independent component analysis: a tutorial introduction: *MIT press*.

166. Taha, M. R., Noureldin, A., Lucero, J., & Baca, T. (2006). Wavelet transform for structural health monitoring: a compendium of uses and features. *Structural Health Monitoring, 5*(3), 267-295.

167. Takens', F. (1981). Detecting strange attractors in turbulence. *Lecture notes in mathematics, 898*(1), 366-381.

168. Tang, B., Dong, S., & Song, T. (2012). Method for eliminating mode mixing of Empirical mode decomposition based on the revised blind source separation. *Signal Processing, 92*(1), 248-258.

169. Todd, M., Erickson, K., Chang, L., Lee, K., & Nichols, J. (2004). Using chaotic interrogation and attractor nonlinear cross-prediction error to detect fastener preload loss in an aluminum frame. *Chaos: An Interdisciplinary Journal of Nonlinear Science, 14*(2), 387-399.

170. Todd, M., Nichols, J., Pecora, L., & Virgin, L. (2001). Vibration-based damage assessment utilizing state space geometry changes: local attractor variance ratio. *Smart Materials and Structures, 10*(5), 1000.

171. Tong, L., Soon, V., Huang, Y., & Liu, R. (1990). AMUSE: a new blind identification algorithm. *IEEE International Symposium on Circuits and Systems, Los Angeles, USA.*

172. Torkamani, S., Butcher, E. A., Todd, M. D., & Park, G. (2012). Hyperchaotic probe for damage identification using nonlinear prediction error. *Mechanical Systems and Signal Processing, 29*, 457-473.

173. United-Nations. (2017). *World Population Ageing 2015*.

174. Van Den Abeele, K. E., Sutin, A., Carmeliet, J., & Johnson, P. A. (2001). Micro-damage diagnostics using nonlinear elastic wave spectroscopy (NEWS). *Ndt & E International, 34*(4), 239-248.

175. Van Overschee, P., & De Moor, B. (1996). Continuous-time frequency domain subspace system identification. *Signal Processing, 52*(2), 179-194.

176. Wahab, M. A., & De Roeck, G. (1999). Damage detection in bridges using modal curvatures: application to a real damage scenario. *Journal of Sound and Vibration, 226*(2), 217-235.

177. Wall, M. E., Rechtsteiner, A., & Rocha, L. M. (2003). Singular value decomposition and principal component analysis. *A practical approach to microarray data analysis* (pp. 91-109): Springer.

178. Wandowski, T., Malinowski, P., & Ostachowicz, W. (2011). Damage detection with concentrated configurations of piezoelectric transducers. *Smart Materials and Structures, 20*(2), 025002.

179. Wang, D., & Haldar, A. (1994). Element-level system identification with unknown input. *Journal of Engineering Mechanics, 120*(1), 159-176.

180. Wang, D., & Haldar, A. (1997). System identification with limited observations and without input. *Journal of Engineering Mechanics, 123*(5), 504-511.

181. Winkel, B. (2017). Simplified Multi-Storey Shear Building Model. https://www.simiode.org/resources/4044.

182. Wong, K. Y. (2004). Instrumentation and health monitoring of cable-supported bridges. *Structural Control and Health Monitoring, 11*(2), 91-124.

183. Worden, K., Farrar, C. R., Haywood, J., & Todd, M. (2008). A review of nonlinear dynamics applications to structural health monitoring. *Structural Control and Health Monitoring, 15*(4), 540-567.

184. Worden, K., Farrar, C. R., Manson, G., & Park, G. (2007). The fundamental axioms of structural health monitoring. *Proceedings of the Royal Society of London A: Mathematical, Physical and Engineering Sciences, 463*(2082), 1639-1664.

185. Worden, K., Manson, G., & Fieller, N. R. (2000). Damage detection using outlier analysis. *Journal of Sound and Vibration, 229*(3), 647-667.

186. Xin, Y., Hao, H., Li, J. J. S. C., & Monitoring, H. (2019). Operational modal identification of structures based on improved Empirical wavelet transform. *Structural Control and Health Monitoring*, *26*(3), e2323.

187. Yamaguchi, H., Matsumoto, Y., Kawarai, K., Dammika, A. J., Shahzad, S., & Takanami, R. (2013). Damage detection based on modal damping change in bridges. *Digital Library, University of Moratuwa, Srilanka.*

188. Yan, A.-M., Kerschen, G., De Boe, P., & Golinval, J.-C. (2005). Structural damage diagnosis under varying environmental conditions—part I: a linear analysis. *Mechanical Systems and Signal Processing, 19*(4), 847-864.

189. Yan, Y., Cheng, L., Wu, Z., & Yam, L. (2007). Development in vibration-based structural damage detection technique. *Mechanical Systems and Signal Processing, 21*(5), 2198-2211.

190. Yan, Y., & Yam, L. (2002). Online detection of crack damage in composite plates using embedded piezoelectric actuators/sensors and wavelet analysis. *Composite Structures, 58*(1), 29-38.

191. Yang, J., & Chang, F.-K. (2006). Detection of bolt loosening in C–C composite thermal protection panels: I. Diagnostic principle. *Smart Materials and Structures, 15*(2), 581.

192. Yang, J. N., & Huang, H. (2007). Sequential non-linear least-square estimation for damage identification of structures with unknown inputs and unknown outputs. *International Journal of Nonlinear Mechanics, 42*(5), 789-801.

193. Yang, J. N., Huang, H., & Lin, S. (2006). Sequential non-linear least-square estimation for damage identification of structures. *International Journal of Nonlinear Mechanics, 41*(1), 124-140.

194. Yang, J. N., Lei, Y., Lin, S., & Huang, N. (2004). Hilbert-Huang based approach for structural damage detection. *Journal of Engineering Mechanics, 130*(1), 85-95.

195. Yang, J. N., Lin, S., Huang, H., & Zhou, L. (2006). An adaptive extended Kalman filter for structural damage identification. *Structural Control and Health Monitoring, 13*(4), 849-867.

196. Yang, Y., & Nagarajaiah, S. (2012). Time-frequency blind source separation using independent component analysis for output-only modal identification of highly damped structures. *Journal of Structural Engineering, 139*(10), 1780-1793.

197. Yang, Y., & Nagarajaiah, S. (2013a). Blind modal identification of output-only structures in time-domain based on complexity pursuit. *Earthquake Engineering and Structural Dynamics, 42*(13), 1885-1905.

198. Yang, Y., & Nagarajaiah, S. (2013b). Output-only modal identification with limited sensors using sparse component analysis. *Journal of Sound and Vibration, 332*(19), 4741-4765.

199. Yang, Y., & Nagarajaiah, S. (2014a). Blind identification of damage in time-varying systems using independent component analysis with wavelet transform. *Mechanical Systems and Signal Processing, 47*(1-2), 3-20.

200. Yang, Y., & Nagarajaiah, S. (2014b). Data compression of structural seismic responses via principled independent component analysis. *Journal of Structural Engineering, 140*(7), 04014032.

201. Yao, R., & Pakzad, S. N. (2012). Autoregressive statistical pattern recognition algorithms for damage detection in civil structures. *Mechanical Systems and Signal Processing, 31*, 355-368.

202. Yeager, M., Gregory, B., Key, C., & Todd, M. (2018). On using robust Mahalanobis distance estimations for feature discrimination in a damage detection scenario. *Structural Health Monitoring*, *18*(1), 245-253.

203. Yim, H. C., & Krauthammer, T. (2009). Load–impulse characterization for steel connection. *International Journal of Impact Engineering, 36*(5), 737-745.

204. Ying, Y., Garrett Jr, J. H., Oppenheim, I. J., Soibelman, L., Harley, J. B., Shi, J., & Jin, Y. (2012). Toward data-driven structural health monitoring: application of machine learning and signal processing to damage detection. *Journal of Computing in Civil Engineering, 27*(6), 667-680.

205. Yu, K., Yang, K., & Bai, Y. (2014). Estimation of modal parameters using the sparse component analysis based underdetermined blind source separation. *Mechanical Systems and Signal Processing, 45*(2), 302-316.

206. Yu, L., Cheng, L., Yam, L., Yan, Y., & Jiang, J. (2007). Online damage detection for laminated composite shells partially filled with fluid. *Composite Structures, 80*(3), 334-342.

207. Zagrai, A., Donskoy, D., Chudnovsky, A., & Golovin, E. (2008). Micro-and macroscale damage detection using the nonlinear acoustic vibro-modulation technique. *Research in Nondestructive Evaluation, 19*(2), 104-128.

208. Zang, C., Friswell, M. I., & Imregun, M. (2004). Structural damage detection using independent component analysis. *Structural Health Monitoring, 3*(1), 69-83.

209. Zhang, Q., Tse, P. W.-T., Wan, X., & Xu, G. (2015). Remaining useful life estimation for mechanical systems based on similarity of phase space trajectory. *Expert Systems with Applications, 42*(5), 2353-2360.

210. Zhang, W., Li, J., Hao, H., & Ma, H. (2017). Damage detection in bridge structures under moving loads with phase trajectory change of multi-type vibration measurements. *Mechanical Systems and Signal Processing, 87*, 410-425.

211. Zheng, H., & Mita, A. (2009). Localized damage detection of structures subject to multiple ambient excitations using two distance measures for autoregressive models. *Structural Health Monitoring, 8*(3), 207-222.

212. Zhong, S., Oyadiji, S. O., & Ding, K. (2008). Response-only method for damage detection of beam-like structures using high accuracy frequencies with auxiliary mass spatial probing. *Journal of Sound and Vibration, 311*(3), 1075-1099.

213. Zhou, W., & Chelidze, D. (2007). Blind source separation based vibration mode identification. *Mechanical Systems and Signal Processing, 21*(8), 3072-3087.

214. Zou, Y., Tong, L., & Steven, G. P. (2000). Vibration-based model-dependent damage (delamination) identification and health monitoring for composite structures—a review. *Journal of Sound and Vibration, 230*(2), 357-378.

215. Zugasti, E., González, A. G., Anduaga, J., Arregui, M. A., & Martínez, F. (2012). NullSpace and AutoRegressive damage detection: a comparative study. *Smart Materials and Structures, 21*(8), 085010.